The Search for the Angiotensin Converting Enzyme Sheddase Recognition Domain

A PhD thesis by

Anthony James Chubb BSc (Med) (Hons)

Thesis Presented for the Degree of

DOCTOR OF PHILOSOPHY

in the Division of Medical Biochemistry, Faculty of Health Sciences

UNIVERSITY OF CAPE TOWN

December 2001

Declaration:

I, ***Anthony James Chubb***, declare that this dissertation is my own, unaided work (except where acknowledgments indicate otherwise). Neither the whole work nor part thereof has been, is being, or is to be submitted for any degree or examination at any other university.

I empower the University to reproduce for the purpose of research either the whole or any part of the contents of this dissertation, in any manner whatever.

Signed by candidate

Signature of applicant:

Signed on the 4th day of December, 2001

For my sister, Kathy

Our shared future of beautiful memories
That we will never have
I will never forget

Dr Kathy Chubb
28 May 1970 - 15 April 1994

Acknowledgements

I would like to express my sincere appreciation to…

… my mentor, Prof. Mario R. W. Ehlers, for his unbelievable encouragement and support over the years. Not only are many of the ideas expressed in this thesis a direct result of many fruitful and enjoyable conversations, but also his infectious enthusiasm and passion for this project are its foundation. His scrutiny of this thesis and consistent advice and support has helped immeasurably. I cannot thank him enough for all his help, and above all for inspiring a love of science.

… Sylva Schwager for the metabolic labelling studies, the construction of the sepharose-[28A]-lisinopril columns, antibody preparation, much of the protein purification and all cleavage site analyses. Her almost maternal love and support has been a major source of motivation and her caring, gentle education have taught me all I know about cell biology and protein chemistry. Her genius in protein biochemistry is unmatched and has obliterated numerous obstacles on this project. I am eternally grateful to Sylva for her maternal love, support and generosity on this project. Words cannot describe my appreciation for all that she has done for me over the years.

… Dr Edward D. Sturrock for taking me on as a student and guiding me through the final stages. His clear and thoughtful guidance have been a significant education. His challenging conversations have forced me to examine numerous different angles, making the write-up (and years of labwork) an exciting, if exhausting, time. His careful reading of this thesis, and innumerable comments, deserves my sincerest gratitude.

… my parents, Peter and Karin Chubb, for their unfailing love and support (both financial, emotional and gastronomical) over the years. Their generosity and understanding have made this thesis possible.

… Marian Brennan for her love, dedication and the zillion late nights she stayed with me in the lab. I hope to have a lifetime of loving her to repay a part of my debt.

... my colleagues, Zenda Woodman and Kerry Gordon, for their friendship, laughter, warmth and fun. Not only have innumerable conversations with Zenda and Kerry helped in conceiving this work, but also their friendly, cheerful and expert help have solved many of the technical problems I've encountered. Zenda, especially, has seen me through my worst lows and greatest highs and somehow pulled me through it all.

... my friends Renen, Zeke, Ben, Heidi, Hoppie, Ros and Kate for their relentless support and encouragement. They pushed me back into the lab when I wasn't focused and pulled me away again when it was all too much. I will never forget their phenomenal support.

... Dr. Reinhard Mentele and Monica Zobawa (Protein Analysis Group, Max Planck Institute, Martinsreid, Germany) for doing some of the cleavage site determinations. Thanks also go to Prof. Wolf Brandt (Biochemistry Dept., UCT) for the N-terminal sequencing of HPLC fractions isolated by Sylva.

... Liz van der Merve (Cell Biology dept., UCT) for the confocal microscopy work. Dr. D. James (Microbiology dept., UCT) for the automated sequencing of the DNA constructs.

... the FRD for generously funding me over many years. Similarly I would like to thank the Guy-Elliot foundation, Investec and Hoffmann-La Roche for funding me after the FRD scholarships ended.

... Pablo, my dog, for smiling at me when there was little to smile about and keeping me company on many a long and lonely night.

Contents

Acknowledgements i
Contents iii
Abstract vi
Introduction vii
Chapter 1: Ectodomain Shedding 1
Cleavage Secretion of Ectoproteins 1
1.1) Characteristics of ectoproteins and shedding 3
1.1.1) Ectoprotein structure 3
1.1.2) Ectodomain shedding 5
1.1.3) Inhibition of ectodomain shedding 10
1.1.4) Cellular control of shedding 13
1.2) The sheddases 19
1.2.1) TACE/ADAM-17 (α-secretase) 20
1.2.2) Kuzbanian/ADAM-10 22
1.2.3) MDC9/ADAM-9 24
1.3) Alzheimer's disease: A Complex Case of Shedding 25
1.3.1) α-Secretase (TACE and/or ADAM-10) 25
1.3.2) β-Secretase (BACE) 27
1.3.3) γ-Secretase (PS1/PS2) 27
1.4) Physiological importance of ectodomain shedding 30
1.5) Finding the sheddase recognition domain 31
1.5.1) In the stalk region? 34
1.5.2) In the ectodomain? 36
In conclusion 41
Chapter 2: Angiotensin-Converting Enzyme 42
2.1) Angiotensin-Converting Enzyme (ACE) 42
2.1.1) The discovery of ACE 42
2.1.2) Somatic ACE 44
2.1.3) Testis ACE 47
2.1.4) Catalytic activity 50
2.1.5) ACE Inhibitors 52
2.1.6) Phylogeny 54
2.2) The Renin-Angiotensin Aldosterone System 57
2.2.1) Localised RAS 59
2.2.2) Hypertension 60
2.3) ACE and fertility 63
2.4) ACE shedding 69
2.5) Finding the sheddase recognition motif 75
An experimental approach 76
Chapter 3: Materials and Methods 78
3.1) Vector construction 78
3.1.1) Deletion mutants 78
3.1.2) Swap-over mutants 81
3.2) Tissue Culture 82
3.2.1) $CaPO_4$ co-transfection of CHO-K1 cells 82
3.2.2) ACE shedding kinetics 83
3.2.3) TAPI inhibition 83

3.2.4) Surface expression – FITC labelling of CHO cells 84
3.2.5) DEAE-Dextran transfection of COS-1 cells 85
3.3) ACE activity assays and protein analysis 86
3.3.1) HHL substrate assay for ACE activity 86
3.3.2) Fluorogenic peptides 86
3.3.3) Western blot analysis 87
3.3.4) Metabolic labelling 87
3.3.5) Triton X-114 phase separation 88
3.4) Protein purification 89
3.5) Cleavage site determination 90
3.5.1) Reduction and protection of disulphides 90
3.5.2) Lys-C digestion and HPLC fractionation 90
3.5.3) ACE peptide deglycosylation 92
3.5.4) MALDI-TOF mass spectroscopy 92
Chapter 4: The Juxtamembrane Region 93
The ACE stalk deletion mutants 93
4.1) The 'headroom' 96
4.1.1) ACE-Δ6JM 97
4.1.2) ACE-Δ11JM 108
4.1.3) ACE-Δ16JM 113
4.2) The Cleavage Site 116
4.2.1) ACE-ΔR627 116
4.3) The 'Footroom' 122
4.3.1) ACE-Δ5JM 124
Conclusions 129
Chapter 5: The Cytoplasmic Tail 131
5.1) ACE-ΔCYT 132
5.2) The actin cytoskeleton and ACE shedding 137
Chapter 6: The Ectodomain 144
Defining the ectodomain 146
6.1) The C-terminal end 146
6.2) The N-terminal end 148
6.2.1) ACEΔ36N-wt 148
6.2.2) ACEΔ61E 150
Swapping the ACE ectodomains 154
6.3) ACE-Ndom 156
6.4) ACE-NBcl 161
Chapter 7: Conclusions 167
Appendix I: Supplementary Tables and Figures 191
Abbreviations: 191
Stalk region sequences 194
Taxonomic lineage of species whose ACE cDNA is cloned 198
The Taxonomic 'history' of ACE Evolution 199
ACE homologues 200
Appendix II: Methods 201
AII.1) Recombinant DNA methods 201
AII.1.1) Polymerase chain reaction (PCR) 201
AII.I.2) Restriction enzyme digestion of DNA and electrophoresis 201
AII.1.3) DNA extraction from *Escherichia coli* 202
AII.1.4) Cloning a DNA fragment into a plasmid vector 202

AII.1.5) Transforming *Escherichia coli* 202
AII.1.6) DNA sequencing 203
AII.2) Tissue culture 203
AII.2.1) CaPO4 Transfection 203
AII.2.2) Cloning CHO cells 203
AII.3) Protein analysis 204
AII.3.1) Western Blot analysis 204
AII.3.2) Protein concentration determination 204
AII.3.3) Triton X114 separation of ACE 204
AII.3.4) Affinity purification of ACE 205
Appendix III: Reagents and Miscellaneous data 206
Reagents 206
Primers 214
Protein Sequences used in alignments 215
Useful websites 221

Abstract

Numerous physiologically important cytokines, receptors and ectoenzymes are released from the cell surface by a defined proteolytic cleavage event ("shedding"), e.g., TNF-α, TNFR, β-APP, TGF-α, IL-6R, L-selectin, and ACE. Shedding therefore contributes to diverse processes including inflammation, neutrophil rolling, cell growth, metastasis, apoptosis, and amyloid plaque formation in Alzheimer's disease.

Angiotensin-converting enzyme (ACE) is a type I ectoprotein that plays a central role in blood pressure regulation and has recently been implicated in fertility. The shedding of ACE was investigated as it shows characteristic induction with phorbol esters and is inhibited with hydroxamate-based inhibitors like TAPI. Mutations were constructed in the juxtamembrane stalk, cytoplasmic and ectodomain regions of human testis ACE and their effect on ACE shedding from transfected Chinese hamster ovary (CHO) cells was examined.

Large deletions in the juxtamembrane stalk region above (Δ6, Δ11) and below (Δ5, Δ17, Δ24) the normal cleavage site were tolerated by the sheddase. The cleavage site was determined for each mutant using MALDI-TOF analysis, most of which were cleaved at the R_{627}/S_{628} bond. The cleavage site shifted closer to the membrane when an N-linked glycosylation site was introduced (Δ6), or the preferred cleavage-site arginine was removed (ΔR_{627}). Interestingly, shedding was deregulated when the cytoplasmic tail was removed, possibly through loss of an inhibitory interaction with an actin binding protein.

As shedding was not abolished by deletions in the stalk or cytoplasmic tail regions, we mutated the ectodomain by replacing sections with equivalent sequences from the highly homologous N-domain of somatic ACE. ACE-Ndom, where the entire 'C-domain' of human testis ACE was replaced, was not shed and accumulated on the cell surface. ACE-NBcl (where only the proximal ectodomain was swapped) was released very efficiently. The ACE sheddase recognition domain is thus not located in the stalk, cytoplasmic or proximal ectodomain regions, but likely resides in the distal ectodomain.

Introduction

Ectodomain shedding, or the proteolytic cleavage of ectoproteins from the surface of cells, is emerging as a cellular process of increasing importance as its role in normal physiology and numerous pathologies unfolds. Over the past decade and a half, the number of ectoproteins found to be shed has increased dramatically, and the first sheddases responsible for this shedding have been isolated and characterised. These recent insights have irrevocably changed the perceived importance of ectodomain shedding. This field of study is still in its infancy with ongoing and future work focusing on how sheddases are regulated; which signals activate and inactivate shedding; which ectoproteins are shed under differing conditions; and even the number of sheddases. Our particular interest has involved investigating how these sheddases recognise their substrates out of the myriad of different ectoproteins on the cell surface. In this thesis, I use angiotensin-converting enzyme (ACE) as a model system to study the criterion needed for sheddase recognition of its substrate ectoprotein. More specifically, we are interested in resolving whether the sheddase recognises the juxtamembrane stalk region or the ectodomain region prior to cleavage in the stalk. Deletion, insertion, and chimeric mutants of ACE were made and their cleavage-release monitored, in order to identify the exact substrate requirements for ectodomain shedding (see Fig. 0.1).

The introductory Chapter 1 is in the form of a literature review introducing ectoproteins, of which integral membrane proteins such as ACE are a subset, and the differing modes of ectoprotein secretion. The ACE sheddase is stimulated by phorbol esters, which activate protein kinase C (PKC), the central effector of numerous signal transduction pathways. A brief explanation of the regulation of sheddases is given and the signal transduction pathways involved in ectodomain shedding is outlined. Another important characteristic of sheddases is their inhibition by hydroxamate-based inhibitors such as the TNFα protease inhibitor (TAPI). The importance of ectodomain shedding in normal and aberrant physiology is now well establishead and there are an increasing number of

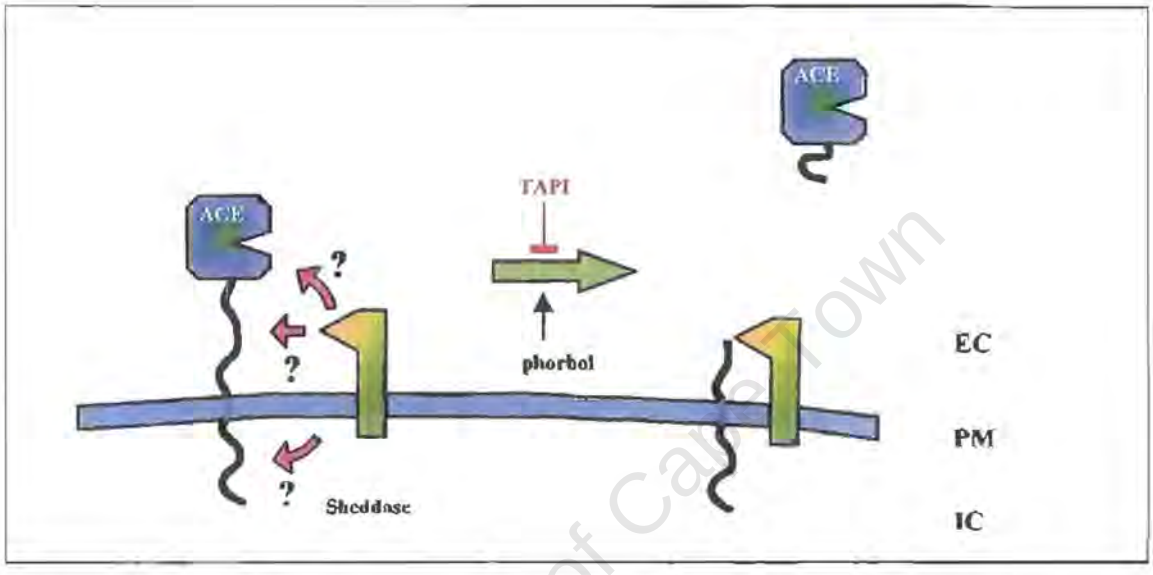

Figure 0.1) Schematic representation of ACE shedding

After cleavage by the sheddase, the ACE ectodomain is free to diffuse into the aqueous extracellular fluid. Intracellular, (IC); Extracellular, (EC); plasma membrane (PM), light blue; ACE ectodomain, blue/green; juxtamembrane stalk and cytoplasmic tail, black line; transmembrane (TM) domain, blue line; hypothetical ACE sheddase, orange/green; the proposed recognition by the sheddase, mauve arrows. Stimulation by phorbol ester (e.g. PDBu) is indicated with a solid arrow, while inhibition by hydroxamate-base inhibitors (e.g. TAPI) is shown with a red bar.

ectoproteins that appear to be shed in a regulated fashion from the cell surface, examples of which are given in Chapter 1.

The controversy surrounding the exact motif or domain used by the sheddase(s) to identify their substrate ectoprotein prior to cleavage in the juxtamembrane stalk region needs clarification and is outlined in Chapter 1. Briefly, the early assumption that the sheddases recognise specific amino acid sequences at or near the cleavage site has been superseded by the hypothesis that the sheddase first recognises the ectodomain of the substrate ectoprotein, prior to a sequence-independent cleavage in the stalk region. We attempt to resolve some of these issues using the ectoenzyme ACE as a model system. The characteristics of ACE, the renin-angiotensin system and the physiological importance of ACE shedding are given in Chapter 2. Furthermore the use of ACE mutants to tease out the substrate requirements of the ACE sheddase is discussed.

As most shed ectoproteins, including ACE, are cleaved in the juxtamembrane stalk region, between the proximal ectodomain and the transmembrane domain, this seemed the obvious place to start an exploration to identify the sheddase recognition motif. In Chapter 4, I present the results of experiments involving stalk deletion mutants in ACE. The sheddase requirement for 'footroom' and 'headroom' are clarified, as well as the need (or lack thereof) for the R_{627} at the P_1 position.

The stalk deletion mutants we made failed to abolish shedding, indicating that the sheddase recognition motif did not reside in this region. It was therefore proposed that the sheddase simply recognises an unstructured, 'open' stalk of minimum length. Our stalk insertion experiments, in which we inserted the tightly knotted EGF domain or highly glycosylated sequences into the ACE stalk, are also detailed in Chapter 4. Surprisingly, these mutants were also shed from the surface of cells indicating that the ACE sheddase is extremely promiscuous in terms of cleavage site sequence. We were, at best, only able to 'force' the sheddase to use alternative cleavage sites, but could not abolish shedding indicating that sheddase recognition of the stalk region was not sequence-specific.

This led to the hypothesis that the ACE sheddase, and by inference other sheddases, first recognises its substrate ectoprotein in a region outside of the stalk, prior to cleavage in an open, extended stalk, with little regard for the exact amino acid sequence at this site. The cytoplasmic tail of numerous ectoproteins has been shown to be involved in protein localisation and signalling. Thus, the possibility exists that the sheddase recognises the cytoplasmic tail of ACE and this signal is transferred to the extracellular proteolytic domain of the sheddase. A C-terminal truncation mutant of ACE lacking the cytoplasmic tail was also shed, with enhanced efficiency, as shown in Chapter 5.

In the absence of a 3D structure of the 616 residue ACE ectodomain, we hypothesised that the N-terminal sequence may be folded back, close to the TM, and thus may provide a region for sheddase recognition. The first truncation mutant, in which the highly O-glycosylated 35-residue 5′-region was deleted, has already been published [Ehlers, 1992]. This soluble enzyme tolerated limited N-terminal truncation, but needed to be converted to the membrane bound form for shedding analysis. Shedding experiments showed that the first 36 amino acids of testis ACE are not involved in shedding. Further truncations were impossible as the enzyme is disrupted.

This implied that the sheddase does not recognise the stalk region, the cytoplasmic domain, or the first 36 amino acids as a prerequisite for shedding. The transmembrane domain was also shown not to be involved in shedding by other workers at this time. This forced us to take a completely different approach to isolating the sheddase recognition domain which, by default, resides in the ectodomain.

When aligning the N- and C-domains of ACE isolated from different animals, we noticed that numerous amino acids are completely conserved across the different species and both domains, implying a conserved function. Clearly, the hydrolysis of angiotensin I is the most likely function. However, the possibility exists that some of the residues conserved in the C-domain, but not necessarily in the N-domain, are involved in sheddase recognition. I therefore swapped the C-domain of ACE for the N-domain, at the exactly equivalent position, in an attempt to knock out the sheddase recognition motif, while

preserving the tertiary structure and activity of the proximal ectodomain. Indeed, I found that the catalytic activity of the ACE N-domain was preserved, but the ACE-Ndom chimera was completely resistant to shedding. These results are given in Chapter 6 along with the first of many shorter swap-over mutants, which should narrow down the region and, eventually, the exact motif used by the ACE sheddase to recognise its substrate.

The discussion in Chapter 7 draws conclusions from the results of deletion, insertion and swap-over mutations in ACE described above, and offers my working hypothesis regarding the nature of the sheddases active on the surface of cells. All the abbreviations and reference tables, which are too large to add into the text, appear in Appendix I. The methods used in this thesis appear in Chapter 3 and Appendix II, while Appendix III contains the recipes for all reagents used and miscellaneous DNA, primer or protein sequences.

Chapter 1: Ectodomain Shedding

Cleavage Secretion of Ectoproteins

Cell-surface bound amphipathic proteins and receptors are attached to the membrane through hydrophobic anchors and are termed ectoproteins. These hydrophobic anchors can be covalently attached lipids (GPI-anchored proteins) or stretches of hydrophobic amino acids (integral membrane proteins). Ectoproteins define the phenotype of each cell and are involved in intercellular binding and communication, internalisation of nutrients, and proteolysis. The importance of a wide repertoire of ectoproteins in the evolutionary development of multicellular, vertebrate animals is illustrated by the direct relationship between the number of ectoprotein architectures (and transmembrane proteins) encoded in the genome and the complexity of the organism [Venter *et al.*, 2001; IHGSC, 2001].

Numerous membrane-bound ectoproteins have been found to occur in a soluble form, through proteolytic cleavage of their juxtamembrane stalk region [reviewed in Ehlers and Riordan, 1991; Ehlers *et al.*, 1996; Hooper *et al.*, 1997b; Rose-John and Heinrich, 1994]. Shedding affects a surprisingly wide range of ectoproteins including receptors, receptor ligands, cell adhesion molecules, leukocyte antigens, ectoenzymes, viral membrane proteins and others, with subsequent effects dependent on the substrate ectoproteins (see Fig. 1.1.1.1). These effects include rapidly releasing a cytokine ligand, thereby converting a localised signal to a systemic one (e.g. TNFα), or equally rapidly down-regulating the paracrine signal by cleaving off the target cells' surface receptors (e.g. TNFRI). The soluble receptor may also chelate the soluble ligand, thereby reducing the effective signal (e.g. GHBP), or even stimulate a new set of target cells through transactivation (e.g. IL-6R). Certain ectoenzymes may be down-regulated by cleavage from the membrane, thereby either increasing turnover, or reducing localised action (e.g. ACE). Localised intercellular interactions can also be modulated rapidly by cleaving off surface-bound ligands (e.g. Delta), or adhesion molecules (e.g. L-selectin).

Shedding is, by necessity, a tightly controlled process where alterations can have major pathological implications such as Alzheimer's disease and inflammation. The overriding features that distinguish this process from other proteolytic events are that: (1) the protease and substrate are both membrane-bound [Parvathy *et al.*, 1997; Ehlers *et al.*, 1991]; (2) cleavage occurs extracellularly at (or near) the cell surface [Rose-John and Heinrich, 1994]; (3) it is stimulated by activation of intracellular second messenger pathways such as the protein kinase C (PKC), and Ca^{2+} [Massague and Pandiella, 1993; Bosenberg *et al.*, 1993]; and (4) inhibited by hydroxamate-based inhibitors such as TAPI, Batimistat [Mohler *et al.*, 1994; Parvathy *et al.*, 1997]. A few interesting examples that illustrate the pathophysiological importance of ectodomain shedding are highlighted in Table 1.4.1, below.

The past decade has seen a plethora of publications appear in the literature examining the identity and characteristics of the sheddases. Although there is a wealth of information pertaining to the mechanism by which the sheddases recognise and cleave their substrate ectoproteins, consensus has not been reached regarding the exact requirements for shedding. The aim of this review is to introduce the data, and the controversy, surrounding sheddase recognition, and to briefly explain how mutations in angiotensin converting enzyme (ACE) have been used in an attempt to resolve this issue.

1.1) Characteristics of ectoproteins and shedding

1.1.1) Ectoprotein structure

The basic structure of ectoproteins is shown in Fig. 1.1.1.1. Most ectoproteins follow the classical secretory route in which they are extruded into the lumen of the endoplasmic reticulum (ER), transfered through the Golgi apparatus and exocytosed at the plasma membrane [for reviews see Scheele, 1988; Dalbey and Von Heijne, 1992; Wilkinson *et al.*, 1997; Keenan *et al.*, 2001]. The hydrophobic N-terminal signal peptide is recognised by the cytoplasmic signal recognition particle (SRP) immediately after translation [Keenan *et al.*, 2001], leading to co-translational extrusion into the lumen of the rough endoplasmic reticulum (RER) [Wilkinson *et al.*, 1997]. In the ER the signal peptidase removes the signal peptide [Dalbey and Von Heijne, 1992], releasing either a soluble ectoprotein (Fig. 1.1.1.1a), or the type I ectoprotein with its hydrophobic anchor tethering it to the membrane (Fig. 1.1.1.1b). Similarly, the GPI-linked protein precursors (Fig. 1.1.1.1d) and multiple membrane-spanning proteins (Fig. 1.1.1.1e) have outward-facing N-termini. Type II ectoproteins (Fig. 1.1.1.1c) escape cleavage by the signal peptidase, and are thus tethered to the membrane via their non-cleavable signal peptides, appearing on the cell surface with an extracellular carboxyl-terminus. Type III integral membrane proteins also span the plasma membrane, except that they have many more transmembrane regions (2 to 24), and are never released from the membrane in their entirety [Hooper *et al.*, 1997a]. Some, however, have large globular ectodomains that are shed (e.g. Thyroid Stimulating Hormone Receptor (TSHR), [Couet *et al.*, 1996]), while others are activated through cleavage and remain membrane associated (e.g. Presenilin 1 (PS1), [Levitan *et al.*, 2001]). GPI-linked proteins are modified in the ER, where the hydrophobic C-terminus is removed and the glycosylphosphatidylinositol (GPI) moiety covalently attached to the new C-terminal carbonate [Kendrew and others, 1995]. These proteins appear to accumulate into cholesterol-rich micro-domains on the cell surface called lipid rafts, as shown by Marcic *et al.* when they swapped the 3′ region of ACE with a GPI anchor signal [Marcic *et al.*, 2000b].

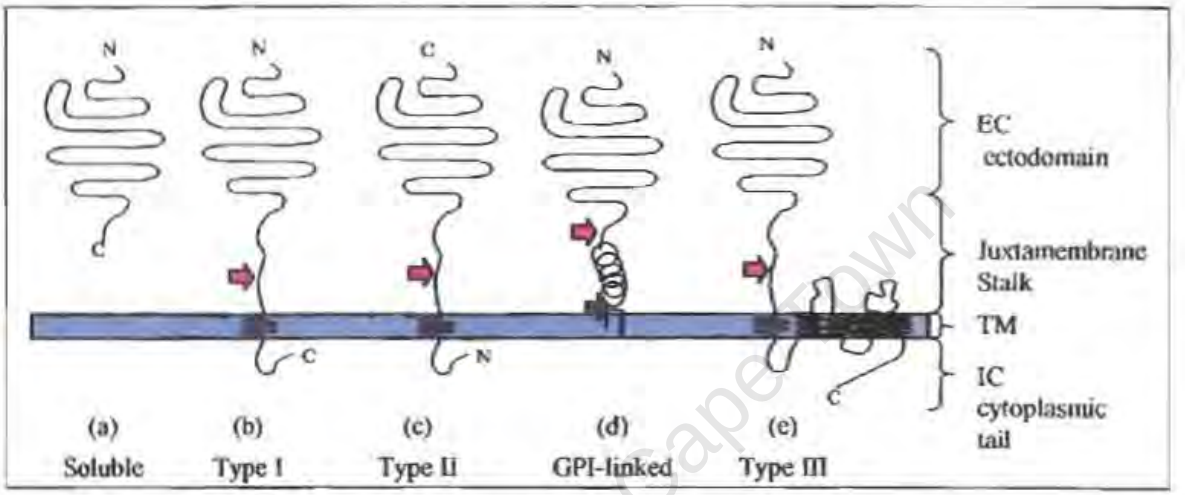

Figure 1.1.1.1) Types of ectoprotein topologies.

Ectoproteins are defined by their orientation in the plasma membrane. Type I, cleavable signal peptide and C-terminal TM; Type II, uncleaved signal peptide; Type III, cleavable signal peptide and multiple membrane-spanning transmembrane domains (2-24) [Ehlers, 1991; Hooper, 1997]. N, NH_2-terminus; C, COOH-terminus; GPI, glycosylphosphatidylinositol; TM, transmembrane; EC, extracellular; IC, intracellular; red arrows, proteolytic cleavage; black arrow, phospholipase C digestion; blue, plasma membrane.

Interestingly, the recent completion of the first draft sequence of the human genome by HUGO (Human Genome Organisation) [IHGSC, 2001] and Celera BioScience [Venter *et al.*, 2001] has made it possible to compare a vertebrate genome to that of invertebrates (fly and worm) and the unicellular eukaryotic yeast, which revealed that the human genome has approximately twice the number of ectoprotein architectures compared to that of the fly and worm genome respectively.

1.1.2) Ectodomain shedding

Soluble forms of membrane-bound proteins can be formed through alternative splicing, examples being IL-6R, CSF-1, NCAM and EGF-R (reviewed in Ehlers and Riordan, 1991 and Rose-John and Heinrich, 1994). However, it was noticed that other ectoproteins could be solubilized in a time- and temperature-dependent, post-translational manner through proteolytic cleavage, probably at the cell surface [Hooper *et al.*, 1987; Ehlers *et al.*, 1991], and that this cleavage-release can be inhibited by certain protease inhibitors, leading to the hypothesis that a protease is responsible for ectodomain shedding. Cleavage-release of ectoproteins was further investigated with the creation of chemically mutated CHO cells which were unable to shed TGF-α and numerous other ectoproteins from their cell surface [Arribas and Massague, 1995; Arribas *et al.*, 1996]. This work proved that the major solubilising activity was post-translational and occurred on the cell surface. It also showed that numerous different ectoproteins (TGF-α, TNFα, L-selectin, and ACE) use the same sheddase, or sheddase regulatory pathway.

Two groups independently cloned the first mammalian sheddase, TNFα converting enzyme (TACE), in 1997 [Black *et al.*, 1997; Moss *et al.*, 1997], with the crystal structure of the catalytic domain appearing only months later [Maskos *et al.*, 1998]. The domain structure of TACE identifies it as a member of the adamalysin/ADAM (A Disintegrin And Metalloprotease domain) family of proteases [for review see Black and White, 1998]. Analysis of the shedding capability (or lack thereof) of $TACE^{-/-}$ cells transfected with different membrane-bound ectoproteins proved that TACE is the major sheddase responsible for releasing a subset of ectoproteins (e.g. TNFα, TNFRI, L-selectin, TGF-α; [Peschon *et al.*, 1998]) but not all (e.g. ACE, L1,

syndecan1; [Sadhukhan *et al.*, 1999; Beer *et al.*, 1999; Fitzgerald *et al.*, 2000]). The sheddases probably constitute a family of similar proteases, each with broad specificities for differing substrate ectoproteins, but regulated through a similar pathway [Merlos-Suarez *et al.*, 1998].

Although all sheddases have not, as yet, been identified [Fitzgerald *et al.*, 2000; Beer *et al.*, 1999; de Bernard *et al.*, 1999; Sadhukhan *et al.*, 1999; Althoff *et al.*, 2000], one is still able to gain valuable information about their mode of action by examining their activation, inhibition and substrate specificity. Shedding usually occurs in the juxtamembrane stalk region of ectoproteins, between the proximal ectodomain and the transmembrane domain (Fig. 1.1.1.1), and has been comprehensively reviewed [Ehlers and Riordan, 1991; Ehlers *et al.*, 1996; Hooper *et al.*, 1997b; Rose-John and Heinrich, 1994]. These authors have found that shedding through limited proteolysis affects a wide range of ectoproteins, of all classes, as mentioned above. It has even been suggested that, during the evolution of eukaryotic cells, extracellular proteolysis was responsible for producing the first soluble forms of ectoproteins [Colman, 1991; Pandiella *et al.*, 1992].

Shedding allows for the rapid release of cytokines from a membrane bound pool, thus rapidly changing a localised signal into a systemic one (e.g. tumor necrosis factor α (TNFα), colony stimulating factor-1 (CSF-1); Fig. 1.1.2.1a). This may be useful physiologically when a very rapid secretion of a cytokine at high concentrations is needed, a criterion which cannot be fulfilled by *de novo* synthesis of an alternatively spliced product alone. Ectodomain shedding also allows a cell to rapidly down-regulate the surface expression of proteins, and thereby modulate its response to external stimuli (e.g. p55 TNFα receptor I (TNFRI), interleukin-6 receptor α (IL-6R); Fig. 1.1.2.1b). The stable expression of receptors is needed to ensure that target cells are primed for response to a cytokine ligand at all times. This same stability may be detrimental to the target cell that needs to down-regulate its response, especially when that response can be potentially disastrous for the organism, as in excessive inflammation [McDermott *et al.*, 1999].

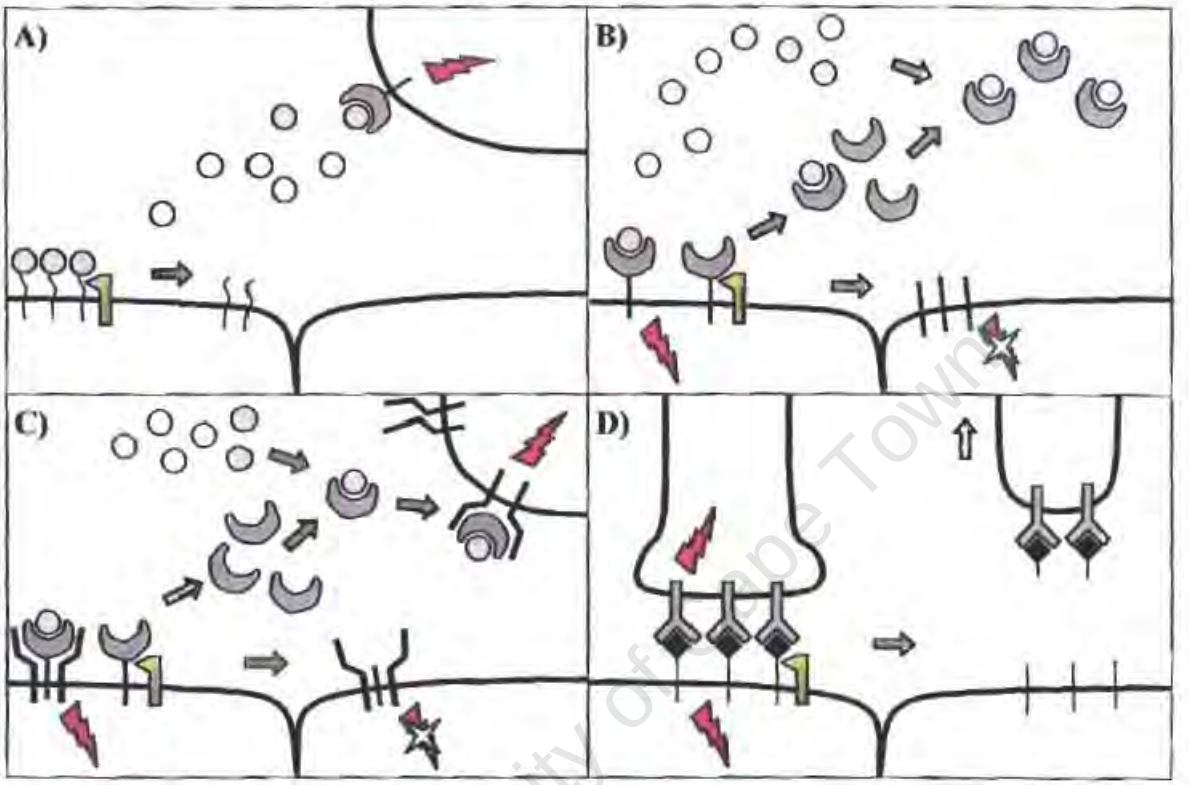

Figure 1.1.2.1) The various effects of ectodomain shedding

Membrane-bound cytokine precursors can be released rapidly into the bloodstream to create a systemic signal from a pool of cell-associated cytokine (A). Cleaving the receptors from the surface of cells can down regulate target cell stimulation resulting in soluble receptors that can then chelate unbound ligand (B). The soluble receptor/ligand complexes can further stimulate cells that do not express the receptor, called transactivation (C). Cell-cell contact recognition can result in repulsion by cleaving the membrane bound receptor or ligand (D). Curved thick lines indicate cell plasma membranes; the red lightning bolt indicates cell stimulation, while the sheddase is orange/green.

Soluble receptors may also chelate out their ligands in the blood, thereby either reducing the cytokine signal (e.g. TNFα), stabilise the cytokine (e.g. growth hormone binding protein {GHBP}, [Alele *et al.*, 1998]) or inducing trans-signalling in an otherwise unstimulated cell that does not express the receptor (e.g. IL-6R, [Rose-John and Heinrich, 1994]; Fig. 1.1.2.1c) .

Direct cell-cell contact recognition is mediated through ligand/receptor binding and activation. This tight binding of receptors and ligands creates a paradox when the interaction of these cells directs their repulsion from each other, as is the case in axon/axon repulsion (Fig. 1.1.2.1d). It has been shown that the ligand involved in this contact-induced repulsion, ephrin-A2, is proteolytically released from the surface of cells [Hattori *et al.*, 2000]. Similarly, L-selectin shedding from the surface of leukocytes may be important in limiting the aggregation of inflammatory cells at the site of infection, or releasing the cells after extrusion from the blood vessel [Walcheck *et al.*, 1996]. It has also been found that cancer cells shed their adhesion molecules, thereby allowing them to migrate [Kajita *et al.*, 2001].

Finding the exact location of the shedding activity in cells is not trivial. It could be due to a soluble protease, like trypsin, or a membrane-bound sheddase on a neighbouring cell with an affinity for accessible stalk regions. Alternatively, cleavage could occur anywhere in the secretory pathway, with exocytosis of the secretory vesicle releasing the soluble form. The rapid turnover of cell-surface membrane at steady state means that the early endosomes may be the site of cleavage of a rapidly recycling ectoprotein. Biotinylation, surface radioiodination and FITC labelling studies have shown that the shed forms of numerous shed ectoproteins were cell-surface derived [Ramchandran *et al.*, 1994; Haass *et al.*, 1992; Haass *et al.*, 1994; Sisodia, 1992]. Furthermore, cell-impermeant biotinylated forms of sheddase inhibitors have been used to show the surface localisation of α-secretase-like shedding of TNFα [Moss *et al.*, 1997] and β-APP [Parvathy *et al.*, 1999].

Ehlers *et al.* have further shown that the ACE-sheddase does not cleave the amphipathic form of ACE in solution, indicating that ACE needs to be inserted in a lipid bilayer for cleavage to occur [Ehlers *et al.*, 1996]. This was corroborated by

Parvarthy *et al,* who also showed that the ACE sheddase is itself an integral membrane protein [Parvathy *et al.*, 1997]. Furthermore, the requirement of an integral membrane sheddase for the cleavage of a membrane-bound substrate has also been shown in the shedding of β-APP [Sahasrabudhe *et al.*, 1992; Sisodia, 1992; Roberts *et al.*, 1994; Citron *et al.*, 1995], KL-1 [Cheng and Flanagan, 1994], TGF-α [Bosenberg *et al.*, 1993] as well as ACE [Oppong and Hooper, 1993; Ramchandran *et al.*, 1994; Ramchandran and Sen, 1995; Ehlers *et al.*, 1996; Parvathy *et al.*, 1997]. In support of this, Reddy *et al.* recently found that TACE needs its membrane-anchoring domain for PMA induced shedding of TNFα, p75 TNFRII and IL-1R-II [Reddy *et al.*, 2000]. Secretion of β-APP is unaltered in the presence of chloroquine, which neutralises acidic intracellular compartments, indicating that shedding is not due to partial degradation in the lysosome [Zhong *et al.*, 1994; Caporaso *et al.*, 1992; De Strooper *et al.*, 1995]. A cell-impermeable, biotinylated hydroxamate inhibitor was used to show that α-secretase cleavage of β-APP occurred at the cell-surface [Parvathy *et al.*, 1999].

1.1.3) Inhibition of ectodomain shedding

The sheddases are a unique group of proteases that are not inhibited by classical inhibitors of the aspartyl, cysteine or serine classes of protease, nor inhibitors of ACE, enkephalinase, endothelin converting enzyme or aminopeptidase [Oppong and Hooper, 1993; Mohler *et al.*, 1994; Gearing *et al.*, 1994]. Sheddases were instead found to be inhibited by the metal ion-chelating zinc-metalloprotease inhibitors 1,10-phenathroline and EDTA, and this inhibition could be reversed with the addition of $ZnCl_2$ [Oppong and Hooper, 1993; Mohler *et al.*, 1994; Arribas *et al.*, 1996].

Initially it was suggested that the sheddases were soluble matrix metalloproteases (MMPs) in the intercellular milieu that cleaved the stalk region of ectoproteins on the cell surface. Similarly, a membrane type MMP (MT-MMP) in the same, or even adjacent, plasma membrane might be responsible for shedding. However, studies using the 28-kDa glycoprotein tissue inhibitors of matrix metalloproteases (TIMPs) have shown that the sheddases are a separate class of protease. For instance, TIMP-2 inhibits MT1-MMP and MT2-MMP activity [Butler *et al.*, 1997], but has no effect on the shedding of TNFα [Gearing *et al.*, 1994] or syndecan-1 [Fitzgerald *et al.*, 2000]. Similarly, TIMP-3 inhibits the shedding of TNFα and L-selectin from human monocytes [Borland *et al.*, 1999], indicating that the metalloprotease sheddase(s) are distinct from the MMPs.

This started a frenzied search for specific zinc-metalloprotease inhibitors that could be used to inhibit the release of TNFα, particularly, as this has immediate potential as a treatment for inflammatory diseases such as arthritis. The first of these compounds that effectively block the processing of TNFα was compound 2 (TNFα protease inhibitor, TAPI) developed by Immunex, Inc., which caused a dose-dependent decrease in TNFα shedding from cells, protected mice from the lethal TNF-mediated response to injected endotoxin [Mohler *et al.*, 1994], and showed anti-inflammatory activity in animal arthritis models [McGeehan *et al.*, 1994]. Hydroxamic acid-based zinc-metalloprotease inhibitors (some of which are shown in Fig. 1.1.3.1c) have now been shown to block the cleavage-release of a wide range of ectoproteins, including

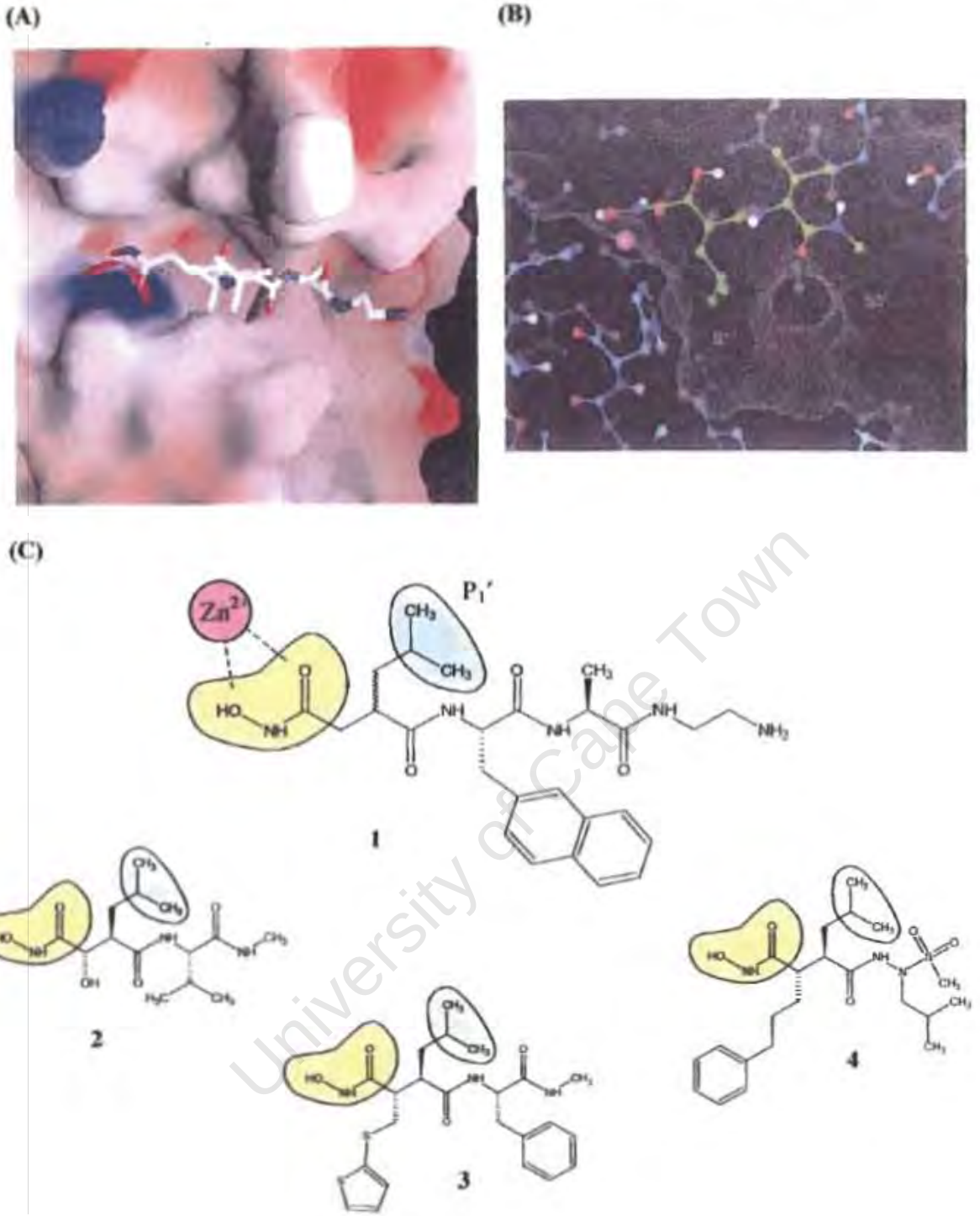

Figure 1.1.3.1) The Sheddase inhibitors

The 3D structure of the metalloprotease domain of TACE is shown in (A) (δ-, red; δ+, blue; [copied from Maskos *et al.*, 1998]). The inhibitor IC3 was cocrystallized and is seen buried in the catalytic cleft, with the hydroxamate bound to the zinc ion (pink). The column in (A), just right of centre, is seen as a hole in the perpendicular view shown in (B), which is a model of the binding of marimastat bound to TACE (H, white; O, red; N, blue; Zn^{2+}, magenta; inhibitor, green; [copied from Moss *et al.*, 2001]). Note the deep S_1' and S_3' pockets. The structures of sheddase inhibitors TAPI (IC2, **1**), marimastat (BB2516, **2**), batimastat (BB94, **3**), and Ro327315 (**4**) are shown in (C) [Moss *et al.*, 1997; see refs in Moss, *et al.*, 2001; Hooper *et al.*, 1997]. The zinc-binding hydroxamate group is highlighted in yellow, while the P_1' isobutyl group is highlighted in blue.

TNFα, APP, ACE, L-selectin, TGF-α, IL-6R, TNFRI and II [Parvathy *et al.*, 1997; Hooper *et al.*, 1997b; Arribas *et al.*, 1996]. The finding that TAPI is effective against the ACE sheddase [Parvathy *et al.*, 1997] allows us to use TAPI as a means of ensuring that the ACE shedding studied in this thesis is due to metalloprotease activity, and not a spurious artefact (apoptosis, bacterial infection, etc).

The refinement of these hydroxamate-based inhibitors for use against the TNFα sheddase culminated in the use of the biotinylated form of GW9471 (GW9277) to affinity-purify TACE [Moss *et al.*, 1997]. The isolation of TACE [Black *et al.*, 1997; Moss *et al.*, 1997], and the subsequent crystallisation and structural determination of the metalloprotease domain [Maskos *et al.*, 1998], has fundamentally changed the sheddase field, as one now has a 3D structure on which to model and refine potent inhibitors and future anti-inflammatory drugs [reviewed in Moss *et al.*, 2001]. For instance, the structures of similar zinc-metalloproteases (adamalysin II and matrix metalloprotease-3 {MMP-3}) were compared to that of TACE, facilitating the rational design of TACE-specific inhibitors that exploit subtle differences in structure [Maskos *et al.*, 1998].

The crystal structure of the TACE/Immunex compound 3 complex revealed that the inhibitor fits into a groove, with the hydroxamate 'head-group' (highlighted in yellow in Fig. 1.1.3.1c) binding the zinc ion (Fig. 1.1.3.1a). The structure therefore explained why numerous of the potent sheddase inhibitors have hydrophobic groups at the P_1' position (highlighted in blue in Fig. 1.1.3.1c), as this appeared to fit into the deep S_1' pocket of TACE (Fig. 1.1.3.1a, shown more clearly from 'below' in Fig. 1.1.3.1b). Clearly, the development of highly specific inhibitors to TACE [reviewed in Moss *et al.*, 2001] and the other sheddases is potentially of enormous value in the treatment of arthritis, inflammation, Alzheimer's disease and possibly even metastatic cancers. For instance, the compound Ro327315 (**4**; Fig. 1.1.3.1c), which inhibits both TACE (K_i = 3nM) and release of TNF from THP-1 cells (IC_{50} = 375 nM), has entered Phase I clinical trials [Moss *et al.*, 2001]. However, due to the broad range of substrates cleaved by each sheddase (e.g. the non-amyloidogenic cleavage of β-APP by TACE), it is clear that each sheddase will have to be inhibited in a substrate-specific fashion, else potentially fatal side-effects may occur, such as the development of Alzheimer's disease after an anti-inflammatory treatment with TACE inhibitors.

1.1.4) Cellular control of shedding

Numerous, diverse stimuli have been found to stimulate shedding, including the mitogenic activators of Ras and PKC, growth factors that activate either G-protein coupled receptors (GPCR) or receptor tyrosine kinases (RTK), unknown serum components and calcium ionophores (see Table 1.1.4.1).

Protein kinase C is a second messenger to G_q-protein coupled receptors (see Fig. 1.1.4.1). These receptors, once bound by their respective ligand, stimulate phospholipase C-β (PLC-β) hydrolysis of phosphatidylinositol 4,5-bisphosphate (PIP_2) and include the adrenergic, histamine, acetylcholine and vasopressin receptors [Kendrew and others, 1995]. This hydrolysis yields two products: water-soluble inositol 1,4,5-triphosphate (IP_3), and lipid-soluble 1,2-diacylglycerol (1,2-DAG). 1,2-DAG remains associated with the cytoplasmic surface of the plasma membrane, where it, binds to and activates PKC (in association with Ca^{2+}), initiating protein kinase cascades that culminate in the activation of mitogenic transcription factors NF-κB, cJun and Elk1 [Henkel *et al.*, 1993; Kendrew and others, 1995; Mudher *et al.*, 2001]. The tumorogenic phorbol esters, namely phorbol 12-myristate 13-acetate (PMA), 12-O-tetradecanoylphorbol-13-acetate (TPA) and phorbol-12,13-dibutyrate (PDBu), are analogues of 1,2-DAG and activate PKC-induced phosphorylation of serine or threonine residues in numerous target proteins. PKC stimulation induces ectodomain shedding both *in vitro* [Mullberg *et al.*, 1992; Ehlers *et al.*, 1995; Haass and Selkoe, 1993; Bosenberg *et al.*, 1993] and *in vivo* [Rossner *et al.*, 2000]. This response is, however, extremely rapid, occurring in minutes and does not involve *de novo* protein synthesis [Mullberg *et al.*, 1992] or cytosolic components [Bosenberg *et al.*, 1993], and therefore probably does not involve downstream components of the 'classical' PKC pathway. Direct phosphorylation of the sheddases' cytoplasmic regions by PKC, or another closely related kinase, may be the activating force in shedding [Walter *et al.*, 2001]. The phosphorylation of the cytoplasmic tail of the substrate ectoprotein may also be a signal for cleavage. However it has been shown by us (Chapter 5), and others [Brakebusch *et al.*, 1992; Mullberg *et al.*, 1994; Sadhukhan *et al.*, 1998], that the cytoplasmic tail can be deleted without adversely effecting ectodomain shedding of certain ectoproteins, but not all [Zhao *et al.*, 2001]. The

possibility remains that a cytoplasmic-tail-binding factor may be inhibited by PKC-stimulated phosphorylation, although this has not been shown.

Table 1.1.4.1) Stimuli that induce ectodomain shedding

Stimulus:	Type of stimulus:	Ectoprotein:	Cell line/tissue:	References:
Phorbol esters (PMA, TPA, PDBu)	PKC activator	All shed ectoproteins	Numerous	Reviewed in Ehlers *et al.*, 1996; Hooper *et al.*, 1997b; Schlondorff and Blobel, 1999; Rose-John and Heinrich, 1994
Receptor ligand(s)	Ligand binding to receptor	ErbB-4	NIH 3T3	Vecchi *et al.*, 1998
EGF	Growth factor, RTK	Syndecan-1/-4	SVEC4-10	Subramanian *et al.*, 1997
A23187	Calcium ionophore	HB-EGF	VSMC	Eguchi *et al.*, 2001
Serum factors	Growth factor, probably RTK	ACE, TGF-α	CHO	Ehlers *et al.*, 1995; Ehlers *et al.*, 1996; Fan and Derynck, 1999
Thrombin	Wound repair, GPCR	Syndecan-1/-4	SVEC4-10	Subramanian *et al.*, 1997
TRAP	14 aa thrombin R agonist	Syndecan-1/-4	NMuMG	Fitzgerald *et al.*, 2000
NGF	Growth factor, RTK	TrkA	PC12	Cabrera *et al.*, 1996
Cell attachment	Cell morphology, possibly through integrins, fyn & Src kinase	L1, HB-EGF	CHO	Beer *et al.*, 1999; Gutwein *et al.*, 2000; Gechtman *et al.*, 1999
Tissue damage	Ischemia/reperfusion	ACE	Lung endothelium	Atochina *et al.*, 1997
Hydrogen peroxide	PKC activator	TNFRI	A549	Hino *et al.*, 1999
Pervanadate	PTPase inhibitor	Amphiregulin, ErbB-4, L1, ACE	MDCK, CHO, NIH-3T3, AR, OVCAR-3, T47D, Kelly,	Vecchi *et al.*, 1998; Gutwein *et al.*, 2000; Santhamma and Sen, 2000
Phenylarsine oxide	PTPase inhibitor	ErbB-4	NIH-3T3	Vecchi *et al.*, 1998
Sodium salicylate	Apoptosis inducing toxin	TNFRI	HUVEC	Madge *et al.*, 1999
Staurosporine	Apoptosis inducing toxin	TNFRI	HUVEC	Madge *et al.*, 1999
C_6-ceramide	Apoptosis inducing toxin	TNFRI	HUVEC	Madge *et al.*, 1999
Arachidoyl trifluoromethylketone	Apoptosis inducing toxin	TNFRI	HUVEC	Madge *et al.*, 1999
LasA	virulence factor (*P. aeroginosa*)	Syndecan-1	NIH-3T3, C127, NMuMG, LA-4,	Park *et al.*, 2000
FMet-Leu-Phe	Peptide activator of p38 MAPK	L-selectin	neutrophils	Fan and Derynck, 1999
Ha-Ras^D	Oncogenic Ras > PI3K > Cdc42/Rac1 > shedding	CD44	CHO	Kawano *et al.*, 2000
Nitic oxide	Nitrosation of TACE prodomain	TNFα	macrophages	Zhang *et al.*, 2000c
C-reactive protein	Acute phase response protein	IL-6R	neutrophils	Jones *et al.*, 1999
Ethanol	Immunosuppressant	Inhibits TNFα	macrophages	Zhang *et al.*, 2000b
NEM	Not PKC or MAPK pathways	GHR	CHO, NIH-3T3	Guan *et al.*, 2001
TFP, W7, calmidazolium	Calmodulin inhibitors	TrkA, EGFR, β-APP, TGF-α, proNRGα2c	HEK-293, CHO, HeLa, PC12	Diaz-Rodriguez *et al.*, 2000; Kahn *et al.*, 1998

PTPase, Phosphotyrosine phosphatase; PKC, protein kinase C; LasA, virulence factor from Pseudomonas aeroginosa; HUVEC, human umbilical vein epithelial cell line; NIH-3T$_3$, Swiss mouse embryo fibroblasts; NmuMG, Normal murine mammary gland cells; VSMC, vascular smooth muscle cells; see Table AI.1.

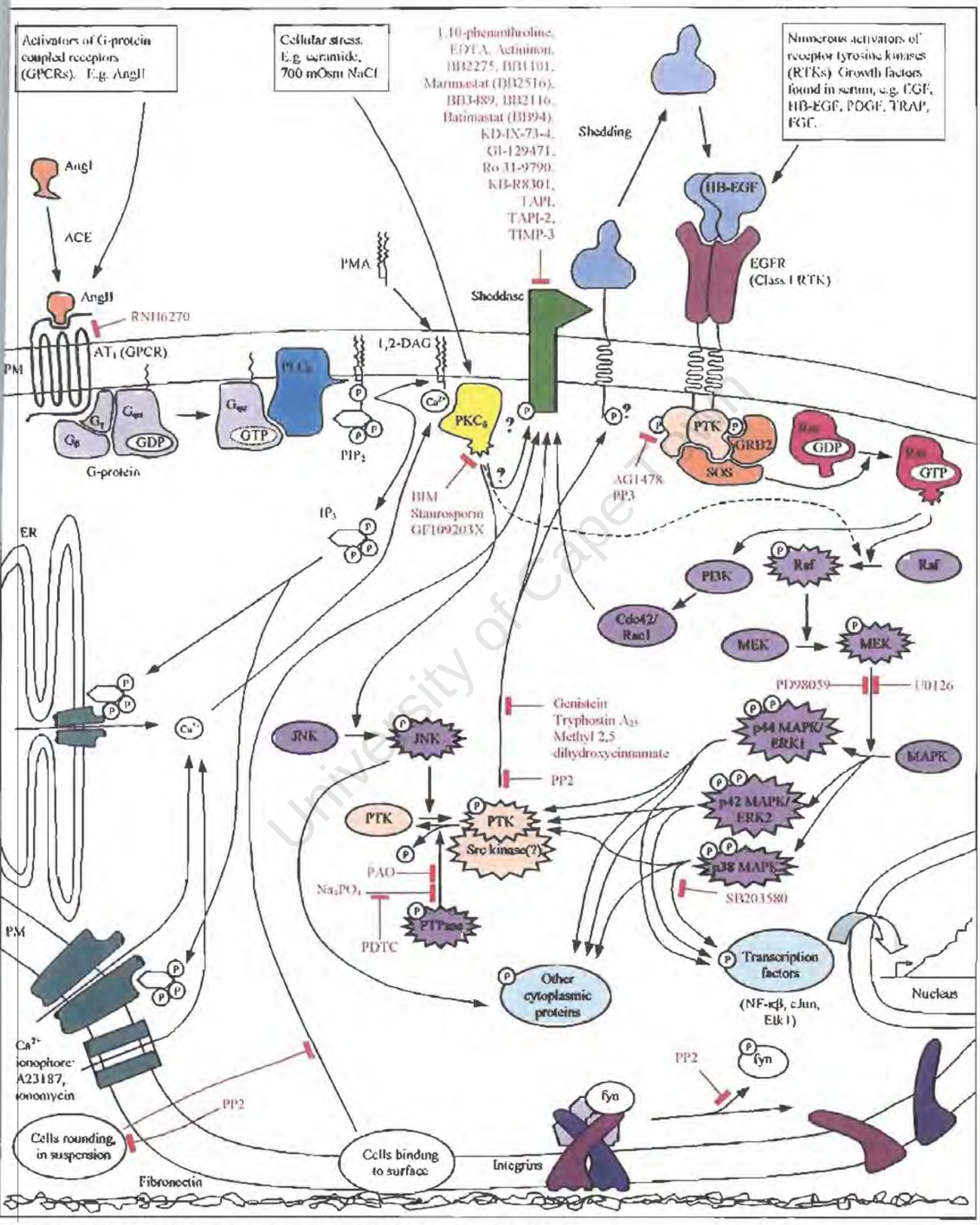

Figure 1.1.4.1) Signal transduction pathways and shedding (cont...)

Figure 1.1.4.1) Signal transduction pathways and shedding

The cartoon overleaf is an illustration of the numerous signal transduction pathways that control ectodomain shedding. As no recent review covers this section of the recent literature in adequate detail, and the characteristics of ectodomain shedding seem to be a cell- and substrate-specific phenomenon, consensus has not yet been reached. This cartoon is an attempt to extrapolate generalisations from limited studies, and should thus be viewed with utmost circumspection. In essence it attempts to connect cellular stimulation from ligands that activate either G-protein coupled receptors, and those that activate receptor tyrosine kinases, to the activation of sheddases (shown in lime green). The major components mentioned here, the 7-transmembrane GPCR, the PLC, the PKC, the sheddase, the RTK and the numerous kinases are all examples that have sibling components. Most importantly, for example, the sheddase is a generic for TACE/ADAM-17, Kuzbanian/ADAM-10, MDC9/ADAM-9, and other unidentified sheddases. Arrows indicate activation, while red, blocked, lines indicate inhibition. Abbreviations are found in Table AI.1. The MAPK pathways are shown in mauve, while PKC is yellow. References: Eguchi *et al.*, 2001; Fitzgerald *et al.*, 2000; Gechtman *et al.*, 1999; Gutwein *et al.*, 2000; Hamm, 2001; Carman and Benovic, 1998; Dong *et al.*, 1999; Jiao *et al.*, 1998; Bosenberg *et al.*, 1993; Walcheck *et al.*, 1996; Mudher *et al.*, 2001; Gebbink *et al.*, 1995; Marron *et al.*, 2000; Holsinger *et al.*, 1998; Kawano *et al.*, 2000; Naor *et al.*, 2000; Murga *et al.*, 1999; Denhardt, 1996; Hunter, 1997; Blobel, 2000; Darnell, 1995; and references in Table 1.1.4.1.

The soluble IP_3 activates ligand-gated Ca^{2+} channels at the ER that rapidly increase the cytoplasmic concentration of Ca^{2+}, which induces the active conformation of calmodulin and thereby glycogen breakdown, smooth muscle contraction and Ca^{2+} excretion from the cell, depending on cell type. Recently it has been shown that the shedding of L-selectin, TGF-α, pro-neuregulin-α2c (neu-α2c), receptor tyrosine kinase (TrkA) and β-APP is induced by calmodulin (CaM) inhibitors in a mechanism that is independent of PKC and Ca^{2+} and is inhibited by hydroxamic-acid based inhibitors [Diaz-Rodriguez *et al.*, 2000]. Calcium ionophores, which create a Ca^{2+} channel in the plasma membrane and an influx of Ca^{2+} ions, are also implicated in ectodomain shedding, although the exact mechanism is not known [Porteu and Nathan, 1990; Porteu and Hieblot, 1994].

Recent interest in understanding the cellular control of sheddases has focused on the mitogen-activated protein kinase (MAPK) cascades, as these enzymes represent one of the major signalling systems used by eukaryotic cells to transduce extracellular signals into cellular responses. These kinases phosphorylate numerous transcription factors, as well as cytosolic proteins, and therefore perform a myriad of rapid (minutes) and gradual (hours) responses, ranging from apoptosis to cell growth and differentiation. It has recently been found that ectodomain shedding is also controlled by MAPKs [Kawano *et al.*, 2000]. Four MAPK subgroups have been identified in humans: the extracellular signal-regulated kinases (ERKs), the c-Jun N-terminal kinases/stress-activated protein kinases (JNK/SAPKs), the ERK5/BMK protein, and the p38 MAP kinases. MAPKs are activated by dual-specificity MAPK kinases

(MAPKKs), also known as MEK (MAPK and ERK kinase) [Darnell, 1995]. To dissect the signalling pathway employed by cells to induce shedding, workers have activated cells with different stimuli (listed in Table 1.1.4.1), and monitored the accumulation of a particular ectoprotein in the culture medium over time. Specific inhibitors of the intracellular signalling pathways are then added, and their effect on stimulated shedding noted.

Classically, MAPKK-kinase (Raf), which is also activated by the oncogenic Ras, was thought to be one of the downstream targets of PKC activity (see dashed arrow in Fig. 1.1.4.1) [Darnell, 1995]. Recently, however, it has been shown that the activation of PKC through the G-protein coupled AngII type-1 receptor (AT_1) does not directly activate the MAPK cascade, but rather uses the ectodomain shedding of HB-EGF and HB-EGF/EGFR binding to transmit the signal to the receptor tyrosine kinase pathway [Prenzel *et al.*, 1999; Eguchi *et al.*, 2001]. This finding is complicated by the fact that the MAPKK (MEK) activity, and therefore ERK MAP kinase cascade activation (see Fig. 1.1.4.1), is needed for the PMA-induced shedding of HB-EGF [Gechtman *et al.*, 1999] and GHR [Guan *et al.*, 2001], and the growth factor-stimulated shedding of TGF-α [Fan and Derynck, 1999]. Fan and Derynck have further shown that constitutive activation of MEK and Erk2 MAPK stimulated the shedding of TGF-α, indicating that ERK MAP kinase stimulation is upstream of ectodomain shedding. They also show that basal (non-induced) shedding is due to p38 MAPK activation [Fan and Derynck, 1999].

Using inhibitors of PKC, MEK, and PTK, namely BIM, PD98059 and genistein respectively, Fitzgerald *et al.* were able to show that EGF-induced MAPK activation, and PMA, osmotic shock and ceramide-induced PKC activation, converge with the activation of a protein tyrosine kinase that activates shedding of syndecan-1 [Fitzgerald *et al.*, 2000]. Similarly, Nath *et al.* have recently shown that both EGF and lysophosphatidic acid (LPA, a GPCR agonist) stimulation can activate c-Met shedding via the ERK MAP kinase cascade [Nath *et al.*, 2001]. This correlates nicely with the finding that pervanadate (Na_3VO_4), a protein tyrosine phosphatase (PTPase) inhibitor activates shedding, probably by stabilising the activated form of the as-yet unidentified sheddase activator [Vecchi *et al.*, 1998; Gutwein *et al.*, 2000].

It is tempting to summarise the shedding activation pathways into two direct lines, namely [ligand > GPCR > PKC > JNK > sheddase] or [ligand > RTK > MAPKK > MAPK > sheddase], and that these may overlap [Eguchi *et al.*, 2001], namely [ligand > GPCR > PKC > JNK > sheddase > ligand > RTK > MAPKK > MAPK]. However, it has been found that inhibitors of MAPKK reduce PMA-induced shedding of GHR, TGF-α and HB-EGF [Guan *et al.*, 2001; Fan and Derynck, 1999; Gechtman *et al.*, 1999]. This implies that another pathway exists, namely [ligand > receptor > PKC > MAPK > sheddase]. The list of shedding stimuli in Table 1.1.4.1 also contains some that are PKC- and MAPK-independent (e.g. NEM), further implicating other pathways in the activation of ectodomain shedding.

1.2) The sheddases

At first it was not clear whether one sheddase, with extremely broad substrate specificity, was responsible for cleaving all shed ectoproteins, or each ectoprotein had its own highly specific sheddase. This confusion was partially resolved by Arribas *et al.*, when they chemically mutated CHO cells and created a sheddase-negative cell line (M2) that was unable to shed proTGF-α, β-APP, TNFα, IL-6R and L-selectin [Arribas and Massague, 1995]. This showed that numerous ectoproteins are shed either by a single protease or a family of sheddases controlled by a single pathway. The isolation of TACE (ADAM-17), and the creation of $TACE^{-/-}$ fibroblasts clarified this issue [Black *et al.*, 1997; Peschon *et al.*, 1998]. The $TACE^{-/-}$ fibroblasts did not shed TNFα, β-APP and numerous other ectoproteins. On the other hand, shedding of other ectoproteins (e.g., L1, Met, syndecan-1, TSHR and ACE) was not impaired in $TACE^{-/-}$ cells, indicating that there is probably a family of sheddases, each with broad substrate specificities, on the surface of cells. Fusion of these cells with the proTGF-α $sheddase^{-/-}$ M2 cells restored shedding, indicating that the gene knocked out in M2 codes for a vital regulatory protein that activates TACE and other sheddases, and that a single shedding pathway exists in cells [Merlos-Suarez *et al.*, 1998]. This is further corroborated by the finding that Kuzbanian (ADAM-10) sheds Delta and ephrin-A2 from the cell surface [Hattori *et al.*, 2000], and that MDC9 (ADAM-9) can cleave stalk-like substrate peptides that are also cleaved by TACE, but with differing characteristics [reviewed by Schlondorff and Blobel, 1999].

The ADAM family of ectoproteins is the most likely candidate group of proteases to perform the role of α-secretase-like shedding. ADAM family members all contain a disintegrin and a metalloprotease domain, in addition to other motifs [Black and White, 1998; Schlondorff and Blobel, 1999]. Of the 30 members, 14 have potentially functional zinc-metalloprotease domains, and three have been shown to be sheddases. BACE and PS1, the amyloidogenic β- and γ-secretases of β-APP respectively, are aspartyl proteases that function intercellularly or intramembranously, and are thus not 'classical' sheddases, even though they do release polypeptides from the membrane. They may, in future, be found to play an increasingly important role in normal physiology when their exact substrate profile is characterised.

1.2.1) TACE/ADAM-17 (α-secretase)

Tumour necrosis factor (TNFα/cachectin) is produced by macrophages, eosinophils and natural killer cells, and plays a pivotal role in inflammatory response to bacterial infection and tumours. The inflammatory effects of TNFα have been implicated in rheumatoid arthritis (RA), Crohn's disease, multiple sclerosis, and cancer- or HIV-associated cachexia [Vassalli, 1992].

The mature, soluble form of TNFα is a 17-kDa protein that is derived from the 26-kDa type II ectoprotein precursor (proTNFα) found on the surface of macrophages as a homo-trimer [Tang *et al.*, 1996a]. Soluble TNFα is released from the membrane through proteolytic cleavage by the TNFα converting enzyme (TACE). The pathophysiological importance of the excessive systemic inflammation implicated in sceptic shock, and the shedding activity responsible for releasing TNFα into the bloodstream, is most clearly illustrated in an experiment by Mohler *et al*, in which they showed that a specific inhibitor to TACE (compound 2) protected mice from a lethal dose of lipopolysaccharide (LPS) [Mohler *et al.*, 1994].

TACE was isolated and cloned by Black *et al.* and Moss *et al.* in 1997, making it the first confirmed sheddase to be cloned [Black *et al.*, 1997; Moss *et al.*, 1997]. Both groups used a soluble peptide that corresponded to the TNFα stalk region cleavage site as a substrate for TACE activity, but somewhat different methods for isolating TACE. The Black group purified the enzyme using cell fractionation, while the Moss group made use of affinity purification using a biotin-conjugated form of the TACE inhibitor TAPI.

TACE is a type I ectoprotein containing a signal peptide followed by a pro-domain that needs to be removed to activate the neighbouring metalloprotease domain, which is further followed by the disintegrin, EGF, Crambin, TM and cytosolic domains IT is thus a member of the ADAM family of proteases [for review see Black and White, 1998]. The ADAMs family includes the fertilins-α (ADAM-1) and -β (ADAM-2), MDC9 (ADAM-9), kuzbanian (ADAM-10), and metargidin (ADAM-15) which are involved in proteolysis, adhesion, signalling, and cell fusion. The crystal structure of

the catalytic domain of TACE revealed that it has the same zinc catalytic environment as the snake venom metalloproteinases (SVMP), clarifying TACE as a member of the adamalysin/ADAM proteases [Maskos *et al.*, 1998].

The creation of $TACE^{-/-}$ knockout mice mutants by Black *et al.* showed the profound effect ectodomain shedding has on the normal development of a vertebrate animal [Black *et al.*, 1997; Peschon *et al.*, 1998]. Most of the transgenic mice with a homozygous mutation in the metalloprotease domain ($tace^{\Delta Zn/\Delta Zn}$) died before or just after birth, establishing ectodomain shedding as a vital part of normal development. This effect of TACE goes beyond merely the release of TNFα, as transgenic mutant mice with either the TNFα, TNFRI or TNFRII genes removed are overtly normal. The $tace^{\Delta Zn/\Delta Zn}$ mice have open eyelids (due to failure of the normal fusion event at embryonic day 17.5), attenuated cornea formation, curly vibrissae (nasal hairs) and disorganised hair follicles. Epithelial cell maturation is also drastically affected in these mice, leading to disruption of functionality in the lung, intestine, thyroid, parathyroid, salivary gland, nonglandular stomach and placenta, contributing to rapid mortality. These dramatic effects were shown to be due to the reduction of cleavage-secretion of TGF-α secretion in $tace^{\Delta Zn/\Delta Zn}$ cells, thus implicating TACE in the ectodomain shedding of TGF-α and possibly also other growth factors necessary for normal development [Peschon *et al.*, 1998].

TACE not only cleaves TNFα, but also both receptors (p55 TNFRI and p75 TNFRII) that mediate the immuno-protective and/or potentially fatal inflammatory response initiated by TNFα [Peschon *et al.*, 1998; Reddy *et al.*, 2000]. The two TNFα receptors share 29.5% identity over 150 residues, but have different juxtamembrane stalk region lengths [Ehlers *et al.*, 1996], and are both poorly shed by $tace^{\Delta Zn/\Delta Zn}$ cells. The importance of TNFRI shedding is clearly illustrated by the findings of McDermott *et al.* in which they mapped the cause of the hereditary familial periodic fever (FPF) syndrome to single point mutations in the p55 TNFRI gene which reduce TNFRI shedding [McDermott *et al.*, 1999].

The range and diversity of ectoprotein substrates that are recognised and cleaved by TACE is surprising, and defines TACE as a major sheddase on the surface of cells.

The list of ectoproteins that are shed by TACE is ever increasing, and thus far includes TNFα, TGF-α, p75 TNFRI & L-selectin [Peschon *et al.*, 1998; Merlos-Suarez *et al.*, 1998; Condon *et al.*, 2001], β-APP [Buxbaum *et al.*, 1998]; p55 TNFRII & IL1-R-II [Reddy *et al.*, 2000], neuregulin-α2c [Montero *et al.*, 2000], HER4/ErbB4 receptor [Eisenberg *et al.*, 2000;Rio *et al.*, 2000], GHBP [Zhang *et al.*, 2000a], IL-6R [Althoff *et al.*, 2000], TRANCE [Lum *et al.*, 1999], CD30 [Hansen *et al.*, 2000] and CX3CL1 (fractalkine, [Garton *et al.*, 2001]).

Interestingly, however, an increasing number of ectoproteins are found to be shed by $TACE^{-/-}$ fibroblasts, such as L1 [Beer *et al.*, 1999], CD44 [Shi *et al.*, 2001], thyrotropin receptor (TSHR, [de Bernard *et al.*, 1999], hepatocyte growth factor receptor (Met, [Nath *et al.*, 2001]), syndecan-1 and –4 [Fitzgerald *et al.*, 2000] and testis ACE [Sadhukhan *et al.*, 1999], indicating that other, as yet unidentified, sheddases are responsible for the cleavage-release of these ectoproteins. In addition, Rose-John's laboratory showed that the PMA-inducible shedding of IL-6R was strongly reduced in $TACE^{-/-}$ knockout cells, but that the basal shedding was unaffected, indicating that another, unidentified, sheddase is active in the basal secretion of ectoproteins from cells [Althoff *et al.*, 2000]. Similarly, the basal shedding of β-APP is not abolished in $TACE^{-/-}$ cells [Buxbaum *et al.*, 1998]. A very recent publication from the Arribas laboratory shows that TGF-α is also shed by another, as yet unidentified, sheddase in $TACE^{-/-}$ knockout cells that were stimulated by the mercurial compound 4-aminophenylmercuric acetate (APMA) [Merlos-Suarez *et al.*, 2001].

1.2.2) Kuzbanian/ADAM-10

During neurogenesis, both neurons and nonneuronal cells are produced from a population of initially equivalent cells by first stimulating the cells with neuronal potential and later using lateral inhibition to ensure that only one cell differentiates into a neuron. The *kuzbanian* (*kuz*) gene, a member of the ADAM family, was found in a *Drosophila melanogaster* screen for mutations in lateral inhibition [Rooke *et al.*, 1996]. The human homologue of kuzbanian, ADAM10, was found to efficiently

cleave a TNFα stalk peptide [Rosendahl *et al.*, 1997]. Initially, kuz/ADAM10 was thought to cleave the Notch receptor because of the similarities between the *kuz* and *Notch* knockout phenotypes [Nye, 1997]. This was found not to be the case by Qi *et al.* when they co-transfected a dominant negative form of Kuz (KuzDN) into cells with either Notch or Delta. KuzDN had an inhibitory effect on the shedding of Delta, but not Notch, indicating that Kuz cleaves the ligand, and not the receptor, responsible for lateral inhibition [Qi *et al.*, 1999].

Controversy also surrounds the identity of the β-APP α-secretase. Although Buxbaum *et al.* have shown that the PMA-induced shedding of β-APP is abolished in TACE $^{-/-}$ cells [Buxbaum *et al.*, 1998], Parvathy *et al.* showed that the inhibitor profiles of the α-secretase and that of ACE secretase are distinct from TACE [Parvathy *et al.*, 1998]. Lammich *et al.* have subsequently shown that Kuz/ADAM-10, like TACE, also shows α-secretase activity; peptides spanning the cleavage site of β-APP were cleaved and a dominant negative form of ADAM-10 decreased the PMA-induced shedding of β-APP [Lammich *et al.*, 1999].

Hattori *et al.* have identified the first sheddase recognition motif in the ectodomain of a surface-bound ectoprotein [Hattori *et al.*, 2000]. In an impressive investigation into axon repulsion, these authors unravelled the paradoxical tight-binding ligand-receptor interactions that lead to axon repulsion (Fig. 1.1.2.1d), an integral part of the dynamic process in which embryonic axons explore their environment. The growth cones of axons express the EphA3 receptors, which bind to the GPI-linked ephrin-A2 found on the surface of neighbouring axons. EphA3/ephrin-A2 binding stimulates the shedding of ephrin-A2 by ADAM10/Kuzbanian, which is already primed for action in a stable complex with ephrin-A2 [Hattori *et al.*, 2000]. The authors show that ephrin-A2 is not shed when bound to free EphA3 receptor, or when the ephrin-A2 ligand is clustered using antibodies, but only when clustered receptors bind to ephrin-A2, suggesting that Kuz has a bivalent activation mechanism. Also, this activation could be simulated by a peptide coding for the ephrin-A2 ectodomain region containing the consensus sheddase recognition domain KFEIKFQEFV. Interestingly, it was found that Kuz co-precipitates with ephrin-A2, and that this binding is dependent on the ectodomain of ephrin-A2. A chimera containing the juxtamembrane stalk region is not shed, and the

KuzDN (which lacks the protease domain) binds to ephrin-A2, strongly suggesting that Kuz binds the ephrin-A2 ectodomain in a region outside its active site [Hattori *et al.*, 2000].

1.2.3) MDC9/ADAM-9

MDC9/ADAM-9/Metargidin/Meltrin-γ was cloned well before TACE [Kratzschmar *et al.*, 1996], although its sheddase capability was only confirmed after it was found that mutant MDC9 proteins lacking a functional metalloprotease domain suppressed the shedding of HB-EGF from the cell surface [Izumi *et al.*, 1998]. This ADAM is also likely to have different substrate preferences from TACE, as it cleaves a soluble TNFα stalk peptide at different bonds, and has a different sheddase-inhibitor profile from that of TACE [Roghani *et al.*, 1999]. Interestingly, the cytoplasmic tail of MDC9 has proline-rich regions that have been shown to bind the Src homology 3 (SH3) domain of Src [Weskamp *et al.*, 1996] and the SH3 domain-containing proteins endophilin I and SH3PX1 [Howard *et al.*, 1999], suggesting a role for the cytoplasmic domain regulation.

Only 15 of the 30 members of the ADAM family of disintegrin metalloproteases have potentially functional metalloprotease domains, as judged from the cDNA sequence [Primakoff and Myles, 2000]. Of these three have been shown to have sheddase activity, namely MDC9/ADAM-9 [Izumi *et al.*, 1998; Roghani *et al.*, 1999], Kuz/ADAM-10 [Qi *et al.*, 1999] and TACE/ADAM-17 [Black *et al.*, 1997; Moss *et al.*, 1997]. This suggests that ADAM proteases are good candidates for the family of sheddases, possibly using their disintegrin domain to bind to substrate ectoproteins prior to cleavage [reviewed in Black and White, 1998; Primakoff and Myles, 2000].

1.3) Alzheimer's disease: A Complex Case of Shedding

Alzheimer's disease (AD), discovered by Alois Alzheimer in 1907, is the most common form of senile dementia, affecting more than 10% of the population over the age of 65 years [Sisodia *et al.*, 1990]. It is associated with aggregates of the 42-amino acid amyloid β-peptide (Aβ), and intracellular neurofibrillary tangles composed of tau. The Aβ peptide was isolated, and found to originate from the stalk and transmembrane region of a large, ubiquitously expressed, ectoprotein called β-Amyloid Precursor Protein (β-APP) [Glenner and Wong, 1984; Kang *et al.*, 1987]. The neurotoxic Aβ peptide arises from cleavage of β-APP at both ends of this peptide, at the β- and γ-secretase sites (Fig. 1.3.1), and has been shown to produce memory defects in mice [McDonald *et al.*, 1994; Sisodia and Gallagher, 1998]. Cleavage at the α-secretase site, in the middle of the Aβ peptide, abolishes the substrate for the amyloidogenic β- and γ-secretases, releasing the soluble β-APP$^{s\alpha}$. β-APP that survives cleavage by the α-secretase (on the cell surface), is internalised and cleaved by the β- and subsequently γ-secretases, releasing the soluble Aβ peptide which then spontaneously aggregates in the brain, causing Alzheimer's disease [reviewed in Selkoe, 1991; Hooper *et al.*, 1997b; Ray *et al.*, 1998; Selkoe, 1998].

1.3.1) α-Secretase (TACE and/or ADAM-10)

The normal processing of APP is through cleavage by the PKC-inducible α-secretase after Lys^{16} (numbering from the N-terminus of Aβ) [Seubert *et al.*, 1992]. This soluble form of β-APP is, paradoxically, thought to have memory-enhancing effects. Mice injected intracerebroventricularly with extremely low doses of APP$^{s\alpha}$ were shown to have improved memory [Meziane *et al.*, 1998], while very low levels of APP due to targeted gene disruption [Muller *et al.*, 1994], or high levels due to over-expression [Hsiao *et al.*, 1995], lead to memory deficits in mice. Buxbaum *et al.* showed that TACE/ADAM17 is the α-secretase [Buxbaum *et al.*, 1998], while Lammich *et al.* found that the mammalian form of *Drosophila* Kuzbanian (ADAM-10) also has α-secretase activity [Lammich *et al.*, 1999], illustrating that the ADAM

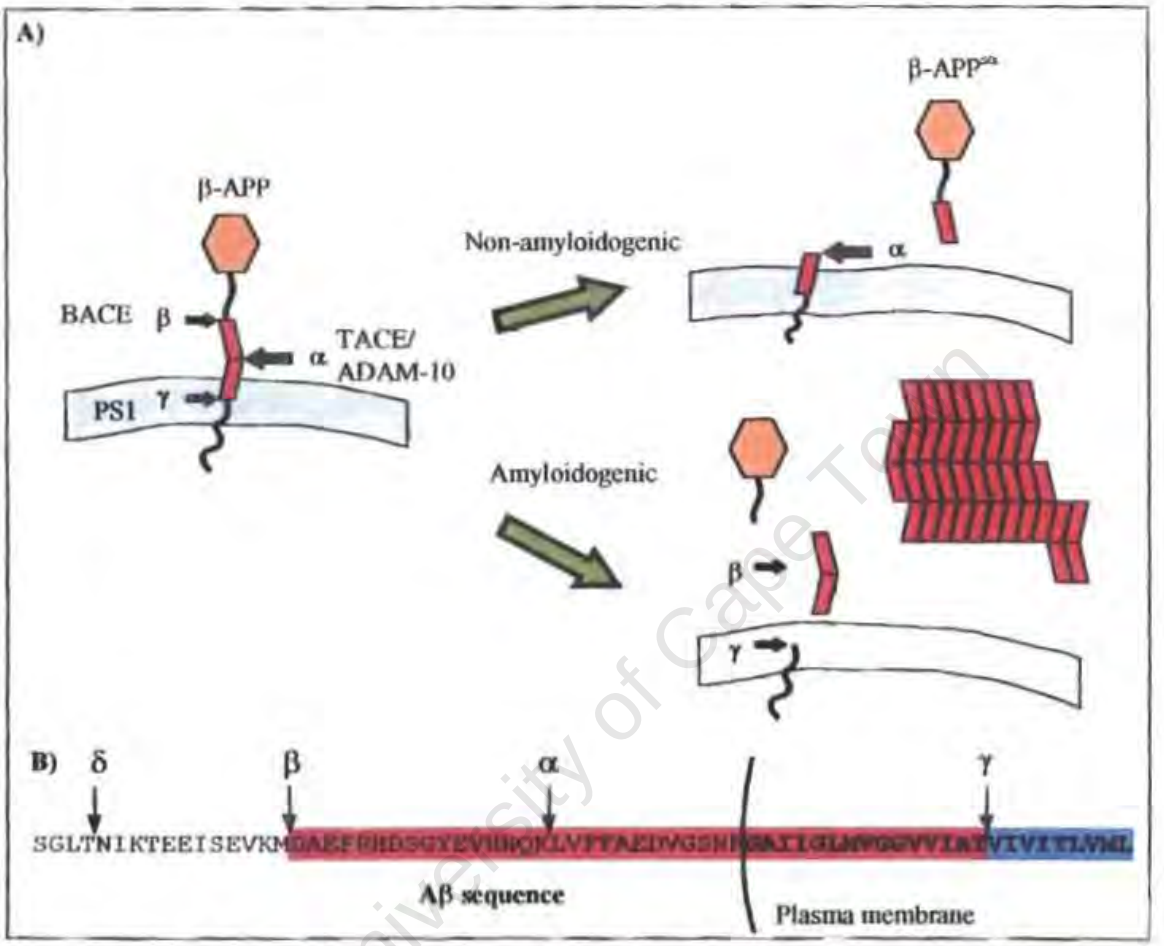

Figure 1.3.1) Schematic representation of APP degradation and Alzheimer's disease

β-APP is cleaved by either the non-amyloidogenic (α-secretase) or amyloidogenic (β-/γ-secretase) pathway, which releases the neurotoxic Aβ peptide that causes Alzheimer's disease (A). The sequence of the β-APP stalk and TM regions is shown in (B), copied from [Hooper *et al.*, 1997]. The α-, β-, γ-, and δ-secretase cleavage sites are indicated by arrows. Intramembranous hydrophobic amino acids are indicated in bold, while the Aβ peptide sequence is highlighted in red. TACE, TNFα convertase; BACE, βAPP converting enzyme (β-secretase); PS1, presenilin 1. α-secretase, [Lammich 1999; Buxbaum *et al.*, 1998]; β-secretase, [Hussain *et al.*, 1999; Yan *et al.*, 1999; Vassar *et al.*, 1999; Sinha *et al.*, 1999]; γ-secretase, [Li *et al.*, 2000; Esler *et al.*, 2000].

family of ectoenzymes may have broad, overlapping specificities for different ectoproteins. Recently it has been shown that the $PKC_{\alpha}/PKC_{\beta I}$ isoforms of PKC mediate the α-secretase cleavage of β-APP in guinea pigs [Rossner *et al.*, 2001].

1.3.2) β-Secretase (BACE)

Cell-surface bound β-APP that escaped α-secretase cleavage is susceptible to the amyloidogenic β/γ-secretase pathway. It is internalised, digested by the β-secretase in the early endosomes, leaving a short membrane-bound stalk, which is then cleaved at the cytoplasmic side of the TM by the γ-secretase, thus releasing the 40-42 amino acid Aβ peptide [Haass and Selkoe, 1993]. The β-secretase, or β-secretase converting enzyme (BACE) was cloned by four groups in 1999 [Hussain *et al.*, 1999; Yan *et al.*, 1999; Vassar *et al.*, 1999; Sinha *et al.*, 1999]. BACE, although technically effective in releasing the ectodomain of APP, differs remarkably from the 'classical' sheddase, in that cleavage occurs intracellularly in the early endosomes and the catalytic action is characteristic of an aspartyl protease, while most sheddases are metalloproteases.

The development of an effective and highly specific inhibitor of BACE is the holy grail of the Alzheimer's disease field. It will be an extremely effective cure, which could have enormous therapeutic applications providing that β-APP is its only target. Unfortunately, this has already been shown not to be the case, as BACE cleaves the Golgi apparatus sialyltransferase ST6Gal I [Kitazume *et al.*, 2001]. The relative toxicity of future BACE inhibitors will be dictated by the physiological importance of this, and possibly other, processing by BACE. In the interim, however, immunization against the Aβ peptide has been shown to decrease the plaque load in mice brain [Schenk *et al.*, 1999], and may be developed as a curative measure.

1.3.3) γ-Secretase (PS1/PS2)

About 10% of Alzheimer's disease cases are familial, involving single gene mutations that are autosomal dominant. Many of these mutations have been characterised, and found to reside in one of three genes, namely β-APP, presenilin 1 (*PS1*) and the

homologous presenilin 2 (*PS2*). The connection between mutations in β-APP and Alzheimer's is clear, as they either favoured shedding by the β-secretase (and thus the amyloidogenic pathway), or increased the length of the Aβ peptide (thereby creating a peptide that is particularly prone to aggregation). However, the role of the *PS1* and *PS2* genes, implicated in AD by genetic analysis, was less easy to unravel, as these genes had no known function or homology to known enzymes.

The finding that missense mutations in the *PS1* and *PS2* genes affect γ-secretase activity (by increasing the length of Aβ) did not necessarily imply that the presenilins are the γ-secretase [Sherrington *et al.*, 1995]. The fact that the presenilins are hydrophobic proteins with 6-8 transmembrane regions and no homology to any known proteases, made it extremely difficult to prove categorically that they are in fact the γ-secretase, and not merely involved in activating the real γ-secretase. A similar argument was used to question the conclusions of De Strooper *et al.* when they found that γ-secretase cleavage of β-APP was significantly reduced in $PS^{-/-}$ knockout mice, an experiment that is usually definitive [De Strooper *et al.*, 1998]. More compelling evidence was presented in 1999, when it was shown that two transmembrane aspartate residues in presenilin-1 are required for γ-secretase activity [Wolfe *et al.*, 1999], and γ-secretase-like protease releases the cytoplasmic tail of Notch [De Strooper *et al.*, 1999]. Li, *et al.* and Esler, *et al.* independently showed that the presenilins could be cross-linked to transition-state-specific inhibitors of the γ-secretase, demonstrating that PS1 and PS2 either are the γ-secretase or are very tightly associated with the real protease [Li *et al.*, 2000; Esler *et al.*, 2000], thereby finally putting the controversy to rest.

The mode of action of γ-secretase is intriguing in that it cleaves the substrate (β-secretase-cleaved β-APP membrane-bound remnant) intramembranously, apparently by means of two aspartate residues, one from either fragment of the cleaved, activated presenilin [Wolfe *et al.*, 1999]. This intramembranous cleavage releases the Aβ peptide from the extracellular surface, into the interstitial fluid of the brain where it spontaneously aggregates [reviewed in Hardy, 1997; Haass and Selkoe, 1998; Wolfe and Haass, 2001].

Interestingly, PS1 has also been implicated in cleavage of the cytoplasmic tail of the activated Notch receptor, releasing a nuclear signalling molecule [Struhl and Greenwald, 1999; De Strooper *et al.*, 1999]. This is a vital step in Notch-mediated lateral inhibition and thus neuronal development [Nye, 1997; Ye *et al.*, 1999]. PS1 may also process Ire1, which controls the unfolded-protein stress response [Katayama *et al.*, 1999].

It is curious to note that, although ACE is used as a model system in this thesis, it has also been found, very recently, to significantly inhibit aggregation, deposition and cytotoxicity of Aβ [Hu *et al.*, 2001] and thus may well play a pivotal role in Alzheimer's disease. The ACE gene contains an insertion/deletion (I/D) polymorphism in intron 16 (involving 287 bp), in which the DD genotype is associated with elevated levels of ACE in serum and an increased risk of heart disease [Rigat *et al.*, 1990; Zee *et al.*, 1992]. Hu *et al.* had previously noted a direct correlation in the Japanese population between the II genotype and sporadic Alzheimer's disease [Hu *et al.*, 1999]. They then discovered that ACE cleaves the Aβ peptide in a lisinopril-inhibitable fashion, at the D_7-S_8 bond, which is uncharacteristic for the dipeptidyl carboxypeptidase ACE. ACE has, however, been shown to cleave the L_7-R_8 bond of luteinizing hormone releasing hormone (LH-RH), three amino acids from the C-terminus [Skidgel and Erdos, 1985]. Thus, this data opens the possibility that ACE may act not only as a dipeptidyl carboxypeptidase, but also as an endopeptidase.

As ACE is widely expressed in the brain [Chai *et al.*, 1990], it is tempting to speculate that the net effect of a progressive decline in α-secretase cleavage of β-APP with aging, combined with a possible simultaneous decrease in ACE shedding and/or activity, may push the flux of Aβ production and degradation over a manageable threshold resulting in the spontaneous aggregation in aging brains. Clearly this needs to be proven, but alludes to the increasing importance in the shedding of ACE, above that noted for kidney development and fertility in Chapter 2.

1.4) Physiological importance of ectodomain shedding

The activities of the substrate ectoprotein, and that of its soluble form, define the physiological significance of shedding. The plethora of shed ectoproteins, and their respective actions in normal and pathophysiology are far too broad to mention in detail in this review. Table 1.4.1, however, briefly illustrates the diversity of diseases and physiological effects that ectodomain shedding has in the body.

Table 1.4.1) Examples of the physiological importance of ectodomain shedding

Disease/ activity:	Ectoprotein:	Role of shedding:	References:
Inflammation, Rheumatoid Arthritis, Toxic Shock	TNFα, TNFRI, TNFRII, ICAM-1	Soluble TNFα, shed from T_H1 CD4 T-cells and macrophages by TACE, induces inflammation at the sites of bacterial invasion. The receptors are down-regulated through shedding. Excessive activation leads to inflammatory diseases like arthritis and toxic shock.	Black *et al.*, 1997; Moss *et al.*, 1997; Nielsen *et al.*, 1994
Alzheimer's Disease	β-APP	Relative defect in true shedding (α-secretase) of APP and relative or absolute overactivity of β- and γ-secretase activities leads to Aβ peptide aggregation in the brain, causing fatal Alzheimer's disease.	Selkoe, 1998; Sisodia and Gallagher, 1998; De Strooper and Konig, 1999; De Strooper, 2000;
Neuro-development	Ephrin-A2, Notch, Delta	Ephrin-A2 is shed by Kuz/ADAM-10, after binding to Eph3 receptor, during axon/axon repulsion. Notch signalling to Delta induces lateral inhibition during the differentiation of neurons from epithelial cells. Kuz cleaves Delta and/or Notch. Cleaved Notch is cut by PS1 – releases cytoplasmic tail as transcription factor.	Pan and Rubin, 1997; Hattori *et al.*, 2000; Qi *et al.*, 1999
Apoptosis	E-cadherin, FasL, TNFα	Unknown.	Steinhusen *et al.*, 2001
Haematopoiesis/ Cell growth	TRANCE, GHBP, IL-6R, GHR	Soluble IL6/IL-6R complexes can stimulate cell growth in cells that do not express gp130 through transactivation. Soluble GHR/GHBP stabilises GH.	Guan *et al.*, 2001; Fischer *et al.*, 1997; Lum *et al.*, 1999;
Cell motility	L-selectin, CD44, ICAM1, VCAM1, Syndecan-1	L-selectin shedding may reduce neutrophil load at the site of inflammation, or release neutrophils post extrusion.	Walcheck *et al.*, 1996
Cancer	Syndecan-1, CD44, L1.	Ras activation has been shown to up regulate the shedding of adhesion molecules, allowing cells to migrate, leading to metastasis.	Gutwein *et al.*, 2000; Alpaugh *et al.*, 2000; Bayer-Garner *et al.*, 2001
Influenza	HA	Influenza virus hemagglutinin cleavage is needed for viral replication. Stalk region glycosylation affects shedding.	Kawaoka and Webster, 1989
Kidney development	Somatic ACE	$ACE^{-/-}$ knockout mice have major structural abnormalities in the kidneys, which cannot be rescued by a soluble N-domain.	Krege *et al.*, 1995; Esther *et al.*, 1997

This table highlights diseases or physiological activities in which the ectodomain shedding plays a role. Abbreviations can be found in Appendix I (Table AI.1).

1.5) Finding the sheddase recognition domain

Future generations of sheddase inhibitors will have to be designed such that they specifically inhibit the shedding of a particular ectoprotein. The lack of specificity of sheddase inhibitors, like TAPI, is their downfall in terms of pharmacological usefulness. Although TAPI has been shown to reduce inflammation in mouse models of toxic shock [Mohler *et al.*, 1994], the inhibition of TACE (and therefore the β-APP α-secretase), may increase the likelihood of an amyloidogenic cleavage of β-APP, and thus Alzheimer's disease. Similarly, it would cause devastating defects in developing embryos, as shown with $TACE^{-/-}$ knockout mice [Peschon *et al.*, 1998]. It is therefore imperative that sheddase inhibitors be uniquely tailored to the exact ectoprotein/sheddase interaction one wishes to inhibit. A useful drug target would therefore be the exact region of the ectoprotein that is specifically recognised by the sheddase.

The most likely region for the sheddase to recognise its substrate ectoprotein is at or near the cleavage site. After comparing the amino acid sequences of the cleavage sites of numerous ectoproteins (listed in Table 1.5.1), it was concluded that no consensus sequence could be found [Hooper *et al.*, 1997b; Ehlers *et al.*, 1996; Rose-John and Heinrich, 1994].

This finding is somewhat surprising, as most proteases are restricted in their cleavage-site specificity [Tyndall and Fairlie, 1999]. Table 1.5.1 also illustrates the variation in distance between the cleavage site and the transmembrane domain. Ehlers *et al.* found, when comparing the stalk regions of different shed ectoproteins, that the stalk needs to be at least 11 amino acids long, with shedding generally occurring at least 8 amino acids from the TM, and 3 residues away from the proximal ectodomain [Ehlers *et al.*, 1996]. Another criterion is that the stalk region should be accessible to the sheddase and unhindered by glycosylation or any tertiary structures such as EGF, Sushi or fibronectin domains [Althoff *et al.*, 2001; Schwager *et al.*, 1998; Ehlers *et al.*, 1996; also see Table AI.2].

Table 1.5.1) Sheddase cleavage sites				
Ectoprotein:	**Cleavage site (...P_1/P_1'...)*:**	**Distance from TM:**	**Sheddase:**	**References:**
Type I				
ACE_S & ACE_T (human, rabbit, pig)	PNSAR↓SEGSL	24	Metallo-, Not TACE	Ehlers *et al.*, 1996
ACE-JMΔ24	PNSAR↓VGQWL	0	Metallo-	Ehlers *et al.*, 1996
ACE-JMΔ6	GRVSF↓LGLDL	24	Metallo-	Schwager *et al.*, 1999
ACE-JMLDL	NSHQA↓LG↓DVAGR	17/15	Metallo-	Ehlers *et al.*, 1996
ACE-JMJGL	TSSQA↓TTSSQ	14	Metallo- /serine	Schwager *et al.*, 1999
ACE-JMEGF	LCPDG↓FQLVA	12	Metallo-	Schwager *et al.*, 1998
ACE-JMfIX	YNWTP↓NSDGD	40	Serine	Schwager SLU, in press
ACE-JMmin23	TPNSL↓MRCKQ	22	Metallo-	Schwager SLU, in press
TNFRI	PQIEN↓VK↓GTEDS	10/8	TACE	Nophar *et al.*, 1990
TNFRII	APGAV↓HLPQP	43	TACE	Nophar *et al.*, 1990
L-selectin	QKLDK↓SFSMI	11	TACE	Kahn *et al.*, 1994
TGF-α	ADLLA↓VVAAS	9	TACE	Derynck *et al.*, 1984
IL-6R	SLAVQ↓DSSSV	1 (or 4)	TACE?	Mullberg *et al.*, 1994
Folate receptor	EEVA↓R↓F↓YAAA	~11	Metallo-	Elwood *et al.*, 1991
Amphiregulin	RCGEK↓SMKTH	14	Metallo-	Plowman *et al.*, 1992; Brown *et al.*, 1998; Vecchi *et al.*, 1998
EGF	WWELR↓HAGHG	9	Metallo-	Bell *et al.*, 1986; Dempsey *et al.*, 1997
HB-EGF	GLSLP↓VENRL	11	MDC9	Goishi *et al.*, 1995; Izumi *et al.*, 1998
β-APP α-secretase	VHHQK↓LVFFA	12	TACE/ ADAM-10	Esch *et al.*, 1990; Maruyama *et al.*, 1991
β-APPΔR601-D619	EEISE↓VKMDA	12	Metallo-?	Maruyama *et al.*, 1991
β-APPΔL613-F616	DSGYE↓VH↓HQKAE	13/11	Metallo-?	Zhong *et al.*, 1994
β-APPΔL613-E618	GYEVH↓HQKDV	9	Metallo-?	Zhong *et al.*, 1994
β-APP β-secretase	SEVKM↓DAEFR	28	BACE	Masters *et al.*, 1985
β-APP γ-secretase	VGGVV↓IATVI	-12	PS1/PS2	Roher *et al.*, 1993
CSF-1	RQSEG↓S↓SPQLQE	8/7	Metallo	Halenbeck *et al.*, 1988; Deng *et al.*, 1996
KL-1	LPPVA↓ASSLR	25	Serine?	Huang *et al.*, 1990; Williams *et al.*, 1990
Type II				
TNFα	PLAQA↓VRSSS	20	TACE	Kriegler *et al.*, 1988
BlyS	SRNKR↓AVQGP	60	TACE?	Moore *et al.*, 1999

Modified from reviews by Ehlers, Hooper and Rose-John [Ehlers *et al.*, 1996; Hooper *et al.*, 1997; Rose-John and Heinrich, 1994]. * nomenclature of Schechter and Berger [Schechter and Berger, 1967]. Metallo- = metalloprotease; ↓ = cleavage site; "-12" = intramembranous cleavage 12 residues from extracellular surface.

The lack of sequence-specificity at the cleavage site implied that the sheddase(s) makes use of another region of the ectoprotein to recognise its substrate, namely either the ectodomain, stalk region, TM or cytoplasmic tail region. Although the

cytoplasmic tails of numerous ectoproteins are phosphorylated and are involved in protein localisation and signal transduction, there is no evidence to implicate the substrate ectoprotein transmembrane- or cytoplasmic-domains in sheddase recognition [De Strooper *et al.*, 1995; Brakebusch *et al.*, 1994; Arribas *et al.*, 1997]. GPI-anchored proteins may be shed through either phospholipase hydrolysis or proteolytic cleavage in the stalk region [Middelhoven *et al.*, 1997; LeBel *et al.*, 1998; Poloso *et al.*, 2002], although the GPI anchor is not sufficient for shedding susceptibility *per se* [Pang *et al.*, 2001]. These anchors, may, however, inhibit shedding by trapping certain ectoproteins in lipid rafts on the cell-surface [Marcic *et al.*, 2000b]. Consensus has therefore been reached that, if it is present, the sheddase recognition motif resides on the extracellular portion of an ectoprotein, either in the stalk or proximal ectodomain.

An alternative explanation that should be considered to account for the apparent lack of stalk-sequence specificity is that sheddases are generally promiscuous and have no specific active site recognition requirements. According to this view, sheddases merely require an accessible juxtamembrane sequence that is sterically unhindered to enable cleavage and release of the ectoprotein [Althoff *et al.*, 2001]. Since it is known that shedding is tightly regulated, this implies that sheddases are held in check until activated by an appropriate signal, after which they indiscriminately cleave all accessible/unstable ectoproteins from the cell surface.

However, since there is clearly more than one sheddase, each incapable of cleaving all cleavable ectoproteins, there is *a priori* evidence for some kind of recognition system, which targets, for example, TACE to TNFα and L-selectin but not to ACE or CD4. Hence, we favour the view that there is a putative recognition motif that confers class-specificity to each sheddase. The existence of such a recognition motif in susceptible substrate proteins is the central hypothesis that I endeavoured to test in this thesis.

1.5.1) In the stalk region?

The most compelling evidence that the stalk region contains the sheddase recognition motif derives from work involving swap-over chimera mutants where the stalk region of a shed ectoprotein induces shedding when inserted into the same region of a non-shed ectoprotein. Brakebusch *et al.* did the first of these experiments in 1994 [Brakebusch *et al.*, 1994]. Their exhaustive deletion and swap-over analysis of the stalk region of the p55 TNF-RI showed that: (i) the stalk region of TNF-RI could induce cleavage of the otherwise non-shed EGF-R, (ii) the EGF-R stalk abolished shedding of TNF-RI, and (iii) that the cleavage-site residues were specifically necessary for cleavage. Later, Arribas *et al.* inserted the 14 amino acid stalk region of TGF-α and β-APP into the juxtamembrane region of the non-shed TGF-β accessory receptor β-glycan, and found that this induced shedding [Arribas *et al.*, 1997]. Similarly, Rose-John *et al.* inserted the IL-6R, TGF-α and TNFα stalk regions into that of gp130, inducing shedding in an otherwise non-cleaved receptor [Althoff *et al.*, 2000].

At first glance this appears solid proof that the stalk region is all-important in sheddase recognition. However, the possibility exists that the stalk regions of β-glycan, gp130 and EGF-R may be highly refractory to cleavage. The EGF-R stalk is only 10 amino acids long, and contains three prolines and a disulphide-linked cysteine 10 amino acids from the membrane, whereas the cleavable TNF-RI stalk (in the EGF-R chimera) is 14 amino acids long and contains no prolines or cysteines (see Table AI.2). The β-glycan stalk contains 6 prolines, while the TGF-α and β-APP stalks contain none. Most importantly, however, Rose-John has found that, on closer examination of their IL-6R/gp130 chimeric mutants, that the IL-6R does not in fact contain the elusive sheddase recognition motif [Althoff *et al.*, 2001]. In fact, the authors found, after structural modelling of the gp130 stalk, that the insertion mutants had probably disrupted a fibronectin type III domain, and thus exposed the stalk region to proteolysis [Althoff *et al.*, 2001].

A similar line of reasoning can be used when examining the ectodomain shedding of an ACE-MDP chimera [Pang *et al.*, 2001]. It was shown that a chimera in which the

stalk region of MDP (a non-shed GPI-linked ectoprotein found on the surface of cells as a disulphide-linked homodimer) was replaced with the stalk, TM and cytosolic domains of ACE, was shed into the medium. It is possible that the homodimer formation through the disulphide bond 8 amino acids away from the TM is refractory to sheddase accessibility of the stalk region [Ehlers *et al.*, 1996]. It is then possible that, by introducing the open, random-coil ACE stalk into MDP, moving the disulphide-linkage cysteine 30 amino acids distal from the TM, that shedding may occur due to accessibility of the stalk region and not through a specific motif recognition in the stalk region [see Table AI.2].

The stalk region of CD4 abolishes cleavage secretion of the ectoprotein syndecan-1 when inserted into its stalk region [Fitzgerald *et al.*, 2000]. Examination of the crystal structure of CD4 reveals that the stalk region of CD4 is only 9 amino acids long, and is probably refractory to cleavage because of an obstructive tertiary structure and short stalk length. The authors replaced 15 amino acids of the syndecan-1 stalk with 15 residues from the juxtamembrane region of CD4, including the 9-residue stalk. The syndecan-CD4 chimera was not shed (unlike wild-type syndecan-1), and this could be ascribed to (a) the CD4 stalk was refractory for the reasons noted, or (b) the CD4 juxtamembrane sequence was misfolded in the chimera. Whatever the explanation, this experiment does not demonstrate unequivocally that the stalk contains the information required for sheddase recognition and cleavage.

De Strooper *et al.* showed in 1995, when developing an assay for β-APP shedding, that the ectodomain of β-APP is not necessary for α-secretase cleavage secretion [De Strooper *et al.*, 1995]. He removed the ectodomain of β-APP (N-terminal to the Aβ sequence) and replaced it with the horseradish peroxidase (HRP) enzyme. Expression of this chimera in COS-1 and MDCK cells revealed that although basolateral sorting was affected, the α-secretase activity was not, indicating that the ectodomain of β-APP is not needed for sheddase recognition or that HRP contains a recognition motif.

Another major piece of evidence implicating the stalk region as the site of sheddase recognition is the fact that some sheddases will cleave short, soluble, synthetic peptides coding for stalk regions *in vitro*, at the same cleavage site as the *in vivo*

sheddases [e.g. TACE [Black *et al.*, 1996] and MDC9 [Roghani *et al.*, 1999]]. Clearly, these sheddases do not need to find a recognition motif in the large ectodomain for activation or for that matter a membrane bound substrate. This assay system was exploited in the search for TACE, and proved successful [Black *et al.*, 1997; Moss *et al.*, 1997]. The inability of sheddases to cleave randomised peptide sequences with the same amino acid composition seemed to give credibility to the specificity of both the assay and the sheddases. However, an important caveat to this is that these *in vitro* assay systems require peptide concentrations that are vastly in excess of the likely stalk concentration *in situ* on the cell surface. Moreover, the ACE sheddase is an exception to this rule in that it needs a membrane-bound substrate for cleavage, as explained above [Oppong and Hooper, 1993; Ehlers *et al.*, 1996].

1.5.2) In the ectodomain?

The first evidence that showed that sheddases did not behave like other highly sequence-specific proteases came from early deletion studies. The first stalk region deletion mutations were made by Maruyama *et al,* in which they deleted two amino acids around the β-APP α-cleavage site, and large sections of the β-APP stalk, but surprisingly did not abolish shedding [Maruyama *et al.*, 1991]. N-terminal sequencing of the C-terminal remnant left in the membrane after cleavage showed that the sheddase conserved the distance from the plasma membrane (see Table AI.2). In 1992, Sisodia published work in which they also made a series of deletion mutants in the β-APP stalk, transfected these into COS-1 cells, and analysed shedding [Sisodia, 1992]. All the mutants were cleaved, indicating that the sheddase shows very poor sequence specificity or that numerous sheddases exist that show varied specificities. Another conclusion from that study was that the distance from the TM to the cleavage site was important, as opposed to the exact sequence of the stalk. Zhong *et al.* also made similar mutants, and came to the same conclusion, namely that the α-secretase is highly promiscuous [Zhong *et al.*, 1994]. However, after N-terminal microsequencing of the 9 kDa p3 stalk remaining in the membrane after cleavage, they concluded that there was probably only one sheddase with broad sequence specificity. This correlates well with the more recent finding that TACE (which cleaves many ectoproteins) is the α-secretase [Buxbaum *et al.*, 1998]. It is possible

that this sheddase recognises some motif in the ectodomain, and then cleaves in the stalk region, regardless of the variance of stalk sequence.

A similar conclusion was reached by our laboratory when we replaced the ACE juxtamembrane stalk with the LDL receptor stalk, an O-glycosylated region, an N-glycosylation site, and three EGF domains (an LDL-R EGF domain, the factor IX EGF domain, and the Min-23 EGF-like cysteine knot) [Ehlers *et al.*, 1996; Schwager *et al.*, 1998, Schwager *et al.*, 1999, Schwager *et al.*, 2001]. Surprisingly, cleavage occurred in all of these constructs (see Table 1.5.1), although with remarkably differing kinetics. It is extremely difficult to reconcile these data with the concept that the ACE sheddase recognises an exact sequence motif in the stalk region, as these stalks and cleavage sites are entirely different. A more reasonable conclusion is that the ACE sheddase recognises some part of ACE (other than the stalk) and cleaves the stalk region in a sequence independent manner. Two additional conclusions that must be considered with this type of experiment, i.e., domain swapping, are that (a) the heterologous domain misfolds, essentially providing access to a disordered, unhindered stalk, or (b) alternative shedding enzymes are recruited. Evidence for both of these possibilities has been presented (Schwager *et al.*, 1999, Schwager *et al.*, 2001; Althoff *et al.*, 2001). Nevertheless, these different interpretations are not mutually exclusive.

Although Brakebusch *et al.* concluded in 1994 that the stalk region of TNFRI was sufficient and necessary for shedding, shedding was independent of the stalk sequence [Brakebusch *et al.*, 1994]. The deletion of one or two amino acids in this stalk was tolerated (except around the cleavage site Val^{173}), while the deletion of 3, 5 or 10 residues inhibited shedding, indicating that the TNFRI stalk needs to be at least 14 amino acids long for shedding to occur. The non-shed EGFR stalk (9 amino long), and the proximal cysteine, was replaced by the 16 amino acid long TNFR stalk. The introduction of shedding susceptibility by the longer TNFRI stalk in the EGFR context was given as proof that the ectodomain of EGFR is incapable of directing cleavage–release, ignoring the possibility that the EGFR may contain a 'silent' recognition motif elsewhere, that is blocked due to an obstructed stalk. It is unfortunate that the definitive experiment, using a duplicated EGFR stalk (i.e.,

doubling the length of the stalk by tandem duplication) in the EGFR context, was not performed, as this would have resolved the stalk length issue.

The conclusion that the TNFRI ectodomain does not play a role in ectodomain shedding may need to be revised in light of an impressive collaborative effort, led by McDermott, that mapped the cause of the familial periodic fever (FPF) syndrome in a large Australian family of Scottish pedigree to mutations in TNFRI that disrupt its shedding from the surface of leukocytes [McDermott *et al.*, 1999]. The point mutations disrupt the second, third and fifth disulphide linkages of the ten disulphide bridges in TNFRI and reduce cleavage-secretion of the receptor without affecting receptor function. These receptors therefore cause excessive stimulation and signalling through impaired sheddase-mediated down-regulation of the TNFα-chelating soluble form of TNFRI [McDermott *et al.*, 1999]. These mutations occur in the ectodomain (at least 94 amino acids from the TM), and thus implicate the TNFRI ectodomain in shedding.

Certain ectoproteins have sheddase cleavage sites that are extremely distant from the TM domain and it is tempting to speculate that the sheddase recognises the proximal ectodomain and cleaves 'below' this structure. Ehlers *et al.* noted in 1996 that many of the heregulin isoforms seem to share a cleavage site 6 amino acids downstream of the proximal EGF domain, even though their stalks had widely differing lengths and sequences [Ehlers *et al.*, 1996]. The type I ectoprotein p75 TNFRII has a sheddase cleavage site that is 14 amino acids from the proximal ectodomain cysteine, while 43 amino acids from the TM domain [Brakebusch *et al.*, 1994]. Similarly, the type II ectoprotein BlyS (B lymphocyte stimulator) has a cleavage site 60 amino acids from the TM, 12 amino acids proximal to the first ectodomain cysteine [Moore *et al.*, 1999]. This variation in cleavage site distance from the TM, and relative constraint to the proximal ectodomain is highly suggestive of a sheddase recognition motif in the ectodomain that directs cleavage in the stalk region.

The concept of 'headroom', or the stalk region between the proximal ectodomain and the sheddase cleavage site (as introduced by Ehlers *et al.* in 1996), has been investigated with regard to the cleavage-secretion of proTNFα, and found to be

important in allowing the sheddase access to the cleavage site [Tang *et al.*, 1996a; Tang *et al.*, 1996b]. Maskos *et al.* concluded, after using their crystal structure of the TACE catalytic domain to perform docking experiments between TACE and the TNFα substrate, that TACE might bind to the base of the TNFα-trimer cone [Maskos *et al.*, 1998]. This again alludes to the possibility that the cell-surface localised sheddase might recognise the proximal ectodomain of TNFα prior to non-specific cleavage in the stalk region, a concept explored further in a review by Black & White [Black and White, 1998]. This control mechanism might be overridden by relatively high concentrations of soluble stalk substrate used in the cell-free assay of TACE activity.

Sadhukhan and colleagues published the first study providing strong evidence that the ectodomain is involved in the cleavage-release of ACE [Sadhukhan *et al.*, 1998]. They made numerous deletion and point mutations in the stalk and cytoplasmic regions of rabbit testis ACE and analysed the relative shedding of these mutants expressed in COS-1 cells. They concluded, like Ehlers *et al*, that the ACE stalk region sequence is not essential for shedding [Ehlers *et al.*, 1996; Sadhukhan *et al.*, 1998; see Chapter 4]. Their cytoplasmic region deletion mutants were shed more effectively than the wild type controls, indicating that the cytoplasmic tail may, if anything, have an inhibitory role in shedding (this is also examined in Chapter 5). The work using chimeric forms of the shed type I ectoprotein ACE and the non-shed type I ectoprotein CD4 were even more illuminating. The ectodomain of ACE was fused onto 62 amino acids of the CD4 stalk and TM and cytoplasmic regions, resulting in effective shedding with cleavage occurring C-terminal to I_{361} (see Table AI.2). This result indicated not only that the ectodomain of ACE was able to direct cleavage of the non-shed ectoprotein CD4, but also that the TM and cytoplasmic regions were not directly involved. This conclusion was corroborated by another of their ACE/CD4 chimeras in which they fused the ectodomain of CD4 onto the stalk, TM and cytoplasmic domain of testis ACE. This chimera ($CD4/ACE_T$-1) was processed to the cell surface but was not shed into the medium, indicating that the ACE stalk, which is usually cleaved very efficiently, was not sufficient for ectodomain cleavage [Sadhukhan *et al.*, 1998].

But where exactly in the ectodomain does this putative sheddase recognition motif reside? One of the first tentative sheddase recognition motifs located in the ectodomain was identified by Pischitzis *et al.* when they compared the human, shed, form of *N*-Benzoyl-L-tyrosyl-*p*-aminobenzoic acid hydrolase β (PPHβ), with the mouse, non-shed, form (meprinβ) [Pischitzis *et al.*, 1999]. After exchanging different domains, and expressing the chimeras in COS-1 cells, they narrowed down the 'sheddase-inducing' section of PPHβ to a 13-amino acid long peptide (QIQLTPAPSVQDL) distal to the juxtamembrane EGF domain (see Table AI.2). PPHβ does, however, contain an EGF domain in its stalk region, which is probably refractory to sheddase cleavage. This 'cleavage-inducing' peptide motif may instead be the proximal, accessible, stalk-like sequence needed by the sheddase to cleave PPHβ, as opposed to a true recognition motif in the ectodomain. Also, our laboratory has recently shown that the ACE sheddase can side step a tightly folded EGF domain, when inserted in the ACE stalk region, to cleave distal to this structure [Schwager *et al.*, 2001].

As mentioned above, Hattori *et al.* have identified the first sheddase recognition motif in the ectodomain of a surface-bound ectoprotein [Hattori *et al.*, 2000]. They found a putative consensus sequence [KFEIKFQEFV] when aligning other shed ectoproteins. Kuz-mediated shedding of Ephrin-A2 was activated using the peptide spanning this region, while a scrambled peptide with the same amino acid composition was inactive. This indicates that the consensus-spanning peptide may be able to mimic the receptor/ligand clustering needed for Kuz activation. This motif has not been found in the ACE amino acid sequence. Nonetheless, the consensus sequence found in the ectodomain of ephrin-A2 may play an important role in substrate/sheddase recognition. Importantly, the authors showed that the ephrin-A2 ectodomain was necessary for binding to Kuz, using a chimera of alkaline phosphatase and the ephrin-A2 stalk. This chimera was unable to bind to Kuz, indicating that the juxtamembrane region (where cleavage occurs) was not sufficient for Kuz-mediated cleavage. Also, this binding occurred in a region of Kuz outside the pro- and protease domains, implying that stalk proteolysis occurs after Kuz/{ephrin ectodomain} binding [Hattori *et al.*, 2000].

In conclusion....

Numerous cell surface-bound ectoproteins are shed from the membrane through proteolytic cleavage of their juxtamembrane stalk regions by one or more sheddase. The sheddases are a family of surface-bound, hydroxamate inhibited, Zn^{2+}-metalloproteases with broad substrate specificity, which are activated by cell stimulation. Some surface-bound ectoproteins escape shedding, likely by either containing an inaccessible stalk region, or lacking a sheddase recognition domain. The recognition domain does not reside in the TM or cytoplasmic domains, but is rather in either the extracellular stalk or proximal ectodomain regions.

In this thesis I have made numerous deletion/insertion mutants in the type I ectoprotein angiotensin-converting enzyme (ACE), in an attempt to resolve the exact location and sequence identity of the sheddase recognition motif.

Chapter 2: Angiotensin-Converting Enzyme

2.1) Angiotensin-Converting Enzyme (ACE)

ACE is a dipeptidyl carboxypeptidase that plays a central role in the control of blood pressure, electrolyte homeostasis, kidney and heart development, and fertility [for reviews see Erdos and Skidgel, 1987; Ehlers and Riordan, 1989; Ehlers and Riordan, 1990;Ehlers and Riordan, 1991b; Hooper, 1991a; Corvol *et al.*, 1995]. ACE is differentially expressed as two membrane-bound isoforms: the ubiquitously expressed somatic form, and the testicular form found only in sperm. Both are shed from the membrane through proteolytic cleavage of their juxtamembrane stalk regions. The somatic form of ACE is expressed primarily on the luminal surfaces of lung and kidney endothelia, where it plays a central role in the renin-angiotensin aldosterone system (RAAS). It increases blood pressure by hydrolysing angiotensin I (AngI) to form the potent vasopressor angiotensin II (AngII), which in turn stimulates aldosterone secretion and sodium reabsorption by the kidneys. ACE also inactivates the vasodilator bradykinin. An over-active RAAS therefore causes hypertension, with eventual renal and cardiac failure.

This chapter will introduce the structure and function of ACE, and its role in both systemic and localised renin-angiotensin system (RAS), hypertension and fertility. Finally, I will discuss the shedding of ACE from the surface of cells and the rationale for using ACE as a model system to study ectodomain shedding.

2.1.1) The discovery of ACE

The original naming of 'ACE' was fraught with confusion, and illustrates many aspects of the discovery of ACE. This enzyme was first discovered in 1954 as a factor in horse blood that converted hypertensin I to the octapeptide hypertensin II by removing the C-terminal dipeptide His-Leu [Skeggs, Jr. *et al.*, 1954; Skeggs, Jr. *et al.*, 1956], and was thus called hypertensin-converting enzyme. Similarly, Helmer noted that a factor in plasma converted his angiotonin preparations, which he called

angiotonin-converting enzyme [Helmer, 1957]. Angiotonin is an early name for the decapeptide angiotensin. ACE was independently isolated from human kidneys as an enzyme that degraded bradykinin through the sequential removal of two C-terminal dipeptides [Yang and Erdos, 1967; Yang *et al.*, 1970]. It was named kininase II to distinguish it from kininase I (carboxypeptidase N). Ng & Vane proposed that both the activation of AngII and inactivation of bradykinin might be due to the same enzyme, primarily found in the lungs [Ng and Vane, 1967, Ng and Vane, 1968]. The first proof for this hypothesis was the finding that the bradykinin-potentiating (and thus vasodilatory) factor isolated from *Bothrops jararaca* venom [Ferreira and Rocha e Silva, 1965] also inhibited ACE [Bakhle, 1968; Ferreira *et al.*, 1970b].

The advent of solid-phase peptide synthesis provided a source of synthetic substrates for ACE. Synthetic angiotensin I peptides were used to further confirm the identity of kininase II as ACE [Yang *et al.*, 1970; Dorer *et al.*, 1974]. However, the analysis of the substrate specificity of ACE added complexity (for reviews see Ehlers and Riordan, 1990; Erdos, 1990 and Hooper, 1991a), and refuted the explicit definition of ACE as a specific dipeptidyl carboxypeptidase. Apart from cleaving the C-terminal dipeptide from angiotensin I and bradykinin, ACE is also able to cleave either two or three amino acids from the carboxy terminus of substrates such as substance P, enkephalins, neurotensin and luteinizing hormone-releasing hormone (LH-RH). Further, ACE is able to cleave either free or amide-blocked carboxytermini [Erdos, 1990]. Very recently, ACE has even been shown to cleave the Aβ peptide, and is thus able to act as an endoprotease, although the physiological significance of the *in vitro* finding awaits confirmation [Hu *et al.*, 2001]. Thus, numerous terms have been used for Angiotensin I-converting enzyme, namely: dipeptidyl carboxypeptidase, peptidyldipeptide hydrolase, kininase II, carboxycathepsin, hypertensin-converting enzyme, and EC 3.4.15.1. However, I refer to it as ACE in this thesis.

Similar confusion of nomenclature occurred when trying to describe the tissue distribution of ACE. Initially, Ng *et al.* found that the lung was the major site of conversion of AngI to AngII [Ng and Vane, 1967], and therefore described 'pulmonary' ACE (ACE_P). It was later found that ACE is almost ubiquitously expressed throughout the mammalian body, especially in the vascular endothelial

layer [reviewed in Erdos and Skidgel, 1987; Ehlers and Riordan, 1990], and therefore became known as 'endothelial' ACE (ACE_E). Surprisingly, high ACE activity was also found in mature rat testes [Cushman and Cheung, 1971], indicating that ACE may play a role in reproduction.

The importance of testicular ACE became more apparent with the finding that it is encoded by a unique mRNA, expressed only in mature testes, and that it is significantly smaller (90-110 kDa) [El Dorry *et al.*, 1982a; El Dorry *et al.*, 1982b] than that isolated from human pulmonary tissue (150-180 kDa) [Kokubu, 1978; Gronhagen-Riska and Fyhrquist, 1980]. The N-terminal sequences of the two isoforms also vary [Iwata *et al.*, 1982], necessitating the renaming of endothelial ACE to 'somatic' ACE (ACE_S) to distinguish it from the smaller, post-meiotic, germinal form called testicular ACE (ACE_T). Ehlers *et al.* cloned and sequenced the cDNA for human ACE_T in 1989 [Ehlers *et al.*, 1989b]. In this thesis I use this cDNA for human ACE_T to explore the structural or sequence criteria required for ectodomain shedding from the surface of eukaryotic cells.

2.1.2) Somatic ACE

The gene for human ACE_S is found on chromosome 17 (Gene map locus 17q23) [Lander *et al.*, 2001]. It spans ~24-kilobases, contains 27 exons, and transcribes a 4.3-kilobase mRNA in endothelial cells and a 3.0-kilobase transcript in sperm [Soubrier *et al.*, 1988; Ehlers *et al.*, 1989b]. The ACE_S mRNA consists of 26 exons that are spliced together (i.e., all exons except the 13^{th} exon) [Hubert *et al.*, 1991]. An insertion/deletion polymorphism of 287 bp in intron 16 of ACE has been associated with hypertension [Rigat *et al.*, 1990; Zee *et al.*, 1992]. Somatic ACE is a 150-kDa type I ectoprotein made up of 1306 amino acids. It consists of a signal peptide, two highly homologous zinc-metalloprotease domains (the N- and C-domains) separated by a short bridge and followed by a juxtamembrane stalk, a transmembrane domain and a cytoplasmic domain (see Fig. 2.1.2.1) [Soubrier *et al.*, 1988].

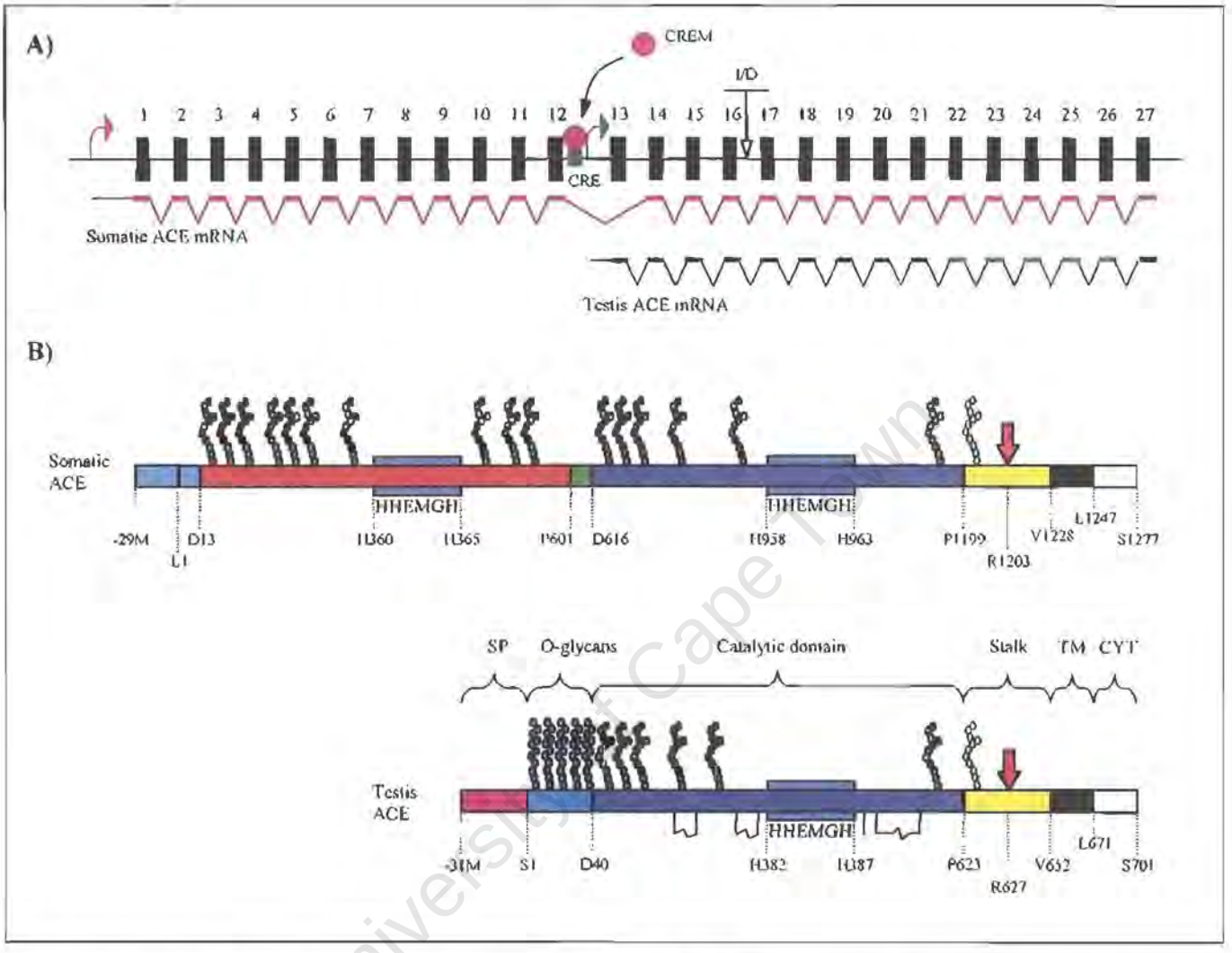

Figure 2.1.2.1) Schematic representation of the structure of ACE

The 24-kilobase ACE gene on chromosome 17p23 is represented schematically in (A). Black bars indicate exons 1-27. Two promoters are differentially active; one in somatic cells that transcribes the 4.3 kb ACE_S mRNA (red, [Soubrier *et al.*, 1988]), and the other in sperm that codes for the 3.0 kb ACE_T mRNA (blue, Ehlers *et al.*, 1989b]. In sperm, the cAMP response element mediator (CREM, pink circle) is necessary for activation of the sperm-specific promoter, by binding to the cAMP response element (CRE, blue square) [Kessler *et al.*, 1998]. The relative position of the 287 bp Insertion/Deletion polymorphism in intron 16 is shown [Zee *et al.*, 1992]. The 1306-amino acid ACE_S and 732-amino acid ACE_T peptides, translated from their respective mRNAs, are shown schematically in (B). Colour scheme: sea green, ACE_S signal peptide; red, N-domain; light green, interdomain 'bridge'; dark blue, C-domain; yellow, juxtamembrane stalk region; black, TM; white, cytoplasmic tail; mauve, ACE_T signal peptide; light blue, N-terminal 36-aa O-glycosylated region; medium blue, catalytic site zinc-binding motif [HHEMGH]. The ACE sheddase cleavage site is indicated with a red arrow, at Arg627/Arg1203 for ACE_T and ACE_S, respectively [Woodman *et al.*, 2000]. Known disulphide linkages are shown with a jagged line, while the single reduced cysteine is shown with a short line [Sturrock *et al.*, 1996]. N- and O-linked glycosylation sites are indicated with green or blue side-chains, respectively. The potential N-glycosylation site that was found not to be glycosylated is shown with a white side-chain [Yu *et al.*, 1997].

Somatic ACE is heavily glycosylated and 26-30% of the protein, by mass, is composed of carbohydrate. It has 17 potential N-glycosylation sites [NX(S/T); X not Pro], while ACE_T has 7 (of which only the first 6 are glycosylated) [Soubrier *et al.*, 1988; Shakin-Eshleman *et al.*, 1996; Yu *et al.*, 1997]. The variation in size and structure of the carbohydrate side-chains accounts for the range in molecular weight, which is given as 170 to 190 kDa for ACE_S, and 90 to 110 kDa for ACE_T. This is reduced to 150 kDa and 80 kDa respectively upon deglycosylation. These hydrophilic carbohydrate side-chains probably protect the molecule from degradation, adding to the overall stability of these enzymes. The higher sialic acid content probably also protects ACE from asialoglycoprotein receptor-mediated uptake and degradation in the liver [Ehlers and Riordan, 1990; Ashwell and Morell, 1974].

Both the somatic and testicular forms of ACE hydrolyse AngI with similar kinetics [Ehlers *et al.*, 1991a; Ehlers and Riordan, 1991a], indicating that the major enzymatic activity controlling blood pressure is due to the C-domain. Corvol and colleagues confirmed that both domains are, in fact, catalytically active by inactivating each domain separately. They did this by introducing point mutations of the zinc-binding histidine (explained below), thereby preserving the 3-dimensional structure of ACE_S, while rendering either domain inactive [Wei *et al.*, 1991a]. They found that the N-domain is independently active as it has an absolute requirement for zinc (like the C-domain), is completely inhibited by captopril and enalaprilat (as is the C-domain), it cleaves Hip-His-Leu with a 10^{th} of the efficiency of the C-domain, and cleaves AngI about 3-fold less efficiently than the C-domain. Interestingly, ACE_S activity is the sum of the activities of both domains, indicating that these domains act as entirely separate catalytic entities, and do not show an allosteric activation. Sturrock *et al.* further showed that each domain could be separated after limited proteolysis with endoproteinase Asp-N, and each preserved its catalytic activity [Sturrock *et al.*, 1997]

The differences in substrate specificity shown by the two domains of ACE is becoming increasing important as new domain-specific substrates are discovered. The tetrapeptide N-acetyl-seryl-aspartyl-lysyl-proline (Ac-SDKP) is a naturally occurring regulator of hematopoiesis, which reversibly blocks pluripotent hematopoietic stem cells and normal early progenitors in the Go-phase of cellular cycle [Lenfant *et al.*, 1989; Bonnet *et al.*, 1993]. ACE was found to be involved with the degradation of this

hemoregulatory peptide, both *in vitro* [Rieger *et al.*, 1993], and *in vivo* [Azizi *et al.*, 1996; Rousseau *et al.*, 1995]. More specifically, the N-domain was found to be the preferential site of Ac-SDKP catabolism [Rousseau *et al.*, 1995], making this the first N-domain specific substrate for ACE. This joined luteinizing hormone-releasing hormone (LH-RH), Met^5-Enk-Arg^6-Phe^7 and Ang 1-7, which were also found to be N-domain specific substrates [Skidgel and Erdos, 1985; Ehlers and Riordan, 1991a; Deddish *et al.*, 1997; Deddish *et al.*, 1998].

Araujo *et al.* developed an internally quenched fluorogenic peptide analogue of Ac-SDKP, Abz-SDK(Dnp)P-OH, and found that it too is N-domain specific [Araujo *et al.*, 2000]. At each end of the peptide, *ortho*-aminobenzoic acid (Abz) and 2,4-dinitrophenyl (Dnp) are added to form a donor/acceptor pair that only fluoresces when separated by substrate hydrolysis [Yaron *et al.*, 1979; Araujo *et al.*, 1999]. We use this internally quenched peptide as a substrate for the enzymatic analysis of an ACE N-domain chimera (ACE-Ndom; Chapter 6).

An alignment of the N- and C-domains of numerous ACE molecules from different species reveals that the catalytic site, in particular, is very well conserved over millennia and that overall they share 54% identity over 616 residues (see Fig. 2.1.4.1; phylogeny, below). The amino acid changes over time have been exploited in this thesis to assist in defining the sheddase recognition motif. A more detailed description of the similarities and differences between these two domains can be found in the introduction to Chapter 6.

2.1.3) Testis ACE

The smaller, germinal form of ACE was first identified during an immunological comparison of ACE in different rat organs [Polsky-Cynkin and Fanburg, 1979]. El-Dorry *et al.* confirmed this when they isolated ACE_T from rabbit testes using affinity purification [El Dorry *et al.*, 1982a] and showed that it had a molecular weight of about 100 kDa. They also showed that the mRNA isolated from testes transcribed a unique isoform of ACE in a reticulocyte lysate assay, alluding to a role for ACE_T in spermatogenesis or fertility (discussed in more detail below) [El Dorry *et al.*, 1982b].

Seven years later Ehlers *et al.* and Lattion *et al.* separately cloned and sequenced the cDNA for testis ACE, and showed that it is transcribed from a sperm-specific promoter in intron 12 of ACE, and contains the C-domain of ACE_S [Ehlers *et al.*, 1989b; Lattion *et al.*, 1989]. This post-meiotic sperm-specific promoter contains a cyclic AMP response element (CRE) that is activated by the cAMP response element modulator (CREM) [Kessler *et al.*, 1998]. Both the CRE and CREM are essential for the transcription of ACE_T.

The ACE_T precursor peptide is 732 amino acids long and is encoded by exons 13 to 27 of ACE_S. It is thus identical to the C-terminal end of somatic ACE (residues 613-1277), except for a unique 67-amino acid-long N-terminal region (see Fig. 2.1.2.1). This region, encoded by exon 13, codes for a 31-residue signal peptide (which is removed in the ER) [Iwata *et al.*, 1982], and a highly O-glycosylated stretch of 36-amino acids [Ehlers *et al.*, 1992]. Although unique to testis ACE, the removal of this domain does not affect the enzymatic activity or stability of ACE_T [Ehlers *et al.*, 1992]. Interestingly, this N-terminal O-glycosylated region has recently been implicated in fertility (see below, [Kessler *et al.*, 2000; Hagaman *et al.*, 1998]).

The fact that ACE_T is in essence a smaller, simplified, form of ACE_S that shares its catalytic properties has facilitated its use in the characterisation of the unique ACE catalytic domain. In the absence of a 3D structure it is difficult to define the stalk length, the limits of the catalytic domain, or even which residues are facing the exterior (and thus may play a role in sheddase/substrate interaction). Disulphide linkages are usually very informative, although in the case of ACE there are only 7 cysteines, linked in a 'nearest-neighbour' manner [aabbcc], i.e. C_{152}/C_{158}, C_{352}/C_{370} & C_{538}/C_{550}, which is not characteristic of any known domain [Sturrock *et al.*, 1996]. Furthermore, disulphide loops account for only 5% of the peptide sequence. Sturrock *et al.* also found that the fifth cysteine, C_{496}, is present in the reduced form. Interestingly, the N- and C-domains show almost exact identity with regard to their cysteines, indicating that the [aabbcdd] linkage found in ACE_T is probably conserved across domains.

Testis ACE contains 7 putative N-linked glycosylation sites, the last of which (N_{620}) is not glycosylated [Yu *et al.*, 1997]. The large, 'bulky', side chains are a major

hindrance in efforts to crystallise ACE, and numerous approaches have been employed in an attempt to reduce the glycosylation. Methods employed thus far include the removal of the sugars with deglycosidases, transfection of ACE into *Escherichia coli* or N-acetylglucosamine transferase$^{-/-}$ cell lines, and growth of transfected cells in the presence of the N-acetylglucosamine transferase inhibitor, tunicamycin. Unfortunately, these methods have all failed to provide a suitable, active, simplified form of ACE that can be used for crystal structure determination. The laboratories of Sen and Corvol have both successfully expressed ACE in the yeast *Pichia pastoris*, in an attempt to obtain large quantities of minimally glycosylated enzyme, and to study the cleavage-release of ectoproteins in a simplified eukaryotic cell system [Sadhukhan *et al.*, 1996; Williams *et al.*, 1997].

The mutagenesis approach of removing the 7 putative N-glycosylation sequons [NX(S/T)] from ACE has not resulted in a crystal structure to date. Mutant rabbit ACE_T protein, in which all the putative N-linked sites were removed (ACE_Tg0), was inactive and rapidly degraded when expressed in HeLa cells [Sadhukhan and Sen, 1996]. The authors found that either the 1st or 2nd N-glycosylation sites were needed for expression of active ACE, while the 3rd site alone was insufficient. Surprisingly, when the ACE_Tg3 mutant, containing only the 3rd glycosylation site, was transfected into yeast, they obtained an active protein that was cleavage-secreted [Sadhukhan and Sen, 1996].

The finding that ACE is cleavage-secreted from yeast cells [Sadhukhan and Sen, 1996; Williams *et al.*, 1997] is of fundamental importance to my thesis. Numerous tools exist for the molecular manipulation of these rapidly growing eukaryotic cells, thus making them extremely tempting for the study and isolation of the ectodomain sheddase. Sadly, both groups showed that the sheddase activity in *P. pastori* happen over days (not minutes), and is not significantly inhibited by the hydroxamic acid sheddase inhibitor Compound 3. In fact, Williams *et al.* state that; "although yeast are capable of cleavage-secreting ACE, it is possible that the protease/s responsible are not homologous to those observed in mammalian cells," thereby aborting any attempts to isolate the sheddase from yeasts [Williams *et al.*, 1997].

2.1.4) Catalytic activity

The amino acid sequence of the zinc-binding site is used to classify zinc-metalloproteases into various families, namely: gluzincins, metzincins, inverzincins, carboxypeptidases and DD-carboxypeptidases [for reviews see: Hooper, 1994; Rawlings and Barrett, 1995]. ACE belongs to the gluzincin family because it contains the [***H***EXX***H***] short zinc-binding consensus sequence, in which the two histidines and a downstream glutamate that acts as the third zinc ligand bind Zn^{2+} (catalytically active amino acids are in bold, and zinc-binding residues are also in italics).

The zinc-binding residues in ACE_S have been identified by Wei *et al*, and shown to be H_{361}/H_{365} and H_{959}/H_{963} in the N- and C-domain respectively (see Fig. 2.1.4.1) [Wei *et al.*, 1991a]. The third zinc coordinating glutamate residue in each domain was found to be 29 amino acids downstream of the zinc-binding motif (numbering from H_{361} and H_{959}) in the [***E***XIX**D**] motif (E_{389} and E_{987}). This secondary zinc-binding motif is shared with thermolysin (TLN) and neutral endopeptidase-24.11 (NEP) [Williams *et al.*, 1994], and is characteristic of the gluzincins [Hooper, 1994]. Comparison of all ACE-like zinc-metalloprotease domains shows that the consensus sequence for the ACE catalytic site is [H***H******E***(M/L)G***H***(I/V)(Q/E)Y] followed C-terminally by the secondary zinc-binding motif [NXGFH***E***A(V/I)G**D**]. Other zinc-metalloproteases such as the thermolysin, endopeptidase-24.11, aminopeptidase and endopeptidase-24.15 families, and the tetanus and botulism neurotoxins, do not share these consensus sequences, except for the core [***H***EXX***H***] & [***E***XIX**D**] motifs [Hooper, 1994]. If one excludes the highly divergent forms of ACE and examines only the zinc-binding consensus sequences in vertebrate ACE one sees substantially greater conservation around the catalytic site, with the consensus region now [H***H***EMG***H***(I/V)QYXXQY] and [ANPGFH***E***AIG**D**] (see Fig. (2.1.4.1)).

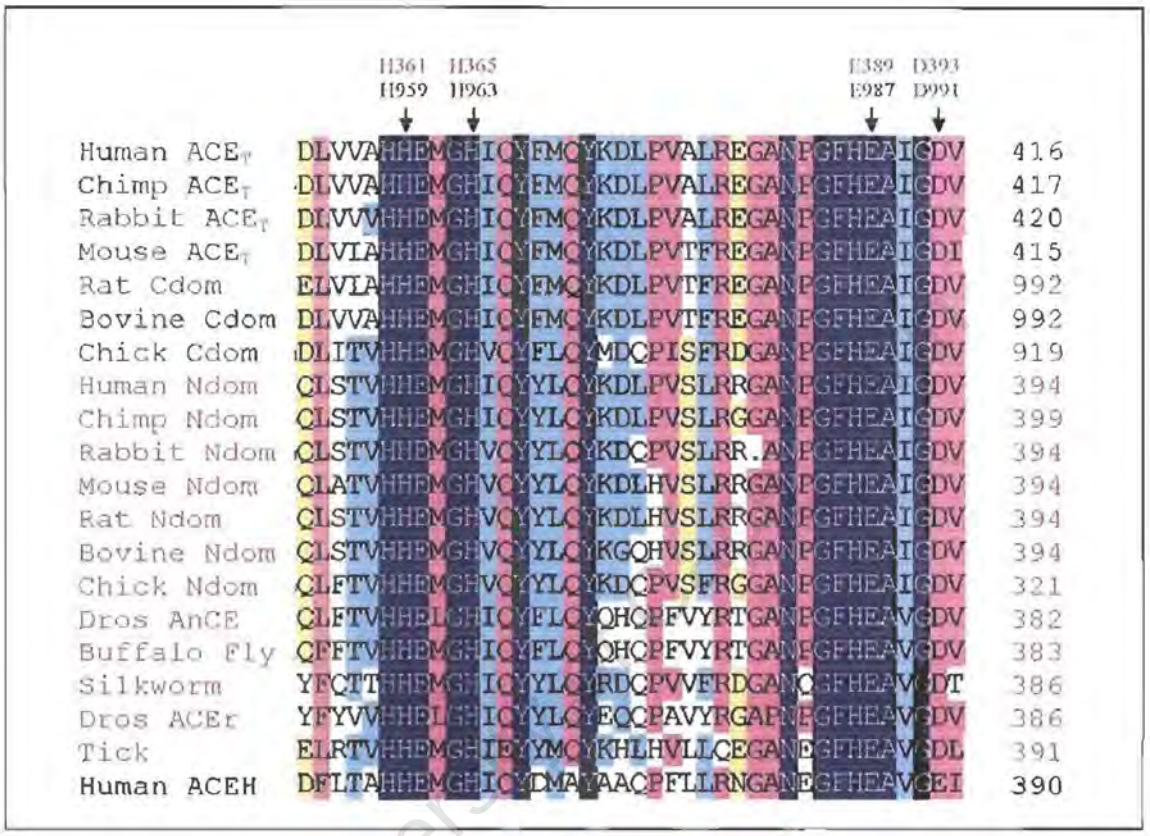

Figure 2.1.4.1) The ACE catalytic site compared (different species/domains)

The full-length (precursor) ACE sequences of different species are compared at the zinc-metalloprotease catalytic site. The conservation around the catalytic site is particularly noticeable with the vertebrate consensus region being [*HH*EMG*H*(I/V)QYXXQY] and [ANPGFH*E*AIGD]. Testicular or C-domain sequences are labelled in blue, while N-domain sequences are labelled in red. Alignment performed using Lynnon BioSoft DNAMAN using sequences listed in Appendix III, and numbered accordingly on right. Black, pink, blue and yellow highlighted regions refer to 100%, >= 75%, >= 50%, and >= 35% identity respectively. Common names are used for species; see Table (2.1.2) for names. Ndom, ACE N-domain from M1 to A618; Cdom, ACE C-domain from D616 to the COOH-terminus; Dros, Drosophila. Note that chicken ACE is only a partial sequence, and does not start from the N-terminus. Note also that the catalytic HHEMGH motif is highly conserved. The catalytic site residues which were mutated by Corvol *et al* (mature ACE$_S$ numbering used) are indicated with the arrow [Wei *et al.*, 1991; Williams *et al.*, 1994].

The general mechanism of action of zinc metalloproteases is based on that of thermolysin and carboxypeptidase A, for which crystal structures are known [for reviews see Ehlers and Riordan, 1990, Hooper, 1994 and Corvol *et al.*, 1995]. The major protagonists in this [***H***EXX***H***] & [***E***XIX**D**] proteolytic motif are the zinc-binding histidines (1 & 5) and glutamic acid (29), and the catalytic glutamate (2) (numbering of Hooper, 1994).

An interesting anomaly with ACE, however, is its anion dependence for activation [for review see Ehlers and Riordan, 1990]. As early as 1954, it was found that ACE activity is greatly enhanced with the addition of NaCl [Skeggs, Jr. *et al.*, 1954]. Surprisingly, the effect of anion enhancement was found to be highly sensitive to the substrate examined [Shapiro *et al.*, 1983]. Shapiro *et al.* also showed that Cl^- binds to the active site, as both chloride and a competitive ACE inhibitor block the reductive methylation of a critical lysine, indicating that this lysine is in the catalytic site [Shapiro and Riordan, 1983]. Recently, Lui *et al.* have shown that R_{1098} in the C-domain is responsible for Cl^- binding and the chloride dependence of human ACE [Liu *et al.*, 2001]. The authors mutated ten basic residues in the C-domain (R/K) to glutamine, and found that only the $R_{1098}Q$ mutant had lost its chloride dependence for AngI hydrolysis. Interestingly, the authors also found that the hydrolysis of tetrapeptides was adversely affected by this mutation, suggesting that the Cl^- site is in fact evolutionarily conserved for the hydrolysis of short peptides substrates, but not Ang I. Ehlers & Riordan suggested that Cl^- binding may be required for the correct alignment of the substrate binding residues in ACE, allowing the catalytic site to act as a **di**peptidyl carboxypeptidase as opposed to a carboxypeptidase [Ehlers and Riordan, 1990].

2.1.5) ACE Inhibitors

The development of effective anti-hypertensive agents that inhibit ACE started with the discovery that a peptide from the venom of *Bothrops jararaca* could potentiate the effects of bradykinin [Ferreira and Rocha e Silva, 1965]. This Brazilian pit viper accounts for 90% of snakebite accidents in Brazil, and can cause oedema and shock due to inhibition of ACE with resulting vasodilation. Later, Bakhle *et al.* showed that

crude peptide extracts from *B. jararaca* venom could inhibit the conversion of AngI to AngII and the inactivation of bradykinin [Bakhle, 1968]. Ondetti *et al.* isolated, sequenced and synthesized six peptides from *B. jararaca* venom that could inhibit the Hip-His-Leu-digesting activity of ACE, and found that some were similar or identical to the nine peptides that Ferreira *et al.* had isolated from the same venom for their bradykinin-potentiating activity [Ondetti *et al.*, 1971; Ferreira *et al.*, 1970a]. This helped confirm that ACE and kininase II was the same enzyme, as mentioned above [Ferreira *et al.*, 1970b].

The rational design of orally active antihypertensive drugs was achieved by Ondetti *et al.* using the catalytic properties of carboxypeptidase A as the basis for constructing a hypothetical model of the ACE catalytic site. They designed carboxyalkanoyl and mercaptoalkanoyl derivatives of proline, such that the carboxyl or thiol group would coordinate with the zinc atom [Ondetti *et al.*, 1977]. One of these (Captopril, SQ 14225) was extremely effective at inhibiting rabbit lung ACE and was subsequently developed and marketed throughout the world as a potent antihypertensive and cardio-protective agent. Numerous derivatives and modified forms of these original ACE inhibitors, such as Enalapril and Lisinopril, have been developed and used clinically in the treatment of hypertension and cardiac failure [Hooper, 1991b]. Interestingly, Dive *et al.* have recently discovered that the phosphinic peptide RXP 407 is an N-domain-specific inhibitor of ACE [Dive *et al.*, 1999], and have subsequently shown that it can be used *in vivo* for the selective inhibition of acetyl-Ser-Asp-Lys-Pro (AcSDKP, a hemoregulatory peptide) degradation by ACE, without effecting blood pressure regulation [Junot *et al.*, 2001].

The development of effective ACE inhibitors was not only a major breakthrough clinically in the control of hypertension, but it was also enormously useful in the purification of ACE. In this thesis I use a sepharose-[28Å linker]-lisinopril affinity resin to purify ACE from transfected CHO cells and culture medium [Pantoliano *et al.*, 1984; Ehlers *et al.*, 1986; Turner *et al.*, 1987]. The relative ease with which one can isolate purified ACE (and mutants thereof) from the cells and medium of transfected CHO cells is one of the reasons ACE is a good model system for examining ectodomain shedding.

2.1.6) Phylogeny

The evolutionary history of ACE is instructive in terms of its distribution in the animal kingdom, and what this can tell us about its role as a carboxydipeptidase and a shed ectoprotein. When comparing the sequence of ACE from different species, one immediately wonders why certain amino acids are conserved throughout evolution, and what possible role they might play in ACE activity and/or as possible motifs for sheddase recognition.

Full-length ACE (or ACE-like) mRNA sequences containing the HHE(M/L)GH zinc-metalloprotease catalytic site have been isolated and sequenced in numerous different species including diverse taxa: Mammalia (human, chimpanzee, rabbit, rat, mouse, cow); Aves (chicken); Lepidoptera (silkworm); Diptera (fruit fly, buffalo fly) and Acari (southern cattle tick). In addition, an enzyme with ACE-like activity has been isolated from *Musca domestica* (house flies) [Lamango and Isaac, 1993] and the electric organ of the fish *Torpedo marmorata* (marbled electric ray) [Turner *et al.*, 1987]. This shows that, to date, ACE has been found in such divergent species that the only common taxonomic root is: Eukaryota; Metazoa; Bilateria; Coelomata (multicellular animals having differentiated tissues, two halves and a body cavity). This is not due to the skewed scientific emphasis on mammalian animals as (i) 63 microbial genomes have been completely sequenced thus far, and do not contain an ACE-like enzyme sequence in any of their hypothetical open reading frames (ORFs) [NCBI Entrez Genome, November 2001] and (ii) the genomes of *Caenorhabditis elegans* and *Saccharomyces cerevisiae* have been completely sequenced [The C.elegans Sequencing Consortium, 1998], and do not contain an ACE-like ORF with a zinc-binding site [Sanger Centre, June 2001]. One may thus postulate that the ACE enzyme evolved sometime after the divergence of Coelomata from their Pseudocoelomata taxonomic neighbours (See Fig. AI.2, Table AI.3).

Interestingly, ACE-like homologues of human ACE (ACEH, ACE2) [Tipnis *et al.*, 2000; Donoghue *et al.*, 2000] have been found in Drosophila [Cornell *et al.*, 1995; Tatei *et al.*, 1995], mice [Komatsu T, 2001, unpublished] and the zebrafish EST database [Zebrafish WashU MPIMG EST, 1999, unpublished], and allude to an as yet

undefined function that is also highly conserved. Surprisingly, even though this homologue contains the [HHE(M/L)GH] catalytic site characteristic of the ACE carboxydipeptidase, and shares 41% identity to ACE_T, it acts solely as a carboxypeptidase, is not inhibited by captopril, and does not cleave hippuryl-His-Leu [Tipnis *et al.*, 2000]. The authors also find that the exon structure of ACEH, found on the X-chromosome at position Xp22, is more closely related to the ACE_S N-domain than that of the C-domain, even though ACEH has a transmembrane domain.

Phylogenetic analysis shows that the ACE gene probably duplicated before our common ancestor diverged from ticks, flies and moths (which contain only one ACE domain), to form the predecessors of the ACE N-domain, the human ACE homologue (ACE2/ACEH) and the ACE-like homologues found in Drosophila. About 415 million years ago, about the time of divergence of our ancestors from fish and amphibia [Rawlings and Barrett, 1995], the ACE N-domain duplicated internally, giving rise to the N- and C-domains which are more closely related to each other than to ACEH (see Fig. 2.1.6.1). Both ACE_S and ACEH separately evolved transmembrane domains, which are absent in the Arthropoda forms. It is only at this point that the ectodomain shedding of ACE would have become physiologically relevant. Interestingly, Collectrin (a 222 amino acid collecting duct-specific transmembrane glycoprotein) shows 47.8% identity to the juxtamembrane region and TM, and cytosolic domains of ACE2 [Zhang *et al.*, 2001]. It is thus highly likely that ACE2/ACEH acquired its transmembrane domain through a gene duplication and fusion event with Collectrin, which would also explain the uncharacteristically long stalk region of the ACE homologue.

Another evolutionary peculiarity is that chickens have lost the ability to transcribe the testicular form of ACE [Esther, Jr. *et al.*, 1994]. The requirement for ACE_T in fertility is therefore probably restricted to mammals.

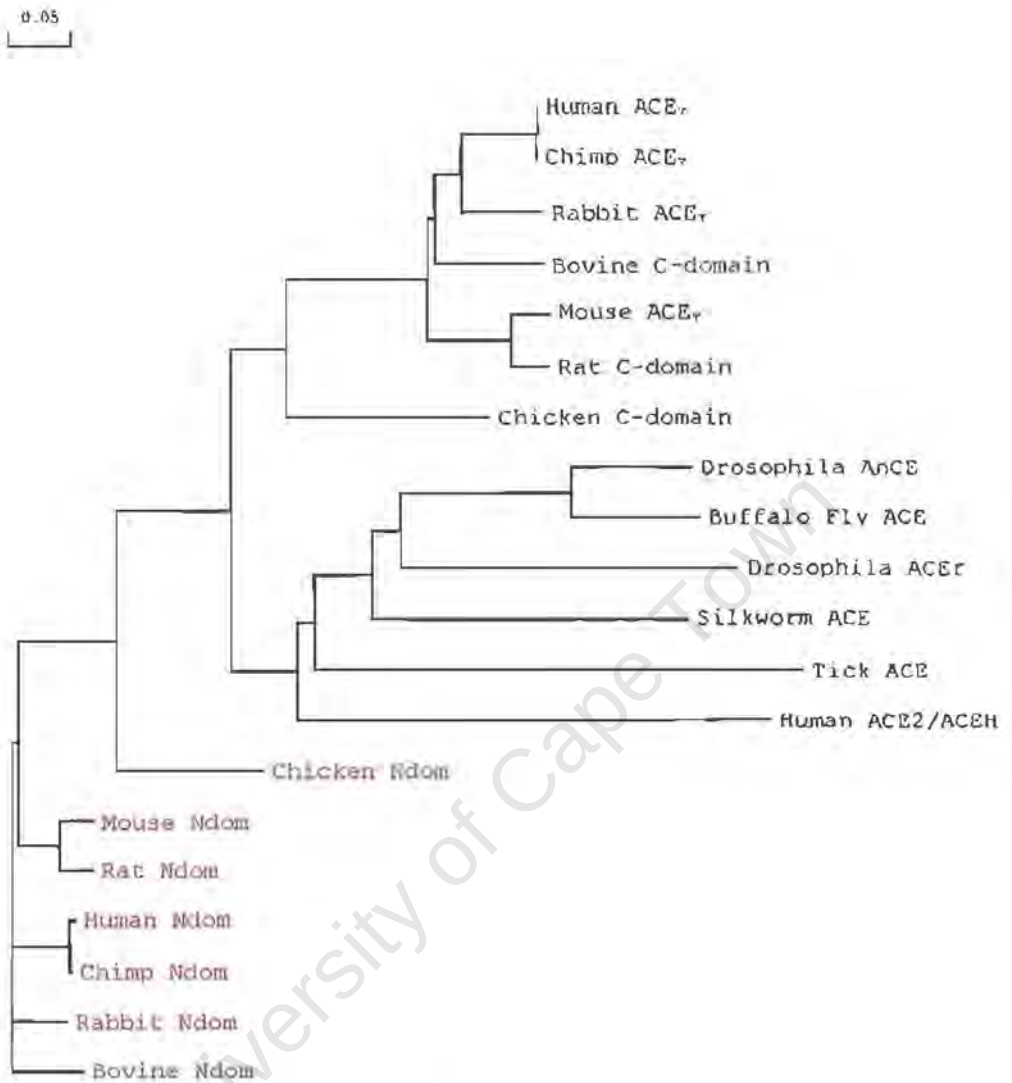

Figure 2.1.6.1) The ACE phylogenetic tree

This unrooted phylogenetic tree was generated using the ACE homologue sequences shown in Appendix III. Scale is in arbitrary branch length units. References: Human ACES [Soubrier *et al.*, 1988]; Human ACET [Ehlers *et al.*, 1989; Lattion *et al.*, 1989]; Human ACEH/ACE2 [Tipnis *et al.*, 2000; Donoghue *et al.*, 2000; Suzuki Y, unpublished;]; Chimpanzee [Dufour *et al.*, 2000]; Cow [Shai *et al.*, 1992]; Rat [Tatei *et al.*, 1995]; Mouse [Bernstein *et al.*, 1988]; Rabbit ACE [Kumar *et al.*, 1991]; Chicken [Esther, Jr. *et al.*, 1994b]; Drosophila [Cornell *et al.*, 1995; Tatei *et al.*, 1995]; Buffalo Fly ACET [Wijffels *et al.*, 1996]; Silkworm [Quan *et al.*, 2001]. Note that the chicken ACE sequence is only a partial cDNA clone.

2.2) The Renin-Angiotensin Aldosterone System

The correct maintenance of blood pressure and fluid and electrolyte homeostasis is vital. Excessive decrease in blood volume with concomitant low pressure, through blood loss, sweating, diarrhoea, or vomiting will result in: necrosis due to poor tissue perfusion, followed by hypoxia-induced coma and death. On the other hand, excessively high blood pressure, or hypertension, is the leading cause of cardiovascular disease and death due to cerebral haemorrhage (stroke), myocardial infarction (heart attack) and kidney disease. The renin-angiotensin system plays a major role in regulating blood pressure and electrolyte balance in the body, as shown in Fig. (2.2.1). This system is comprehensively characterised and reviewed [Inagami, 1994; Ariel Gomez and Norwood, 1995; Swales, 1995], and appears in most physiology texts [Marieb, 1995].

The primary role of the RAAS is normal maintenance of blood volume, pressure and sodium concentration. It achieves this by controlling blood vessel diameter and the re-absorption of sodium ions (Na^+) in the kidneys. Vascular constriction increases the total peripheral resistance, while the increased Na^+ uptake (in the presence of sufficient anti-diuretic hormone (ADH)), draws water osmotically out of the collecting ducts and into the efferent capillaries of the kidney, increasing blood volume and thus pressure.

The primary effector of RAAS is AngII, an octapeptide vasopressor. It is produced by the removal of a C-terminal dipeptide from AngI, a reaction catalysed by ACE. AngI, in turn, is produced from angiotensinogen (Ao) after cleavage by renin, which removes the N-terminal decapeptide. Ao is constitutively secreted into the plasma by the liver, while renin production by the juxtaglomerular apparatus of the kidney is rapidly up-regulated in conditions of low plasma Na^+ concentration or low blood pressure. ACE not only activates the vasoconstricting AngII, it also inactivates the nonapeptide vasodilator bradykinin (see 2.1.1). ACE is therefore doubly effective in increasing blood pressure as it activates a vasoconstrictor and inactivates a vasodilator. The control of ACE activity using ACE inhibitors thus forms the basis for the treatment of chronic hypertension.

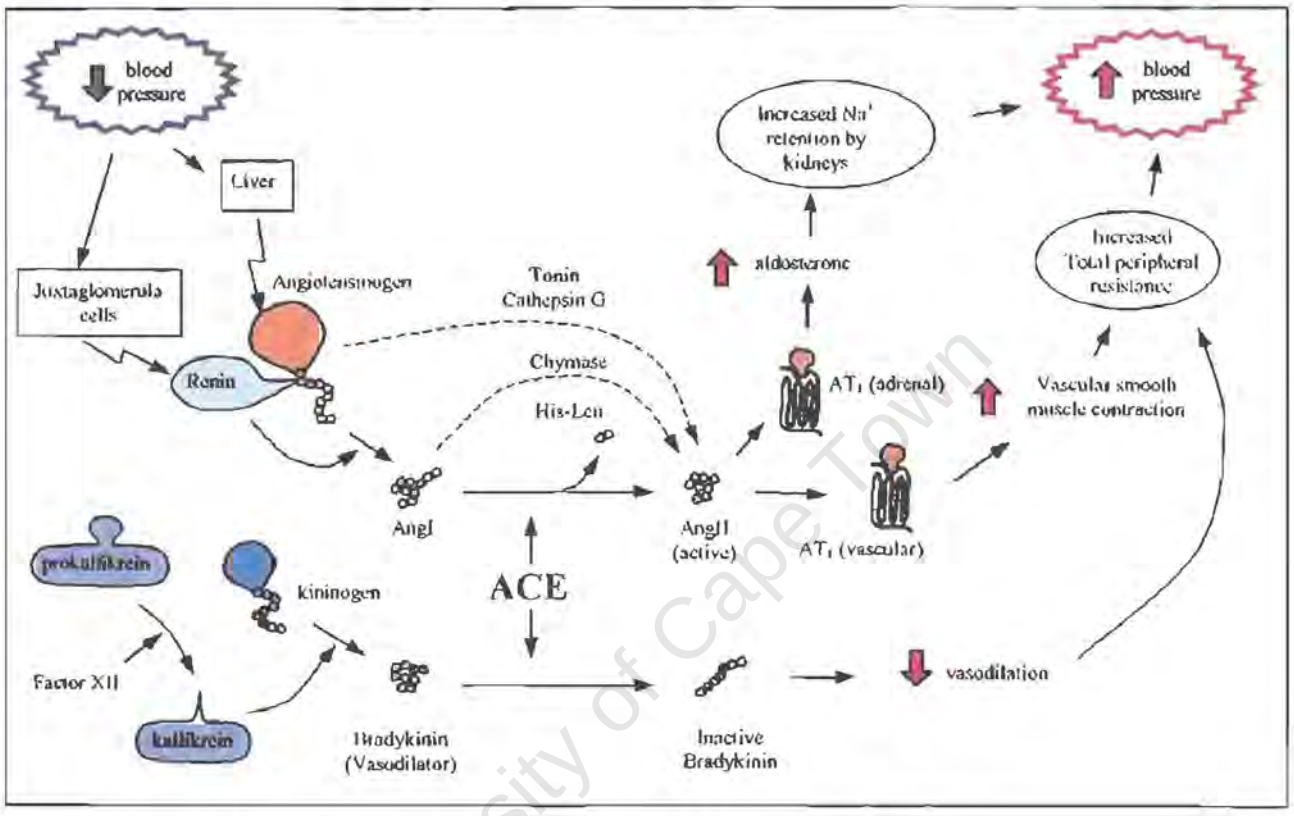

Figure 2.2.1) The Renin-Angiotensin Aldosterone (RAAS) system

Activation is indicated with solid, straight arrows. Increased expression is indicated with jagged arrows. The dashed arrows indicate the alternative, renin- and/or ACE-independent conversion of angiotensinogen to AngII.

Angiotensin II binds to the 7-transmembrane angiotensin II receptor (AT_1), which activates G_q and/or G_i type G-proteins [reviewed in Unger *et al.*, 2000]. Signalling from the AT_1 receptor in the adrenal gland leads to increased secretion of aldosterone, which in turn stimulates the kidneys to increase Na^+ reabsorption, which results in greater water reabsorption and an increase in blood volume. AT_1 activation in vascular smooth muscle cells leads to increased contractility, thus narrowing the blood vessels and increasing blood pressure (see Fig. 2.2.1). The signalling pathways involved are discussed in more detail in Chapter 1 (see Fig. 1.2.2).

A more recent advance in the treatment of hypertension is the development of new antagonists of the angiotensin II receptors, such as candesartan cilexetril (reviewed in Unger *et al.*, 2000). The argument used in favour of AT_1 antagonists over existing ACE inhibitors is that ACE inhibitors competitively bind the catalytic site of ACE, and can thus be overwhelmed by excessive AngI production. This occurs when the negative feedback of AngII, namely the inhibition of angiotensinogen production, is abolished with the administration of ACE inhibitors. Also, the ACE inhibitors do not abolish the non-ACE pathways for AngII production, such as cathepsin G (see Fig 2.2.1), which may be up-regulated with increasing concentrations of AngI. AT_1 receptor antagonists will therefore block the effects of AngII, no matter which pathways are involved in its production, and also preserve the negative feedback on angiotensinogen production by AngII [Johnston, 2000; Swedberg, 2000]. It has also been proposed that the retroviral insertion of antisense mRNA to the AT_1 receptor could be used as a therapeutic method [Raizada *et al.*, 2000].

2.2.1) Localised RAS

The possibility also exists that a localised RAS may occur at both extra-renal and/or intracellular sites [Dzau VJ 1988; Re R 1988; Ehlers & Riordan, 1989; Dostal DE 1999; Unger T 2000; Phillips MI, 1993]. This assertion is based on the finding that many of the proteins involved in the RAS are expressed in extra-renal tissues, and could therefore produce AngII without the need for kidney-derived plasma renin or liver-derived angiotensinogen. AngII may even be generated directly from angiotensinogen by serine proteases like tonin and cathepsin G in the, hypothetical,

nonrenin-angiotensin system (NRAS) [Phillips MI, 1993]. Adding weight to this argument is the finding that angiotensin II can also be formed by proteolysis by the mast cell chymase (a serine protease), which cleaves AngI at the Phe^{8}-His^{9} bond [Caughey *et al.*, 2000; Chandrasekharan *et al.*, 1996; Ariel Gomez and Norwood, 1995].

2.2.2) Hypertension

Cardiovascular disease (CVD) accounts for a third of global deaths. It is the leading cause of death in the USA (33.3% of total deaths), and is projected to become the leading cause of death in developing countries by 2010 [CDC, 01; World Health Organisation, 01]. The cardiovascular diseases are a collection of diseases of the heart and blood vessels that includes: hypertension (high blood pressure), coronary heart disease (angina and heart attack), cerebrovascular disease (stroke), peripheral vascular disease, heart failure, rheumatic heart disease, congenital heart disease and cardiomyopathies. It is estimated that 3 million of the 17 million deaths due to CVD globally are the direct result of essential hypertension (i.e., hypertension with no known cause) [World Health Organisation, 01]. In addition, hypertension is the leading risk factor for both heart attacks and strokes, and is thus one of the major indirect causes of death globally.

It is estimated that 600 million people globally suffer from hypertension. The relatively innocuous symptoms for hypertension, which include headaches, tiredness, nausea, anxiety, perspiration and chest pain, belie the seriousness of this disease. It is 'arbitrarily' defined as a resting systolic and diastolic blood pressure (BP) of greater than or equal to 140 and 90 mm Hg, respectively, while normal BP is 120 and 80 mm Hg, respectively. Hypertension can be seen as something of a gateway disease, having numerous aetiologies (such as kidney failure which increases sodium and water retention), but also causing numerous secondary cardiovascular diseases that are often debilitating or fatal.

The discovery of Hypertension timeline		
Ancient Chinese	'Hardening of the pulse' first described.	
W. Harvey (1578-1657)	Discovered the circulation of blood.	
Rev S. Hales (1677-1761)	Developed blood pressure measurement in horses (found to be 8 feet and 3 inches of blood in a vertical glass tube).	
R. Bright (1789-1858)	Observed left ventricular hypertrophy in patients with chronic renal disease.	
Sir W. Withey Gull (1816-1891)	Showed thickening of small artery walls independent of renal disease.	
F. Mahomed (1849-1884)	Adapted Marey's sphygmograph for BP crude measurement, showed independence of increased BP from renal disease and association with cardiac failure and strokes.	
S. Riva-Rocci (1863-1920)	Designed air-filled rubber bag for brachial systolic BP measurement.	
N. S. Korotkoff (1874-1920)	Noticed that the first sound on deflation of a Riva-Rocci cuff relates to systolic BP, and pressure at the disappearance (or muffling) of blood sounds is diastolic BP. This rapidly led to epidemiological studies relating hypertension to CVD.	
Tigerstedt & Bergman	Showed kidneys contained vasopressor substance when injected into rabbits	
Ambard & Beaujerd (~1900)	Showed increased BP in renal disease patients with salt loading. Found to be due to Na^+, not Cl^-, in 1920's with the development of the flame photometer.	
H. Goldblatt (1934)	Produced hypertension in dogs by partial constriction of renal arteries.	
Framingham Study (1948-)	1948	5209 residents of Framingham (USA) start longest-running major epidemiological project in medicine.
	1960	Cigarette smoking found to increase the risk of heart disease
	1961	Cholesterol level, blood pressure, and electrocardiogram abnormalities found to increase the risk of heart disease
	1967	Physical activity found to reduce the risk of heart disease and obesity to increase the risk of heart disease
	1970	High blood pressure found to increase the risk of stroke
	1976	Menopause found to increase the risk of heart disease
	1978	Psychosocial factors found to affect heart disease
	1988	High levels of HDL cholesterol found to reduce risk of death
	1994	Enlarged left ventricle shown to increase the risk of stroke
	1996	Progression from hypertension to heart failure described

Table 2.2.2.1) Timeline for the discovery of Hypertension
Adapted from [Swales, 1995]. See also: http://rover.nhlbi.nih.gov/about/framingham/index.html

The discovery of blood pressure and hypertension, shown in Table 2.2.2.1, highlights some of the major advances in modern medicine. The ability to rapidly and easily measure brachial blood pressure led to large epidemiological studies that soon showed a clear correlation between elevated blood pressure and the risk of heart disease. Initial studies compared the average blood pressure of different human populations, and found that people in 'westernised' societies showed both elevated BP, and a progressive increase in BP with age, which is absent in rural communities. The major changes associated with urbanisation and 'development' is predominantly an increase in stress, smoking, salt intake and weight (due to an increase in consumption of

animal proteins, simple carbohydrates and saturated fats, combined with a reduction in exercise). More precise data regarding the epidemiologically associated causes of hypertension were, and still are, gathered from the Framingham study, initiated in 1948 and co-opting the help of 20% of the town of Framingham in the USA (see Table 2.2.2.1). Most importantly, this study showed that heart failure occurred six times more commonly in hypertensives than in normotensive subjects.

How does the elevated blood pressure, derived from numerous different causes, result in elevated risk of heart disease and strokes? It appears that chronic hypertension and the sustained vasoconstricting stimulus induces the arteriosclerotic remodelling and/or hypertrophy of the walls of the larger arteries, resulting in a permanently narrowed lumen. Smooth muscle cells migrate through the elastic lamina layer of the arteries and lay down collagen, obstructing blood flow and thus further increasing blood pressure. Eventually the heart, the left ventricle of which becomes enlarged to compensate for the increased resistance against which it works, is unable to sustain sufficient cardiac output. Tissue perfusion drops, as the arteries are unable to dilate in response to the compensatory vasodilation, causing localised oxygen starvation and necrosis in the affected tissues (infarction). In the cerebrum this results in stroke, in the kidney it results in renal failure (and thus exacerbation of the hypertension), while in the heart muscle tissue it results in heart attack and an extremely poor prognosis [reviewed in Swales, 1995].

It is therefore vital that hypertension is effectively treated by either removal of the excess water load by diuretics, increasing vasodilation, or switching off the vasopressor drive. The latter can be achieved by inhibiting either the RAAS, using ACE inhibitors (e.g. Lisinopril) or angiotensin II receptor antagonists (e.g. Losartan), or the central sympathetic drive with Reserpine, or the effect of catacholamines with beta-blockers.

Although it is tempting to speculate that ACE activity may be down-regulated by shedding from the endothelial surface, this is unlikely as both the soluble and membrane-bound forms of ACE have similar half lives and enzymatic activity. The membrane-bound form, however, is involved in kidney development (detailed below), although its exact function is as yet unclear.

2.3) ACE and fertility

By the early 1970's the RAAS had been clearly established, the corner stone of which was the endothelium-bound ACE found in the vascular beds of numerous organs. It was therefore somewhat surprising that the testes and epididymis of rats contained high concentrations of ACE (but less in the prostate, vas deferens and penis) [Cushman and Cheung, 1971]. Cushman & Cheung were the first to propose not only that ACE was associated with mature sperm cells and readily released ('shed') into the tubular fluid, but also that the enzyme plays a role in spermatogenesis or sperm motility [Cushman and Cheung, 1971]. At the time it was assumed that the ACE activity measured from these tissue extracts was due to the 'pulmonary' form of ACE. However, the identification [Polsky-Cynkin and Fanburg, 1979], isolation [El Dorry *et al.*, 1982a], cloning [Ehlers *et al.*, 1989a], and localisation [Yotsumoto *et al.*, 1984, Langford *et al.*, 1991] of testicular ACE showed that elongating spermatids specifically expressed ACE_T, and that this form was likely to be involved in mammalian fertility (see Table 2.3.1).

Krege *et al.* showed that *ace*$^{-/-}$ knockout mice, in which both the somatic and testis forms have been inactivated, have much reduced blood pressure, major renal abnormalities, and male (but not female) infertility (see Fig. 2.3.1, [Krege *et al.*, 1995]). Esther *et al.* excluded the reduced blood pressure in these animals as a cause for infertility by creating transgenic mice that expressed a soluble form of the somatic ACE N-domain, and showed significant levels of plasma ACE activity [Esther *et al.*, 1997]. These mice lacked both membrane-bound forms of ACE and males remained infertile, indicating that a membrane-bound form of ACE is necessary for male fertility.

Male fertility in mice was restored in *ace*$^{-/-}$ mice using the sperm-specific expression of testis ACE [Hagaman *et al.*, 1998; Ramaraj *et al.*, 1998]. These transgenic mice expressed wild type membrane-bound ACE_T in sperm, but expressed no ACE in any other tissues, and thus showed reduced blood pressure. The authors therefore concluded that somatic ACE is not essential for normal male fertility, while the sperm-specific expression of ACE_T is essential. This raises the question of whether or

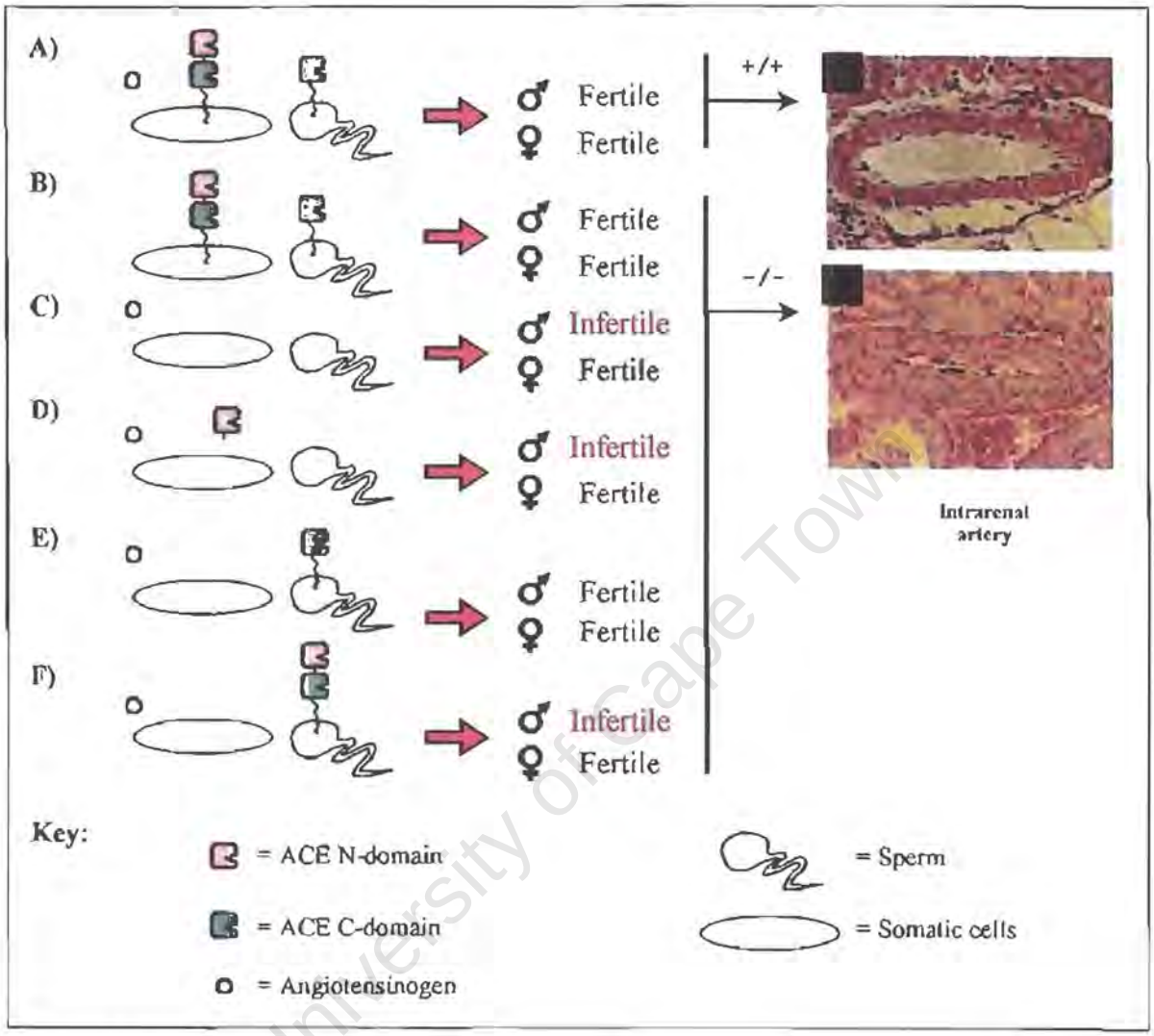

Figure 2.3.1) ACE and fertility

The genotypes of different transgenic mice are indicated as expressing angiotensinogen, ACE_T, ACE_S or combinations thereof, expressed either in somatic cells or the sperm in these mouse strains. The wild-type genotype, showing normal renal development, and fertility is shown in (A), while the *angiotensinogen*$^{-/-}$ mice (B) die shortly after birth, have reduced blood pressure, show thickening of the intrarenal arterial wall (section shown on right) and thin, atrophied renal cortex, while remaining fertile [Tanimoto *et al.*, 1994; Kim *et al.*, 1995]. The *Ace*$^{-/-}$ knockout (KO) mouse (C) shows similar renal abnormalities, but also shows male infertility [Krege *et al.*, 1995] which could not be rescued by the systemic expression of a soluble ACE N-domain (D) [Esther *et al.*, 1997], or the sperm-specific expression of ACE_S (F) [Kessler *et al.*, 2000]. Fertility was, however, restored with the sperm-specific expression of ACE_T (E) [Hagaman *et al.*, 1998; Ramaraj *et al.*, 1998].

not ACE acts as a protease in this context, or whether it acts structurally to bind sperm to the egg or to the female reproductive tract.

Support for the enzymatic activity of ACE_T being involved in fertility comes from early work showing that Captopril treatment of isolated sperm reduces acrosome reaction and oocyte penetration [Foresta *et al.*, 1991]. However, it is unlikely that the ACE_T substrate is Angiotensin I in this instance, as *angiotensinogen*$^{-/-}$ mice show normal fertility in both sexes (Fig. 2.3.1b, [Tanimoto *et al.*, 1994; Kim *et al.*, 1995]).

The intriguing possibility that ACE_T acts non-enzymatically by binding in a lectin-like manner to the oviductal epithelia or the zona pellucida (surrounding the egg) is gaining support, although evidence is as yet circumstantial. During their arduous migration from the vagina to the oocyte, sperm are stored in the oviductal isthmus prior to fertilization. This brief respite requires tight binding of the sperm's periacrosomal plasma membrane to the oviductal epithelium. Sperm-oviduct binding is likely a lectin-like interaction, as it can (i) be inhibited with the addition of sugars, (ii) carbohydrates can bind spermatozoa, and (iii) the oviductal epithelia show a species-dependent differential glycosylation pattern (see refs in Dobrinski *et al.*, 1997). In this context it is interesting to note that Hagaman *et al.* showed that the reduced fertility shown by *ace*$^{-/-}$ mice was due to reduced binding of sperm to the zona pellucida, and not to other sperm parameters such as number, longevity, motility or the capacity for acrosome reaction [Hagaman *et al.*, 1998]. Added to this, Kessler *et al.* have recently shown that somatic ACE cannot act as a substitute for ACE_T to restore male fertility in *ace*$^{-/-}$ mice [Kessler *et al.*, 2000]. This is a very surprising result, as ACE_S contains the C-domain of ACE_T and therefore should compensate for the enzymatic function missing in $ACE_T^{-/-}$ sperm. It is all the more perplexing if one hypothesises that ACE_T acts on an as yet unidentified substrate in sperm or in the female genital tract as a pre-requisite for acrosome reaction and oocyte penetration [Foresta *et al.*, 1991; Tanimoto *et al.*, 1994]. However, ACE_T contains a unique 36-residue highly O-glycosylated region that is not present in ACE_S (see Fig. 2.3.2) [Ehlers *et al.*, 1992]. It is thus highly likely that the N-terminal region of ACE_T acts in a lectin-like binding manner between sperm and either the oviductal epithelium or the zona pellucida of the egg in a (species) specific manner that is essential for fertilization to take place; however, this has not been proven.

The recent knockout experiments in mice also indicate that the localised, intraovarian RAS is not likely involved in fertility, as both *angiotensinogen*$^{-/-}$ and *ace*$^{-/-}$ knockout female mice are fertile [Tanimoto *et al.*, 1994; Krege *et al.*, 1995]. These data also indicate that the recently isolated homologue of ACE (ACEH/ACE2, [Tipnis *et al.*, 2000; Donoghue *et al.*, 2000]) is probably not involved in fertility, although it shows similarities in structure to ACE_T, with a single zinc-metalloprotease domain showing 42% identity over 556 residues to ACE_T. Furthermore, ACEH does not contain the highly O-glycosylated 36 residue N-terminal region of ACE_T.

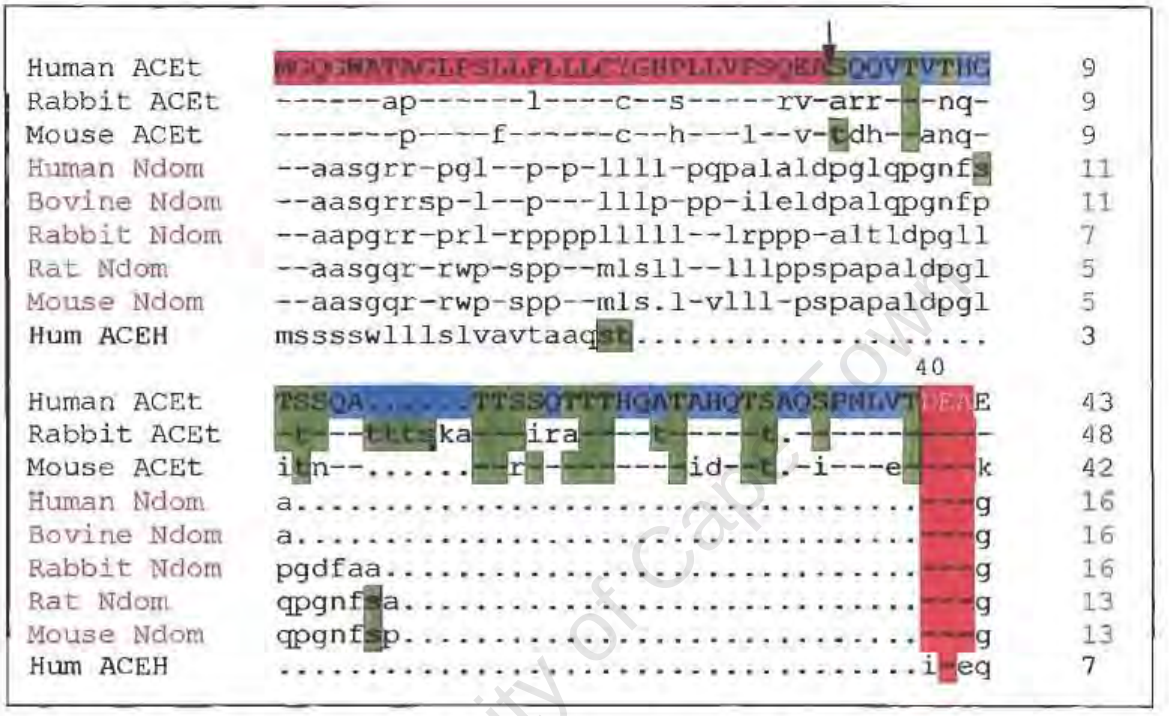

Figure 2.3.2) The O-glycosylated N-terminal region of testis ACE

The N-terminal regions of human, rabbit and mouse ACE_T (blue labels) are compared to the somatic forms of human, rabbit, mouse, bovine and rat ACE_S (red labels). The ACE homologue ACEH/ACE2 is also compared. The ACE_T signal peptide is shown in mauve, with the signal peptidase cleavage site indicated by an arrow. The beginning of the ACE domain ([DEA...], N- and C-domains) is highlighted in red. The highly O-glycosylated N-terminal region on ACE_T is highlighted in blue, with Ser and Thr residues (attachment sites for O-glycosylation) highlighted in green. Note the relative paucity of possible O-glycosylation sites in the region downstream of the signal peptide of somatic ACE. Full sequences are in Appendix III.

ACE and fertility timeline:		
~1970	ACE established as the central enzyme in RAS.	
1971	High concentrations of ACE found in mature rat testes and epididymis. Proposal that ACE is predominantly in mature sperm, is 'released' into seminal fluids and may play a role in fertility.	Cushman and Cheung, 1971
1978	ACE_S found in seminal plasma.	Depierre *et al.*, 1978
1979	ACE_T identified through cross-reactivity with pulmonary antibodies.	Polsky-Cynkin and Fanburg, 1979
1982	Human ACE_T isolated using affinity purification. *In vitro* translation of testis mRNA shows smaller ACE isoform.	El Dorry *et al.*, 1982a; El Dorry *et al.*, 1982b
	The NH_2- and COOH-terminal sequences of rabbit lung and testis ACE differ.	Iwata *et al.*, 1982
1983	Soluble seminal fluid ACE found to be $sACE_S$ not $sACE_T$.	El Dorry *et al.*, 1983
1984	Pig ACE localised to the spermatids and residual bodies in the Sertoli cells of the testis using immunofluorescence. ACE found in the cytoplasmic droplet of epididymal sperm and in detached cytoplasmic droplets in semen.	Yotsumoto *et al.*, 1984
	Rat ACE found in acrosomal region of sperm ([3H]Captopril). Epididymis ACE is same as ACE_P, but testis ACE is unique (mAb to ACE_P).	Strittmatter and Snyder, 1984
1985	Two active isoforms of ACE found in testes. 140 kDa form & 90 kDa form.	Lanzillo *et al.*, 1985
1987	Ovarian RAS identified. Immunoreativity of renin and AngII in follicular fluid.	Lightman *et al.*, 1987
1988	Mouse ACE_S cDNA cloned and sequenced.	Bernstein *et al.*, 1988
1989	Human ACE_T cDNA cloned and sequenced.	Ehlers *et al.*, 1989a
1990	Captopril treatment of rats does not affect epididymal ACE or fertility.	Wong and Uchendu, 1990
1991	Captopril treatment of isolated human sperm did not affect sperm motility, nor viability, but significantly reduced acrosome reaction and oocytes penetration.	Foresta *et al.*, 1991
	Testis specific promoter identified in intron 12 of the *ace* gene using a beta-galactosidase reporter gene.	Langford *et al.*, 1991
1993	Mouse ACE_T mRNA first expressed in late pachytene spermatocytes	Langford *et al.*, 1993
1994	*Angiotensinogen*$^{-/-}$ knockout mice created. Males and female are fertile.	Tanimoto *et al.*, 1994
	AngII and OVRAS proposed to be involved in follicular atresia, polycystic ovarian syndrome and oocytes maturation and ovulation.	Pepperell *et al.*, 1994
1995	*ace*$^{-/-}$ knockout mice created (both $ACE_S$$^{-/-}$ and $ACE_T$$^{-/-}$). Females show normal fertility, while males are infertile. Both sexes show severe renal abnormalities and low blood pressure.	Krege *et al.*, 1995
1997	Plasma levels of ACE in *ace*$^{-/-}$ KO mice 'rescued' with soluble form of ACE N-domain. Renal abnormalities and male infertility persist, indicating importance of membrane-bound ACE in fertility and renal development.	Esther *et al.*, 1997
1998	Human ACE_T localised to plasma membrane of acrosomal region, equitorial segment, postacrosomal region and midpiece of sperm.	Kohn *et al.*, 1998
	cAMP response element in promoter (and CREM) required for ACE_T expression	Kessler *et al.*, 1998
	Male fertility in *ace*$^{-/-}$ mice restored with sperm-specific ACE_T expression. Sperm from *ace*$^{-/-}$ mice show reduced binding to zona pellucida.	Hagaman *et al.*, 1998; Ramaraj *et al.*, 1998
	AT_{1A} and AT_{1B} AngII receptor knockouts in rat.	Oliverio *et al.*, 1998
2000	Sperm-specific expression of ACE_S could not restore male fertility in *ace*$^{-/-}$ mice. Implicates the necessity of the N-terminal 36 aa of ACE_T in fertility.	Kessler *et al.*, 2000
2001	ACE_T measured in human spermatozoa membranes	Kamata *et al.*, 2001

Table 2.3.1) ACE and fertility timeline.

2.4) ACE shedding

Although ACE was initially isolated from horse blood, far higher activities were noted in the vascular epithelium of the lung and kidneys, indicating that the soluble plasma form may have been incidental. Later it became increasingly clear that a stable form of ACE is present in blood plasma and most body fluids [Yotsumoto *et al.*, 1983; Erdos and Skidgel, 1987], and that this form of ACE may be due to 'shedding' of the membrane bound form (see Table 2.4.1) [Matsuo *et al.*, 1985; Gronhagen-Riska *et al.*, 1985]. The sequencing of the ACE_S cDNA showed that ACE contains a hydrophobic anchor at its C-terminus and is thus a type I ectoprotein [Soubrier *et al.*, 1988]. Hooper & Turner excluded the possibility that this region was a signal for GPI-linkage [Hooper and Turner, 1989]. They found that the amphipathic form of pig kidney ACE_S is not cleaved by glycosylphosphatidylinositol-specific phospholipases C or D, and does not contain inositol. This indicated that ACE is in fact bound to the cell surface through its hydrophobic transmembrane region, and that release into the medium would have to occur through proteolytic cleavage, probably at the juxtamembrane stalk region.

Ehlers *et al.* delivered the definitive proof that ectodomain shedding occurs through limited proteolysis when examining the spontaneous release of a hydrophilic form of ACE into the medium of CHO cells expressing the newly cloned human ACE_T cDNA [Ehlers *et al.*, 1991b]. They showed, using Triton X114 phase separation, that the large quantity of soluble ACE_T appearing in the medium of the transfected CHO cells was hydrophilic, and thus not due to the destruction/release of plasma membrane, but was instead due to the proteolytic removal of the hydrophobic anchor. This was corroborated by Wei *et al.* when they found that full-length ACE_S cDNA expressed in CHO cells is secreted into the medium through post-translational processing at the C-terminus [Wei *et al.*, 1991b].

Shedding is also stimulated with phorbol ester (PKC activator), and this stimulation is abolished with staurosporin, a PKC inhibitor [Ehlers *et al.*, 1995]. The shedding of ACE from isolated pig membranes is strongly inhibited by EDTA and 1,10-phenanthroline, but not EGTA and numerous inhibitors specific for different classes

of protease, indicating that shedding is due to a zinc-metalloprotease [Oppong and Hooper, 1993]. These authors also show that shedding is not an autocatalytic event because the ACE inhibitors Captopril, Enalaprilat and Zofenoprilat have no effect on shedding [Oppong and Hooper, 1993].

The suggestion that ACE_S is solubilized through alternative splicing [Sugimura *et al.*, 1998] is hard to reconcile with the PKC activation of the ACE secretase [Parvathy *et al.*, 1997], which occurs in seconds and does not require cytosolic components or *de novo* translation [Ramchandran *et al.*, 1994]. Also, Soubrier *et al.* found a single mRNA transcript in endothelial cells, which would rule out alternative splicing of a common transcript [Soubrier *et al.*, 1988], and Oppong and Hooper developed a cell-free assay system for ACE shedding and showed that the ACE sheddase is completely inhibited by the zinc metalloprotease inhibitors 1,10-phenanthroline and EDTA [Oppong and Hooper, 1993].

The development of cell-free assay systems for analysing ACE shedding has also been instrumental in showing that the ACE sheddase is an integral membrane protein [Oppong and Hooper, 1993; Ramchandran and Sen, 1995], that requires its substrate to be membrane bound [Parvathy *et al.*, 1997; Sadhukhan *et al.*, 1999]. Ramchandran *et al.* used purified membranes from ACE-expressing CHO cells [Ramchandran and Sen, 1995], while Parvathy *et al.* found that pig microvillar membranes contain significant quantities of membrane-bound ACE and lack detectable secretase activity [Parvathy *et al.*, 1997]. The finding that Triton X-100 solubilized secretase needs ACE either to be stabilised by lisinopril-sepharose [Sadhukhan *et al.*, 1999], or inserted in a bilayer [[Parvathy *et al.*, 1997], is of fundamental importance to the study of ACE shedding, as other sheddases like TACE were isolated using a soluble stalk peptide as substrate [Black 1997; Moss 1997], a method that can thus not be used in the isolation of the ACE sheddase.

The cleavage site for both rabbit [Ramchandran *et al.*, 1994] and human [Ehlers *et al.*, 1996] testis ACE was found to be at the R_{627}/S_{628} bond (human ACE_T numbering). This cleavage site differs markedly from both the proposed C-terminal end (A_{1116}) of an alternatively spliced form of ACE [Sugimura *et al.*, 1998], or the cleavage site (R_{1137}/L_{1138}), 90 amino acids from the transmembrane domain, proposed by the

Corvol laboratory [Beldent *et al.*, 1995]. Woodman *et al.* have also recently shown that both porcine and human ACE_S are cleaved at R_{1203}, the same cleavage site found in ACE_T, in both *in vivo* and *in vitro* systems [Woodman *et al.*, 2000]. It is now well established that both testis and somatic ACE are cleaved at the R_{627}/S_{628} and R_{1203}/S_{1204} bond respectively, 24 residues from the TM [Ramchandran *et al.*, 1994; Ehlers *et al.*, 1996; Woodman *et al.*, 2000].

Although they share a cleavage site, the shedding kinetics is markedly different for ACE_S and ACE_T, with the rate of phorbol-activated shedding of ACE_S a 10^{th} that of ACE_T [Woodman *et al.*, 2000; Beldent *et al.*, 1995]. The large, glycosylated, N-domain may cause steric hindrance of the sheddase cleavage site, or occlude a recognition motif in the C-domain, thus making the smaller ACE_T a more convenient model for the study of ectodomain shedding.

The soluble form of ACE is catalytically active and stable, and thus the role of shedding of ACE in normal physiology is unclear, and is probably not involved in the down-regulation of ACE [Lanzillo and Fanburg, 1977]. Further, plasma ACE is probably protected from degradation in the liver by sialic acid moieties at the ends of its extensive carbohydrate chains [Ehlers and Riordan, 1990]. However, the creation of a transgenic mouse lineage that contained only a soluble form of ACE, by Esther *et al*, helped to elucidate the role of the membrane-bound form of ACE in normal blood pressure regulation and renal development and physiology [Esther *et al.*, 1997]. These authors created a transgenic mouse mutant that could only express the soluble N-terminal domain of somatic ACE. The homozygous mutant mice had 34% of the wild-type plasma ACE activity, and no tissue- or sperm-associated ACE activity, which resulted in infertile mice with low blood pressure, high urinary flow and renal histological pathologies similar, but not as extreme, as the $ace^{-/-}$ knockout mice [Esther *et al.*, 1997]. This implies either that the C-domain is essential for blood pressure regulation, or that the membrane-bound form of ACE, specifically, plays the major part in ACE-related blood pressure regulation, renal development and urine concentration, possibly through a pivotal role in an extremely localised RAS. This membrane bound form may also play a role in male fertility through a ligand-receptor interaction between sperm and egg or oviductal epithelium. It is unfortunate that a knockout mouse expressing only a soluble form of ACE_S, containing both the N- and

N- and C-domains, was not created. This would clarify the effect of relative importance of the absence of the active C-domain or the loss of the cell-associated ACE in this mouse model. A detailed understanding of how the membrane-bound form of ACE is shed through limited proteolysis may help to clarify the physiological role of ACE shedding.

Curiously, another soluble form of ACE has been isolated from the luminal fluid of the ileum, and appropriately named ileal ACE (ACE_I) [Deddish *et al.*, 1994]. It was found to be the N-domain of somatic ACE that had apparently been cleaved in the bridge region between the two domains (see Fig. 2.4.1). The function of this soluble form of ACE is unknown, as is the identity of the releasing protease, which may be any of a number of intestinal proteases.

Table 2.4.1) ACE and shedding timeline		
1982	Bovine aortic cell cultures produce soluble form	Mendelsohn *et al.*, 1982
1983	A catalytically active 90-kDa fragment of ACE generated from 140kDa human plasma $sACE_S$ after treatment with 6M urea, trypsin, chymotrypsin, V8 proteinase, ammonium hydroxide and H_2O_2. Shows that core structure of ACE is stable. Degradation not autocatalytic.	Yotsumoto *et al.*, 1983
1985	Immune complexes of ACE 'shed' from rabbit oocyte oolemma onto zona pellucida.	Matsuo *et al.*, 1985
	Thyroid hormones may increase plasma ACE through 'shedding'.	Gronhagen-Riska *et al.*, 1985
1986	Porcine aortic endothelial cells produce soluble ACE.	Dickinson *et al.*, 1986
1987	EDTA-sensitive hydrolase releases ACE from lung and kidney.	Hooper and Turner, 1987
1991	Transfection of full-length, membrane-bound ACE into CHO cells results in spontaneous release of a soluble form. Shedding of ACE proposed.	Ehlers *et al.*, 1991b
	Transfected mouse epithelial cells secrete rabbit testis ACE. Soluble ACE is smaller, contains no hydrophobic domain.	Sen *et al.*, 1991
	Plasma ACE hydrophilic, lacks cytoplasmic tail.	Wei *et al.*, 1991b
1993	ACE shedding found not to be autocatalytic.	Oppong and Hooper, 1993
1994	Mouse ACE cleavage-secretion identified at cell surface, post Golgi apparatus, not in lysosomal compartment. Shedding is stimulated with phorbol esters. Cleavage site identified for mouse ACE, R663/S664 (same as R627/S628).	Ramchandran *et al.*, 1994
1995	Secreted and cell-bound ACE show similar ACE activities (in both domains).	Jaspard *et al.*, 1993
	ace$^{-/-}$ knockout mice created (both $ACE_S^{-/-}$ and $ACE_T^{-/-}$). Females show normal fertility, while males are infertile. Both sexes show severe renal abnormalities and low blood pressure.	Krege *et al.*, 1995
	ACE sheddase is an integral membrane protein. Cell free assay system developed.	Ramchandran and Sen, 1995
1996	Human ACE sheddase cleavage site found (R627/S628). Sheddase recognition not in footroom, can cleave alternative stalk sequences. Min stalk 11 residues.	Ehlers *et al.*, 1996
	Cleavage-secretion of rabbit ACE_T in yeast.	Sadhukhan *et al.*, 1996
1997	Plasma levels of ACE in *ace*$^{-/-}$ KO mice 'rescued' with soluble form of ACE N-domain. Renal abnormalities and male infertility persist, indicating importance of membrane-bound ACE in fertility and renal development.	Esther *et al.*, 1997
	Sheddase is inhibited by zinc metalloprotease inhibitors and needs substrate ACE in lipid bilayer. Pig microvillar membranes contain no sheddase, used in cell-free assay.	Parvathy *et al.*, 1997
1998	ACE/CD4 chimeras show that the ACE ectodomain is essential for shedding. ACE stalk, TM and cytoplasmic tail not necessary for shedding.	Sadhukhan *et al.*, 1998
	ACE and βAPP are not cleaved by TACE.	Parvathy *et al.*, 1998
	Cleavage-secretion even occurs with an EGF-knotted stalk. Tethering through third disulphide may be used by receptors to escape shedding.	Schwager *et al.*, 1998
1999	TACE is not the ACE sheddase. TACE$^{-/-}$ knockout cells are able to shed ACE. Triton X-100 solubilized sheddase needs lisinopril-sepharose-stabilised substrate for cleavage.	Sadhukhan *et al.*, 1999
	Cleavage-secretion also occurs with highly glycosylated stalks, but site shifted. ACE sheddase has broad cleavage site sequence specificity, if any.	Schwager *et al.*, 1999
2000	Human and porcine, testis and somatic, *in vivo* and *in vitro* cleavage site found to be 24 amino acids from the TM at R627/S628 and R1203/S1204 respectively.	Woodman *et al.*, 2000
2001	ACE stalk directs cleavage of non-shed GPI-linked MDP, at wt R_{627}/S_{628} site. ACE-Ndom (ACEDeltaC), in which C-domain deleted, is not shed.	Pang *et al.*, 2001

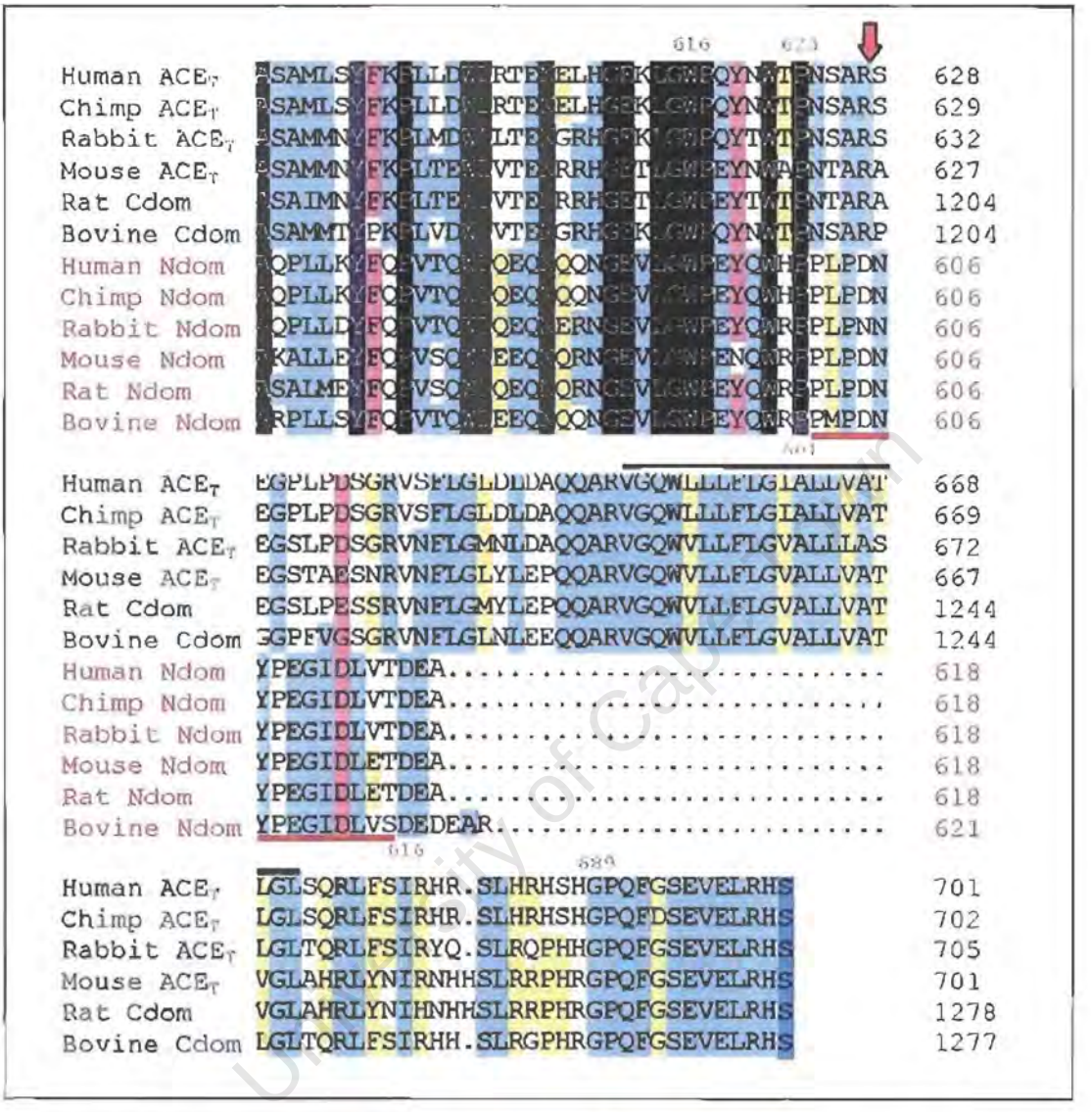

Figure 2.4.1) Comparison of all mammalian ACE juxtamembrane stalks

The primary sequences of both the N-domain (in red) and C-domain (in blue) of ACE molecules from different mammalian species are compared. Note that the last conserved amino acid between the N- and 'C'-domains are P_{623} and P_{601} for human testis and somatic ACE respectively. Note also that the 'bridge' region between the two domains in ACE_S (indicated by a red bar) spans P_{602} thru T_{613}, with the C-domain starting at D_{616}. Curiously, the last 13 amino acids of all mammalian ACE molecules are highly conserved. Alignment performed using Lynnon BioSoft DNAMAN using sequences listed in Appendix III. Black, pink, blue and yellow highlighted regions refer to 100%, >= 75%, >= 50%, and >= 35% identity respectively. The transmembrane region is indicated with a black bar. The human ACE_T sheddase cleavage site is indicated with a red arrow.

2.5) Finding the sheddase recognition motif

From the literature reviewed in Chapter 1, it is clear that numerous ectoproteins are released from the cell surface by a sheddase (or family of sheddases) through cleavage in the juxtamembrane stalk region, and that the universal sheddase recognition motif(s) remains elusive.

The variety of shed ectoproteins (and thus 'stalks') cleaved by the same sheddase is most clearly illustrated by the work of Peschon *et al*, when they created $TACE^{-/-}$ mice by knocking out the mouse TNFα convertase gene and showed that the shedding of not only TNFα, but also TNFR, L-selectin, TGF-α and APP was abrogated in these mice [Peschon *et al.*, 1998]. One would expect that these stalk regions, although very different, would show some sequence or structural homology (see Fig. AI.3). However, homology alignments using the stalk region of shed ectoproteins have thus far failed to shed further light on the sheddase recognition motif other than a predicted open, extended structural conformation which is a universal characteristic of all protease substrates [Tyndall and Fairlie, 1999]. Furthermore, $TACE^{-/-}$ cells are able to cleave-secrete ACE, showing that TACE is not the ACE sheddase [Sadhukhan *et al.*, 1999], a finding which corroborates *in vitro* studies [Parvathy *et al.*, 1998].

The only reported consensus region for shedding reported to date is that found in the Ephrin-A2 ectodomain, which is proposed to direct the cleavage-release of Ephrin-A2 by Kuz [Hattori *et al.*, 2000]. This region, [(K/R)FE(I/V/L)(K/R)(F/Y)QEFV], is apparently conserved in the ectodomain of numerous Kuz substrates, namely all 8 vertebrate ephrins, Delta, TNF-α and βAPP. It has not been found in ACE, nor has it been shown to direct the shedding of a non-shed ectoprotein. Thus there is still a pressing need to find the 'universal' sheddase recognition motif, or at least understand how the membrane bound sheddase decides the fate of numerous ectoproteins.

An experimental approach

The finding that ACE, a type I ectoprotein, is shed from the surface of cells makes this enzyme a useful model system for studying ectodomain shedding. The flexibility of substrate specificity shown by ACE has been exploited in the development of sensitive assays for ACE that make use of substrate analogues, e.g. hippuryl-$_L$-histidyl-$_L$-leucine (Hip-His-Leu) and furylacryloyl-Phe-Gly-Gly [Holmquist *et al.*, 1979; Piquilloud *et al.*, 1970; Ryan, 1988]. ACE catalytic activity can thus be measured in cells and medium, to monitor the rate of ACE shedding into the medium, without the need for radioactive immunoprecipitation. This makes ACE an excellent candidate for the dissection of ectodomain shedding, as the medium-associated ACE activity not only indicates the rate of shedding, but that the enzyme is structurally sound, an advantage over immunoprecipitation. ACE is also expressed in numerous different tissues in the body, and is therefore likely to be expressed in many cell-culture systems.

The shedding of human testis ACE from CHO cells has been extensively characterised [Ehlers *et al.*, 1991b; Sen *et al.*, 1991]. The mammalian expression vector encoding the human testis ACE cDNA (pLEN-ACEVII) was constructed by Ehlers *et al.* [Ehlers *et al.*, 1991b], and shown to be capable of inducing the expression of significant quantities of membrane-bound wtACE in the CHO-K1 cell culture system. Although CHO cells do not express endogenous ACE, the transfected membrane-bound form of both recombinant human ACE_T and ACE_S are shed from the cell surface into the culture medium, and this cleavage site is the same as that used *in vivo* to release human seminal ACE_S [Ehlers *et al.*, 1996; Woodman *et al.*, 2000].

In an attempt to identify and characterise the sheddase recognition motif, we deleted sections of ACE_T with the expectation that at least one of these deletions would result in a non-shed ACE mutant, from which we could infer that a region involved in sheddase recognition had been removed. Our initial attempts focused on mutating regions of the ACE juxtamembrane stalk region (see Chapter 4), as this seemed the most likely site for sheddase recognition of ACE. We also examined the relative importance of stalk accessibility for shedding, by either decreasing the distance from

the proximal ectodomain and the cleavage site (termed 'headroom'), or inserting an N-linked glycosylation site just upstream of the cleavage site. Furthermore, we have established the lack of sequence specificity of the sheddase by inserting entirely different peptide sequences into the ACE stalk and identifying the cleavage site used by the sheddase. The cytoplasmic tail (Chapter 5) and the ectodomain (Chapter 6) were also analysed using mutagenesis to define their respective roles in ectodomain shedding.

Chapter 3: Materials and Methods

The methods used in this thesis include: recombinant DNA methods to construct expression vectors containing mutant human testis ACE proteins; transfection and expression of these constructs in CHO or COS1 cells; detection of protein using enzyme assays, Western blotting and metabolic labelling; analysis of the rate of shedding into the culture medium; surface FITC labelling of fixed CHO cells; affinity purification of the soluble protein and identification of the cleavage site using mass spectroscopy. Protocols that are described explicitly in Appendix II and recipes for buffers that appear in Appendix III are highlighted in bold. Boehringer Mannheim supplied all restriction enzymes and Sigma Aldrich Company Inc. supplied all other reagents, unless otherwise indicated.

3.1) Vector construction

All expression vectors encoding mutant human testis ACE (ACE_T) proteins are based on the vector pLEN-ACEVII [Ehlers *et al.*, 1991a,b]. Three basic methodologies were used, based on the two-stage PCR-based mutagenesis protocol described previously [Ehlers *et al.*, 1996], to either insert or delete residues from the stalk region of ACE_T, or swap the N- and C-domains. All constructs were verified by restriction mapping and sequencing of PCR-products in the pBS-SK sequencing vector (Stratagene). All primers used are listed in Table AIII.1.

3.1.1) Deletion mutants

ACE-Δ6JM: The plasmid encoding the ACE-Δ6JM mutant, namely pLEN-ACE-Δ6JM, was constructed using the two-stage **polymerase chain reaction** (PCR) strategy, involving the amplification of nucleotides (nt) 1854-1975 and nt 1994–2221 of full length ACE_T cDNA [Ehlers *et al.*, 1989] with pairs of primers designed to generate overlapping hybrid sequences (see Fig. 3.1.1.1, Fig. 4.1.1). The products were mixed and re-amplified using the outside primers (ACE-MP2 and ACE-MP3) to generate a recombinant sequence from which nt 1976-1993 [encoding W_{621}-A_{626}]

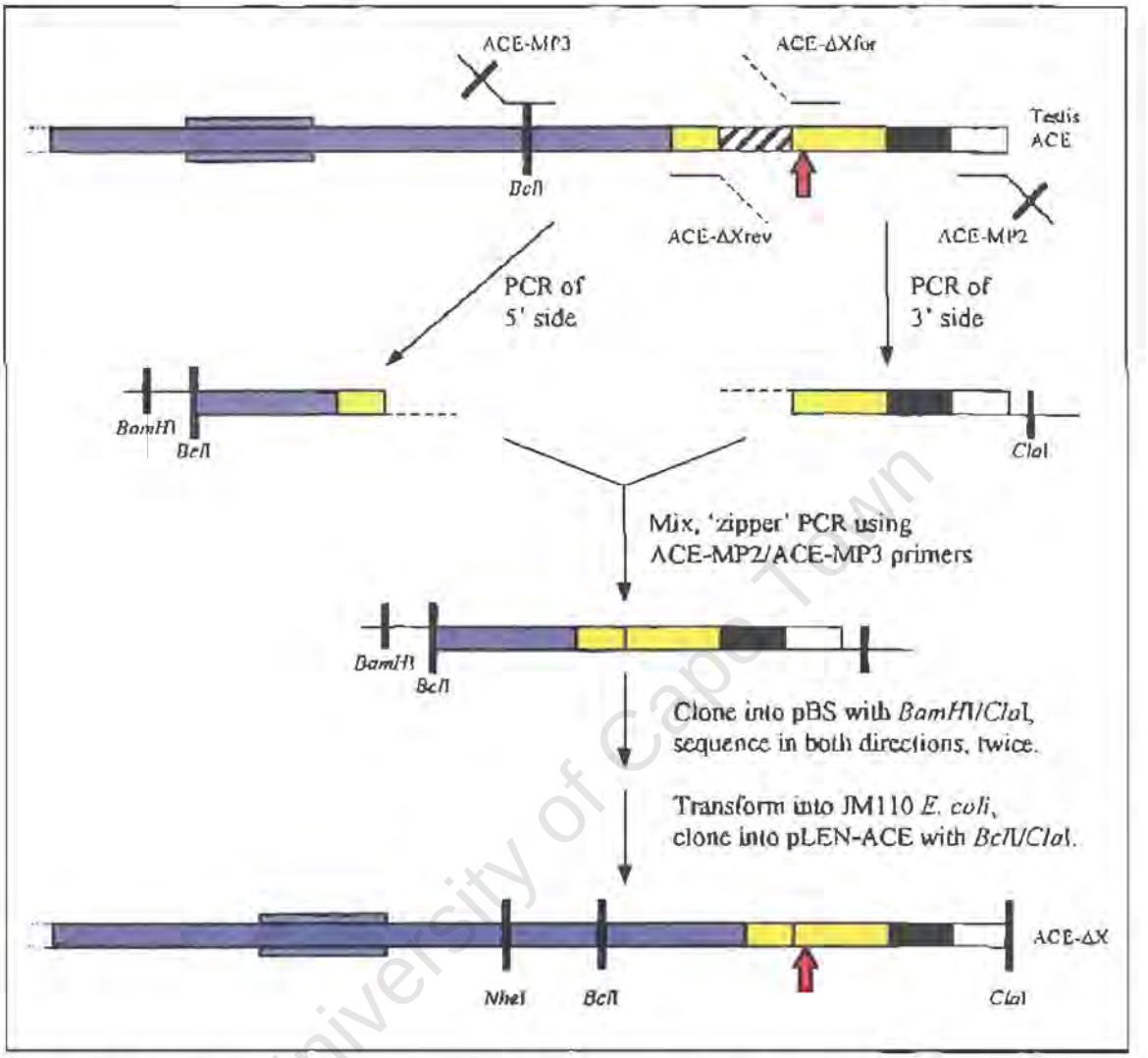

Figure 3.1.1.1) Construction of the pLEN-ACE deletion mutants

A schematic representation of the human testis cDNA ACE gene in pLEN-ACEVII is shown, with the ectodomain in red, the stalk region yellow, the TM in black and the cytoplasmic tail in white and the sheddase cleavage site indicated by a red arrow. The 5' and 3' regions flanking the region to be deleted (hatched) were **PCR** amplified using pairs of primers designed to generate overlapping hybrid sequences. The products were mixed and re-amplified using the outside primers (ACE-MP2 and ACE-MP3) to generate a recombinant sequence from which different sections of the stalk region are deleted. The 'zippered' PCR product was then restriction digested with both *BamH*I and *Cla*I, and ligated into similarly digested pBS (Stratagene), and **transformed** into XL1 Blue *Escherichia coli* (Stratagene). Insert-containing vectors were identified using the miniprep DNA extraction method and restriction mapping. DNA was then extracted using the MIDI DNA extraction kit (Qiagen) and sequenced in both directions using **SequiTherm Cycle Sequencing** (Epicentre), and again confirmed using the **ALFexpress DNA Automated Sequencer** (APBiotech). To facilitate digestion with the methylation sensitive *Bcl*I site, the insert-containing vector was transformed into the methylation negative JM110 *E. coli* (ATCC), isolated and cloned into pLEN-ACEVII using *Bcl*I and *Cla*I digestions. The final vector was then identified using restriction mapping.

were deleted. **DNA sequencing**, using both SequiTherm [α-^{35}S]-dATP sequencing (Epicentre technologies) and ALF automated sequencing (APBiotech), in both directions, was used to verify that no errors had been introduced. The insert-containing vector was **transformed** into the methylation-negative JM110 *Escherichia coli* strain, to facilitate digestion with the methylation-sensitive *Bcl*I enzyme. The final PCR product was then ligated into pLEN-ACEVII using the *Bcl*I and *Cla*I restriction endonucleases.

ACE-Δ11JM: pLEN-ACE-Δ11JM was constructed in the same manner except that nt 1961-1993 [encoding W_{616}-A_{626}] were deleted and a *Hind*III site was introduced through the silent mutation $G_{1957}T$.

ACE-Δ16JM: Similarly, pLEN-ACE-Δ16JM was constructed such that nt 1928-1975 [encoding T_{605}-N_{620}] were deleted and an *Eco*RI site introduced through the silent mutation $C_{1987}T$.

ACE-ΔR_{627}: In pLEN-ACE-ΔR627, three nucleotides were removed (nt 1994-1996), thereby deleting the P_1 cleavage site residue R_{627}.

ACE-Δ5JM: For pLEN-ACE-Δ5JM, nt 2006-2020 [encoding P_{631} to S_{635}] were deleted and a silent mutation ($C_{2029}A$) introduced a *Hind*III site.

ACE-ΔCYT: For pLEN-ACE-ΔCYT, a single PCR step was needed to introduce a stop codon directly 3′ of nt 2137, thereby truncating ACE at R_{674} and thus deleting the C-terminal 27 amino acids of human ACE_T.

ACEΔ36N-wt: The construction of pLEN-ACEΔ36N-wt involved substituting the 3′ end of wtACE (the *NheI*/*Cla*I fragment) for the same region of pLEN-ACEΔ36N. ACEΔ36N [Ehlers *et al.*, 1992] lacks the highly Ser/Thr-rich region at the N-terminus of testis ACE, via the deletion of residues Q_2-N_{36} (see Fig. 2.3.2), as well as the TM and cytoplasmic region. The ACEΔ36N-wt mutant therefore also lacks the O-glycosylated N-terminus (Q_2-N_{36}), but includes the wtACE TM and cytoplasmic domains.

ACEΔ61E: The ACEΔ61E mutant was constructed such that the N-terminal residues of human ACE_T, Q_3-E_{61}, were deleted. Suitable primers were used to separately PCR amplify nucleotides 3-121 and nt 299-638, using pLEN-ACEVII as template. The overlapping internal primers were then used to 'fuse' these PCR products in a second PCR using the outside primers only. After the sequence was confirmed in pBS, the

insert was excised using *Bam*HI/*Xho*I and inserted into partially digested pLEN-ACEVII. The correct orientation was confirmed using restriction analysis.

3.1.2) Swap-over mutants

ACE-Ndom: The construction of pLEN-ACE-Ndom was achieved with a similar two-stage PCR strategy to delete the section in somatic ACE (ACE_S) from P_{602}-T_{1198}, thereby fusing the human somatic ACE N-domain [M_{-29}-P_{601}; Soubrier *et al.*, 1988] directly onto the stalk, TM and cytoplasmic regions of human testis ACE [N_{624}-S_{701}; Ehlers *et al.*, 1989]. Suitable PCR primers were used to amplify nucleotides 1697-1912 of the full-length somatic ACE cDNA [Soubrier *et al.*, 1988] and nt 1982-2221 of full-length testis ACE cDNA containing the testis stalk sequence, TM domain and cytoplasmic region [Ehlers *et al.*, 1989]. The PCR products containing overlapping hybrid sequences were mixed and the flanking primers used to re-amplify a fusion product that was cloned into pBS using *Eco*RI/*Cla*I digestions. After sequencing, the PCR product was cloned into pBACE (pBS containing somatic ACE cDNA, obtained from Professor P. Corvol, INSERM U36, College de France, 75005 Paris), using *Pin*AI/*Cla*I digestions and exploiting a unique *Pin*AI site in ACE_S. The complete ACE-Ndom construct was then cloned into the mammalian expression vector pLEN-ACEVII [Ehlers *et al.*, 1991a] using *Bam*HI/*Cla*I restriction digestions.

ACE-NBcl: The mutant vector pLEN-ACE-NBcl was constructed using a single PCR step to amplify the proximal ectodomain region of pLEN-ACE-Ndom, thereby introducing a *Bcl*I site 3′ of the region coding the ACE_S N-domain sequence G_{561}-P_{601} fused to ACE_T sequence N_{624}-S_{701} of testis ACE (containing the stalk, TM and cytoplasmic domain regions of ACE_T). This was ligated into pLEN-ACEVII using *Bcl*I/*Cla*I digests. The ACE-NBcl chimeric mutant therefore consisted almost entirely of the testis ACE sequence except for the 41 amino acid proximal ectodomain region (G_{583}-P_{623}), which was replaced with the complementary region of the somatic ACE N-domain (G_{561}-P_{601}). Final amino acid sequences for ACE-Ndom and ACE-NBcl are shown in Appendix III.

3.2) Tissue Culture

The pLEN-ACE mutant vectors were stably co-transfected into CHO-K1 cells with pSV2NEO using the calcium phosphate method and/or transiently transfected into COS-1 cells using the DEAE-Dextran method. All tissue culture cells were grown in a humidified incubator at 37°C with 5% CO_2. CHO-K1 cells were maintained in **complete medium** [Dulbecco's modified Eagle's medium (DMEM)/Ham's F-12 supplemented with 20 mM 4-(2-Hydroxyethyl)-1-piperazineethanesulfonic acid (HEPES), pH 7.5, 20 mM *L*-glutamine and 10% foetal calf serum (**FCS**; heated to 56°C for 30 minutes before use)], while COS-1 cells were propagated in 10% FCS in **DMEM/P/S** [DMEM supplemented with penicillin (100 U/ml) and Streptomycin (100 µg/ml)). Cells were cryopreserved by resuspending in FCS supplemented with 10% DMSO and frozen to -200°C in liquid nitrogen. To resuscitate frozen cells, the cells were thawed rapidly to 37°C, washed with complete medium and allowed to settle in DMEM/Ham's F-12 supplemented with 30% FCS and 20 mM HEPES, pH 7.5 overnight (O/N).

3.2.1) Calcium phosphate co-transfection of CHO-K1 cells

All pLEN-ACE mutant vectors were stably transfected into CHO-K1 cells (adherent epithelial cells derived from a Chinese hamster [*Cricetulus griseus*] ovary; American Type Culture Collection (ATCC), CCL-61 CHO-K1; [Puck TT, 1958]), using the ProFection Calcium Phosphate Mammalian Transfection System kit, according to the manufacturer's instructions (Promega). A 1:20 molar ratio of pSV2NEO (containing the neomycin-resistance cassette under the control of the SV40 early region promoter; ATCC; [Southern and Berg, 1982]) to mutant pLEN-ACEVII was used. This was achieved by mixing 10 µg pLEN-ACE and 0.33 µg of pSV2NEO with 62 µl **2M $CaCl_2$** in a final volume of 500 µl water. This was slowly added to 500 µl **2× HBS** in a 10-ml tube, with gentle vortexing. After 30 minutes at RT, the fine precipitate of DNA/calcium phosphate was added to a 100mm dish containing CHO-K1 cells at 30% confluence and incubated with fresh **complete medium** for 4 hours prior to transfection. After a further 4 hours the medium was removed and replaced with 3 ml of **glycerol shock solution** [15% glycerol in PBS], for exactly 2 minutes at RT. The

cells were then washed twice with 10 ml PBS and grown O/N in fresh complete medium. Transfected cells were then selected using **0.8 mg/ml G418** (Geneticin, Sigma) in complete medium. Clones were selected using either **cloning rings** or **limiting dilution**.

3.2.2) ACE shedding kinetics

Neomycin-resistant CHO colonies, co-transfected with pLEN-ACE mutant constructs and pSV2NEO, were grown to confluence in 6-well plates (9.5 cm^2) for shedding-kinetics studies. After an overnight incubation with **induction medium** [DMEM/Ham's F-12 supplemented with 20 mM HEPES, pH 7.5, 20 mM *L*-glutamine, 2% foetal calf serum (heated to 70°C for 15 minutes before use) and 40 μM $ZnCl_2$], the medium was removed at zero time and replaced with 1 ml of fresh induction medium or induction medium supplemented with either 1 μM phorbol 12,13-dibutyrate (PDBu), 10 μM TNFα protease inhibitor (TAPI; [Mohler *et al.*, 1994]), 200 μM 3,4-dichloroisocoumarin (DCI) or 1 μg/ml cytochalasin D (cytoD). At the indicated times (usually 0-, 0.5-, 1-, 2-, 4- and 8-hour time points) the medium (1 ml) was removed and the cells dissolved in 1 ml of **Triton-lysis buffer** [1% Triton X-100, 50 mM HEPES, pH 7.5, 0.5 M NaCl and 1 mM PMSF]. ACE activity was determined using the HHL substrate.

3.2.3) TAPI inhibition

The IC_{50} was determined for TAPI inhibition of ACE shedding in the confluent 6-well CHO cell system used in this thesis, using a range of TAPI concentrations (from 0.1 to 100 μM TAPI). The percentage of shedding relative to the control (no additions) ACE activity in the medium after 4 hours of incubation was found for each concentration of TAPI and the IC_{50} determined using non-linear regression (Prism, GraphPad software Inc.). The IC_{50} for TAPI was found to be 0.5 ± 0.3 μM (n=4) in this system, thus the concentration used to characterise the shedding of the ACE mutants from transfected CHO cells (10 μM) was well in excess of this IC_{50}. The IC_{50} for TNF-α shedding by TAPI was ~0.1-0.2 μM [McGeehan *et al.*, 1994], which was

thus within an order of magnitude of the IC_{50} for ACE shedding found for this CHO cell system.

3.2.4) Surface expression – FITC labelling of CHO cells

Transfected CHO-K1 cells were seeded on flame sterilised glass coverslips in 12-well plates, cultured to 40% confluence in **complete medium** and ACE expression induced O/N in 1 ml **induction medium**. The cells were washed in **PBS^{++}** [phosphate-buffered saline (PBS) supplemented with 1 mM $CaCl_2$ and 1 mM $MgCl_2$], fixed for 5 minutes on ice using ice-cold **3% paraformaldehyde** (PFA) in PBS^{++} and washed in PBS^{++}. Alternatively, intracellular proteins were examined by permeabilising fixed cells with ice-cold methanol for 5 min on ice and again washing with PBS^{++}. The cells were then incubated with blocking buffer [**3% bovine serum albumin** (BSA) in PBS^{++}] for 30 minutes and washed in PBS^{++}. The cells were probed with a 1:300 dilution of either the rabbit polyclonal antibody R147 (anti-human kidney ACE) [Ehlers *et al.*, 1991a] or the rabbit polyclonal antibody 'A' (anti-recombinant human testis ACE), washed and incubated with fluorescein isothiocyanate-conjugated goat anti-rabbit IgG (1:500) in a humidified chamber in the dark. For nuclear staining, the cells were permeabilised with ice-cold methanol and inverted on a 50 µl drop of **2 µM propidium iodide** for 10 minutes at RT in the dark, followed by extensive washing with PBS^{++}, and a brief wash in H_2O to remove any salts. Finally, the coverslips were mounted onto glass microscope slides by inversion on a 10 µl drop of **MOWIOL mounting solution** and viewed under a scanning confocal microscope (Leica DMIRBE inverted confocal microscope, Leica Microsystems Heidelberg). An FITC control slide was included with each experiment to ensure that no non-specific binding of the secondary antibody occurred (i.e. the primary antibody was excluded). The baseline laser intensity levels were set such that the CHO cells showed no signal and these settings were applied rigorously to each subsequent analysis, to ensure that the observed signal was specific to the transfected cells and was semi-quantitative. Digital pictures were modified in Adobe Photoshop, again using the same adjustments for each picture to keep the 'exposure' settings identical. When no FITC label was detected, the red channel picture (i.e. propidium iodide stain) was used to show that cell nuclei were indeed present.

3.2.5) DEAE-Dextran transfection of COS-1 cells

COS-1 cells (*Cercopithecus aethiops* [African green monkey] cell line; ATCC, CRL-1650) were transiently transfected using DEAE-Dextran and 2.5 µg DNA per well in a 12-well tissue-culture dish (4.0 cm^2). Cells were seeded the day before transfection ($2x10^5$ cells) into 1 ml **10% FCS/DMEM/PSH** [DMEM supplemented with 10% FCS, 100 U/ml penicillin, 100 µg/ml streptomycin and 20 mM HEPES, pH7.5]. After washing with **DMEM/PS**, 2.5 µg pLEN-ACE DNA was added to each well in 0.5 ml **1× DEAE-Dextran/DMEM/PS**. This was followed 4 hours later by a 1 hour 'chloroquine-shock' [DMEM/PS supplemented with 2 µM chloroquine and 2% FCS] at 37°C, 5% CO_2. A 'DMSO-shock' step was then performed by adding 1 ml 10% DMSO (in DMEM/PS) to washed cells for exactly 2 minutes at RT. Fresh 10% FCS-DMEM/PSH medium was then added (zero time-point) and the cells allowed to recover O/N. The medium was replaced 24 hours later with 10% FCS/DMEM/PS medium containing 40 µM $ZnCl_2$. At 44 hours, the start of the shedding experiment, the medium was replaced with 1 ml of fresh medium containing 40 µM $ZnCl_2$ with 1 µM PDBu, 10 µM TAPI or no additions. A set of Triton-lysed cell samples was also collected. The cells were then harvested at 48 hours (after 4 hours of shedding) and the cell-extract and medium samples assayed for ACE activity using the HHL substrate.

3.3) ACE activity assays and protein analysis

3.3.1) HHL substrate assay for ACE activity

ACE activity was assayed using the Hippuryl-His-Leu (HHL) substrate and spectrophotometrically measuring the amount of histidinyl-leucine (HL) produced. The cellular and soluble fractions (5-50 µl) were added to 120 µl **HHL assay solution** [5 mM Hippuryl-His-Leu in 50 mM HEPES, pH 7.5, 0.3 M NaCl] and incubated for 15-30 minutes at 37°C. The reaction was stopped with 750 µl 0.28 M NaOH and the HL dipeptide product conjugated to ***o*-phthaldialdehyde** (20 mg/ml in methanol) by adding 50 µl of a fresh stock, for 10 minutes at RT. The conjugation was stopped by adding 100 µl 3 M HCl and the conjugate was assayed for fluorescence (λ_{ex} = 360 nm and λ_{em} = 485 nm) using a Perkin-Elmer LS-5 Luminescence Spectrometer. Fluorescence units were converted to nmol of HL produced using an HL standard curve (1.4, 2.8, 7, 14 and 20.9 nmol HL). 1 unit (U) of ACE activity is defined as the quantity of ACE that converts 1 mmol of HHL in 1 minute at 37°C in 50 mM HEPES, pH 7.5, 0.3 M NaCl.

3.3.2) Fluorogenic peptides

The activity of the ACE-Ndom swap-over mutant was assayed using the internally quenched fluorescent peptide Abz-SDK(Dnp)P-OH (defined in [Araujo *et al.*, 2000]; a gift from Adriana K. Carmona [Dept. Biophysics, Universidade Federal de Sao Paulo, Brazil]). The basic concept behind intramolecularly quenched fluorogenic substrates, developed by Yaron *et al.* [Yaron *et al.*, 1979] is that an *o*-aminobenzoic acid and a 2,4-dinitrophenyl group can only fluoresce once one of the connecting peptide bonds that separates them has been hydrolysed. This was converted for use as an ACE assay by Araujo *et al.* [Araujo *et al.*, 1999], who also discovered that some peptides showed domain-specificity, such as the modified tetrapeptide Abz-SDK(Dnp)P-OH, which is preferentially cleaved by the ACE_S N-domain [Araujo *et al.*, 2000]. Culture medium or Triton-lysed cell-extract samples were assayed at 37°C using 8 µM Abz-SDK(Dnp)P-OH as substrate in **Abz/Dnp-substrate solution** [0.1 M Tris/HCl, pH 7.0, 50 mM NaCl and 10 µM $ZnCl_2$]. Substrate hydrolysis was

monitored continuously by measuring the fluorescence at λ_{ex} = 320 nm and λ_{em} = 420 nm for 5 min after 5-50 µl of each sample was added to 2.5 ml temperature-equilibrated Abz/Dnp-substrate solution. The initial, linear slope was converted to nmoles of substrate hydrolysed per minute by using fluorescence measurements for standard peptide solutions (20, 40, 100, 200 and 400 nmoles) after total hydrolysis (2hours at 37°C) [Araujo *et al.*, 1999].

3.3.3) Western blot analysis

Western blotting was also performed on the samples collected during the shedding-kinetics experiments described above. Sodium dodecyl sulphate-polyacrylamide gel electrophoresis (**SDS-PAGE**) was performed through a 10% acrylamide gel in a Western blotting apparatus (BioRad) using 24 µl of each sample mixed with 6 µl **5× SDS reducing buffer** [0.15 M Tris (pH 6.8), 5% SDS, 25% Glycerol, 0.0025% Bromophenol Blue and 12.5% β-mercaptoethanol]. The gel was blotted against nitrocellulose, blocked using skim milk powder and probed using a 1:1000 dilution of the rabbit polyclonal anti-human kidney ACE antibody R147 [Ehlers *et al.*, 1991a], followed by a 1:2000 dilution of a goat anti-rabbit IgG antibody conjugated to horse radish peroxidase (HRP). All antibodies were diluted in **blocking buffer** [PBS containing 2% (w/v) BSA and 0.1% Tween-20]. After extensive washing, the nitrocellulose was analysed for peroxidase activity using the ECL chemiluminescence kit (Amersham) according to the manufacturer's instructions and Kodak BioMax MR X-ray film for autoradiography.

3.3.4) Metabolic labelling

Metabolic labelling and pulse-chase analysis of the biosynthesis and release of ACE mutant proteins was performed as described previously [Schwager *et al.*, 1999]. Stably transfected CHO-K1 cells were grown to confluence in 6-well dishes with **complete medium**. ACE expression was induced O/N, after which the cells were washed twice with **PBS** and 'starved' for 30 minutes in 500 µl **starvation medium** [2% dialysed FCS in minimal Eagles medium (MEM) supplemented with 4 mM L-glutamine]. The medium was removed and the cells 'pulsed' with 500 µl [^{35}S]

labelling medium [starvation medium supplemented with 100 µCi [^{35}S]-methionine and [^{35}S]-cysteine per ml] for 30 minutes at 37°C in 5% CO_2. The cells were washed with PBS and 1 ml fresh induction medium, containing no additions, 1 µM PDBu, 10 µM TAPI or 200 µM DCI, was added at zero time. The metabolically labelled proteins were then 'chased' for up to 24 hours. Cell-lysate and medium samples were collected at the indicated times, centrifuged for 10 minutes in a benchtop microcentrifuge, and 700 µl of the 'hot' supernatant was carefully collected. Fifty µl of each sample was used for ACE activity assay (using the substrate HHL). ACE in the remaining sample was affinity-precipitated by adding 50 µl of lisinopril-sepharose slurry [~50% sepharose-[28Å linker]-lisinopril affinity resin and 50% **column wash buffer** (20 mM HEPES, pH 7.5; 0.5 M NaCl)] and ACE binding was facilitated by continuous vortexing for 30 minutes. The beads were centrifuged, washed three times with column wash buffer and resuspended in 50 µl **2× SDS reducing buffer**. The beads were then loaded onto 10% SDS-PAGE gels and the protein electrophoresed O/N. The gel was vacuum-dried onto filter paper and autoradiographed.

3.3.5) Triton X-114 phase separation

Triton X-114 phase separation of cell-associated and soluble proteins was performed to confirm the presence or absence of a hydrophobic anchor region [Bordier, 1981; Hooper *et al.*, 1987; Ehlers *et al.*, 1996]. Medium and cell extract samples were centrifuged in 1.5 ml Eppendorf tubes for 3 minutes to remove any cells or cell-debris. Fifty µl of each sample was mixed with 50 µl **Triton X-114 extraction buffer** [10 mM Tris, pH 7.5, 150 mM NaCl]. An equal volume (100µl) of **2% Triton X-114** in Triton X-114 extraction buffer was added and mixed thoroughly. After allowing the cloudy solution to clear on ice (5 minutes), the samples were incubated at 30°C for 3 minutes. The samples were immediately centrifuged at RT for 3 minutes. The aqueous phase (~180 µl) was carefully removed and transferred to a new Eppendorf tube. To equalise the volumes, the detergent droplet was resuspended in 146 µl Triton X-114 extraction buffer and placed on ice to allow the micelles to dissolve. HHL assays were performed on 20 µl of both the detergent- and aqueous-phase samples and the fraction of soluble ACE expressed as a percentage of total ACE activity.

3.4) Protein purification

Soluble ACE, released into the medium from the surface of CHO cells, was purified to homogeneity using affinity-chromatography [Pantoliano *et al.*, 1984; Ehlers *et al.*, 1986, 1989; Hooper and Turner, 1987]. The sepharose-28Å-lisinopril affinity column used consists of the highly specific and tight-binding ACE inhibitor lisinopril bound to epoxy-activated sepharose 6B via a 28Å-long linker [Pantoliano *et al.*, 1984; Hooper and Turner, 1987]. The linker consists of aminocaproic acid coupled to aminobenzoic acid (via an *N*-hydroxysuccinimide linkage), which is in turn bound to the epoxy activated sepharose 6B [Cuatrecasas and Parikh, 1972; Pantoliano *et al.*, 1984]. Transfected CHO-K1 cells were grown to confluence in four T 175 cm^2 tissue culture dishes (Nunc) in **complete medium**. ACE production was induced for 48 hours in 25 ml **induction medium**/flask. The medium was collected and a further 25 ml induction medium was added for another 48 hours. The cells were allowed to recover in 20 ml complete medium for 24 hours, before the induction and collection were repeated. All medium was centrifuged in 50-ml tubes at 2500 rpm in a Beckman benchtop centrifuge at 4°C, to remove any cell debris, prior to freezing at -20°C. The pooled, thawed, medium was then passed over a 10-ml sepharose-28Å-lisinopril affinity column, which had been pre-equilibrated with **column wash buffer** [0.5 M NaCl, 20 mM HEPES, pH 7.5]. For the isolation of cell-associated ACE, the wash buffer was supplemented with 1% Triton X-100 and 1 mM PMSF. Contaminating proteins were washed off with ~50 column volumes of wash buffer, prior to elution with 50 mM borate, pH 9.5. Fractions (2 ml) were collected and assayed for ACE activity. ACE-containing fractions were pooled and dialysed into H_2O at 4°C O/N using SnakeSkin dialysis tubing (Pierce, 10 000 MWCO). The dialysed ACE was then frozen to -20°C, freeze-dried O/N and resuspended in 200 µl H_2O. A small amount (~1 µg) was then analysed on SDS-PAGE with **Coomassie blue stain**. The specific activity of the purified protein was calculated by assaying enzymatic activity (**HHL activity**) and the protein concentration (**BioRad Bradford method**, [Bradford, 1976]).

3.5) Cleavage site determination

Soluble ACE_T that has been released from the surface of CHO cells does not contain the hydrophobic transmembrane region of its membrane-bound precursor and its COOH-terminal end is the P_1 residue of the sheddase cleavage site [Ehlers *et al.*, 1991b, 1996; Hooper *et al.*, 1987]. To determine the identity of this cleavage-site residue, a mass-spectrometry method of cleavage site determination was employed [Ehlers *et al.*, 1996; Schwager *et al.*, 1998, 1999]. Briefly, the purified soluble (released) ACE proteins were reduced, the cysteines protected with vinylpyridine and the peptide digested with endoproteinase cleavage. The peptides were analysed using MALDI-TOF mass spectrometry and correlated with the calculated masses of all potential COOH-terminal peptides. The COOH-terminal peptide was confirmed by fractionation using HPLC, N-terminal sequencing via automated Edman degradation and MALDI-TOF analysis (see Fig. 3.5.1).

3.5.1) Reduction and protection of disulphides

Purified soluble ACE was reduced by adding **6 M GnCl buffer** [6M GnCl, 0.1 M Tris, pH 8.5], β-mercaptoethanol and incubating the mixture at 40°C for 3 hours with gentle agitation. The free thiol groups were then protected from re-forming disulphides by adding vinylpyridine (100%) for 30 minutes at RT in the dark. One drop of formic acid (100%) was used to acidify the sample prior to removal of any unreacted vinylpyridine using reverse phase high performance liquid chromatography (RP-HPLC). The sample was loaded onto a 'desalting' Aquapore RP-300 7 μm C8 column (30 × 2.1 mm; Perkin-Elmer) and developed with a linear gradient of 0-80% acetonitrile in 0.1% TFA over 20 minutes. The samples were freeze-dried.

3.5.2) Lys-C digestion and HPLC fractionation

The vinylpyridine-protected protein (~250 μg) was then resuspended in 100 μl Lys-C digestion buffer [25 mM Tris, 1 mM EDTA, pH 8.5], to which 5 μl (5 μg) of endoproteinase Lys-C (Boehringer Mannheim) was added and the protein digested O/N at 37°C. Alternatively, the purified protein was digested with cyanogen bromide

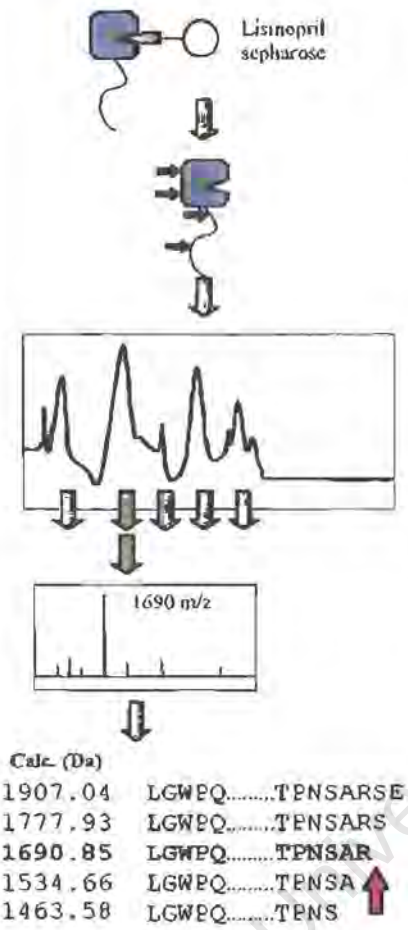

Soluble, released, ACE was affinity-purified from culture medium using a sepharose-28-lisinopril affinity column.

Purified ACE was reduced, vinylpyridine protected, 'cleaned' using C_8 HPLC and digested with Lys-C or CNBr.

Peptides were separated using C_{18} HPLC and fractions collected for each peak.

The COOH-terminal peptide was found by N-terminal sequencing using the Edman degradation method.

MALDI-TOF mass spectroscopy analysis of the COOH-terminal peptide revealed its exact mass (*m/z*).

The cleavage site was thus identified by comparison with the hypothetical masses for C-terminal peptides derived from all possible cleavage sites.

Figure 3.5.1) A Schematic representation of the cleavage site determination protocol
ACE_T (blue/green) binds the affinity column thru the lisinopril ligand (purple), which is in turn bound covalently to sepharose beads (orange). Endoproteinase (Lys-C) cleavage sites are represented by black arrows. The sheddase cleavage site is indicated with a red arrow.

(CNBr) using standard procedures [Gross E, 1967]. The peptide mixture was then analysed using MALDI-TOF mass spectroscopy and the mass of the C-terminal peptide determined. To confirm the identity of the *m/z* peak relating to the C-terminal peptide, the peptides were fractionated using HPLC and sequenced using Edman degradation. The sample was acidified with formic acid and loaded onto a Jupiter 5 μm C_{18} HPLC column (150 × 1.0mm; Phenomenex). The peptides were separated using a gradient of 0-60% acetonitrile in 0.08% TFA over 120 min. Fractions were collected for each peak and the COOH-terminal peptide fraction found by MALDI-TOF analysis and sequenced using automated Edman degradation in a gas-phase sequenator 473A (Applied Biosystems, Weiterstadt, Germany).

3.5.3) ACE peptide deglycosylation

An exception occurred with the ACE-Δ6JM mutant, as its COOH-terminal peptide was found to be glycosylated and the glycan needed to be removed before its peptide mass could be determined. The HPLC-fractionated COOH-terminal peptide (~1 nmol) for ACE-Δ6JM was resuspended in 20 mM NaH_2PO_4, pH 8.0, 25 mM EDTA, to which 1 unit (5 μl) *N*-glycosidase F (Boehringer Mannheim) was added. After deglycosylation for 2 hours at 37°C, the peptide was N-terminally sequenced prior to MALDI-TOF mass spectrometry.

3.5.4) MALDI-TOF mass spectroscopy

Matrix-assisted laser-desorption-ionisation time-of-flight (MALDI-TOF) mass spectroscopy (MS) was preformed on either the isolated COOH-terminal peptide or the mixed peptides directly following Lys-C digestion of purified ACE. The exact mass measurement (*m/z*) can then be correlated with hypothetical masses for an ACE C-terminal peptide that was cleaved at any peptide bond in the stalk region as well as the known Lys-C peptides. MALDI-TOF analysis was done using either a PerSeptive Voyager Elite Biospectroscopy Workstation (PerSeptive Biosystems, Framingham, MA) or a Bruker Reflex III time-of-flight mass spectrometer (Bruker-Franzen, Bremen, Germany). The matrixes 2,5-dihydroxybenzoic acid (DHB) and α-cyano-4-hydroxycinnamic acid (CHCA) were used.

Chapter 4: The Juxtamembrane Region

The ACE stalk deletion mutants

From the literature reviewed in Chapter 1, it is clear that numerous ectoproteins are cleaved in the juxtamembrane stalk region by a sheddase (or family of sheddases), and that the universal sheddase recognition motif(s) remains elusive.

The obvious place to start looking for the sheddase recognition motif is at the cleaved site, as most, if not all, proteases recognise the residues either at or near the scissile peptide bond. Ehlers *et al.* showed that the recombinant human testis ACE sheddase cleavage site used in CHO cells is at the R_{627}/S_{628} bond, 24 amino acids from the transmembrane domain [Ehlers *et al.*, 1996], which was later shown to be the same as that used to cleave both porcine and human somatic ACE [Woodman *et al.*, 2000]. Thus, knowing where the ACE sheddase must have interacted with its substrate, at least transiently, one can use this as a starting point for closer examination of the stalk region by deleting or mutating sections above and below this cleavage site and monitoring how these deletions affect the shedding of ACE. This forms the logical basis for the work presented in this thesis.

Ehlers *et al.* showed that large deletions C-terminal to the sheddase cleavage site, of 17 or 24 amino acids (see Fig. 4.1), did not abolish shedding, although the rate of shedding was affected [Ehlers *et al.*, 1996]. Interestingly, the deletion of 17 amino acids adjacent to the transmembrane domain **increased** the rate of shedding ~4 fold, while the deletion of a further 11 amino acids resulted in an ~8 fold **decrease** in the rate of shedding relative to wtACE. The shedding of ACE-JM24 mutant is particularly surprising, as the cleavage-site R_{627} is directly adjacent to the predicted transmembrane region, indicating that the sheddase needs no 'footroom' for cleavage to occur. This work also strongly suggests that the sheddase has a preference for R_{627}, which was also tested by deleting this single amino acid. The fact that the ACE-JM24 mutant is shed at all implies that the sheddase recognition domain is probably not C-terminal to R_{627}, leaving the N-terminal 'headroom' region between the proximal

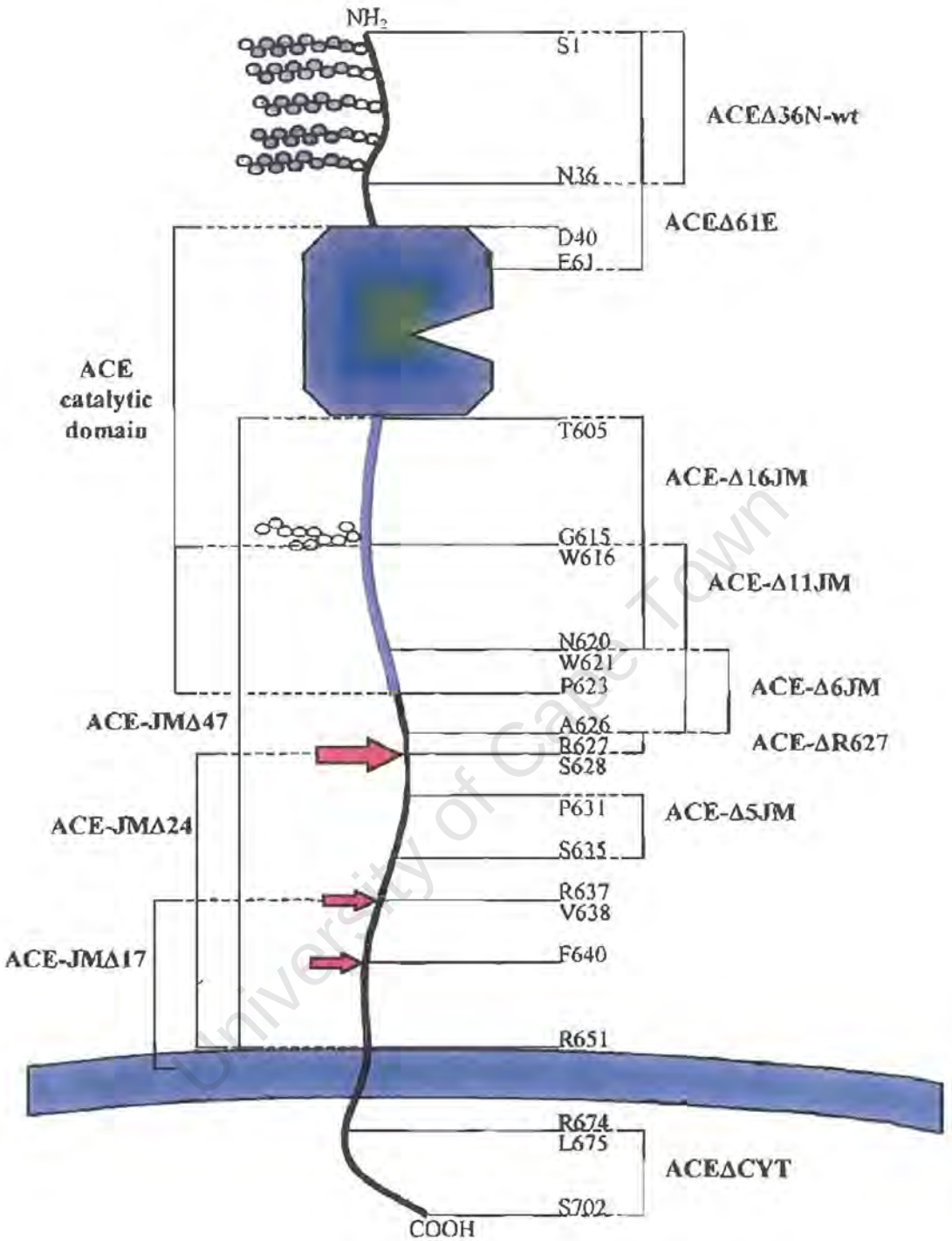

Figure 4.1) The ACE deletion mutants

Schematic representation of ACE showing the deletion mutants analysed in this thesis. The ACE catalytic domain is blue/green while the plasma membrane is light blue. The major sheddase cleavage site is shown with a large red arrow, while alternative cleavage sites are shown with smaller arrows. The 5' O-glycosylated region is shown with blue circles, while the 7th putative N-glycosylation site, which is unglycosylated in wtACE, is shown with open circles. Numbering is for mature human testis ACE [Ehlers *et al.*, 1989]. Mutants ACE-JM17, -JM24 and –JM47 were constructed and analysed previously [Ehlers *et al.*, 1996].

ectodomain and the cleavage site as the only remaining stalk region for protease recognition. The ACE-JMΔ6, -JMΔ11 and –JMΔ16 mutants (see Fig. 4.1) were constructed in an attempt to knock out this potential sheddase recognition site directly N-terminal to the cleavage site.

The concept of 'headroom', and its importance in positioning the promiscuous sheddase(s) to cleave its substrate ectoprotein(s) was introduced by Ehlers *et al.* after aligning the stalk regions and cleavage sites of numerous shed ectoproteins [Ehlers *et al.*, 1996]. 'Headroom' is defined here as the distance between the proximal ectodomain and the sheddase cleavage site, both of which are difficult to define. However, the cleavage site was determined for numerous ectoproteins which, when aligned, revealed that the sheddase appears to cleave various ectoproteins at a defined distance from the ectodomain [Ehlers *et al.*, 1996; see Table AI.2]. This implies that the sheddase first recognises a motif either in the ectodomain or in the region just N-terminal to the cleavage site and then cleaves in the stalk region at a defined distance from the proximal ectodomain, likely in a sequence-independent manner.

But how does one define the boundary of the proximal ectodomain of ACE in the absence of any discernable structural motif, or 3D structure? It was noted that the ACE-JMΔ47 mutant, in which all of the 'stalk' region was removed, was both inactive and not shed, indicating that this stalk deletion may have encroached on a structurally important motif needed for the stability and correct processing of ACE to the cell surface. The ACE-Δ16 mutant was constructed in an attempt to define the boundary of the proximal ectodomain, and potentially knock out a cleavage recognition motif (see Fig. 4.1, Table 4.1.1).

4.1) The 'headroom'

As large deletions of the ACE stalk region between the sheddase cleavage site and the transmembrane domain did not abolish shedding [Ehlers *et al.*, 1996], it seemed likely that the 'headroom' region between the ACE ectodomain and the sheddase cleavage site might play a role in ectodomain shedding. We therefore deleted 6, 11 and 16 amino acids from the stalk region of human testis ACE, thereby removing the peptides WTPNSA, WPQYNWTPNSA and TENELHGEKLGWPQYN respectively, as shown in Table 4.1.1. Furthermore, these 'headroom' deletions would bring the proximal ectodomain closer to the wtACE cleavage site, which may sterically hinder the sheddase from accessing its favoured cleavage site, namely the R_{627}/S_{628} bond. Interestingly, a $P_{1199}L$ mutation in the stalk region of somatic ACE has recently been shown to increased shedding and thus elevate the plasma ACE levels of three unrelated individuals [Eyries *et al.*, 2001]. This proline, equivalent to P_{623} in testis ACE, is the last completely conserved amino acid in both domains of numerous ACE homologues and was deleted in the ACE-Δ6JM and ACE-Δ11JM mutants (see Table 4.1.1).

Table 4.1.1) The ACE stalk deletion mutants

Mutant	Stalk sequence	Shed
WtACE	WLRTENELHGEKLGWPQYNWTPNSARSEGPLPDSGRVSFLGLDLDAQQARVGQWLL	Y
ACE-JMΔ17	WLRTENELHGEKLGWPQYNWTPNSARSEGPLPDSGR.....WLL	Y
ACE-JMΔ24	WLRTENELHGEKLGWPQYNWTPNSAR.....VGQWLL	Y
ACE-JMΔ47	WLR.....VGQWLL	N
ACE-Δ6JM	WLRTENELHGEKLGWPQYN.....RSEGPLPDSGRVSFLGLDLDAQQARVGQWLL	Y
ACE-Δ11JM	WLRTENELHGEKLG.....RSEGPLPDSGRVSFLGLDLDAQQARVGQWLL	Y
ACE-Δ16JM	WLR.....WTPNSARSEGPLPDSGRVSFLGLDLDAQQARVGQWLL	N
ACE-Δ5JM	WLRTENELHGEKLGWPQYNWTPNSARSEG.....GRVSFLGLDLDAQQARVGQWLL	Y
ACE-ΔR627	WLRTENELHGEKLGWPQYNWTPNSA.SEGPLPDSGRVSFLGLDLDAQQARVGQWLL	Y

The amino acid sequence of the stalk region of human testis ACE, from W_{602} to L_{657}, and mutations thereof, are shown. The transmembrane domain and proximal ectodomain are highlighted in blue and yellow respectively. The putative TM domain suggested by Soubrier is underlined [Soubrier *et al.*, 1988]. Cleavage sites are indicated with an arrow and distance from the TM shown on the right. The cleavage sites and shedding characteristics of wtACE, ACE-JMΔ17, -JMΔ24 and -JMΔ47 are published previously [Ehlers *et al.*, 1996], as is that of ACE-Δ6JM [Schwager *et al.*, 1999]. The N-glycosylation site created by the deletion of 6 amino acids in the ACE-Δ6JM mutant is shown in bold, as is the seventh putative glycosylation site in human testis ACE, which is not glycosylated in wtACE [Yu *et al.*, 1997]. The last lysine in the sequence of human ACE_T is highlighted in green. The $Pro_{1199}Leu$ mutation found by Eyries *et al.* to elevate the shedding of ACE is highlighted in purple [Eyries *et al.*, 2001].

4.1.1) ACE-Δ6JM

The ACE-Δ6JM mutant was constructed using a two-step PCR mutagenesis approach described previously [Schwager *et al.*, 1999]. Primers were designed to delete the region W_{621}-A_{626} of recombinant human ACE_T (see Table 4.1.1). The construct vector pLEN-ACE-Δ6JM was co-transfected with pSV2NEO into CHO-K1 cells using the calcium phosphate co-transfection method, as described in Chapter 3. Although numerous stable lines were analysed for HHL activity, similar activity levels were found for each. Transfected CHO cells were grown to confluence in 6-well 9.5 cm^2 dishes, ACE expression induced overnight and the cells-extracts assayed for ACE activity using the HHL substrate method. The cell-associated ACE activity for ACE-Δ6JM was found to be 24.0 ± 4.0 mU ACE per confluent 9.5 cm^2 well (n = 5), approximately an order of magnitude lower than that of wtACE, 177.9 ± 15.0 mU ACE/well (n = 8).

To examine the effect of phorbol ester stimulation and TAPI inhibition on the shedding of ACE-Δ6JM from CHO cells, the rate of accumulation of ACE activity in the culture medium of transfected CHO cells was monitored over 8 hours, as described [Schwager *et al.*, 1999]. The ACE activity associated with both the medium and cell-extract samples was measured using the substrate HHL (see Fig. 4.1.1.1 and Fig. 4.1.1.2). The shedding profile for wtACE (wild-type human testis ACE), seen in Fig. 4.1.1.1, was consistent with that shown previously by our laboratory [Ehlers *et al.*, 1996; Schwager *et al.*, 1999; Woodman *et al.*, 2000]. Not only was there a characteristic 5-fold **increase** in shedding of wtACE on stimulation with 1 μM PDBu in the initial period (2-4hrs), there was also a dramatic inhibition by 10 μM TAPI, shown by a 10-fold **decrease** in release of soluble ACE (see Fig. 4.1.1.1a). Interestingly, in the case of the ACE-Δ6JM mutant, a similar burst of shedding activity was seen when the transfected CHO cells are stimulated with phorbol ester, resulting in a 2.4-fold increase in soluble ACE activity (see Fig. 4.1.1.2a). There was also a 4-fold reduction in ACE release when the sheddase is inhibited with 10 μM TAPI, indicating that this shedding activity was similar to that seen previously for ACE and numerous other ectoproteins.

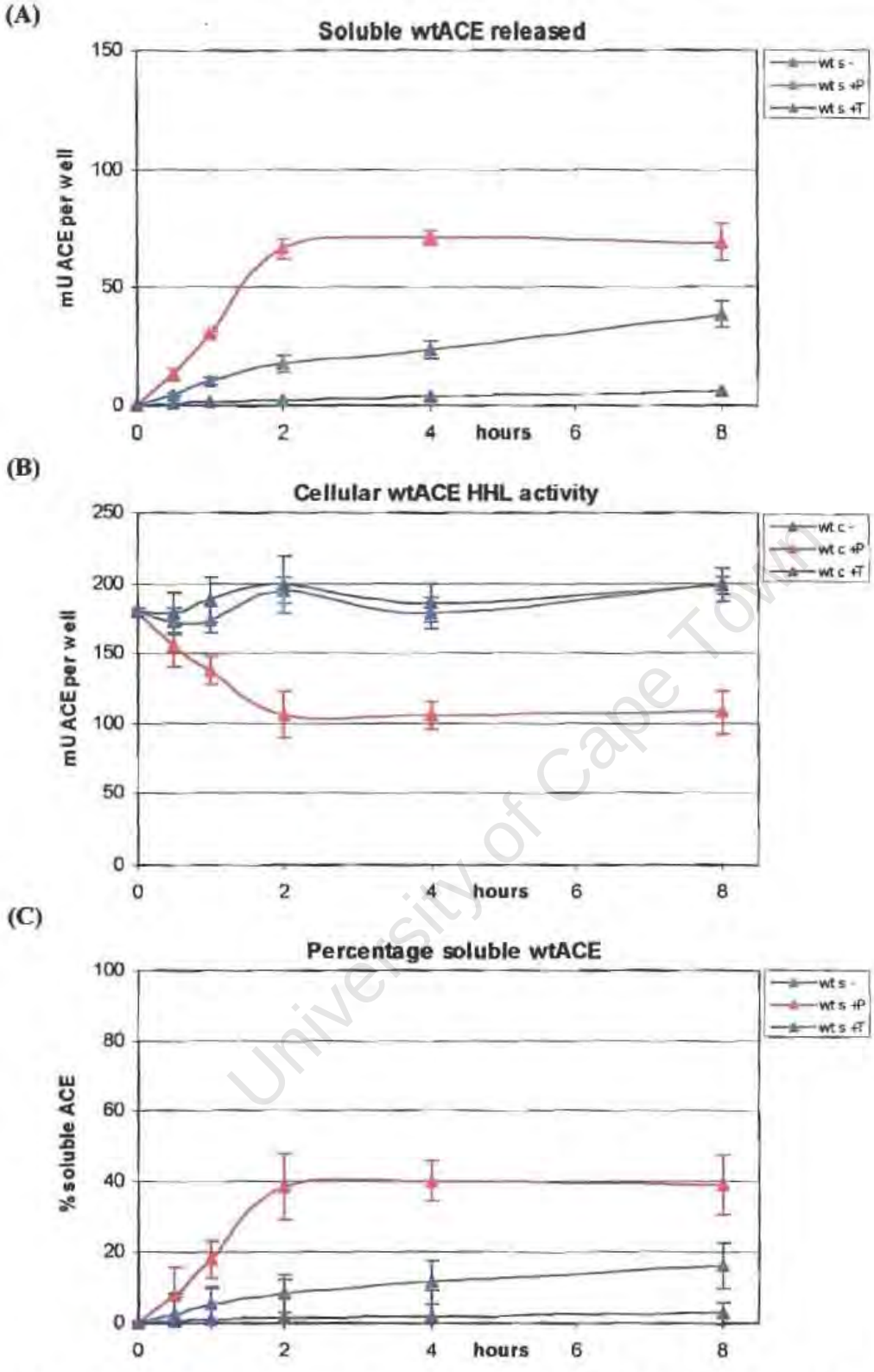

Figure 4.1.1.1) The shedding of wtACE – effect of PDBu and TAPI over 8 hours

CHO-K1 cells transfected with pLEN-ACEVII were grown to confluence in 6-well dishes and ACE expression induced overnight using 1 ml induction medium. At zero time the medium was replaced with 1 ml fresh induction medium supplemented with either nothing (blue), 1 μM PDBu (red) or 10 μM TAPI (dark blue). At the indicated times the medium was retained and the cells lysed using Triton lysis buffer. ACE activity of the medium (A) and cell extract (B) was determined using the HHL assay. The percentage soluble ACE in (C) is determined by dividing the soluble activity by the total ACE activity in the well (cell plus medium) [n=4].

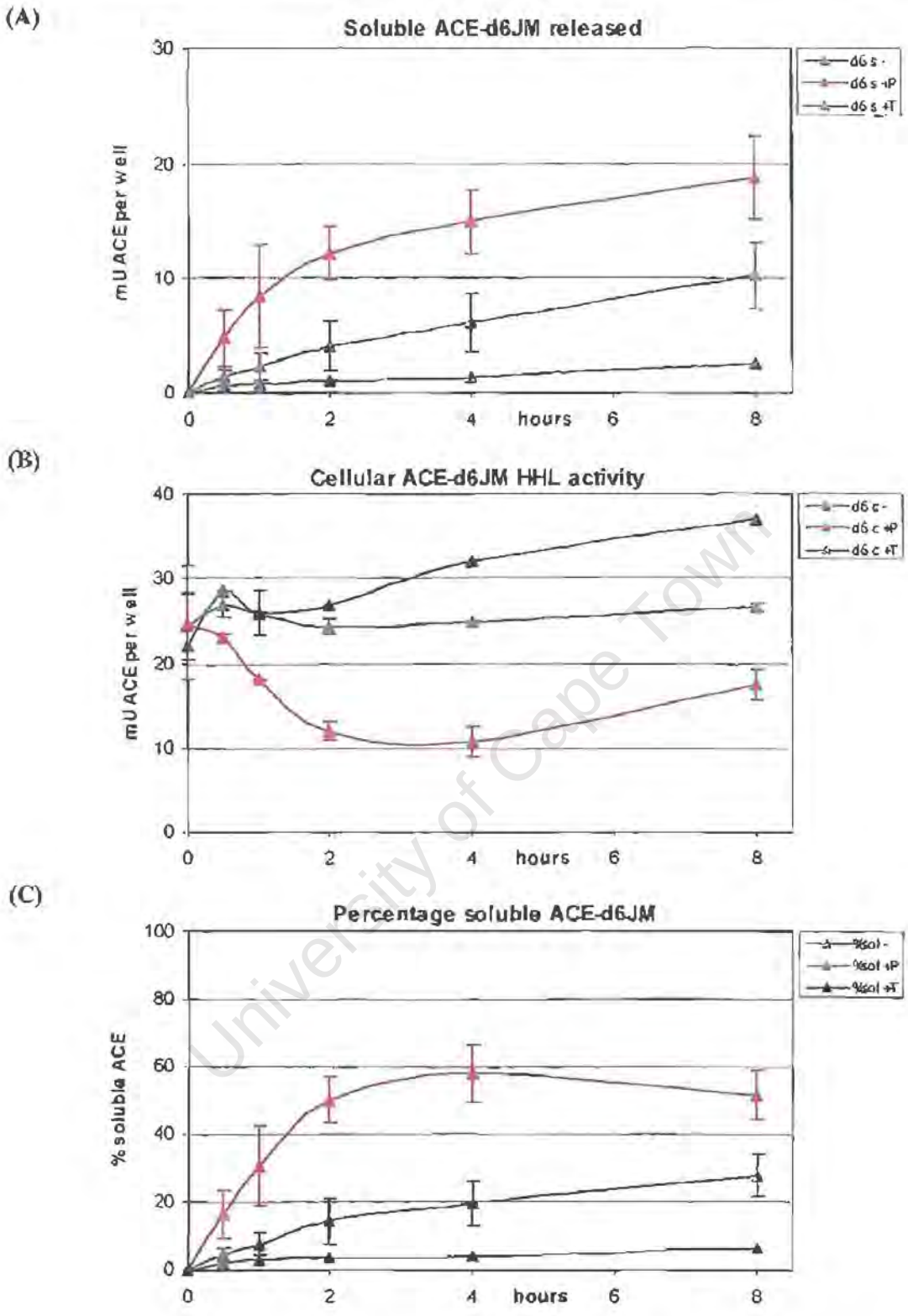

Figure 4.1.1.2) The shedding of ACE-Δ6JM – effect of PDBu and TAPI over 8 hours
CHO-K1 cells transfected with pLEN-ACE-Δ6JM were grown to confluence in 6-well dishes and the 8hr shedding kinetics assay performed as described in Fig. 4.1.1.1, using induction medium supplemented with either nothing (blue), 1 μM PDBu (red) or 10 μM TAPI (dark blue). ACE activity of the medium (A) and cell extract (B) was determined using the HHL assay, with the percentage soluble ACE at each time-point shown in (C) [n=2].

The expression of shed ACE as a percentage of soluble activity was based on the finding that both the soluble and cellular form of recombinant human testis ACE expressed in CHO cells have the same K_m and k_{cat} for both Fa-FGG and Angiotensin I hydrolysis, and thus show essentially identical enzymatic activity [Ehlers *et al.*, 1991], which can thus be compared (see Fig. 4.1.1.1c). This is useful when comparing the shedding activity of CHO cells transfected with different ACE mutants that have differing expression levels, as the effective release of ACE into the culture medium is corroborated by the concomitant reduction in cell-associated ACE. Thus in Fig. 4.1.1.2c the distinctive increase in shedding of ACE-Δ6JM with phorbol ester stimulation and the inhibition by TAPI closely matched that seen in Fig. 4.1.1.1c for wtACE when expressed as a percentage of total ACE activity in the well.

The processing and shedding of the membrane-bound form of ACE-Δ6JM from CHO cells was further investigated using metabolic labelling and pulse-chase analysis (see Fig. 4.1.1.3; [Schwager *et al.*, 1999]). Analysis of affinity-precipitated ACE-Δ6JM (Fig. 4.1.1.3b) showed the progression of radioactive label through the precursor form (90 kDa) to the mature, fully glycosylated ~105 kDa form, which was almost identical to that seen with wtACE (Fig. 4.1.1.3a). It can be inferred that this signal was due to nascent ACE being glycosylated as it progressed through the Golgi apparatus, to appear on the cell surface as a fully glycosylated, mature enzyme. The larger mature form had the same relative molecular mass as the biotin-labelled form isolated from the cell-surface (data not shown). As biotin is a hydrophilic molecule that cannot enter cells, the isolation of only the larger form of ACE using streptavidin-linked sepharose beads, SDS-PAGE and Western blot analysis implied that this 'mature' form was predominantly on the cell-surface.

This larger, cell-surface-derived form was then cleaved from the cell surface by the ACE sheddase, and appeared in the medium after about an hour (Fig. 4.1.1.3, left panel), the cleavage of which was entirely abolished by the addition of 10 μM TAPI (right panel). The metabolic labelling studies also showed very clearly that phorbol ester stimulated the rapid release of both wtACE and ACE-Δ6JM from the cell (middle panel), with significant signal appearing in the medium fractions as early as 1 hour after fresh 'cold' medium was added. This was corroborated by a rapid decrease

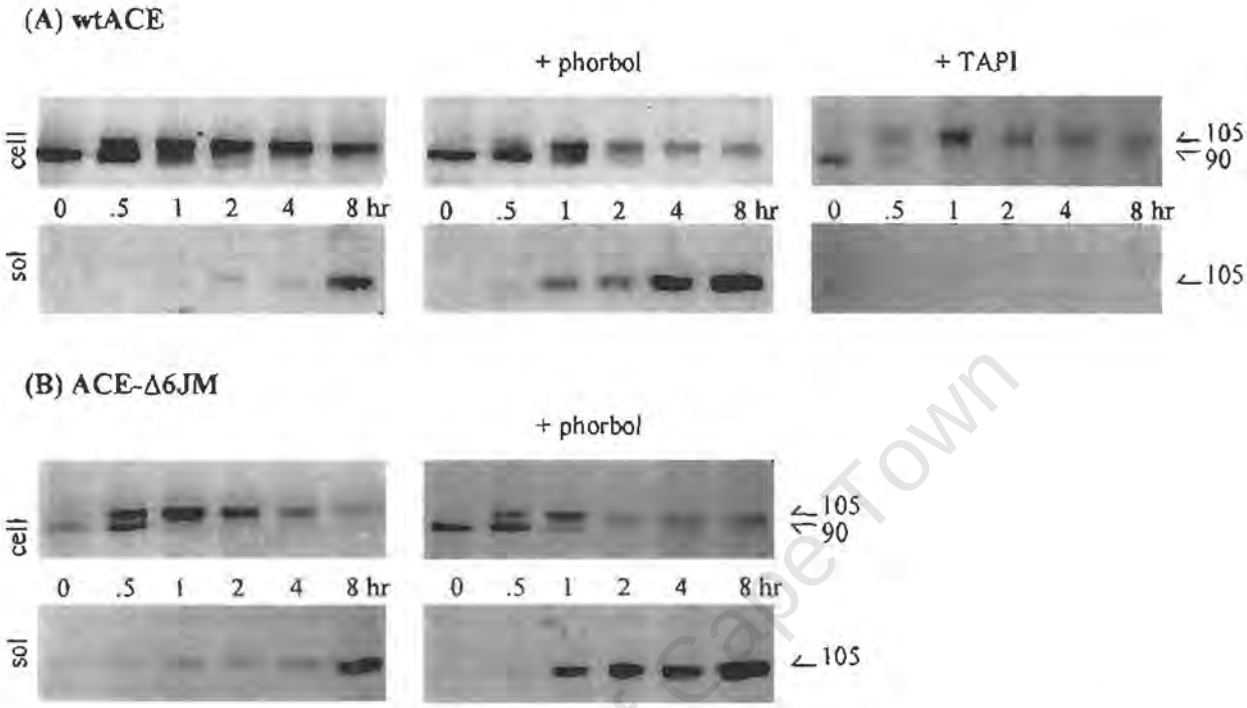

Figure 4.1.1.3) Metabolic labelling and pulse-chase analysis of wtACE and ACE-Δ6JM
CHO cells expressing either wtACE (A) or ACE-Δ6JM (B) were grown to confluence in 6-well dishes and starved for 30 minutes in 'starvation medium' prior to metabolically labelling with starvation medium supplemented with [^{35}S]-methionine and [^{35}S]-cysteine for 30 minutes. The cells were then washed and 'chased' in fresh induction medium for up to 10 hours as described in Chapter 3. The 'chase' medium was supplemented with nothing (left panels), 1 μM PDBu (middle) or 10 μM TAPI (right). The TAPI inhibition study was omitted in (B). At the indicated times, cell lysate (cell) and medium (sol) samples were affinity-precipitated with lisinopril-[28Å]-sepharose, subjected to SDS-PAGE and autoradiographed. Estimated molecular masses (in kDa) of the major bands are shown on the right.

in cell-associated signal, which was less obvious when cells were grown in medium without supplements (left panel).

To verify that this shedding effect was reproducible in other cell lines, COS1 cells were transiently transfected with pLEN-ACEVII (wtACE) and pLEN-ACE-Δ6JM plasmids using the DEAE-Dextran transient transfection method. The culture medium on the confluent 12-well dishes was replaced with fresh medium containing 1 μM PDBu 44 hours after the chloroquine/DMSO shock step had been completed. Shedding was allowed to proceed for a further 4 hours before both the cell-extract and medium samples were assayed for ACE activity using HHL as substrate. Although the expression levels were low for both wtACE and ACE-Δ6JM (see Fig. 4.1.1.4a), they nonetheless showed that 21% of the total ACE-Δ6JM appeared in the soluble fraction (see Fig. 4.1.1.4b). This was qualitatively similar to that seen for wtACE, which shed 34% of the total ACE over 4 hours of phorbol ester activation. These cells also showed the same dramatic inhibition with 10 μM TAPI and an increase in shedding on treatment with 200 μM 3,4-dichloroisocoumarin (DCI, a serine protease inhibitor shown to stimulate shedding [Schwager *et al.*, 1999]).

The shedding experiments, using both enzymatic activity and metabolic labelling studies, showed that the ACE-Δ6JM mutant was shed in the same manner as wtACE, both in the CHO and COS-1 cells. This indicated that the region just N-terminal of the human testis ACE cleavage site (R_{627}) was not crucial for sheddase recognition.

Of key interest then was the cleavage site. Did the ACE sheddase locate and cleave the same Arg-Ser bond at R_{627} in the stalk region, as is the case for wtACE [Ehlers *et al.*, 1996; Woodman *et al.*, 2000], or was it constrained by the reduction of 'headroom' and forced to find an alternative cleavage site closer to the transmembrane region? To find the cleavage site, MALDI-TOF mass spectrometry analysis was performed on fractionated peptides produced by endoproteinase Lys-C digestion of purified soluble ACE-Δ6JM.

Soluble ACE-Δ6JM was purified from the culture medium of transfected CHO cells using affinity chromatography over a lisinopril-28-sepharose column. The purified

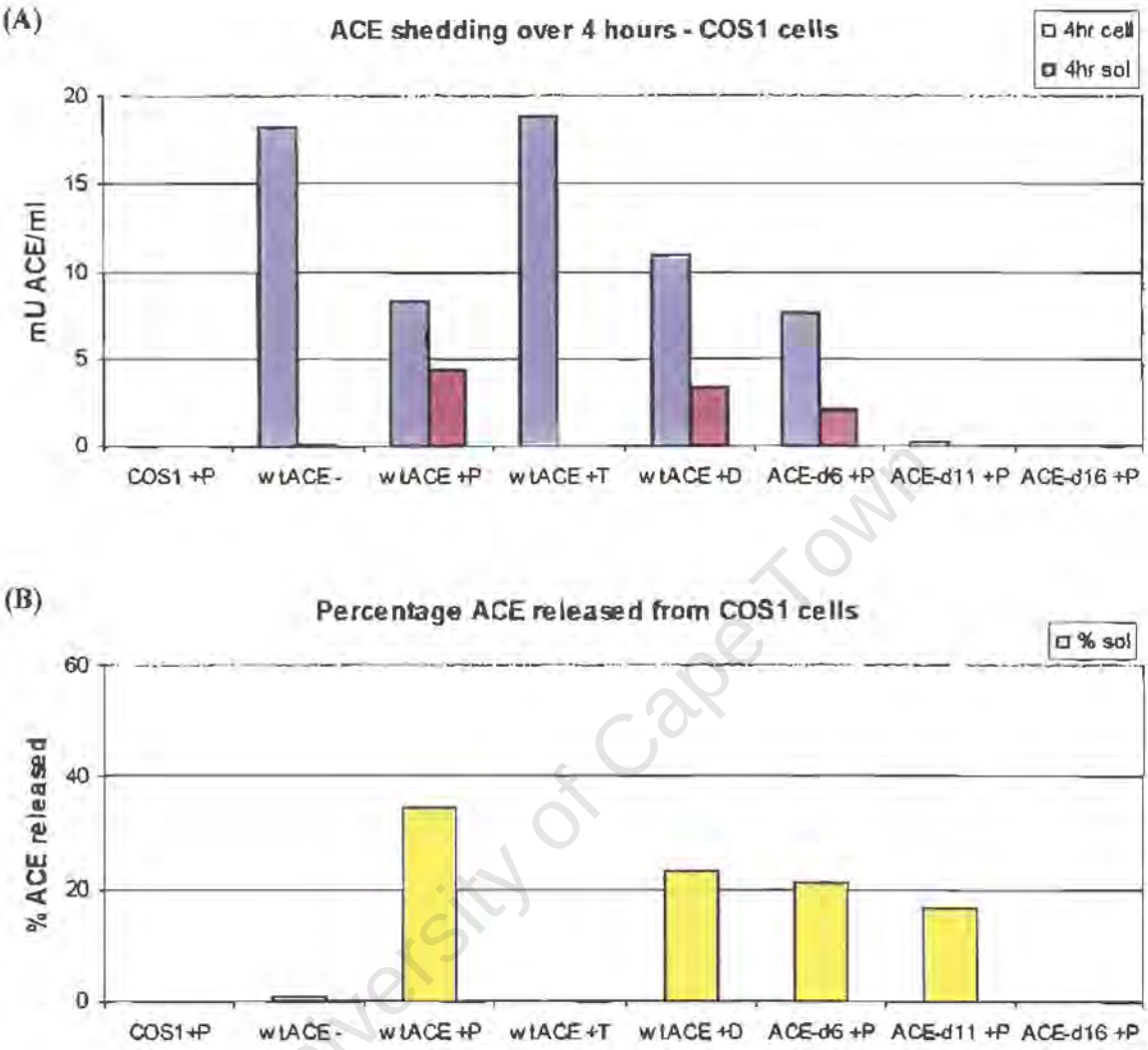

Figure 4.1.1.4) Transient transfection of COS1 cells and the shedding of ACE

COS1 cells grown to confluence in 12-well 4 cm^2 dishes were transiently transfected with 2.5 µg of either pLEN-ACEVII (wtACE) or pLEN-ACE-Δ6JM (ACE-d6), -Δ11JM (ACE-d11) or -Δ16JM (ACE-d16) mutant construct plasmid DNA, as described in Chapter 3. After 44 hours the medium was replaced with fresh culture medium [10% FCS, 40 µM $ZnCl_2$ in DMEM] supplemented with either nothing (-), 1µM PDBu (+P), 10 µM TAPI (+T) or 200 µM DCI (+D). After 4 hours of incubation at 37°C, 5% CO_2, humidified, the medium (sol) and cell-extract (cell) samples were assayed for HHL activity and converted to mU ACE per ml (A), and the soluble ACE activity expressed as a percentage of the total (cell-associated plus soluble) ACE (B).

protein was then denatured, the disulphide bonds reduced and protected with vinylpyridine, followed by complete digestion with endoproteinase Lys-C. The peptides were fractionated on HPLC, and the peak corresponding to the COOH-terminal peptide of soluble ACE-Δ6JM was then identified using N-terminal sequencing (automated Edman degradation). This produced the sequence [LGWPQY?RSEG], which was almost exactly identical to the expected sequence for this C-terminal peptide, namely [LGWPQY**N**RSEG…] (see Table 4.1.1).

This COOH-terminal peptide was also subjected to MALDI-TOF analysis, producing a strong peak at *m/z* 4130.4, and another at *m/z* 4421.4, neither of which related to cleavage after a defined number of residues in the ACE stalk (see 4.1.1.5a). The difference between these peaks was 291 Da, which is the mass of sialic acid (N-acetylneuraminic acid; monoisotopic mass change = 291.0954 Da). This curious result indicated that the N_{620}, adjacent to the section deleted in ACE-Δ6JM, might well be glycosylated, which was not entirely surprising as it now conforms to the putative N-glycosylation sequon (NXS/T, where X is not proline; [Ronin *et al.*, 1981]).

To confirm this, we removed the N-glycosylated sugars from the purified COOH-terminal peptide with N-glycosidase F treatment. The re-purified, deglycosylated, peptide was again sequenced using Edman degradation, yielding the sequence [LGWPQY**D**]. This change is consistent with deglycosylation at N_{620} as the deglycosylation reaction converts the peptide asparagine to aspartic acid, releasing the complete oligosaccharide.

The re-purified, N-glycosidase F-treated peptide was analysed using MALDI-TOF mass spectrometry, which yielded a single peak at *m/z* 2363.4. This corresponded to the peptide L_{614}-F_{640} (calculated *m/z* 2363.6; Table 4.1.1.1), implying that the ACE sheddase had cleaved ACE-Δ6JM at the F_{640}-L_{641} bond, 11 amino acids away from the transmembrane domain.

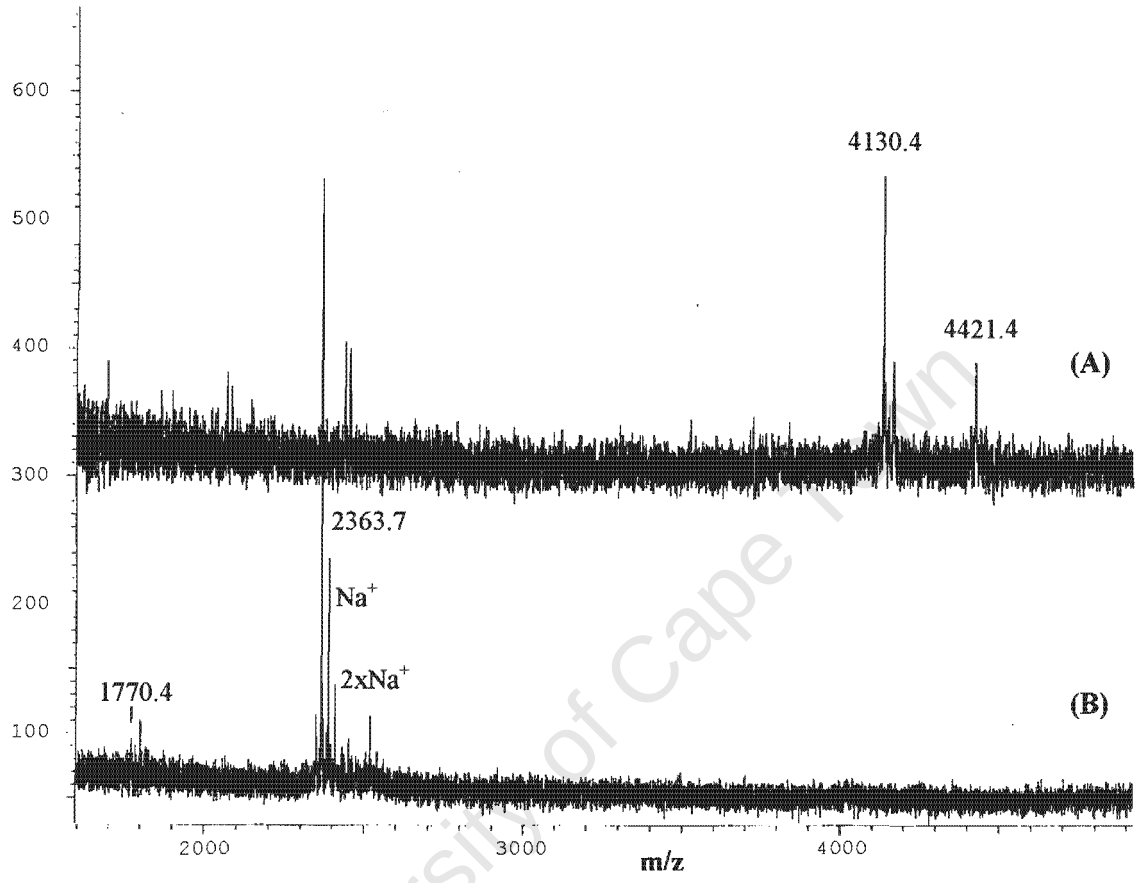

Figure 4.1.1.5) MALDI-TOF analysis of the COOH-terminal peptide of ACE-Δ6JM
Purified soluble ACE-Δ6JM was digested with Lys-C, the peptides separated using HPLC, and the fraction containing the COOH-terminal peptide found using Edman degradation. This fraction was subjected to MALDI-TOF analysis both prior to (A) and directly following deglycosylation with *N*-glycosidase F treatment (B). Note the absence of the larger peak at *m/z* 4130.4 after deglycosylation, and the appearance of a peak at *m/z* 2363.7, which was found to account for the peptide component after re-purification. One of the minor peaks (*m/z* 1770.4) possibly constitutes the complete N-glycan oligosaccharide, the possible structures of which are shown in Fig. 4.1.7. Relative mass (*m/z*) is shown on the x-axis, and arbitrary intensity units are shown on the y-axis.

Table 4.1.1.1) Calculated $[M+H]^+$ ions for putative COOH-terminal ACE-Δ6JM peptides	
Calc. $[M+H]^+$	COOH-terminal ACE-Δ6JM peptide
2762.03	LGWPQYDRSEGPLPDSGRVSFLGLD
2646.94	LGWPQYDRSEGPLPDSGRVSFLGL
2533.78	LGWPQYDRSEGPLPDSGRVSFLG
2476.73	LGWPQYDRSEGPLPDSGRVSFL
2363.57	LGWPQYDRSEGPLPDSGRVSF
2216.39	LGWPQYDRSEGPLPDSGRVS
2129.32	LGWPQYDRSEGPLPDSGRV
2030.18	LGWPQYDRSEGPLPDSGR
1874.00	LGWPQYDRSEGPLPDSG

The peptide molecular ions of all possible deglycosylated COOH-terminal peptides for Lys-C digested ACE-Δ6JM were calculated, and those in the relevant region shown here. Note that N_{620} has changed to an aspartic acid (highlighted in yellow) after N-glycosidase F treatment. The phenylalanine at which the ACE sheddase has cleaved ACE-Δ6JM is highlighted in blue. Notice the close agreement between the calculated $[M+H]^+$ ion for this peptide and that found experimentally for the deglycosylated COOH-terminal peptide (*m/z* 2363.4).

The products from N-glycosidase F treatment were also analysed using MALDI-TOF analysis, prior to re-purification of the deglycosylated peptide. The peptide accounted for the *m/z* 2363.7 peak, with secondary peaks containing either 1 or 2 sodium ions (Fig. 4.1.1.5b). Another minor peak appeared at *m/z* 1770.4, which may have been due to the complete oligosaccharide that was removed through N-glycosidase F treatment. A search of the www.GlycoSuite.com database [Proteome Systems, Ltd.] of known glycan structures using the mass of the released oligosaccharide revealed four completely different structures all having the same monoisotopic mass (1770.6552 Da), the structures of which are shown in Fig. 4.1.1.6. In addition, an oligosaccharide with mass 1769.6 Da was found previously to form the basic structure of the other six N-linked oligosaccharides found in ACE_T [Yu *et al.*, 1997]. A putative glycan structure would also have to take into account the sialic acid that is incorporated into the *m/z* 4421.4 glycopeptide peak seen in Fig. 4.1.1.5a.

The combinatorial variation in possible glycan structures thus precluded any hope of defining the exact structure without further oligosaccharide sequencing, which was outside of the scope of this thesis. It was, however, clear that a large N-glycan oligosaccharide was covalently linked to N_{620}, an asparagine that was usually not glycosylated in wild-type human testis ACE [Yu *et al.*, 1997]. This implied that the N-glycosyl transferases responsible for glycosylating this potential N-linked glycosylation sequon, 32 amino acids from the transmembrane domain, are not

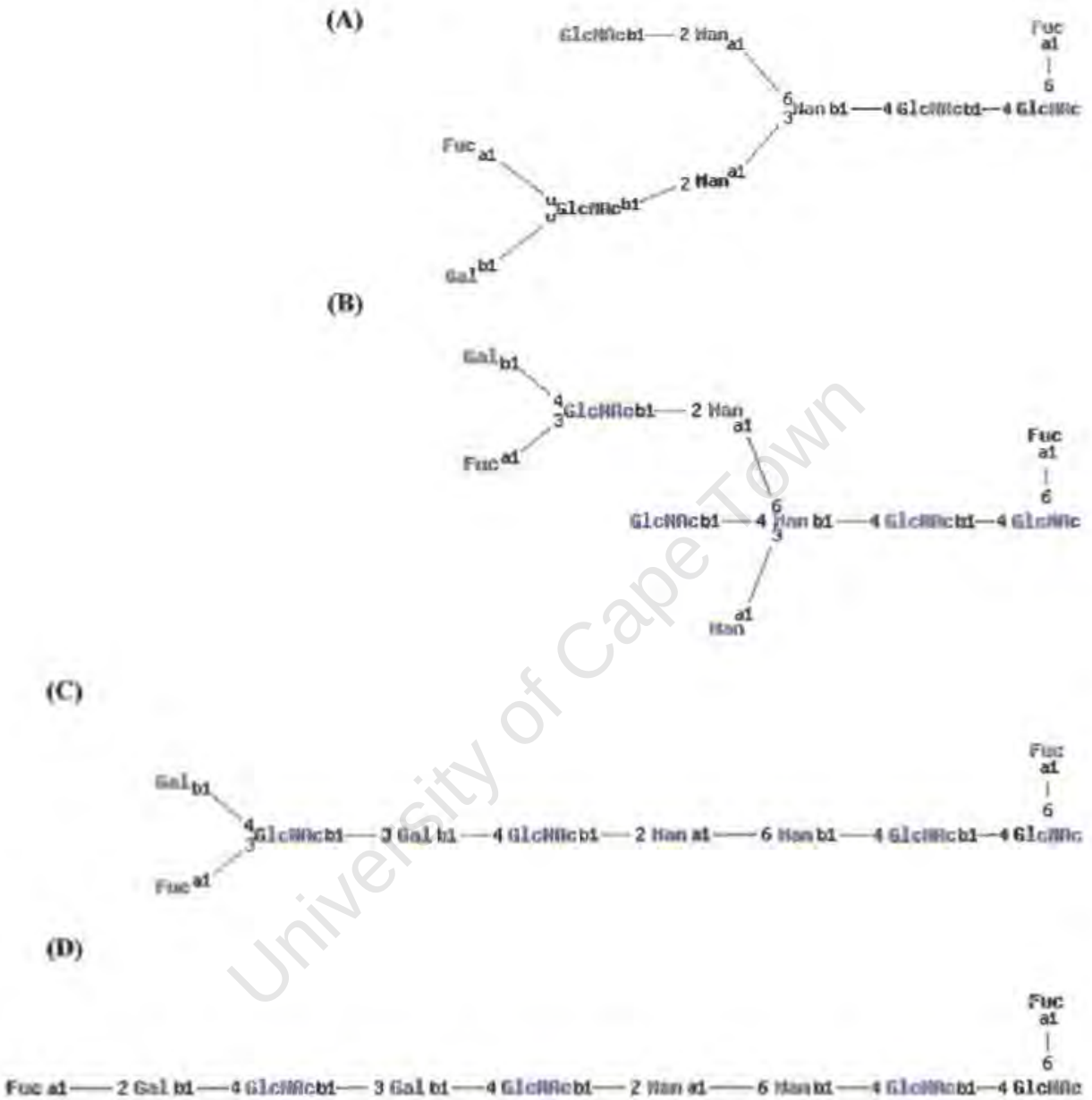

Figure 4.1.1.6) Putative glycan structures

A search of the GlycoSuite.com database (http://www.glycosuite.com/query) revealed four N-linked structures relating to a monoisotopic mass of 1770.6552 Da, which closely matches that found released by *N*-glycosidase F treatment of the purified COOH-terminal Lys-C digested peptide of ACE-Δ6JM. (A) was found attached to both recombinant HIV protein gp120 expressed in CHO cells [Kuster *et al.*, 1997], and human elastase I [Wendorf *et al.*, 1991]. (B) was isolated from the mouse brain protein tenascin-R [Zamze *et al.*, 1999], while both (C) and (D) were isolated from unknown proteins in human urine [Michalski *et al.*, 1991]. Gal, Galactose; Fuc, Fucose; Man, Mannose; GlcNAc, *N*-acetylgalactosamine.

inhibited by steric constraints between the proximal ectodomain and the TM in the native enzyme, as this same N_{620} is glycosylated in the stalk region of ACE-Δ6JM. It also implied that the structure of the native N-glycosylation sequon [NWTP] is probably refractory to glycosylation, whereas the new site [NRSE] is more accommodating. One can thus surmise that the 'bulky' tryptophan and 'helix-breaking' proline create an unfavourable N-glycosylation site in wtACE.

The key finding from the ACE-Δ6JM mutant is that the region directly N-terminal to the native cleavage site is not the site of sheddase recognition, and that the sheddase is able to make use of alternate sites proximal to the transmembrane domain when the 'headroom' is occluded by a large carbohydrate side-chain. However, this does not exclude the possibility that the reduction in headroom may have played a role in re-positioning the sheddase. Thus another mutant was constructed in which a further 5 amino acids were removed from the N-terminal region, the ACE-Δ11JM mutant, which does not contain a putative N-glycosylation site.

4.1.2) ACE-Δ11JM

The ACE-Δ11JM mutant was constructed such that the region W_{616}-A_{626} of human ACE_T was deleted. This deletion removed the peptide [WPQYNWTPNSA] upstream (N-terminal) of the cleavage site, thereby removing the seventh putative N-glycosylation site (NWT), and bringing the proximal ectodomain closer to the wtACE cleavage site.

CHO cells were transfected with pLEN-ACE-JMΔ11, using the calcium phosphate method described above. Although numerous clones from repeated transfections were screened for ACE activity, the activity was consistently low with a cellular ACE activity of 1.6 ± 0.7 mU ACE per well (n = 7), two orders of magnitude lower than that of wtACE.

ACE-Δ11JM showed characteristic inhibition of shedding in the presence of 10 μM TAPI (~75%). Although the 4-hour medium samples did not show a pronounced

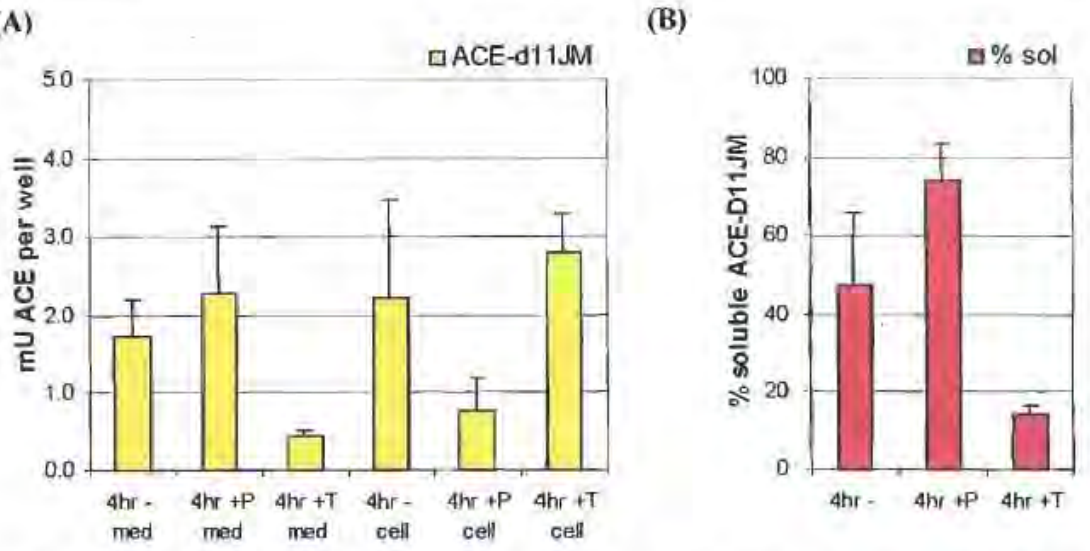

Figure 4.1.2.1) The shedding of ACE-Δ11JM – effect of PDBu and TAPI over 4 hours
CHO-K1 cells transfected with pLEN-ACE-Δ11JM were grown to confluence in 6-well 9.5 cm^2 dishes, ACE expression induced overnight, followed by a 4 hour incubation with fresh induction medium supplemented with nothing (-), 1 μM PDBu (+P) or 10 μM TAPI (+T). After 4 hours the medium (med) and cell-extract (cell) samples were assayed for ACE activity using the HHL assay (A). The percentage of soluble ACE-Δ11JM in the medium fraction after 4 hours (B) was determined by dividing the soluble activity by the total ACE activity in the well (cell plus medium) [n=7].

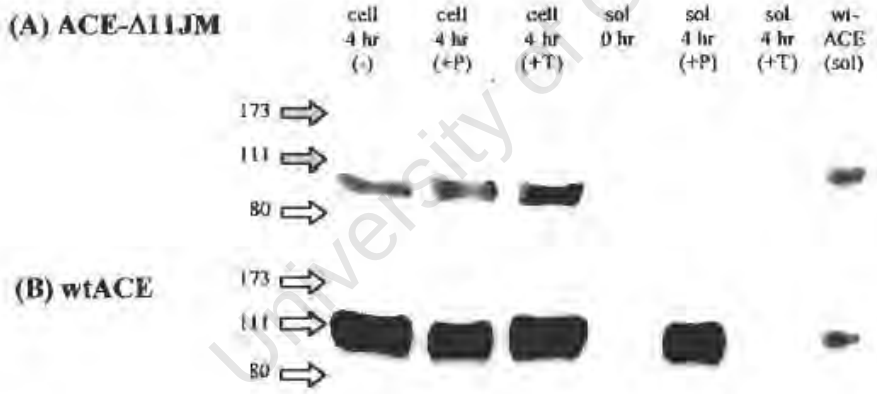

Figure 4.1.2.2) Western blot analysis of ACE-Δ11JM
The 4-hour cellular (cells) and medium (sol) samples in Fig. 4.1.2.1 (A) were further analysed using Western blotting. 24 μl of the 1000 μl samples from the confluent, induced 6-well dish was separated through a 10% SDS-PAGE gel, blotted onto nitrocellulose and probed using a 1:2000 dilution of rabbit anti-human ACE polyclonal antibody followed by a 1:2000 dilution of an anti-rabbit HRP-conjugated antibody. Peroxidase activity was detected using the ECL chemiluminescence kit [APBiotech]. The Western blot for wtACE analysed under the same conditions is shown in (B) for comparison. Note the release of shed wtACE in the medium after 4 hours of phorbol ester stimulation (+P), and the almost complete inhibition of shedding by TAPI (+T). The absence of bands in the 0hr medium lane indicates specificity of the anti-ACE antibody. The soluble ACE-Δ11JM protein was below the detection limit for this anti-ACE antibody. GibcoBRL BenchMark pre-stained protein ladder size marker positions are indicated with grey arrows, the size of each shown in kDa. Purified soluble wtACE protein (25ng) was loaded in the last lane as a size marker for shed ACE.

increase in shedding with phorbol ester stimulation, a statistically significant increase in shedding was observed when the ACE activities were converted to a percentage of total ACE in the well (47% versus 74%; $P = 0.008$; Fig. 4.1.2.1b). This implies that, although expressed very poorly in CHO cells, the ACE-Δ11JM mutant was shed with qualitatively similar kinetics to that of wtACE and the ACE-Δ6JM mutant, and thus the deletion of 6 or 11 amino acids directly distal to the cleavage site did not affect the rate of shedding, but may have affected the efficiency of protein translocation to the cell surface and/or its stability.

The poor expression level for ACE-Δ11JM was tested in a second cell line. pLEN-ACE-JMΔ11 was transiently transfected into COS1 cells using the DEAE-Dextran method. Although the ACE activity detected was extremely low, showing only 1 mU ACE per ml (Fig. 4.1.1.4a), the percentage ACE activity shed over 4 hours of phorbol ester stimulation was 16.7%, qualitatively similar to that of ACE-Δ6JM (see Fig. 4.1.1.4b). Thus, the poor expression of ACE-Δ11JM in COS1 cells is consistent with that observed in CHO cells.

Western blotting analysis of cell-extract and medium samples of CHO cells expressing ACE-Δ11JM showed an ACE specific band in the cellular fractions with a molecular weight of about 90 kDa (Fig. 4.1.2.2b). This is smaller even than the soluble wtACE control band shown on the right of Fig. 4.1.2.2a, and about the same size as the precursor form of wtACE (Fig. 4.1.1.3a) and cannot be accounted for by the change in peptide mass due to the 11-residue deletion (1.3 kDa). This band did not appear in the medium fraction after 4 hours of PDBu stimulation. As the ACE activities of the cellular and medium fractions seen in Fig. 4.1.2.1a were not significantly different, detection of the medium form by Western blot analysis would be expected if the cellular form were detected. The detection limit for this Western blot system was tested using purified ACE, and found to be 5 ng of soluble wtACE, which was the equivalent of a cell-extract or medium sample having an ACE activity of ~25 mU per well (using HHL as substrate; data not shown). The active forms of both the cell-associated and soluble forms ACE-Δ11JM were thus below the detection limit, and the membrane-associated ACE seen in the cellular fractions was therefore likely an inactive precursor form.

The intracellular localisation of the ACE-Δ11JM mutant was investigated using confocal microscopy. Transfected CHO cells were grown on coverslips, ACE expression was induced overnight, and the cells were fixed with ice-cold 3% paraformaldehyde (PFA) for 5 min for surface labelling. For detection of the intracellular ACE, the fixed cells were further permeabilised with ice-cold methanol for 5 minutes. ACE protein was probed using an anti-ACE antibody and a FITC-conjugated secondary antibody. No FITC label was seen when the extracellular, cell-surface ACE was probed in fixed CHO cells expressing ACE-Δ11JM, although intracellular signal was detected (see Fig. 4.1.2.3). This implies that the precursor form seen in the Western blots (Fig. 4.1.2.2b) did not reach the cell surface to any appreciable degree. Furthermore, the low levels of enzymatically active, mature ACE-Δ11JM that reached the cell surface were likely cleaved off the membrane too rapidly to allow detection using either Western blotting or FITC labelling and confocal microscopy.

Thus, it can be concluded that although appreciable quantities of the precursor form were expressed in CHO cells, the ACE-Δ11JM mutant was much less stable than the native form of ACE. These proteins were probably rapidly degraded, with an undetectable fraction reaching the cell surface as a fully glycosylated form. This could be due to the deletion of the amino acids W_{616}, P_{617}, W_{621}, P_{623}, which are completely conserved in all mammalian forms of ACE and in both domains, and could therefore be evolutionarily conserved for the structural stability of ACE (see Fig. 2.4.1).

Soluble ACE-Δ11JM was affinity-purified for cleavage site analysis. MALDI-TOF mass spectrometry analysis was performed on peptides generated from a cyanogen bromide (CNBr) digest. Cyanogen bromide digestion was used because the COOH-terminal peptide from a Lys-C digest ending at R_{627} would have a calculated mass of only 344.2 Da, which is not easily detected using MALDI-TOF analysis. MALDI-TOF analysis identified a peptide molecular ion at *m/z* 2916.6, which matched that of the calculated mass for the peptide L_{593}–R_{627} (2915.3), the presumptive COOH-terminal peptide. This peptide was isolated using HPLC and identified by Edman degradation, which gave the sequence [LSYFK]. This confirmed the correct

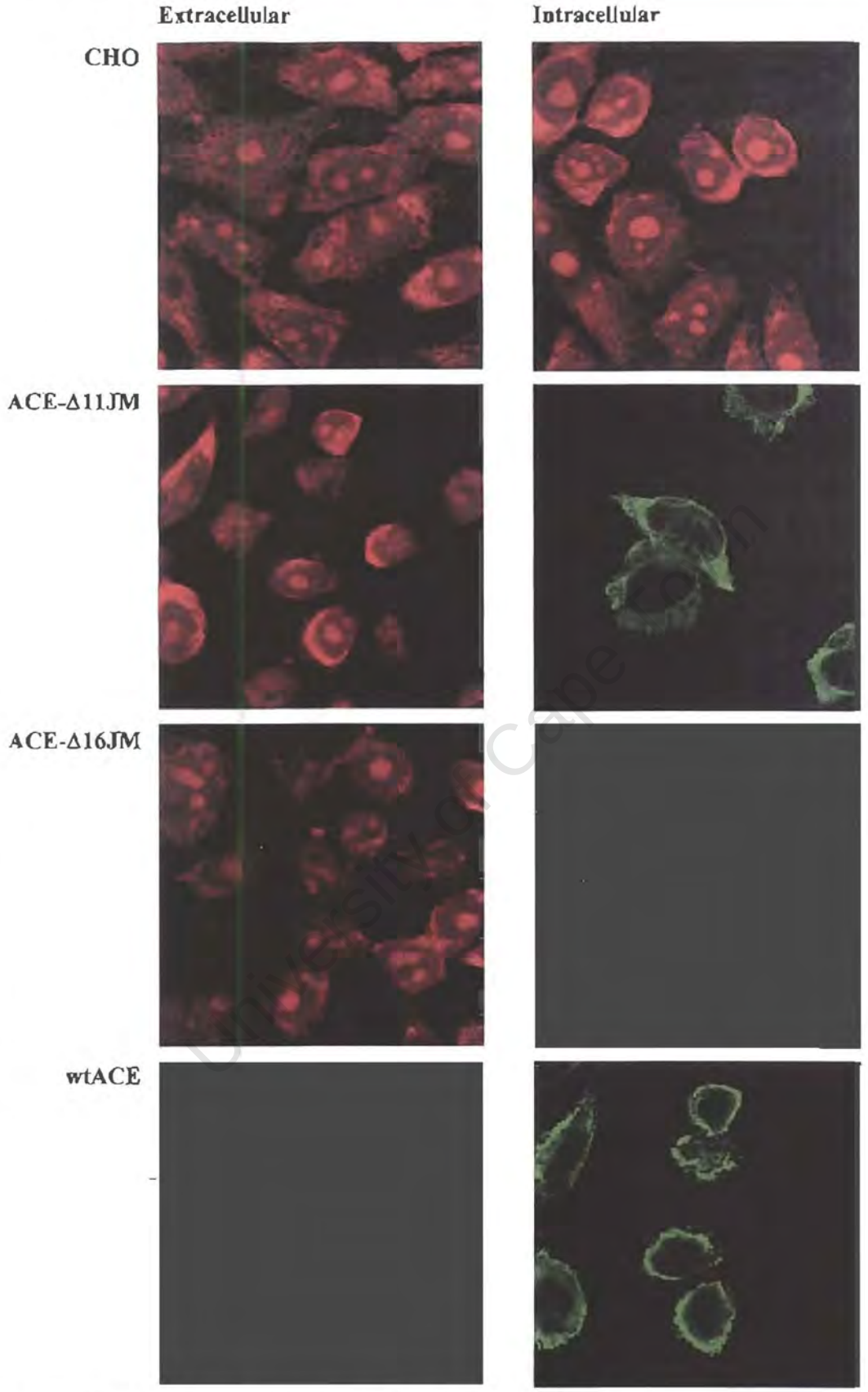

Figure 4.1.2.3) Confocal microscopy of transfected CHO cells

CHO cells expressing wtACE, ACE-Δ11JM or ACE-Δ16JM were grown on coverslips, fixed with 3% PFA (extracellular), or additionally permeabilised with methanol (intracellular). ACE protein was probed, and anti-ACE antibodies probed with a FITC-conjugated antibody. FITC label (green) was detected using confocal microscopy. The DNA-intercalating propidium iodide stain (red) was used to verify that cells (nuclei) were indeed present when no FITC was detected.

construction and isolation of ACE-Δ11JM, as the C-terminal peptide from a wtACE contaminant would have had a significantly different mass. The ACE sheddase cleavage site for the ACE-Δ11JM mutant was therefore at the R_{627}/S_{628} bond, identical to that of wtACE.

The fact that the ACE sheddase, showing the characteristic phorbol ester induction and TAPI inhibition of shedding, was capable of cleaving the mutated stalk region at the same R_{627}/S_{628} bond as in native wtACE, implied that the reduction of headroom by 11 amino acids did not physically hinder the sheddase from reaching this cleavage site. It further implied that the N-glycan that was introduced in the stalk region of ACE-Δ6JM was much more effective at blocking this site, and the sheddase was 'forced' to find an alternate site. Thus the 'headroom', or distance from the proximal ectodomain to the stalk cleavage site, probably does not play a role in shedding *per se*. This region may, however, be involved in protein folding and stability, resulting in reduced expression when critical, evolutionarily conserved, amino acids are deleted.

4.1.3) ACE-Δ16JM

The same two-step PCR mutagenesis protocol described above, with primers shown in Appendix III, was used to create the ACE-Δ16JM mutant in which the stalk region residues T_{605}-N_{620} were deleted (see Table 4.1.1). The plasmid pLEN-ACE-Δ16JM was transfected into CHO cells and neomycin-resistant clones were selected and assayed for ACE activity using HHL as substrate. Surprisingly, no ACE activity was detected in the medium or cell-extracts of selected clones, under the standard assay conditions.

To verify that the protein was indeed expressed, Western blot analysis was performed as described under Methods (Chapter 3). Like the ACE-Δ11JM mutant, only the precursor form of ACE-Δ16JM was detected in the cell extract samples (~90 kDa), and no ACE was detected in the medium (Fig. 4.1.3.1). The calculated difference in relative peptide mass between the mature forms of wtACE and ACE-Δ16JM is only 1.9 kDa. Thus the mature form of both proteins should appear as a broad band (due to

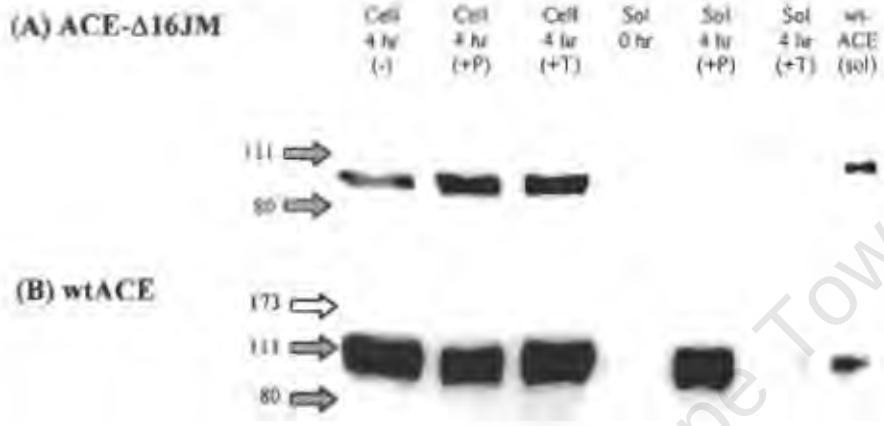

Figure 4.1.3.1) Western blot analysis of ACE-Δ16JM

CHO cells expressing either ACE-Δ16JM (A) or wtACE (B) were subjected to the same 4-hour shedding kinetics study in which cells were incubated for 4 hours with fresh culture medium supplemented with nothing (-), 1 μM PDBu (+P) or 10 μM TAPI (+T). The cellular (cell) and medium (sol) samples were analysed using Western blotting to probe for ACE protein, as described. The molecular masses of the BenchMark pertained marker are indicated in the left, in kDa, the position of which is indicated by the grey arrows. Purified soluble wtACE was loaded in the last lane as a size marker for the soluble form of ACE. Note the complete absence of any shed (soluble) ACE-Δ16JM protein in (A) and the lack of the mature form in the cell-extract samples.

heterogeneous glycosylation) at about the same size (~105 kDa), which was clearly not the case for ACE-Δ16JM (see Fig. 4.1.3.1a). The ACE-specific band seen in the cell-extracts of ACE-Δ16JM was smaller than the soluble wtACE marker on the right of Fig. 4.1.3.1a, indicating that this was an unglycosylated, immature form of ACE. This precursor form was likely not transported to the cell surface and was probably rapidly degraded in the endoplasmic reticulum, explaining the absence of a shed form in the medium.

Confocal microscopy was used to determine the intracellular localisation of the ACE-Δ16JM mutant. No FITC label was seen on the cell surface of the fixed but unpermeabilised cells, although adequate numbers of intact nuclei were seen. A weak but reproducible intracellular signal was seen, indicating that the precursor form of ACE-Δ16JM was produced in these cells, but did not appear on the cell surface (Fig. 4.1.2.3).

Thus, the ACE-Δ16JM mutant was inactive, and was produced as a precursor form which did not mature to the glycosylated form and did not reach the cell surface. This mutant was not shed into the medium, and was probably rapidly degraded intracellularly.

The regions of the ACE stalk deleted in the ACE-Δ16JM, -Δ6JM, -ΔR627 and -JMΔ24 mutants cumulatively span the entire juxtamembrane stalk region (see Table 4.1.1). Based on these results, in particular those of the ACE-Δ16JM mutant, it is likely that inactivation of the ACE-JMΔ47 mutant was due to the deletion of the region T_{605}-G_{615}, and not due to the proximity of the extracellular domain to the TM. As all other stalk mutants with deletions C-terminal to G_{615} were enzymatically active, to varying degrees, one can conclude that the proximal boundary of the ACE ectodomain is likely at, or near, G_{615} (see Fig. 4.1). This therefore precluded more adventurous deletions in the ACE ectodomain with the aim of deleting the sheddase recognition region, a limitation that is discussed in greater detail in Chapter 6.

4.2) The Cleavage Site

The cleavage site of wild-type human testis ACE deserves closer examination. Cleavage-site analysis has shown that the sheddase cleavage sites for the release of human ACE_T and ACE_S, as well as the ACEΔ17, ACEΔ24 and ACE-Δ11JM mutants, is at the R_{627}/S_{628} bond 24 amino acids from the TM [Ehlers *et al.*, 1996; Woodman *et al.*, 2000; above]. This means that large deletions, both N- and C-terminal to the cleavage site, are tolerated by the sheddase and that it continues to use this arginine at the P_1' position for cleavage, even when it is directly adjacent to either the TM or the proximal ectodomain. This is somewhat counter-intuitive, as a comparison of the stalk region and cleavage sites of numerous ectoproteins indicates that sheddases appear to favour cleavage at least 3 residues from the proximal ectodomain and 8 residues from the TM (see Table AI.2; Ehlers *et al.*, 1996). Thus, cleavage at R_{627} suggests that the ACE sheddase may have a preference for this particular amino acid. To test this hypothesis we deleted R_{627} and examined the effect this had on shedding.

4.2.1) ACE-ΔR627

The plasmid pLEN-ACE-ΔR_{627} was constructed in pLEN-ACEVII using the two-step PCR mutagenesis protocol described in Chapter 3 to delete R_{627} from human testis ACE (see Table 4.1.1). The plasmid was stably transfected into CHO-K1 cells using the calcium phosphate transfection protocol. Neomycin-resistant cells were assayed for ACE activity. ACE expressing cells were then grown to confluence in 6-well cm^2 tissue culture dishes and subjected to the same 4-hour shedding kinetics study described previously, the results of which are shown in Fig. 4.2.1.1. Surprisingly, ACE activity in the medium after 4 hours was extremely low compared to that for wtACE, although this did show a 2-fold increase with the addition of phorbol ester, and exhibited TAPI inhibition.

The relative effect of PDBu and TAPI on shedding was more clearly demonstrated with Western blot analysis, where a marked difference was seen in the amounts of soluble ACE-ΔR_{627} when cells were treated with either compound (see Fig. 4.2.1.2).

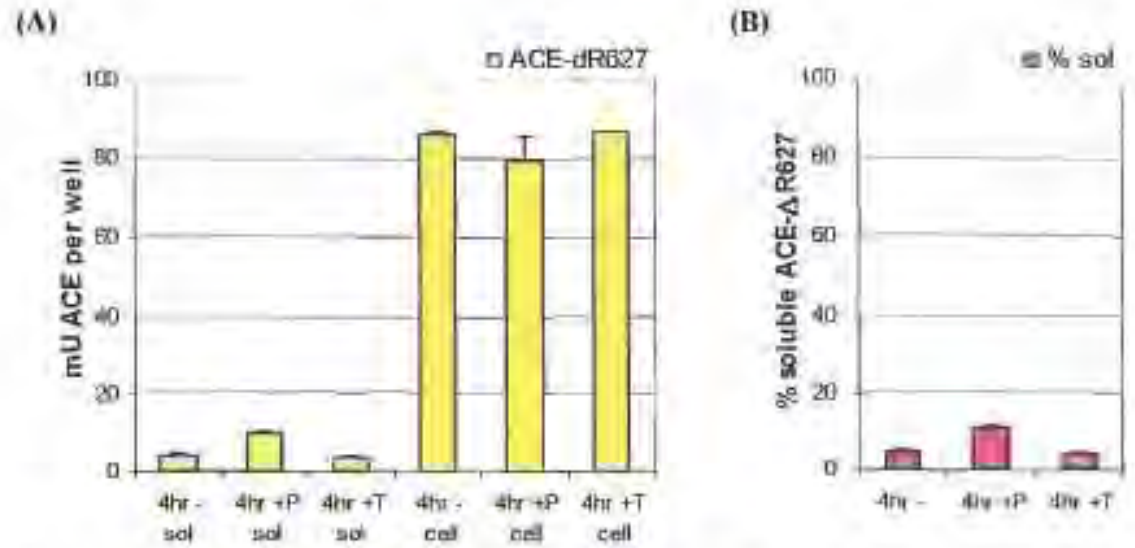

Figure 4.2.1.1) The shedding of ACE-ΔR627 – effect of PDBu and TAPI over 4 hours

CHO-K1 cells transfected with pLEN-ACE-ΔR627 were grown to confluence in 6-well dishes, ACE expression induced overnight, followed by a 4-hour incubation with fresh induction medium supplemented with nothing (-), 1 μM PDBu (+P) or 10 μM TAPI (+T). The medium (sol) and cell-extract (cell) samples were then assayed for ACE activity using the HHL substrate assay (A) and the percentage activity in the medium after 4 hours (B) was determined by dividing the soluble activity by the total ACE activity in the well (cell plus medium) [n=3].

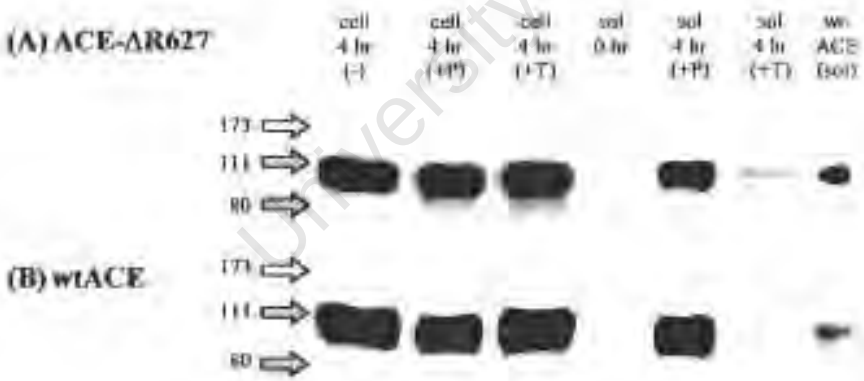

Figure 4.2.1.2) Western blot analysis of ACE-ΔR627

The 4-hour cellular (cells) and medium (sol) samples in Fig. 4.2.1.1 (A) were further analysed using Western blotting to probe for ACE protein, as described. Note the release of shed ACE-ΔR627 in the medium after 4 hours of phorbol ester stimulation (+P) and the almost complete inhibition of shedding by TAPI (+T). The top band seen in the medium samples also occurs in the medium control (0 hr) lane, and is thus a cross-reactive component of FCS. GibcoBRL BenchMark pre-stained protein ladder size marker positions (in kDa) are indicated with grey arrows. Soluble wtACE protein (25ng) is loaded in the last lane as a marker.

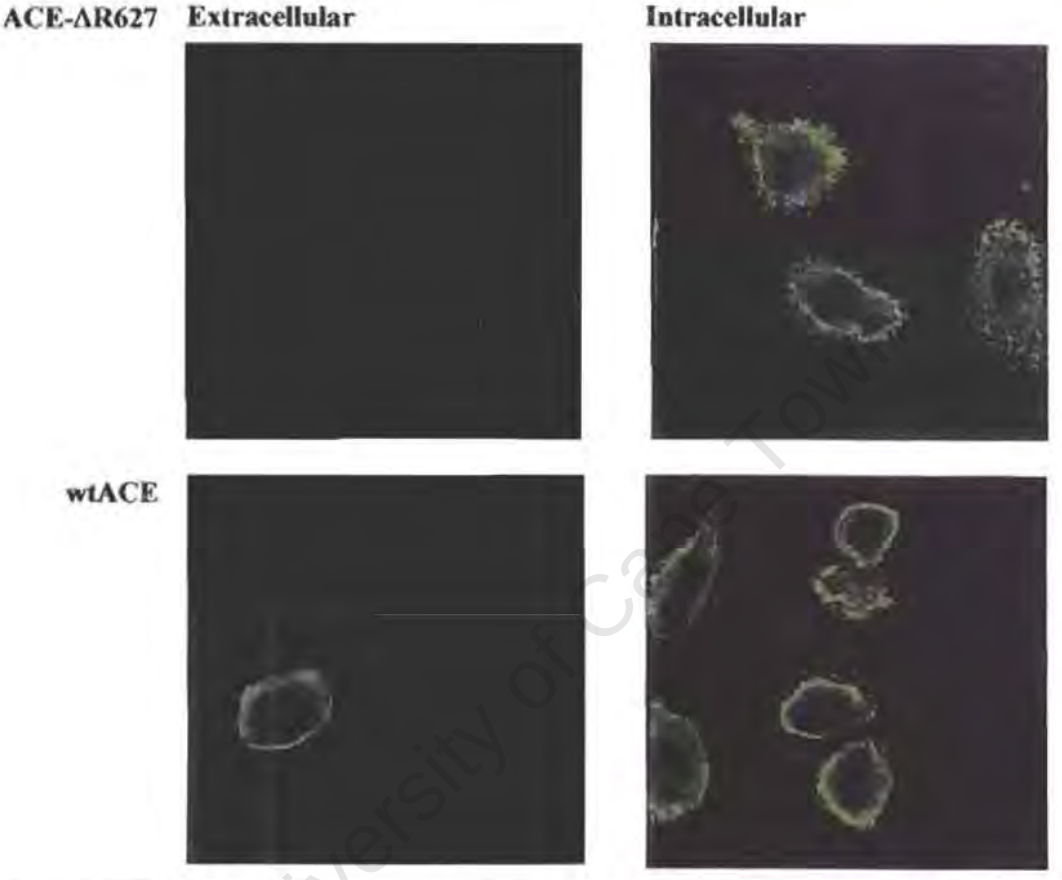

Figure 4.2.1.3) Confocal microscopy of CHO cells – ACE-ΔR627 and wtACE
Transfected CHO cells grown on coverslips were fixed with 3% PFA (extracellular), or additionally permeabilised with ice-cold methanol (intracellular). ACE protein was probed with rabbit anti-ACE antibodies, which was subsequently probed with a FITC-conjugated anti-rabbit antibody and the FITC label (green) detected using confocal microscopy. The propidium iodide stain was omitted for clarity as it obscures the faint FITC signal seen on the surface of ACE-ΔR627-transfected CHO cells. The same intensity setting was used for all pictures, allowing semi-quantitative comparison.

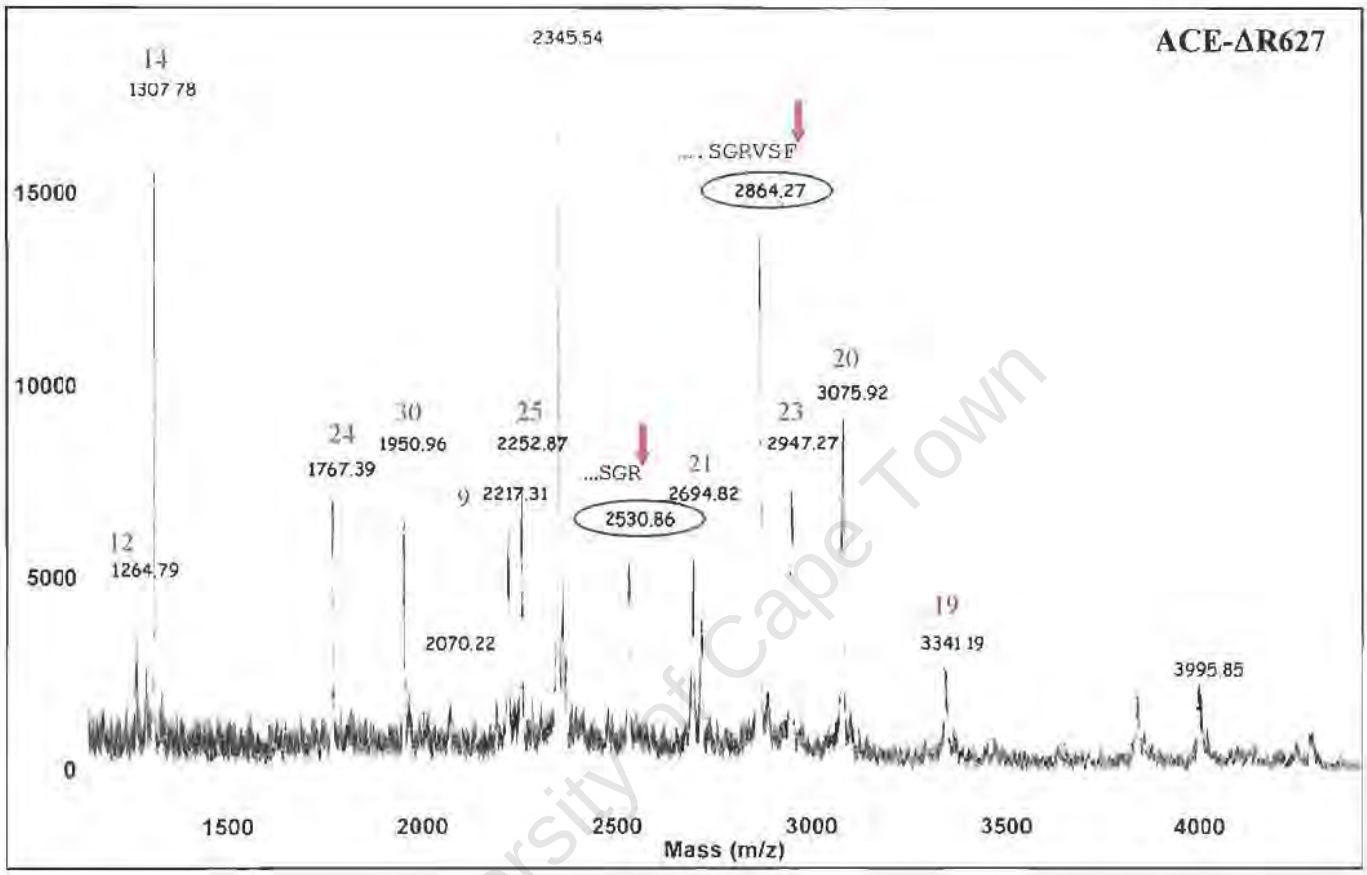

Figure 4.2.1.4) MALDI-TOF analysis of ACE-ΔR627

Denatured, reduced and vinylpyridine-protected, purified ACE-ΔR627 was digested with endoproteinase Lys-C, and the mixed peptides subjected to MALDI-TOF analysis. Numerous *m/z* masses related closely to the calculated masses for expected peptides produced through Lys-C digestion of soluble ACE (red numbers). However, two did not relate to known peptide masses (shown in blue), but instead matched the calculated $[M+H]^+$ sizes of COOH-terminal peptides ending in R637 (2530.7) and F640 (2864.1). Thus ACE-ΔR627 is cleaved at the R637/V638 and F640/L641 bonds (shown with red arrows).

This indicated that the shedding of ACE-ΔR_{627} showed similar characteristics to that of wtACE, although at a reduced efficiency.

Confocal microscopy was performed on paraformaldehyde-fixed CHO cells expressing ACE-ΔR_{627}, using a polyclonal rabbit anti-ACE antibody and a FITC-labelled secondary antibody (Fig. 4.2.1.3). Surprisingly, the fixed cells showed very poor cell-surface signal, while strong intracellular signal was seen when the cells were permeabilised. This implied that the cellular ACE activity was mostly intracellular and that the deletion of a single residue in the stalk region of ACE had profoundly affected the processing of ACE to the cell surface. This would explain the poor shedding results, as ACE was poorly processed to the plasma membrane, thus reducing the amount of substrate available to the sheddase.

Soluble ACE-ΔR_{627} protein was purified from the medium of transfected CHO cells for cleavage-site determination. The purified protein was denatured, the disulphide bonds reduced and free thiols protected with vinylpyridine, and the protein digested using endoproteinase Lys-C. The peptide fragments were then subjected to MALDI-TOF analysis that revealed numerous peaks corresponding to the calculated molecular ions for expected peptides produced by Lys-C digestion of soluble ACE. However, two peaks did not relate to known peptide masses, instead matching the calculated $[M+H]^+$ ions of COOH-terminal peptides ending in R_{637} and F_{640}, namely *m/z* 2530.86 and 2864.27 respectively (Fig. 4.2.1.4). Thus ACE-ΔR627 was cleaved at the R_{637}/V_{638} and F_{640}/L_{641} scissile bonds, 14 and 11 amino acids from the TM domain, respectively (see Table 4.1.1).

In conclusion, the ACE sheddase was able to cleave other bonds in the stalk region when the preferred R_{627} was deleted. Cursory examination of the rate of shedding may suggest that cleavage had been disrupted. However, the confocal microscopy data indicated that this was instead due to a defect in the processing of this mutant to the surface. Thus, the sheddase may in fact be working optimally but with limited ACE-ΔR_{627} substrate. This result also established the promiscuity of the ACE sheddase, as shedding was not abolished with the removal of this cleavage-site residue. These results also suggested the relative importance of the R_{627} residue for cleavage, as the

sheddase did not position itself relative to the S_{628}, otherwise cleavage would still have occurred N-terminal to S_{628} in the ACE-ΔR_{627} mutant. Nor, for that matter, did the sheddase position itself rigorously at a defined distance from the proximal ectodomain (as shown above), otherwise shedding would have occurred C-terminal to S_{628} in the ACE-ΔR_{627} mutant. Furthermore, the assumption that the sheddase recognition domain may be close to the cleavage site requires re-assessment, as the ACE sheddase finds alternate sites for cleavage when the preferred R_{627} is either deleted or blocked by a large N-linked oligosaccharide. These alternate cleavage sites have differing proximal regions, implying that varied sequences are tolerated by the sheddase in the immediate vicinity of the scissile bond. This is most clearly illustrated by the insertion of entirely different sequences into the ACE stalk region of ACE, and finding that they too are cleaved by a sheddase, explained in greater detail below.

In the work of Ehlers *et al*, deletions of 17 and 24 amino acids C-terminal to the cleavage site did not abolish cleavage at the R_{627}/S_{628} bond, implying either that the sheddase had a preference for this bond, or that the distance from the proximal ectodomain to the cleavage site had to be maintained [Ehlers *et al.*, 1996]. The latter has been shown not to be critical for shedding (above), implying that the sheddase shows a preference for cleavage at the R_{627}/S_{628} bond, irrespective of the distance to either the TM or ectodomain. Furthermore, the somatic and testicular forms of human ACE, both *in vitro* and *in vivo*, are cleaved at this bond [Woodman *et al.*, 2000]. The use of this bond is also not limited to humans, as porcine ACE_S is also cleaved at the R_{1203}/S_{1204} bond [Woodman *et al.*, 2000], and rabbit ACE_T is cleaved at a bond homologous to the human ACE_T R_{627}/S_{628} bond [Ramchandran *et al.*, 1994].

The apparent specificity of the ACE sheddase towards this particular bond is somewhat surprising, as it cleaves this bond at a wide range of distances from the membrane (see Table 4.1.1), but does not cleave C-terminally to the other two arginines in similar positions in the wild-type stalk, namely R_{637} and R_{651}. Also, shedding is not abolished when the 'preferred' R_{627} residue at the P_1 position is deleted, indicating that it is not an absolute requirement for shedding, and other sites can instead be utilised. In fact, the cleavage of the stalk insertion mutants described below illustrates the wide range of cleavage sites that can be utilised by the ACE

sheddase. This opens the possibility that the sheddase recognition motif is a structural element, with relaxed sequence requirements, showing redundancy almost anywhere on the stalk region. Thus the 'footroom' region, with its secondary cleavage sites, was re-examined as the last remaining stalk region that may contain a possible shedding motif.

4.3) The 'Footroom'

Ehlers *et al.* showed that large deletions of 17 or 24 amino acids C-terminal to the sheddase cleavage site did not abolish shedding, although the rate of shedding was affected (see Fig. 4.1; [Ehlers *et al.*, 1996]). Interestingly, the deletion of 17 amino acids adjacent to the transmembrane domain **increased** the rate of shedding four fold, while the deletion of a further 11 amino acids resulted in an eight fold **decrease** in the rate of shedding relative to wtACE. This intriguing difference between the shedding rates of ACE-JMΔ17 and ACE-JMΔ24 alluded to the possibility that the there may be a 'shedding enhancing' structural motif in the differential region [SE**GPLPDSG**R], just C-terminal to the cleavage site, that was deleted in the ACE-JMΔ24 mutant. The ACE-Δ5JM mutant was constructed to investigate this possibility, in which residues P_{631}-S_{635} of human testis ACE were deleted (in bold, above; see Table 4.1.1).

Another possible explanation for increased shedding of the ACE-JMΔ17 mutant was that the region just C-terminal to the cleavage site may now be in a more favourable position for the ACE sheddase, or a related sheddase with broad specificity. Two lines of evidence point in this direction: firstly, the α-secretase responsible for cleaving β-APP 12 amino acids from the TM, now found to be TACE [Buxbaum *et al.*, 1998] and/or ADAM-10 [Lammich *et al.*, 1999], cleaves β-APP at about this distance even when 4, 6 or 19 amino acids were removed from the stalk region [Maruyama *et al.*, 1991; Zhong *et al.*, 1994], and secondly, Deng *et al.* found the juxtamembrane sequon [PQLQE] to be important in directing cleavage of colony stimulating factor-1 (CSF-1^{256}) [Deng *et al.*, 1996]. This region, from P_{161}-E_{165} in CSF-1^{256}, occurs three residues C-terminal to the cleavage site and directly adjacent to the TM (see Table 4.3.1.1). Although shedding was abolished when this pentapeptide was deleted,

numerous site-directed mutations were tolerated, as shown in Table 4.3.1.1, such that a vague 'consensus sequence' [PPPEQ] could be postulated. If one then examines the side chains of these residues, and equates proline with leucine (non-polar), aspartic acid with glutamic acids (negatively charged), and serine with glutamine (uncharged polar side chains), then one could envisage that the region [PLPDS] in wtACE may be compatible with the 'consensus sequence' [PPPEQ] found for CSF-1. As this region is also three amino acids C-terminal to the cleavage site, and adjacent to the TM in the ACE-JMΔ17 mutant, it seemed plausible that this may serve as a putative sheddase recognition motif. To examine this possibility, the region [PLPDS] was deleted from the ACE stalk and the proteolytic cleavage-release of this mutant was examined.

Table 4.3.1.1) ACE and CSF-1^{256} stalks compared

Mutant	Stalk sequence	Effic.	Dist.
WtACE	KLGWPQYNWTPNSARSEG↓PLPDSGRVSFLGLDLDAQQARVGQ	++++	24
ACE-Δ5JM	KLGWPQYNWTPNSARSEG↓.....GRVSFLGLDLDAQQARVGQ	+	19
ACE-JMΔ47	MKLGFSRPWPEAMQLITGQPNMSASAMLSYFKPLLDWLRVGQ	-	-
ACE-JMΔ24	ASAMLSYFKPLLDWLRTENELHGE↓KLGWPQYNWTPNSARVGQ	+	0
ACE-JMΔ17	LLDWLRTENELHGE↓KLGWPQYNWTPNSARSEG↓PLPDSGRWLL	+++++	10
CSF-1^{256}	PASEGAARPLPRFNSVPLTDTGHERQSEGSSS↓PQLQESVFHL	++++	~8
CSF-1^{256}-Q162P	PASEGAARPLPRFNSVPLTDTGHERQSEGSSS↓PPLQESVFHL	++++	~8$^{\Psi}$
CSF-1^{256}-L163P	PASEGAARPLPRFNSVPLTDTGHERQSEGSSS↓PQPQESVFHL	++++	~8$^{\Psi}$
CSF-1^{256}-Q164E	PASEGAARPLPRFNSVPLTDTGHERQSEGSSS↓PQLEESVFHL	++++	~8$^{\Psi}$
CSF-1^{256}-E165Q	PASEGAARPLPRFNSVPLTDTGHERQSEGSSS↓PQLQQSVFHL	++++	~8$^{\Psi}$
CSF-1^{256}-L163I,Q164P	PASEGAARPLPRFNSVPLTDTGHERQSEGSSS↓PQIPESVFHL	+	N
CSF-1^{256}-Δ161-162	PASEGAARPLPRFNSVPLTDTGHERQSEGSSS..LQESVFHL	±	N
CSF-1^{256}-Δ161-165	PASEGAARPLPRFNSVPLTDTGHERQSEGSSS.....SVFHL	-	N*
CSF-1^{256}-Δ150-156	PASEGAARPLPRFNSVPLTDT.....SEGSSS↓PQLQESVFHL	++++	Y*

The amino acid sequence of human testis ACE including the stalk region (K_{613}-Q_{654}) and mutations thereof are shown. The transmembrane domain and proximal ectodomain are highlighted in blue and yellow respectively. Cleavage sites are shown with arrows. The putative TM domain for ACE suggested by Soubrier *et al* is underlined [Soubrier *et al.*, 1988]. The start of the TM found for CSF-1^{256} using TMPred is shown in bold. Cleavage sites are indicated with an arrow, and distance from TM (Dist.) are shown. Cleavage efficiency (Effic.) is indicated on a relative scale where +++++ is extremely fast shedding, and ± indicates 2-10% shedding. Shedding efficiency for ACE is measured after cells were incubated for 4 hrs with 1 μM PDBu, while that for CSF-1^{256} is after 3 hrs incubation with 0.5 μM PMA [Deng *et al.*, 1996]. (*) Relative shedding of CSF-1^{256}-Δ150-156 vs. CSF-1^{256}-Δ161-165 only apparent after tunicamycin treatment. (Ψ) The approximate cleavage sites for CSF-1^{256} were estimated using SDS-PAGE gels [Deng *et al.*, 1998].

4.3.1) ACE-Δ5JM

The vector pLEN-ACE-Δ5JM that encodes human ACE_T protein with a deletion of five juxtamembrane residues was constructed using the same two-step PCR mutagenesis protocol mentioned above (see Table 4.3.1.1). The vector was co-transfected with pSV2NEO into CHO-K1 cells using the calcium phosphate method, as described. Neomycin-resistant cells were analysed for ACE activity using the HHL substrate assay, and the cellular expression found to be 55.6 ± 4.6 mU ACE per confluent well in a 6-well dish (n = 3). The cells were then grown to confluence in 6-well dishes and subjected to a 4-hour shedding kinetics study as above. This mutant is shed very poorly, with only 1.2 ± 0.1 mU ACE per well being released over 4 hours in the absence of phorbol (Fig. 4.3.1.1a). Although this shedding is TAPI-inhibitable, and there appears to be a 3-fold induction of shedding with phorbol ester treatment (Fig. 4.3.1.1b), this phorbol-response is insignificant compared to that seen with wtACE (Fig. 4.3.1.1d). In fact the percentage of wtACE released with PDBu stimulation is 7-fold that of ACE-Δ5JM, suggesting either that this mutant is not efficiently processed to the cell-surface, or that this mutant may have lost the ability to be shed by a phorbol-activated sheddase.

COS-1 cells were also transiently transfected with pLEN-ACE-Δ5JM, allowed to recover for 44 hours, and then induced for 4 hours with 1 μM PDBu before the cell-extract and medium samples were assayed for ACE activity using HHL as substrate (Fig. 4.3.1.2). Phorbol-ester activation resulted in the cleavage of only 7.7% of the total ACE in the well, over a 4 hour period, which correlated well with that found for ACE-Δ5JM expressed in CHO cells under the same conditions, namely 6.8% soluble ACE (n = 3). This indicates the poor cleavage-release seen for ACE-Δ5JM in CHO cells was not cell-line specific.

Western blotting analysis showed both the precursor and the fully glycosylated form of ACE-Δ5JM in CHO cells (see Fig. 4.3.1.3), indicating that this mutant was stable enough to be processed through the Golgi and likely appears on the cell surface as a mature protein. The low ACE activity after 4 hours was supported by the absence of a

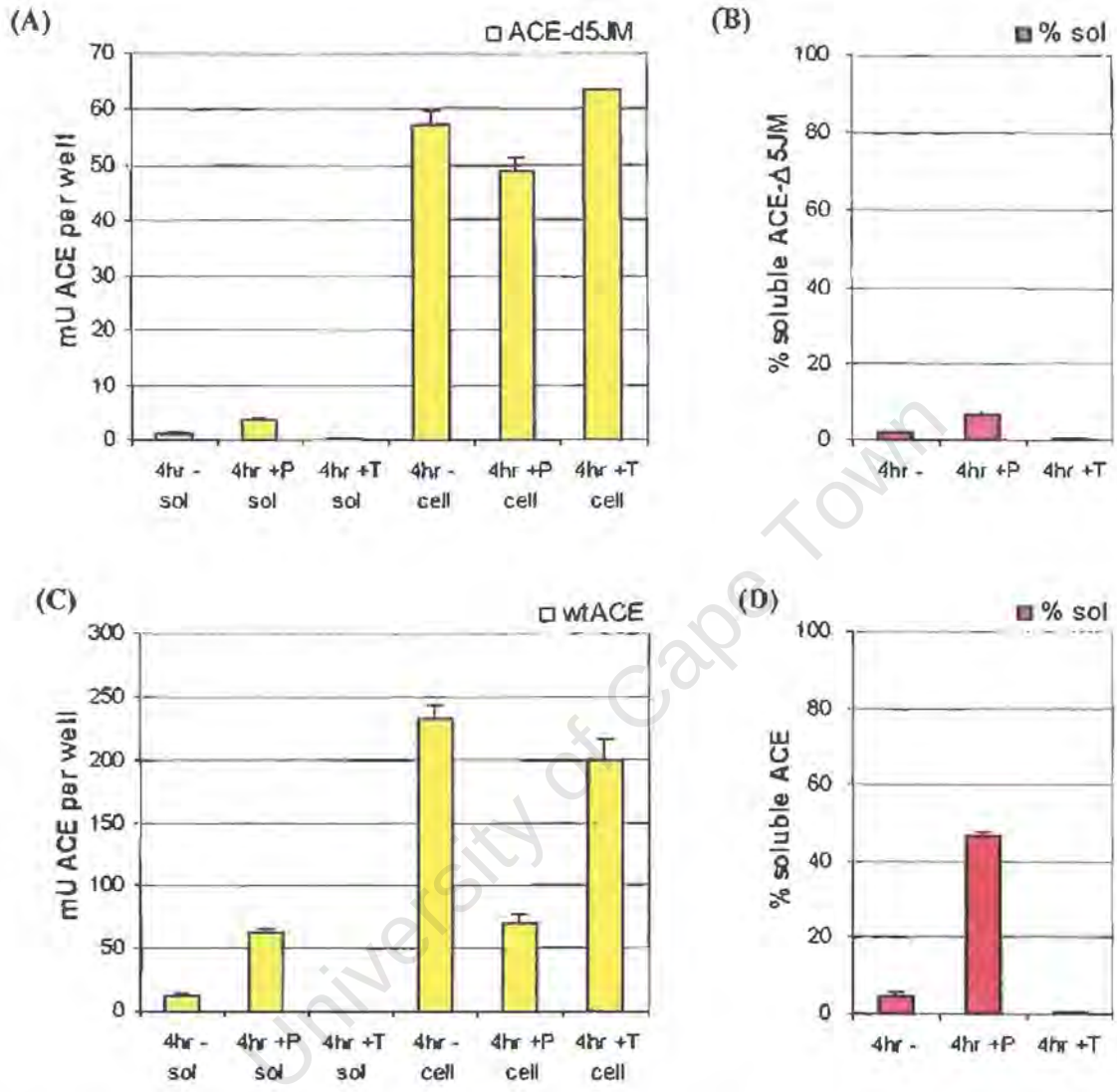

Figure 4.3.1.1) The shedding of ACE-Δ5JM compared to wtACE

CHO-K1 cells expressing ACE-Δ5JM or wtACE were grown to confluence in 6-well dishes, and incubated for 4 hours with fresh induction medium supplemented with either nothing (-), 1 μM PDBu (+P) or 10 μM TAPI (+T). The medium (sol) and cell-extract (cell) samples were then assayed for ACE activity using the HHL substrate assay (A, C). The percentage of total ACE-Δ5JM in the medium fraction after 4 hours is shown in (B, D) [n=3].

band in the medium after 4 hours of phorbol stimulation. Assuming that ACE-Δ5JM had the same specific activity as wtACE, then the enzyme concentration of 3.6 mU ACE per well found for this sample was below the detection limit for the Western blot.

To confirm that the mutant did in fact reach the cell surface, confocal microscopy was performed on fixed, but un-permeabilised, CHO cells expressing ACE-Δ5JM (Fig. 4.3.1.4b). A significant extracellular signal was recorded in these cells, indicating that this mutant was processed to the plasma membrane. Thus, the poor shedding seen for this mutant must have been due to some interference with sheddase recognition, or access of the protease to the cleavage site, and not due to an unforeseen problem with processing to the membrane.

The cleavage site was also determined, using endoproteinase Lys-C digestion of ACE-Δ5JM purified from the medium of transfected CHO cells, and analysis of the peptides by MALDI-TOF. The mixed peptides contained a peptide that had a peak at *m/z* 1690.2, which matched the calculated *m/z* for a C-terminal peptide spanning L_{614}-R_{627} (1690.85), indicating that this mutant was also cleaved at the R_{627}/S_{628} bond, 19 residues from the TM. This was not surprising, as both ACE-JMΔ17 and ACE-JMΔ24 are also cleaved at this bond [Ehlers *et al.*, 1996].

In summary, the ACE-Δ5JM mutant is expressed and processed to the cell surface in CHO cells, but is shed very poorly. Although the shedding of ACE-Δ5JM does occur at the wild-type cleavage site and is enhanced 3-fold with phorbol ester this response is significantly less than that seen for wtACE shedding (6.8% *versus* 46.7%), implying that this mutant may be refractory to cleavage by the phorbol-induced sheddase, but is still susceptible to the basal shedding. Furthermore, this reduction in PDBu-inducible shedding relative to wtACE is not cell-line specific, as the same is seen in COS cells. One can therefore conclude that the poor rate of cleavage of ACE-JMΔ24 compared to that seen for ACE-JMΔ17 was due to the removal of a structural element in the differential region, and not simply because the cleavage site abutted against the TM in the ACE-JMΔ24 mutant.

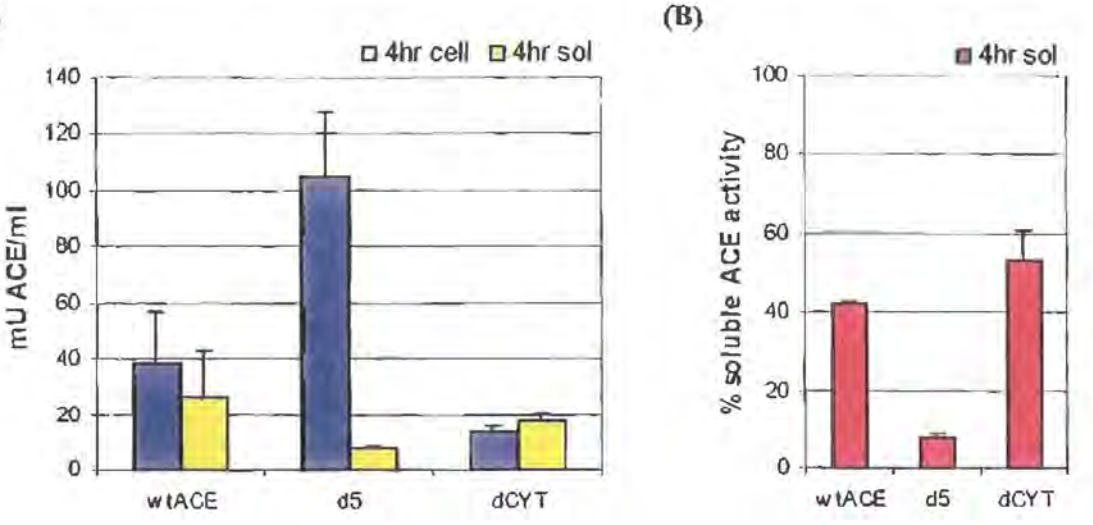

Figure 4.3.1.2) The shedding of ACE-Δ5JM from transfected COS-1 cells

COS-1 cells were transiently transfected with pLEN-ACE-VII, -Δ5JM or -ΔCYT. After 44 hours the cells were stimulated with 1 μM PDBu and the medium and cell-extracts assayed for ACE activity using the HHL substrate (A). The percentage of total ACE in the medium fraction after 4 hours is shown in (B) [n=2].

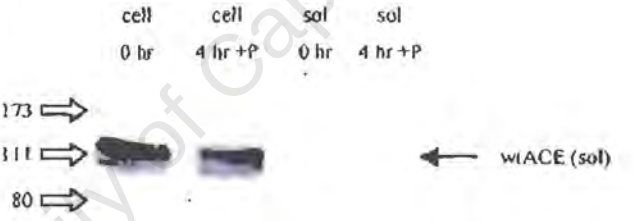

Figure 4.3.1.3) ACE-Δ5JM Western blot

The cell extract and medium samples at zero time and after 4 hours of phorbol ester stimulation (assayed in Fig. 4.3.1.1) were subjected to Western blotting and probed for ACE protein. The BenchMark prestained marker positions and sizes are shown on the left, while the position of a soluble wtACE marker is shown on the right.

Figure 4.3.1.4) Confocal Microscopy of CHO cells expressing ACE-Δ5JM

Confocal microscopy was performed on either untransformed CHO cells (A), or CHO cells transfected with either pLEN-ACE-Δ5JM (B), or pLEN-ACEVII (C). Cells were fixed with 3% PFA, probed with rabbit anti-ACE antibody and labelled with FITC-conjugated anti-rabbit IgG. Nuclei were stained with 2 μM propidium iodide (PI) before mounting. Confocal microscopy overlays of the PI (red) and FITC (green) signal for fixed, but un-permeabilised, cells are shown.

The idea that the structure of the stalk region may dictate its accessibility to shedding by a phorbol-inducible sheddase was proposed by Althoff *et al.* when they showed that PMA-induced shedding, but not basal shedding, of IL-6R was significantly reduced in $TACE^{-/-}$ cells [Althoff *et al.*, 2000]. Furthermore, the authors swapped the stalk regions of TNFα and IL-6R, and found that the PMA-inducible shedding characteristics were transferable with the stalk region. Thus it is possible that similar information is contained within the region just downstream of the ACE cleavage site, explaining the relatively poor phorbol-inducible shedding of both the ACE-Δ5JM and ACE-JMΔ24 [Ehlers *et al.*, 1996] mutants.

The differential region also contained a sequon [PLPDS], which might be equivalent (in terms of sheddase recognition) to the sequon [PQLQE] initially found to be essential for shedding of CSF-1 [Deng *et al.*, 1996]. Clearly, the next step would be to systematically mutate each of these residues to alanine, and/or make smaller deletions, to further characterise this possible recognition motif. However, this was not done for several reasons. Firstly, a subsequent publication by Deng *et al.* showed that cleavage of $CSF\text{-}1^{256}$ still occurred when they inserted the tripeptide Phe-Ala-Glu into this juxtamembrane sequon [PQ**FAE**LQE]. Cleavage also occurred at about the same distance from the membrane, indicating that this sequon was, in fact, not vital for cleavage of $CSF\text{-}1^{256}$ [Deng *et al.*, 1998]. Secondly, subsequent work in our laboratory showed that the ACE sheddase tolerates vastly differing stalk regions, including highly glycosylated or disulphide-linked regions (discussed below). These stalks were all cleaved, indicating that the sheddase does not need to find a specific motif in the ACE stalk, and that the effect seen in ACE-Δ5JM might instead have been due to an unfavourable conformation that reduced protease accessibility, and not due to the deletion of a recognition motif. Thirdly, Sadhukhan *et al.* mutated the sequon [SLPDS] to [SHQDS] without any effect on the shedding of rabbit testis ACE_T [Sadhukhan *et al.*, 1998]. Fourthly, Althoff *et al.* have subsequently shown that there is no PMA-induced-shedding motif in the IL-6R stalk, and that shedding may instead be due to the disruption of ectodomain structure [Althoff *et al.*, 2001]. The authors inserted truncated IL-6R stalk peptides into the stalk region of the non-shed receptor gp130, but were unable to abolish PMA-induced shedding of these chimeras. Finally, shedding was not totally abolished in the ACE-Δ5JM mutant.

Conclusions:

Previously Ehlers *et al.*, showed that the region C-terminal to the ACE cleavage site, between R_{627} and the TM, was not to be necessary for cleavage [Ehlers *et al.*, 1996]. I have shown that the region just N-terminal to the ACE sheddase cleavage site is also not required for shedding as the ACE-ΔR_{627}, ACE-Δ6JM and ACE-Δ11JM mutants were all shed. Furthermore, I have defined the boundary of the proximal ectodomain to be the region just N-terminal to W_{616}, implying that the ACE stalk spans the region W_{616}-R_{651}. From Table 4.1.1 it is clear that the ACE-Δ11JM, ACE-ΔR_{627} and ACE-JMΔ24 mutants collectively delete the whole of this region. Each of these mutants was shed, implying that the ACE sheddase recognition domain does not reside in the juxtamembrane stalk region. Furthermore, the use of alternate cleavage sites for the shedding of the ACE-ΔR_{627} and ACE-Δ6JM mutants shows that there is also not absolute requirement for cleavage to occur at the R_{627}/S_{628} bond.

The concept that the stalk region of ACE may contain a sequence-specific sheddase recognition motif was finally put to rest when numerous stalk-insertion mutants were constructed, all of which were shed from CHO cells (Table 4.6.1). In these experiments, the stalk region of ACE was replaced with widely differing peptides such as the highly O-glycosylated N-terminal region of ACE_T (ACE-JGL) [Schwager *et al.*, 1999] and the tightly disulphide knotted domains of the LDL receptor (ACE-JMEGF), factor IX (ACE-JMfIX) and the synthetic peptide Min23 (ACE-JMmin23) [Schwager *et al.*, 2001]. The fact that these varied stalk sequences and structures could all support shedding indicated that the sheddase has to recognise some other region of ACE before cleavage occurs in the juxtamembrane stalk, irrespective of the exact sequence of the stalk.

The lack of sequence-specificity of the ACE sheddase at the cleavage site was also corroborated by the work of Sadhukhan *et al.* when they mutated the cleavage site P_1' and P_1 residues in rabbit testis ACE (R_{663} and S_{664} respectively) to glycine and/or alanine and found that shedding was not effected [Sadhukhan *et al.*, 1998]. Other point mutations and deletions in the stalk region also did not abolish shedding.

Table 4.6.1) The ACE stalk insertion mutants

Mutant	Stalk sequence
WtACE	FKPLLDWLRTENELHGE LGWPQYNWTPNSARSEGPLPDSGRVSFLGLDLDAQQAR
ACE-JMLDL	FKPLLDWLRTENELHGE LGWPQYNWTPNS.....HQALGDVAGRGNEKKPSSVR
ACE-Δ6JM	FKPLLDWLRTENELHGE LGWPQYN.....RSEGPLPDSGRVSFLGLDLDAQQAR
ACE-JGL	FKPLLDWLRTENELHGE LGWPQYNWTPNS.VTVTHGTSSQATTSSQTTTHQATAR
ACE-JMEGF	HGE LGWPQYNWTPNSEGLGANQGDSH..VGNDLNIGYEGLGPDGTQLVNQRPGER
ACE-JMfIX	LGWPQYNWTPNSDGDQGE..SNPGLVDGSCKIDINSYEGNGPEGFE...GFNGER
ACE-JMmin23	LGWPQYNWTPNS.LMRGKGDS.DGLAGRVGSPNGF...GG.....

The amino acid sequence of the stalk region of human testis ACE, from W_{602} to L_{657}, and mutations thereof, are shown, as in Table 4.1.1. The transmembrane domain and proximal ectodomain are highlighted in blue and yellow respectively. Cleavage sites are indicated with an arrow. The blue arrows indicate the position of the secondary cleavage sites that are used to cleave the ACE-ΔR627 and ACE-Δ6 mutants. The cleavage sites and shedding characteristics of wtACE, ACE-JMLDL, -JMEGF, -JGL, -JMfIX and –JMmin23 are published previously [Ehlers *et al.*, 1996; Schwager *et al.*, 1998, 1999; 2001]. The N-glycosylation site created by the deletion of 6 amino acids in the ACE-Δ6JM mutant is shown in bold, as is the seventh putative glycosylation site in human testis ACE, which is not glycosylated in wtACE [Yu *et al.*, 1997]. The most C-terminal lysine in the sequence of human ACE_T is highlighted in green. The arrangements of the disulphide linkages are indicated with bars below the sequence. Human testis ACE sequence is in blue, while chimeric sequence is in red.

It is possible that by deleting sections of the stalk region we have removed the recognition motif of the specific ACE sheddase, and that shedding has been compensated by another sheddase with extremely similar characteristics but a different recognition domain. Although this cannot be disproved until all sheddases have been identified, we feel it is highly unlikely to be the case as the ACE-JMΔ17, ACE-JMΔ24, ACE-Δ11JM and ACE-Δ5JM mutants are all cleaved at the same site as wt-ACE, namely the R_{627}/S_{628} bond (see Table 4.1.1). Furthermore, cleavage still occurs when the stalk region is entirely replaced by unrelated sequences (see Table 4.6.1).

Thus, as shedding was not abolished by deleting large sections N- and C-terminal to the cleavage site, coupled with the lack of sequence specificity, we showed conclusively that the ACE sheddase recognition motif does not reside in the stalk region. The cytoplasmic tail (Chapter 5) and the ectodomain (Chapter 6) were therefore examined as possible sites for sheddase recognition of ACE.

Chapter 5: The Cytoplasmic Tail

The cytoplasmic tail (endodomain) of numerous ectoproteins (for the purposes of this discussion, ectoproteins refers to single-pass, type I or II, transmembrane proteins) has been shown to play a vital role in their function. Receptors on the surface of cells transmit their signal (e.g. ligand binding) through the lipid bilayer of the plasma membrane and induce a multitude of responses in the cell. The cytoplasmic tail is often involved in this signal transduction, either by activating a kinase domain (e.g., receptor tyrosine kinases; see Fig. 1.2.4), or through a conformational change that induces phosphorylation of serines, threonines or tyrosines in this region by any number of kinases such as PKC [Fagerholm *et al.*, 2001; Bodeau *et al.*, 2001]. Furthermore, the sorting of secreted ectoproteins to different sub-cellular compartments is controlled by motifs in the cytoplasmic tail, such as sorting to the cell surface [Urena *et al.*, 1999], or more specifically the apical/basolateral surfaces [Le *et al.*, 1991], or internalisation via clathrin-coated pits [Pearse, 1988]. Internalisation of receptors is particularly interesting in that it is often rapidly up-regulated on ligand binding, indicating the direct allosteric effect of a change in the structure of the ectodomain.

Signalling may even be directed in the reverse direction, from the cytoplasm to the external environment, via the cytoplasmic tail. High affinity binding of nerve growth factor (NGF) receptor [Hempstead *et al.*, 1990] and the EGF receptor [Livneh *et al.*, 1986b] is lost when the cytoplasmic tail is truncated. Furthermore, a basic amino acid in the cytoplasmic domain of βAPP (R_{747}) is essential for α-secretase cleavage of the ectodomain and directing β-APP through the normal secretory pathway [Tomita *et al.*, 1998].

The cytoplasmic tail may even act as a transcription factor. Notch binding to Delta induces shedding of the ectodomain of Notch by TACE [Brou *et al.*, 2000], which is followed by a γ-secretase-like cleavage-release of the cytoplasmic tail by PS1 [Levitan *et al.*, 2001]. The soluble cytoplasmic tail is then free to translocate to the nucleus where it interacts with the DNA-binding protein CSL and induces transcription [Brou *et al.*, 2000; Ray *et al.*, 1999]. Recently it has been found that γ–

secretase cleavage of βAPP releases the cytoplasmic tail that translocates to the nucleus [Kimberly *et al.*, 2001], and may therefore also act as a transcription factor.

The possibility therefore exists that the ACE cytoplasmic domain may be involved in the recognition of the ACE ectoprotein, which then induces the shedding of the ectodomain through the sequence-independent cleavage of the stalk region. Furthermore, the alignment of testis ACE from numerous mammalian species showed almost perfect conservation of the COOH-terminal 13 residues of ACE (Fig. 5.1.1), implying that these residues may play a role in ACE processing, and possibly shedding. The cytoplasmic truncation mutant ACE-ΔCYT was constructed to test this hypothesis.

5.1) ACE-ΔCYT

The ACE-ΔCYT mutant was constructed in a single PCR step that introduced a stop codon directly downstream of R_{674}, thereby truncating the C-terminal 27 amino acids of human ACE_T. The construct pLEN-ACE-ΔCYT was transfected into CHO-K1 cells, and stably transfected cells were assayed for cell-associated ACE activity, which was found to be 14.0 ± 0.7 mU ACE per well with HHL as substrate.

ACE-ΔCYT-expressing cells were then tested for their ability to shed ACE into the culture medium over 4 hours (Fig. 5.1.2). Surprisingly, induction medium with no supplements induced the release of 58.6% of the total ACE activity from the cells. This was increased slightly to 70.1% on cellular stimulation with phorbol ester, although not significantly. TAPI (the hydroxamate inhibitor of sheddases) was, however, able to inhibit 60% of this release, indicating that a proteolytic activity must have been responsible for much of the release of ACE-ΔCYT into the medium.

However, TAPI inhibition did not prevent the release of 25.2% of total ACE over 4 hours, which was 40-fold greater even than the 'basal' release found with wtACE (Fig. 4.1.2c). This raises the possibility that the ACE-ΔCYT may be produced in the cell as a soluble form that accounted for 25% of the total cell-associated ACE.

```
ACE-ΔCYT     DLDAQQARVGQMLLLFLGIALLVATLGLSQR                    674
Human tACE   DLDAQQARVGQMLLLFLGIALLVATLGLSQRLFSIR.HRS          682
Chimp tACE   ------------------------------.  -                683
Rabbit tACE  n----------v-----v---l-s---t-------.yq-            686
Bovine sACE  n-ee--------v-----v---------t-------.-h-          1254
Mouse tACE   y-ep--------v-----v------v--ah--yn--n-h-          682
Rat sACE     y-ep--------v-----v------v--ah--yn-hn-h-         1259

Human tACE   LHRHSHGPQFGSEVELRH                                701
Chimp tACE   ----------d--------                                702
Rabbit tACE  -rgph--------------                                705
Bovine sACE  -rgphr-------------                               1273
Mouse tACE   -r-phr-------------                                701
Rat sACE     -r-phr-------------                               1278
```

Figure 5.1.1) Cross-species conservation of the ACE endodomain
The TM and cytoplasmic tail regions of sequences for human, chimpanzee, rabbit, bovine, mouse and rat ACE are aligned. Human testis ACE is shown in capitals on the second line. The relative position of the truncation in ACE-ΔCYT is indicated on the top line. Identity to the human testis ACE sequence is indicated with a dash while differences are shown using single letter amino acid codes and spaces shown with a dot. Note that the 20 amino acid long TM domain (highlighted in blue) has 5 changes, while the COOH-terminal 13 amino acids (green) are almost completely conserved in mammals.

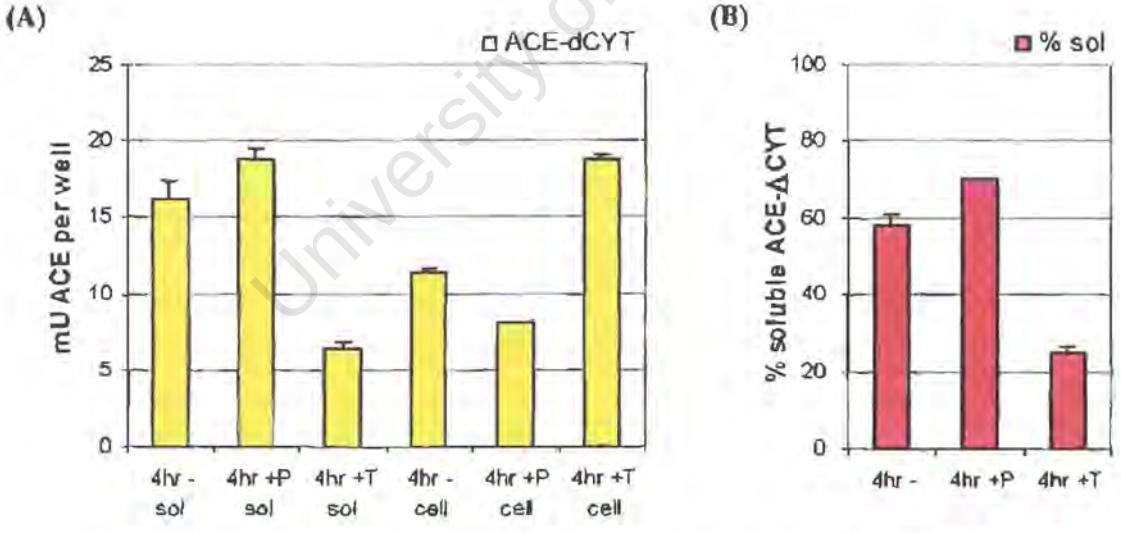

Figure 5.1.2) The shedding of ACE-ΔCYT – effect of phorbol ester and TAPI
Confluent CHO-K1 cells stably transfected with the pLEN-ACE-ΔCYT vector were incubated for 4 hours with fresh induction medium supplemented with nothing (-), 1 μM PDBu (+P) or 10 μM TAPI (+T). The medium (sol) and cell-extract (cell) samples were then assayed for ACE activity using HHL as substrate (A) [n=3]. The percentage of total ACE activity in the medium (soluble) after 4 hours is shown in (B).

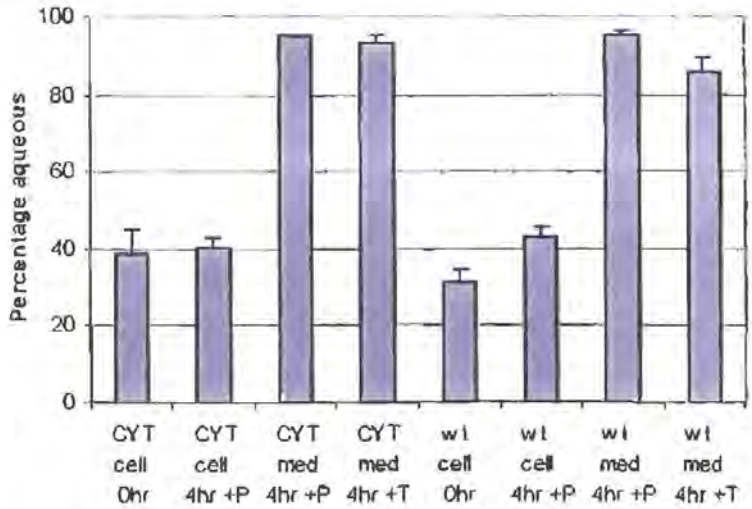

Figure 5.1.3) Triton X-114 extraction of cell-associated and soluble ACE-ΔCYT

Confluent CHO cells expressing either wtACE or ACE-ΔCYT were incubated for 4 hours with fresh induction medium supplemented with nothing (-), 1 μM PDBu (+P) or 10 μM TAPI (+T). The medium (med) and cell-extract (cell) samples were then separated into lipophilic and hydrophilic fractions using Triton X-114, after which all samples were assayed for ACE activity using the HHL substrate. The percentage of soluble (aqueous) ACE activity in each sample is shown [n=4].

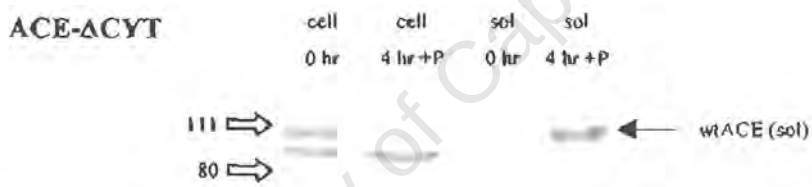

Figure 5.1.4) ACE-ΔCYT Western blot

The cell extract (cell) and medium (sol) samples at zero time and after 4 hours of phorbol ester (P) stimulation (assayed in Fig. 5.1.2) were subjected to Western blotting and probed for ACE protein. The BenchMark prestained marker positions and sizes are shown on the left, while the position of a soluble wtACE marker is shown on the right.

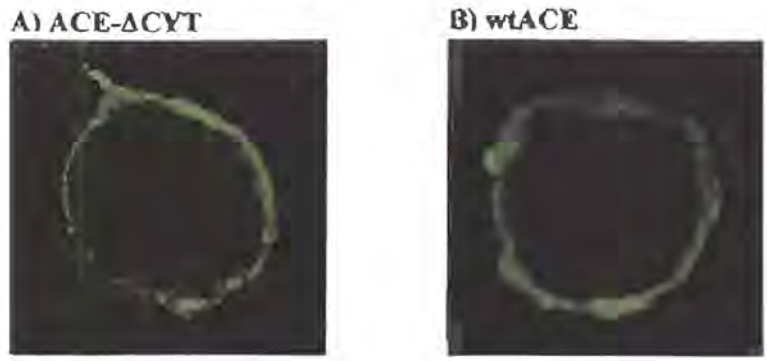

Figure 5.1.5) Confocal Microscopy of CHO cells expressing ACE-ΔCYT

CHO cells expressing ACE-ΔCYT (A) or wtACE (B) were fixed with paraformaldehyde, probed for ACE with an anti-rabbit antibody, and visualised using FITC labelled anti-rabbit antibodies and confocal microscopy. Only the extracellular signal is shown here.

We attempted to pre-empt this potential problem by not deleting the charged 'stop-transfer' sequence [SQR] when constructing ACE-ΔCYT. Triton X-114 extraction of the released and cell-associated protein was therefore performed. The ACE-ΔCYT mutant showed the same fractionation of the cell-associated activity into 60% hydrophobic and 40% aqueous as seen for wtACE (Fig. 5.1.3), indicating that the mutant had the same amphipathic nature as wtACE. Furthermore, the soluble form showed the same hydrophilicity as wtACE (~90%), indicating that it no longer contained the hydrophobic region, and thus must have been proteolytically cleaved to appear in the medium. Interestingly, the ~25% shed protein that is released into the medium in the presence of TAPI, does not contain a hydrophobic anchor and thus is likely the result of proteolytic cleavage-release from the cell (Fig. 5.1.3).

Western blotting analysis of ACE-ΔCYT showed a clear separation between the precursor and mature forms (Fig. 5.1.4), with sizes similar to that of wtACE. The change in mass in the ACE-ΔCYT mutant of 3.2 kDa was not noticeable on the blot. The intensity of the mature form's band in cell-extracts was significantly reduced after 4 hours of phorbol ester stimulation, with a concomitant increase in mature ACE-ΔCYT in the medium.

Confocal microscopy was also performed on fixed, but unpermeabilised, CHO cells expressing ACE-ΔCYT (Fig. 5.1.5a). This showed excellent cell-surface labelling, indicating that the mutant protein appeared in significant quantities on the cell surface. This served as more evidence that the ACE-ΔCYT mutant was correctly tethered to the plasma membrane, via the TM domain, as a more soluble form would have diffused away from the surface and would not have been detected in these studies.

Cleavage-site determination was then performed on ACE-ΔCYT purified from the medium of transfected CHO cells. The denatured, disulphide-reduced and vinylpyridine-protected protein was digested with endoproteinase Lys-C and subjected to MALDI-TOF mass spectrometry analysis. Numerous peaks could be assigned to Lys-C peptides, but one of them, *m/z* 1690.4, related to the calculated size of the peptide L_{614}-R_{627} (1690.85 Da), implying that the ACE-ΔCYT mutant, like

wtACE, was cleaved at the R_{627}/S_{628} bond. Interestingly, a minor peak at *m/z* 2687.3 related well to the calculated mass of the peptide L_{614}-R_{637} (2686.89 Da), indicating that a secondary site (R_{637}/V_{638}) was also used by the sheddase. Curiously, this minor peak was not seen in wtACE when analysed in parallel, although both share the identical extracellular sequence.

COS-1 cells were also transiently transfected with pLEN-ACE-ΔCYT, allowed to recover for 44 hours, and then induced for 4 hours with 1 μM PDBu before the cell-extract and medium samples were assayed for ACE activity using the HHL substrate method. A shedding rate of 53.4% soluble ACE after 4 hours was observed, which was well above that of wtACE, namely 42.1%, indicating that the rapid shedding seen for ACE-ΔCYT in CHO cells was not cell-line specific (see Fig. 4.3.1.2b).

In summary, the ACE-ΔCYT truncation mutant was processed efficiently to the cell surface as a glycosylated 'mature' form that was rapidly shed from the cell after removal of the hydrophobic TM domain, by cleavage predominantly at the R_{627}/S_{628} bond. The characteristic induction of shedding with phorbol ester and inhibition with TAPI were both reduced implying that a different sheddase may be involved. A similar shedding profile was seen for the ACE-JGL mutant in which shedding is rapid, has a reduced response to phorbol ester and is only partially inhibited by TAPI [Schwager *et al.*, 1999], indicative of the activity of a "non-classical" sheddase. Thus the shedding of ACE-ΔCYT may be due to a similar sheddase, or the up-regulation of a basal sheddase similar to that seen in $TACE^{-/-}$ cells [Buxbaum *et al.*, 1998].

An alternative explanation is that the shedding of ACE-ΔCYT was de-regulated, and that the C-terminal 27 residues of wtACE, truncated in ACE-ΔCYT, contain an inhibitory signal that, once removed, allowed for extremely rapid shedding of the ACE ectodomain. This finding was corroborated by the work of Sadhukhan *et al.* in which they too truncated the cytoplasmic domain of rabbit testis ACE and found an increase in shedding [Sadhukhan *et al.*, 1998]. As the C-terminal 13 residues are 99% conserved across 6 mammalian species, it is tempting to suggest that this region is involved in binding to cytoplasmic components that either directly inhibit shedding or constrain ACE to a region of the plasma membrane that is not accessible to the

sheddase. Although finding the identity of this putative 'sheddase inhibitor' is outside of the scope of this thesis, preliminary studies were performed on the likely down-stream effector of this cytoplasmic receptor, the most likely candidate being the actin cytoskeleton.

5.2) The actin cytoskeleton and ACE shedding

Actin filaments (F-actin) are involved in numerous cellular processes in all eukaryotic cells, from the amoeboid movement of white blood cells to muscle contraction. The abundant actin monomer (G-actin) rapidly polymerises to form long filaments (F-actin) by adding to the 'barbed' ends of pre-existing filaments. The F-actin is depolymerised from the 'pointed' end, thus allowing cell motility and structural remodelling of the actin network. A vast array of actin-binding proteins controls this process, resulting in the continuous flux of the 3D matrix that forms the scaffold of the cell [Ellis and Mellor, 2000; Wear *et al.*, 2000].

Cell migration is also mediated by the integrins, an extensive family of ectoproteins involved in cell-cell and cell-substratum binding. The integrins are clustered into focal contacts where the cytoplasmic tail of the integrin β-chain binds actin via the α-actinin, talin and vinculin actin-binding proteins [Kendrew and others, 1995]. Similarly, the EGF receptor binds actin via a profilin domain. By implication, the possibility exists that the cytoplasmic tail of ACE may be involved in actin binding.

Cytochalasin, a fungal metabolite identified in contaminated food [Patwardhan *et al.*, 1974], and phalloidin, a highly toxic alkaloid from the toadstool *Amanita phalloides*, have been shown to bind actin. Whereas phalloidin binds F-actin and stabilises the filamentous network by inhibiting depolymerisation, cytochalasin binds G-actin and inhibits polymerisation. The varied effects of cytochalasin were found to be specific to the de-polymerisation of actin, because cells expressing a mutant form of actin were resistant to cytochalasin B treatment [Toyama and Toyama, 1988]. Furthermore, Holsinger *et al.* showed that the ionomycin- and PMA-stimulated transcription of IL-2 in human peripheral blood lymphocytes **was not** inhibited by cytochalasin D, while that induced by T-cell receptor aggregation **was**, indicating that cytochalasin D affects

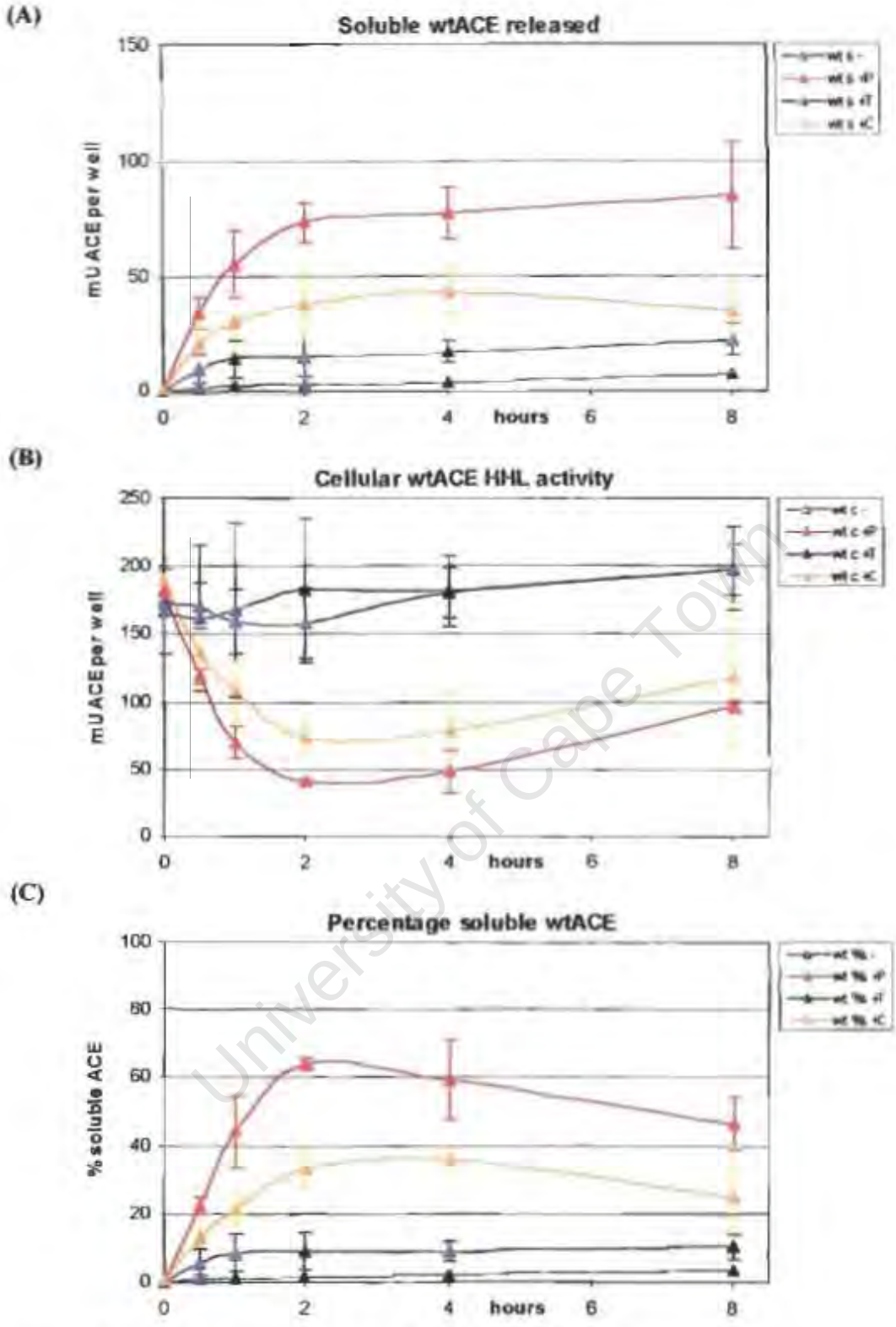

Figure 5.2.1) The shedding of wtACE – effect of cytochalasin D

CHO-K1 cells transfected with pLEN-ACEVII were grown to confluence in 6-well dishes and ACE expression induced overnight using 1 ml induction medium. At zero time the medium was replaced with 1 ml fresh induction medium supplemented with nothing (blue), 1 μM PDBu (red), 10 μM TAPI (dark blue) or 2 μM cytochalasin D (orange). At the indicated times the medium (A) and cell extract (B) samples were assayed for ACE activity using HHL as substrate. The percentage soluble ACE (C) is determined by dividing the soluble activity by the total ACE activity in the well (cell plus medium), expressed as a percentage [n=2].

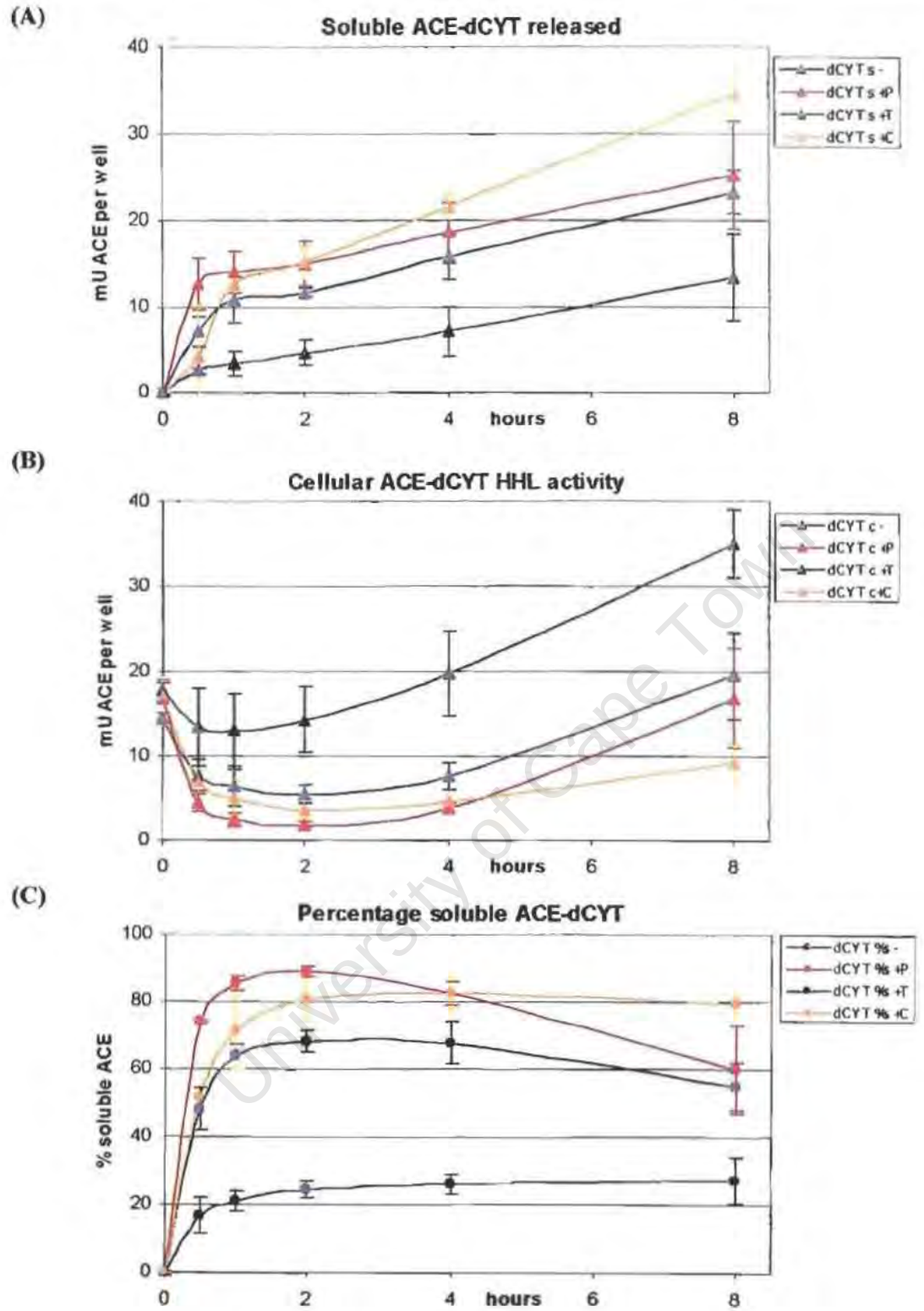

Figure 5.2.2) The shedding of ACE-ΔCYT – effect of cytochalasin D

CHO cells expressing ACE-ΔCYT were grown to confluence in 6-well dishes and ACE expression induced overnight using 1 ml induction medium. At zero time the medium was replaced with 1 ml fresh induction medium supplemented with nothing (blue), 1 μM PDBu (red), 10 μM TAPI (dark blue) or 1μg/ml cytochalasin D (orange). At the indicated times the medium (A) and cell extract (B) samples were assayed for ACE activity using HHL as substrate. The percentage soluble ACE (C) is determined by dividing the soluble activity by the total ACE activity in the well (cell plus medium), expressed as a percentage [n=2].

an upstream component of CD3/CD28 signalling, i.e. the F-actin architecture [Holsinger *et al.*, 1998].

We therefore investigated the effect of cytochalasin D on the shedding of wtACE from the surface of CHO cells. Surprisingly, this actin depolymerising agent induced a 2.5-fold increase in the release of ACE over that seen with medium alone (Fig. 5.2.1a). Although this was not as impressive as the characteristic 4-fold increase seen with phorbol ester stimulation, it is still significantly above the shedding-activation seen with induction medium with no supplements, and is inhibited with TAPI (data not shown). Cytochalasin-induced shedding was not increased when the concentration of cytochalasin D was changed from 2 μM to 20 μM (data not shown).

Interestingly, when CHO cells expressing ACE-ΔCYT were treated with 2 μM cytochalasin D, no significant increase in the percentage soluble ACE-ΔCYT above that of unstimulated cells was seen ($p = 0.3$). This was probably due to the de-regulated shedding of ACE-ΔCYT already occurring at a maximal rate without supplements (Fig. 5.2.2c).

The de-regulation of ectodomain shedding of ACE-ΔCYT indicated that the cytoplasmic region of wtACE may be involved in a sheddase-inhibitory binding to some cytoplasmic component, possibly actin or an actin-binding protein. Santhamma and Sen analysed the proteins bound to ACE using lisinopril affinity chromatography of detergent extracts and identified the endoplasmic reticulum chaperone BiP and the dolichyl-diphophosoligosaccharide-protein glycosyltransferase, ribophorin 1, out of the smear of ACE-bound proteins separated on SDS-PAGE [Santhamma and Sen, 2000]. More importantly, the authors found that the PKC isoforms PKCι, PKCγ, PKCδ and PKCλ are all bound to ACE, presumably in the cytoplasmic domain, while PKCα and PKCβ are not. Significantly, PKCγ and PKCδ dissociate from ACE on PMA stimulation, indicating that this dissociation may be involved in ACE shedding. The de-regulated shedding of the ACE-ΔCYT mutant may thus be the result of 'constitutive' dissociation from PKCγ and PKCδ, proteins that may act as sheddase inhibitors in the normal state. Shedding may therefore be due to the rapid dissociation of an inhibitory shedding regulator from the cytoplasmic tail, rather than the

activation of the sheddase, or a combination of both effects. This regulator may also have actin binding capabilities.

To add weight to this argument, the intracellular calcium regulatory protein calmodulin has recently been shown to act as a negative effector of L-selectin shedding [Kahn *et al.*, 1998]. L-Selectin is a type I ectoprotein, expressed on the surface of leukocytes, involved in neutrophil rolling and recruitment to sites of infection. It is also shed in the membrane proximal region [Kahn *et al.*, 1994] by a phorbol ester-stimulated and hydroxamic acid inhibitable sheddase [Feehan *et al.*, 1996] that was later found to be TACE [Peschon *et al.*, 1998]. Kahn *et al.* discovered the binding of calmodulin to the L-selectin cytoplasmic tail after they identified a 17-kDa band in their immunoprecipitation studies [Kahn *et al.*, 1998]. The calmodulin inhibitors TFP, W7 and calmidizolium have furthermore been shown to accelerate the rate of shedding of L-selectin, TGF-α, EGFR, proNRGα2c, TrkA and βAPP [Kahn *et al.*, 1998; Diaz-Rodriguez *et al.*, 2000].

The binding of calmodulin has recently been mapped to the membrane-proximal region of the cytoplasmic domain [Matala *et al.*, 2001]. Surprisingly, this is the same region where ezrin and moesin, members of the Ezrin-Radixin-Moesin (ERM) family of proteins involved in cross-link type I integral membrane proteins with F-actin [Tsukita and Yonemura, 1999], have been shown to also bind L-selectin [Ivetic *et al.*, 2001]. Using affinity purification of unstimulated or PMA stimulated cells, the authors were able to show that moesin interacts with the L-selectin cytoplasmic tail only under PMA stimulating conditions, while ezrin binds constitutively. One or other of the PKC isoforms, or another kinase, activates the ERM proteins, which then translocate to the cell membrane and cross-link it to the F-actin cytoskeleton. It is therefore possible that the signal transduction cascades that result in shedding may phosphorylate moesin, which in turn binds the cytoplasmic domain of a set of ectoproteins, displacing the potentially inhibitory calmodulin, PKCγ and PKCδ.

A more likely scenario with regard to ACE shedding is that ACE may be localised to a particular sub-compartment of the plasma membrane through an association with a putative actin binding protein, analogous to the focal adhesions that cluster integrins.

The lateral inhibition of movement of ectoproteins in the plasma membrane was investigated by Winckler *et al.* to explain the polarized distribution of axonal and somatodendritic plasma membrane domains in polarised neuronal cells [Winckler *et al.*, 1999]. To study the lateral mobility of the transmembrane protein L1, the authors used optical tweezers to place antibody-coupled beads at various distances from the soma, and then measure the distance the bead could be dragged along the axon. They found that both latrunculin-B (another actin-disrupting drug), and 0.4% DMSO induced a 50-fold increase of the lateral mobility of L1. This implies that cytoplasmic actin-binding proteins may be involved in retarding the lateral mobility of L1, likely in the cytoplasmic tail. This cannot be generalised, as the restricted lateral mobility of the EGF receptor is not affected by large deletions in the cytoplasmic tyrosine kinase domain [Livneh *et al.*, 1986a]. The authors used fluorescence recovery after photobleaching (FRAP) to measure the lateral mobility of their EGFR truncation mutants and found that they all had similar mobility.

It is interesting to note that, in contrast with ACE, the removal of the cytoplasmic domain does not affect the regulated cleavage of L1 [Gutwein *et al.*, 2000], amphiregulin [Vecchi *et al.*, 1998], KL-1 [Cheng and Flanagan, 1994], IL-6R [Mullberg *et al.*, 1994] or GHBP [Amit *et al.*, 2001], while the shedding of L-selectin is reduced [Zhao *et al.*, 2001]. Furthermore, the shedding of L-selectin is not affected by incubation with cytochalasin B [Kahn *et al.*, 1994], although receptor function is affected [Kansas *et al.*, 1993], likely due to α-actinin (an actin-binding protein) that was shown to bind the C-terminal 11 residues of the L-selectin cytoplasmic tail [Pavalko *et al.*, 1995]. Also, the cytochalasin-induced disruption of the actin cytoskeleton reduces the shedding of CD44, but not TNFα [Shi *et al.*, 2001]. Similarly, the pervanadate-induced shedding and tyrosine-phosphorylation of the cytoplasmic domain of ErbB-4 cannot be extrapolated to the shedding of amphiregulin, in which the cytoplasmic tail (with two tyrosine residues) is not required for regulated shedding [Vecchi *et al.*, 1998].

The shedding of all ectoproteins are thus not necessarily increased or de-regulated by removal of the cytoplasmic tail, or incubation with F-actin inhibitors, again indicating

that individual ectoproteins are shed through distinct secretory pathways involving a family of related sheddases.

In conclusion, one could speculate that the de-regulation of shedding seen in the ACE-ΔCYT mutant was due to an increased freedom of lateral diffusion in the plasma membrane. This would give it a greater chance of interacting with the sheddase, thus resulting in cleavage. This notion is corroborated by data from the purified membranes of ACE-expressing CHO cells, which shed ACE extremely rapidly and which has been suggested to be due to the dissolution of the sub-compartment structure of the membrane, allowing greater sheddase-substrate interaction (Z. Woodman, personal communication). The rapid activation of shedding on phorbol ester stimulation of cells was as likely a result of increased sheddase activity as an increased substrate susceptibility, possibly both due to an increased membrane fluidity on cellular activation. The ACE-ΔCYT data argue that the increased lateral movement of the substrate ACE molecule was sufficient to increase shedding, and thus that the sheddase activation may be secondary. However, the specific activation of the sheddase cannot be ruled out, as the cytoplasmic tails of TACE and MDC9 have been found to interact with the spindle assembly checkpoint mechanism proteins MAD2 and MAD2β respectively [Nelson *et al.*, 1999], while that of MDC9 binds endophilin I (involved in synaptic vesicle endocytosis), and MDC15 binds a sorting-nexin-like protein SH3PX1 [Howard *et al.*, 1999]. This shows that the cytoplasmic tails of the ADAM sheddases are probably involved in their sub-cellular localisation and activation at particular points in the cell cycle, although this control may also be through sub-compartmentalisation of the plasma membrane and restricted mobility of the sheddase.

Shedding may therefore be controlled by the relative lateral freedom of movement of both the sheddase and the substrate, possibly through the PKC induced phosphorylation of cytoplasmic tail binding proteins.

Chapter 6: The Ectodomain

The results shown in the previous two chapters provide compelling evidence that the ACE sheddase does not require a sequence-specific 'shedding motif' in the juxtamembrane stalk region or the cytoplasmic tail. This is corroborated by the work of Sadhukhan *et al.* in which they made numerous deletion mutants in rabbit ACE_T and found that shedding was not abolished [Sadhukhan *et al.*, 1998].

This leaves the ectodomain as the last remaining region in which a specific interaction between the substrate ACE molecule and its hypothetical sheddase may exist, resulting in the relatively specific cleavage of ACE. Work carried out on an ACE/CD4 chimera also suggests that the sheddase recognition motif must reside somewhere in the ectodomain of ACE (Chapter 2) [Sadhukhan *et al.*, 1998]. The authors constructed two important chimeras, one of which, ACE_T/CD4-5, contains the rabbit equivalent of human ACE_T residues M_{-31}-Y_{619} fused to 62 amino acids of the stalk region, TM and cytoplasmic domains of human CD4 (Fig. 6.1c). This chimera is **shed** extremely well from the surface of HeLa cells, indicating that the 32 amino acid stalk, TM and cytoplasmic region of rabbit ACE_T are not involved in shedding. The other chimera, CD4/ACE_T-1, contains the region M_{-25}-Q_{352} of CD4 fused to the proximal ectodomain, stalk, TM and cytoplasmic domains of rabbit ACE_T (the rabbit equivalent of M_{578}-S_{701} in human ACE_T; Fig. 6.1d). This chimera is **not shed**, indicating that the CD4 ectodomain does not support shedding, and the stalk region of ACE is insufficient for sheddase recognition [Sadhukhan *et al.*, 1998].

The fact that the ACE juxtamembrane stalk is unable to support ectodomain shedding in this system indicates either; (i) that the stalk region of ACE does not contain a specific recognition motif, (ii) that the ACE ectodomain contains a motif that is absent in the CD4 ectodomain and/or (iii) that the CD4 ectodomain occludes the stalk region, thus sterically blocking the sheddase.

The first hypothesis is supported by the various ACE stalk-insertion mutants produced in our laboratory, including the LDLR stalk, the Factor IX and LDLR EGF domains, the min23 disulphide-knotted structure, a highly O-glycosylated region, and an N-

linked glycan, all of which are cleavage-secreted [Schwager *et al.*, 1998; Schwager *et al.*, 1999; Schwager *et al.*, 2001]. The second option is favoured, as the stalk, TM and cytoplasmic domain of ACE do not direct shedding (see Chapters 4, 5). The third argument is more difficult to prove, although activity studies showing that CD4 is active in this chimeric form would be useful. Although the chimera is produced in appreciable quantities in HeLa cells and is thus likely to be stable, it does not eliminate the possibility that the CD4 ectodomain may occlude the cleavage site.

One approach for finding this elusive sheddase recognition motif is to delete large sections of the ACE ectodomain, thereby narrowing down the relevant region. However, enzymatic activity needs to be maintained to ensure that the protein is structurally similar to the native form, otherwise the truncation mutant may become susceptible to cleavage by a 'non-specific' sheddase that recognises unstable ectoproteins, as has been found for the shedding of gp130/LIFR stalk chimeric mutant [Althoff *et al.*, 2001]. Although this mutant involved swapping only the stalk regions of two non-shed ectoproteins, which resulted in cleavage-secretion of LIFR, the same logic may be used for ectodomains. Alternatively, the sheddase recognition motif may be structurally sensitive and easily disrupted by deletions in a region far removed from the real motif. The shedding of the p55 TNFRI, for example, is disrupted by mutations at or near numerous disulphide-linked cysteines in the ectodomain [McDermott *et al.*, 1999]. As it is unlikely that all of these disulphide-linked regions are involved in sheddase-ectoprotein recognition, it is possible that the global disruption of the ectodomain caused a secondary inhibition of shedding. Surprisingly, these receptors were still functional in terms of response to TNFα, demonstrating the relative sensitivity of sheddase-ectodomain recognition. The very real possibility of false positives is a cause for concern, as structurally disruptive deletions that knock out the shedding of ACE may lead to future detailed analysis in a region unrelated to the true shedding motif. I therefore used ACE activity as a test for ectodomain integrity to avoid this potential problem.

Defining the ectodomain

In the absence of a 3-D structure of ACE, one needs to first characterise the functional boundaries of this enzyme (catalytic domain) before embarking on a deletion-based search for the recognition motif in the ACE ectodomain (Fig. 6.1a,b). Cross-species homology alignments of numerous ACE ectodomains showed that D_{40} of ACE_T is the first completely conserved amino acid (see Fig. 2.3.2) while P_{623} is the last (see Fig. 2.4.1). While this evolutionary evidence strongly suggests that this is the functional boundary of the ACE catalytic domain, it is only through experimentation that this can be confirmed (see Appendix III for sequences used). Thus small sections were deleted from either end of wtACE until enzymatic activity was abolished, thereby defining the minimum requirement for a functional ACE (i.e. the minimum catalytic domain).

6.1) The C-terminal end

The ACE mutants ACE-Δ6JM, -Δ11JM and -Δ16JM have been described in detail above. Although originally developed to analyse the importance of 'headroom' in shedding, the data instead points to the sensitivity of this region in terms of ACE catalytic activity and stability. Repeated transfections showed that the expression of ACE-Δ6JM was an order of magnitude lower than wtACE. Similarly, ACE-Δ11JM was an order of magnitude lower than ACE-Δ6JM and no active ACE was found for ACE-Δ16JM. Western blotting, however, revealed that a significant amount of mutant ACE protein was translated, but not necessarily processed to the cell surface, in cells transfected with these mutants. As the ACE-Δ11JM mutant is active and shed, while the ACE-Δ16JM mutant is not, one can conclude that the C-terminal boundary of the ACE catalytic domain is G_{615}. However, the lower expression levels in these mutants suggests that deletions just C-terminal of G_{615} may destabilise the neighbouring proximal ectodomain.

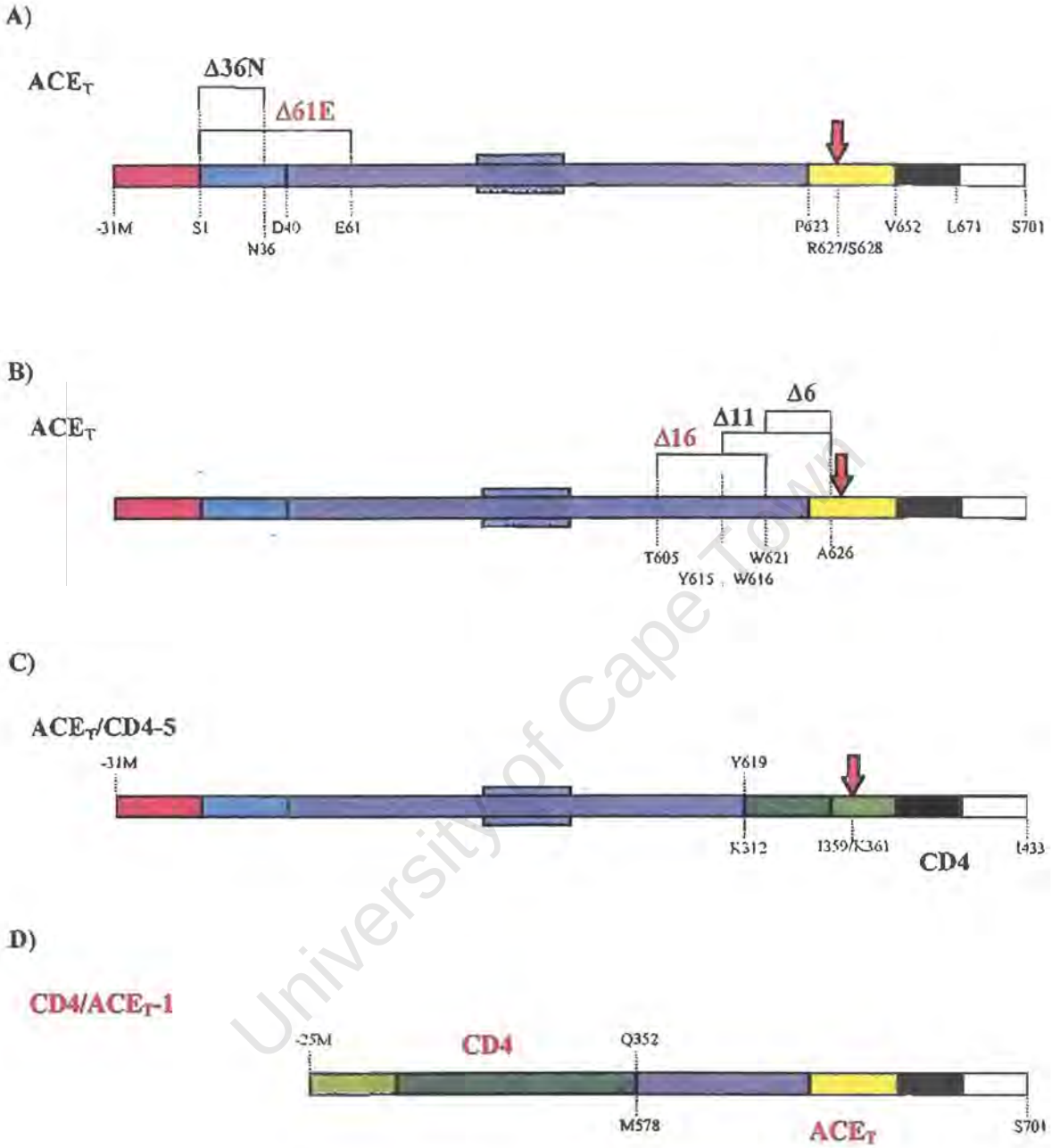

Figure 6.1) Defining the ectodomain

This schematic illustrates the deletion mutants that helped define the minimal catalytic unit of the ACE ectodomain. Mutants that are inactive and/or not shed are labelled in red. Deletions at the N-terminal end are shown in (A), while the C-terminal mutants are shown in (B). The putative ACE catalytic domain (according to amino acid conservation) is shown in dark blue (D40-P623). The CD4/ACE chimeras constructed by Sadhukhan *et al.* are shown in (C) and (D) [Sadhukhan *et al.*, 1998]. ACE and CD4 sequences are shown in blue and green respectively. CD4 sequence numbering from GenBank #P01730.

Further evidence for the boundary being N-terminal to Y_{619} is the fact that when rabbit ACE_T ectodomain containing 655 residues is fused to CD4, the chimera is processed to the surface normally and cleaved efficiently. This corresponds to the region M_{31}-Y_{619} for human ACE_T, indicating that deletions C-terminal of Y_{619} are tolerated. When smaller regions of ACE were used, which equate to human ACE_T ending at L_{306}, Y_{390} or P_{500}, the chimeras were rapidly degraded and did not appear on the cell surface, indicating that major structural damage had occurred [Sadhukhan *et al.*, 1998].

It is therefore clear that sections of the proximal ectodomain N-terminal to W_{616} cannot be deleted without inactivating the protein and disrupting possible structural motifs needed for sheddase recognition.

6.2) The N-terminal end

The N-terminal boundary of the ACE ectodomain was also examined by making progressively larger deletions C-terminal to the signal peptide.

6.2.1) ACEΔ36N-wt

The first N-terminal deletion mutant, ACEΔ36N-wt, was constructed by substituting the 3' end (*NheI*/*Cla*I fragment) of pLEN-ACEΔ36N [Ehlers *et al.*, 1992], with that of pLEN-ACEVII, to create an ACE mutant that lacks the highly O-glycosylated 5' region (Q_2-N_{36} (see Fig. 2.3.2)), but retains the wtACE stalk, TM and cytoplasmic regions. The mutant vector was co-transfected with pSV2NEO into CHO-K1 cells, and neomycin resistant cells selected. Transfected cells were grown to confluence in 6-well dishes, and the cell-extracts assayed for ACE activity using HHL as substrate. The activity was found to be similar to wtACE, at 179 ± 22 mU ACE per ml (n = 9), confirming that the O-glycosylated region is not essential for enzyme integrity.

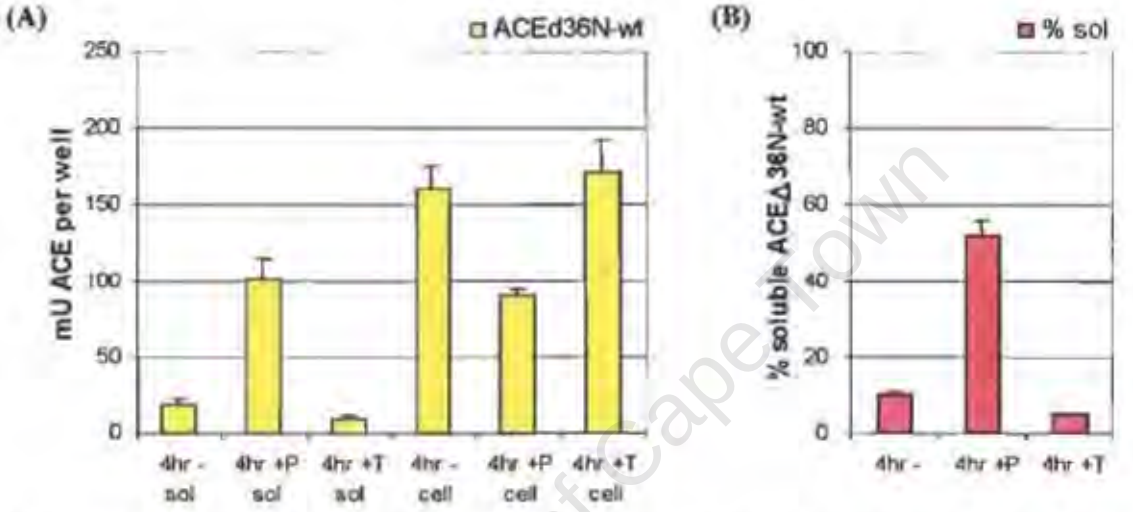

Figure 6.2.1.1) The shedding of ACEΔ36N-wt – effect of phorbol and TAPI over 4 hours
CHO-K1 cells transfected with pLEN-ACEΔ36N-wt were grown to confluence in 6-well dishes, ACE expression induced overnight, followed by a 4 hour incubation with fresh induction medium supplemented with nothing (-), 1 μM PDBu (+P) or 10 μM TAPI (+T). After 4 hours the medium (sol) and cell-extract (cell) samples were assayed for ACE activity using HHL as substrate (A). The percentage of total ACEΔ36N-wt in the medium fraction after 4 hours is shown in (B) [n=6]. This shedding profile is identical to that of wtACE.

Shedding kinetics studies were performed using confluent CHO cells expressing ACEΔ36N-wt (Fig. 6.2.1.1). These assays show the characteristic accumulation of soluble ACE activity in the medium over 4 hours, which is significantly increased with phorbol ester stimulation (5-fold), and decreased with TAPI-inhibition (2-fold), indicating that this truncation mutant undergoes similar processing to wtACE.

The soluble form of ACEΔ36N-wt was purified, reduced and protected with vinylpyridine, prior to endoproteinase Lys-C digestion. Peptides were fractionated on HPLC and analysed using MALDI-TOF mass spectrometry, as described above. A peak of *m/z* 1689.9 was obtained, which closely matches the mass of a C-terminal peptide spanning L_{614}-R_{627} (calculated mass of 1690.8), which is consistent with that found for wtACE. This was confirmed with the Glu-C digestion and MALDI-TOF analysis of purified soluble ACEΔ36N-wt, which revealed a peak of *m/z* 2255.2, almost identical to that calculated for a C-terminal peptide L_{609}-R_{627} (2255.5).

In conclusion, the ACEΔ36N-wt truncation mutant shows the same expression and shedding profile, and is cleaved at the same R_{627}/S_{628} bond, as wtACE. One can therefore conclude that the N-terminal O-glycosylated region is not essential for ACE shedding. Furthermore, this region is not involved in the core ACE catalytic domain of ACE, as published previously for the soluble form, ACEΔ36N [Ehlers *et al.*, 1992; Yu *et al.*, 1997]. In retrospect, this finding is not entirely surprising when considering the sequence alignment of ACE, as D_{40} is the first completely conserved amino acid in the ACE catalytic domain, four amino acids C-terminal to N_{36} (see Fig. 2.3.2).

6.2.2) ACEΔ61E

The mutant ACE vector pLEN-ACEΔ61E was constructed using the same two-step PCR mutagenesis protocol used above, except that residues Q_3-E_{61} were removed, thus deleting the N-terminal O-glycosylated region of human testis ACE, and 22 amino acids from the N-terminal end of the ACE catalytic domain (D_{40}-E_{61}). The mutant vector was repeatedly co-transfected with pSV2NEO into CHO-K1 cells using

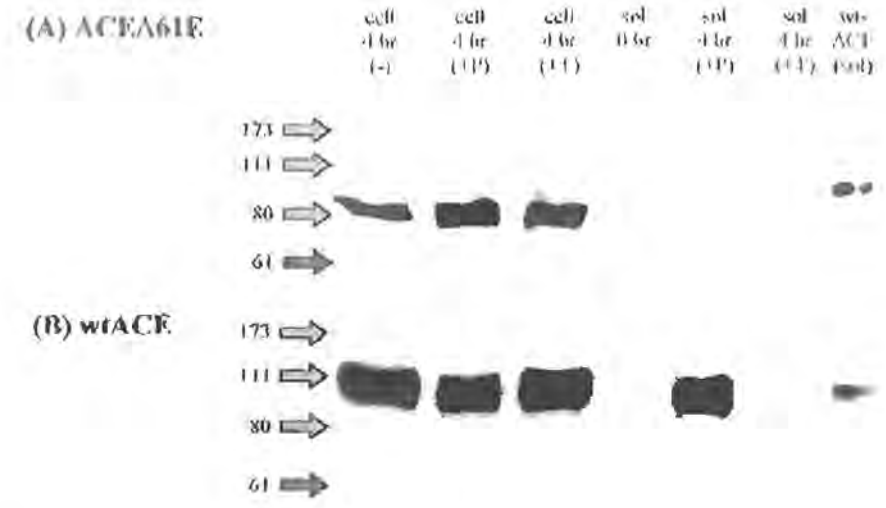

Figure 6.2.2.1) ACEΔ61E Western blot

Western blot analysis was performed on cell extract (cell) and medium (sol) samples of CHO cells transfected with either pLEN-ACEVII or pLEN-ACEΔ61E after 4 hours of either no stimulation (-), phorbol ester stimulation (+P), or TAPI inhibition (+T), and probed for ACE protein, as described above. The medium (med 0hr) is shown as a control. The BenchMark prestained marker (GibcoBRL) positions and sizes are shown on the left, with the pink reference marker band position shown in pink. The soluble wtACE marker (25ng) is in the last lane. The ACEΔ61E precursor protein appears to be much smaller than the wtACE precursor as it has no O-glycosylation sites and a 6.5 kDa reduction in peptide length. ACEΔ61E is not shed in any appreciable amounts, or is below the detection limit of the Western blot.

Figure 6.2.2.2) Confocal microscopy of CHO cells – ACE-Δ61E, wtACE

Transfected CHO cells expressing either ACEΔ61E or wtACE, were grown on coverslips, fixed with 3% paraformaldehyde, and ACE protein probed with rabbit anti-ACE antibodies, followed by a FITC-conjugated secondary antibody. The extracellular green FITC label was detected using confocal microscopy, the digital pictures of which are shown. The same intensity setting was used for all pictures, allowing semi-quantitative comparison.

the calcium phosphate method, and into COS-1 cells using the DEAE-Dextran method. Cell-extract samples of both neomycin resistant CHO cells and transiently transfected COS-1 cells failed, however, to yield any ACE activity using the HHL substrate protocol, suggesting that this mutant is inactive.

Western blotting analysis of CHO cells transfected with ACEΔ61E revealed a band at 80 kDa in the cell-extracts, however nothing was seen in the medium even in the presence of phorbol (Fig. 6.2.2.1). Thus, the transfection had succeeded but the catalytic domain of the ACEΔ61E truncation mutant enzyme is inactive. Interestingly, the ACE-specific band appears to be significantly smaller than expected for a mutant only 6.5 kDa smaller than wtACE. This is, however, consistent with the loss of the highly O-glycosylated N-terminal region [Ehlers *et al.*, 1992].

Confocal microscopy was performed on these cells to examine the subcellular localisation of this inactive mutant. Paraformaldehyde-fixed and un-permeabilised cells were found to contain significant amounts of ACE on the cell surface (Fig. 6.2.2.2). Surprisingly, the fluorescent signal is the most impressive of all the ACE mutants analysed thus far, strongly suggesting that this mutant form of ACE reaches the surface but is not shed and thus accumulates on the surface.

Although this exciting result would, at first glance, suggest that a sheddase recognition motif has been knocked out and that the N-terminal 22 residues of the ACE catalytic domain (D_{40}-E_{61}) are necessary for shedding, some circumspection is needed. Without an active ectodomain, one can assume that the protein is probably incorrectly folded. Thus, shedding may have been abolished due to the disruption of an important structural element elsewhere in the ectodomain, and not due to the removal of a sequence- or structure-specific binding site in the N-terminal 22 residues of the catalytic domain.

In the recent publication by Althoff *et al.*, the authors argue against the existence of a specific shedding motif in the stalk region and instead suggest that the sheddase(s) recognise and cleave disorganised ectoproteins more readily than stable ones, and that structural integrity (at least in the stalk region) is a key determinant for survival and

accumulation on the cell surface [Althoff *et al.*, 2001]. This is an extremely compelling idea as it solves many of the paradoxes found in the sheddase field, mentioned in Chapter 1. The data presented here argues against this model, however, as the ACEΔ61E mutant contains the wtACE stalk region (which is likely to have an open loop structure), is inactive (thus likely disordered/unstable) and should thus be the perfect candidate for a non-specific sheddase that recognises damaged/disorganised ectoproteins. Instead the inactive mutant accumulates impressively on the surface of CHO cells, indicating that a structurally sensitive sheddase-recognition motif has been disrupted.

The disruption in this mutant is not due to the removal of the O-glycosylated region as the ACEΔ36N-wt mutant shares the shedding and enzymatic profile of wtACE. Further deletion of the N-terminal 22 residues of the ACE catalytic domain (D_{40}-E_{61}) is therefore responsible for inactivating the enzyme. Surprisingly, the post-translational processing machinery tolerates this deletion, and the inactive mutant is allowed to proceed to the cell surface where it accumulates. Not only does this mutant suggest that ectodomain organisation is not the only factor involved in sheddase recognition, but it also proves the point that the ACE catalytic domain is extremely sensitive to deletions. Thus, deletion mutagenesis is not a meaningful strategy for isolating the exact shedding motif. This could explain why the chimeric mutants produced by Sadhukhan *et al.* involving sections of the rabbit ACE_T ectodomain fused to the CD4 stalk, TM and cytoplasmic domain were highly unstable and not processed to the cell surface [Sadhukhan *et al.*, 1998]. These unstable chimeras, as mentioned above, also involved fusing the CD4 ectodomain to truncated forms of rabbit ACE_T, equivalent to deleting the N-terminal 306, 390 and 500 residues of human ACE_T.

It is therefore clear that large-scale deletions in the ACE ectodomain have not, and cannot, yield meaningful results with respect to ectodomain shedding. We therefore devised an alternative strategy, exploiting the 55% amino acid identity between the N- and C-domains of somatic ACE, to create chimeric mutants that should retain structural integrity of the ACE catalytic domain, but mutate the hypothetical shedding recognition domain.

Swapping the ACE ectodomains

The homology between the N- and C-domains of somatic ACE is one of the most intriguing aspects of this enzyme. As explained in Chapter 2, the ACE catalytic domain duplicated internally about 400 million years ago, and the C-domain harbours the majority of the angiotensin I-hydrolysing activity of the enzyme, as well as being the sole catalytic domain in testis ACE. The fact that numerous residues have been completely conserved between both domains, and across numerous species strongly suggests that any mutation of these residues may be deleterious to the survival of the organism, and thus probably plays an important role in ACE function and stability. Figures 2.1.2 & 2.3.2 and Table 2.1.1 illustrate the extent of conservation in this molecule. The two domains are 55.2% identical, over the region D_{40}-P_{623} of ACE_T, and both have dipeptidyl carboxypeptidase activity, thus one can assume that these proteins will fold into very similar (if not identical) structures.

The non-identical residues must, however, be responsible for the differences in substrate specificity shown for these two domains. Using a similar line of reasoning, we proposed that by swapping the 'C-domain' of testis ACE for the N-domain of somatic ACE, we could halve the number of residues needing examination as possible shedding motifs. If the chimera containing only the N-domain of somatic ACE fused to the stalk, TM and cytoplasmic domains of testis ACE **is not** shed, then one can assume that the shedding motif has been inactivated, due to changes in the non-conserved amino acids. If, however, the N-domain chimera **is** shed from the cell surface, then one can assume either that the recognition motif lies in the conserved residues that have not changed, or that the motif is a structural one that has not been affected by the changes.

To test this hypothesis we deleted the C-domain from somatic ACE, creating a membrane anchored N-domain (Fig. 6.3.1).

(A)

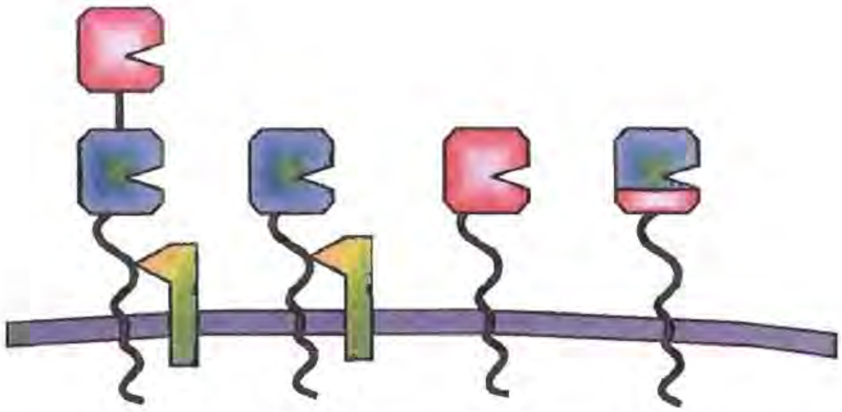

(B)

```
              556                           58[illegible]
WTACE         KEAGQRLATAMKLGFSRPWPEAMQLITGQPNMSASAMLSY
ACE-NBCL      ------------------------------LDALD-QPL-K-
ACE-NDOM      TK--AK-RKVLQA-S-----Q-VLKDMV-LDALD-QPL-K-
                                            561

                           Δ16        Δ11    Δ6
                                            623
WTACE         FKPLLDWLRTENELHGEKLGWPQYNWTPNSARSEGPLPDS
ACE-NBCL      -Q-VTQ--QEQ-QQN--V----E-Q-H-------------
ACE-NDOM      -Q-VTQ--QEQ-QQN--V----E-Q-H-------------
                                            601

                             65[illegible]          67[illegible]
WTACE         GRVSFLGLDLDAQQAR[illegible]SQRL
ACE-NBCL      ----------------[illegible]----
ACE-NDOM      ----------------[illegible]----
```

Figure 6.3.1) The ACE-Ndom and ACE-NBcl chimeric mutants

A schematic representation of the ACE-Ndom and ACE-NBcl chimeric mutants is shown in (A). Somatic ACE consists of the ACE N-domain (red) and a C-domain (blue) separated by a short bridge, followed by the juxtamembrane stalk, TM and cytoplasmic regions that anchor it to the plasma membrane (dark blue). The N-domain is absent in the testicular form of ACE. The ACE-Ndom mutant has the 'C-domain' of testis ACE swapped for the N-domain of somatic ACE. ACE-NBcl has only 41 residues of the proximal ectodomain of testis ACE swapped for the equivalent region of the N-domain. The sequences of each of these mutants are shown in (B), where the testis ACE sequence from K556 to L675 is shown in blue, and the N-domain sequence in red. Identity with testis ACE is indicated with a dashed line, changes are indicated by their single letter code. Amino acid numbering refers to mature proteins. The relative positions of the ACE-JMΔ6, -JMΔ11 and -JMΔ16 mutants are shown with lines, while the wtACE sheddase site (R627/S628) is shown with a red arrow. The section of testis ACE that is swapped with the somatic form in SomNBcl is indicated in bold. The transmembrane region is highlighted in light blue.

6.3) ACE-Ndom

The ACE-Ndom mutant was constructed using the same two-stage PCR protocol described above, except that a unique *Pin*AI site in ACE_S was exploited to insert the 'zipper' PCR product (encoding the I_{530}-P_{601} region of ACE_S fused to the N_{624}-S_{701} region of ACE_T) into ACE_S. This, in effect, removes the whole of the ACE_S C-domain. The wtACE (ACE_T) catalytic 'C-domain' is therefore swapped for the exactly equivalent residues of the ACE_S N-domain, in order to preserve the folding and enzymatic activity.

The vector pLEN-ACE-Ndom was stably co-transfected with pSV2NEO into CHO-K1 cells, and the cell-extract assayed for ACE activity using the HHL substrate assay, as described. Numerous clones, from repeated transfections, were tested, but failed to improve on the ACE activity of only 3.4 ±0.1 mU ACE per well (n = 3). This cell-associated activity did not vary when the cells were subjected to the 4-hour shedding kinetics study described above, and no ACE activity was recorded in the medium of these ACE-Ndom-transfected CHO cells (Fig. 6.3.2). Furthermore, the cells showed no characteristic reduction in ACE activity on stimulation with 1 μM PDBu or increase in activity with TAPI inhibition. There is no statistical difference between each of the cell-extract samples shown in Fig. 6.3.2 ($P>0.2$; n = 3).

The poor HHL-hydrolysing activity found for the ACE-Ndom mutant is to be expected as the N-domain is reported to have an order of magnitude lower catalytic activity than the C-domain for the substrate HHL. The k_{cat} of the N-domain for HHL hydrolysis was found to be 10-fold lower than that of wild-type somatic ACE and the C-domain, although the K_m is the same as the C-domain [Wei *et al.*, 1991].

Even if one takes this into account, wtACE sheds about half the enzyme present in the cells at zero-time, and thus a medium HHL activity of ~1.5 mU ACE per well for a shed ACE-Ndom would be within the limit of assay sensitivity. The absence of any HHL-hydrolysing activity in the medium after 4-hours of phorbol ester activation,

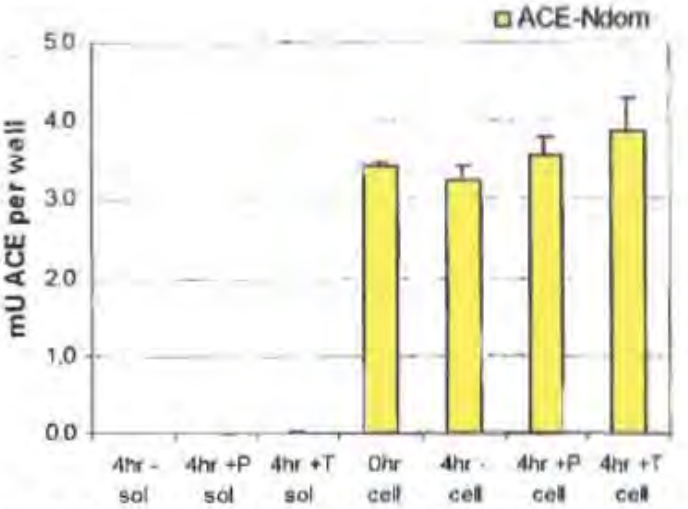

Figure 6.3.2) The shedding of ACE-Ndom – HHL substrate

CHO-K1 cells expressing ACE-Ndom were grown to confluence in 6-well dishes. At zero-hour the cell-extract samples were removed (0hr) and the remaining cells incubated for 4 hours with fresh induction medium supplemented with either nothing (-), 1 μM PDBu (+P) or 10 μM TAPI (+T). The medium (sol) and cell-extract (cell) samples were then assayed for ACE activity using HHL as substrate [n=3].

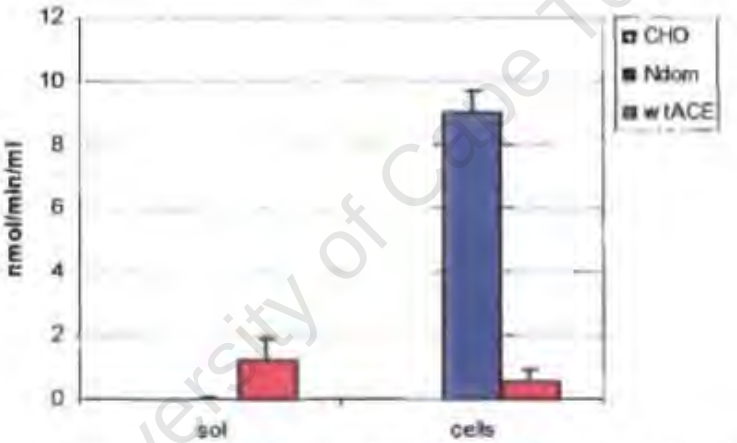

Figure 6.3.3) The shedding of ACE-Ndom – using the Abz-SDK(Dnp)P-OH substrate

The 4hr PDBu stimulated cell-extract (cells) and medium (sol) samples collected above for Fig 6.3.2 were further assayed for the ability to hydrolyse the internally quenched fluorogenic substrate Abz-SDK(Dnp)P-OH. Similarly produced wtACE and CHO samples were used as controls. 50μl of each sample was assayed using 8 μM Abz-SDK(Dnp)P-OH in a final volume of 2.5 ml, at 37°C, with continuous fluorescence measurement at λ_{ex} = 320nm and λ_{em} = 420nm. The change in fluorescence was converted to nmol substrate hydrolysed per minute per ml of sample (y-axis) using a calibration curve of hydrolysed peptide.

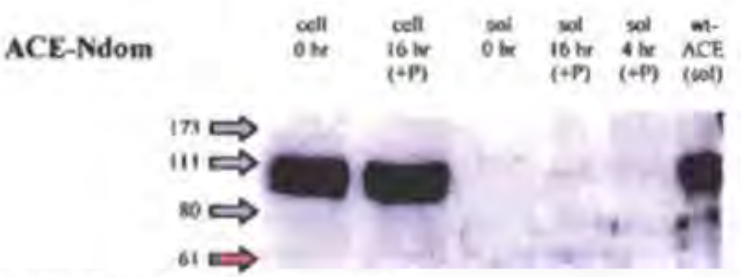

Figure 6.3.4) ACE-Ndom Western blot

Western blot analysis was performed on cell extract (cell) and medium (sol) samples of ACE-Ndom expressing CHO cells, at zero time and after either 4 or 16 hours of phorbol ester stimulation (+P). Markers (in kDa) on left, soluble wtACE (250ng) in last lane.

even when the medium was concentrated 8-fold (data not shown), introduces the possibility that the ACE-Ndom mutant is not shed, or is shed in an inactive form.

In contrast to the poor N-domain substrate HHL, the hemoregulatory peptide Ac-SDKP was found to be a specific substrate for the N-domain [Rousseau *et al.*, 1995]. This was converted for use as an internally quenched fluorogenic peptide substrate for ACE assays [Araujo *et al.*, 2000]. The Ac-SDKP analogue Abz-SDK(Dnp)P-OH was also found to be an N-domain specific substrate [Araujo *et al.*, 2000]. We analysed the cell-extract and medium samples of wtACE, ACE-Ndom and CHO cells subjected to 4 hours of phorbol ester stimulation, using the Abz-SDK(Dnp)P-OH substrate (8 μM) and continuously measuring fluorescence. The initial velocity (Vo) was determined (<5% substrate hydrolysed), and converted to nmol of substrate converted/min/ml of sample using a calibration curve of completely hydrolysed Abz-SDK(Dnp)P-OH. The data clearly shows that, although good enzyme activity was recorded in the cell-extracts of ACE-Ndom expressing CHO cells, none is seen in the medium after 4 hours of shedding stimulation with 1 μM PDBu, again indicating that this chimera is not shed (Fig. 6.3.3). CHO cell-extract and medium samples showed no activity, defining the specificity seen in this crude cell-extract system. The wtACE-expressing cells showed 15-fold less activity, which is not surprising as testis ACE contains only the C-domain. Interestingly, the wtACE enzyme is also seen to be shed over 4 hours, at 69% (n = 2), indicating that this assay is not inhibited by components in the medium or cell-extracts.

Western-blot analysis was also performed on the cell-extract and medium samples of CHO cells expressing ACE-Ndom, at zero time and after 4 or 16 hours of stimulation with 1 μM PDBu. A broad band is consistently seen in the cell-extract samples, with both the precursor and mature forms identifiable. No ACE protein is seen in the medium after 4 hours (see Fig. 6.3.4), which is stark contrast to the signal seen for wtACE after 4 hours of phorbol activation. Thus, ACE-Ndom is considered to be a non-shed ACE mutant.

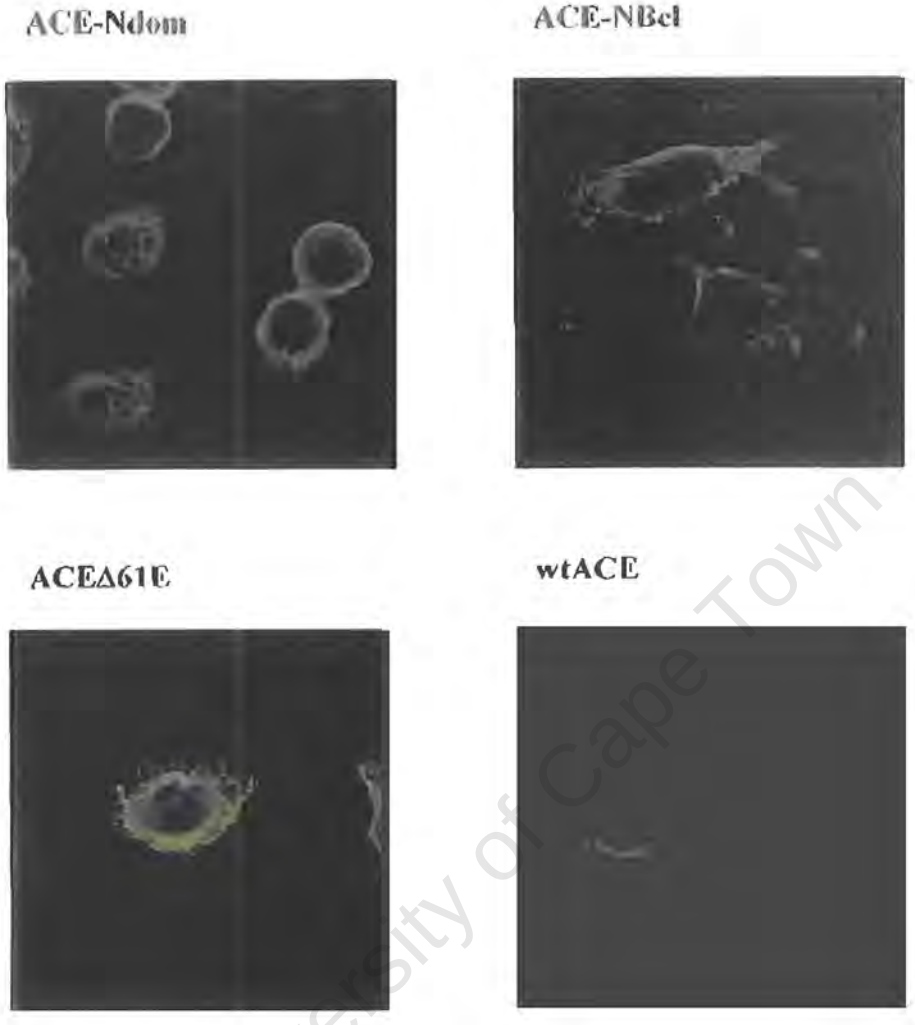

Figure 6.3.5) Confocal microscopy of CHO cells – ACE-Ndom, -NBcl, -Δ61E and -wt
Transfected CHO cells expressing either ACE-Ndom, ACE-NBcl, ACEΔ61E or wtACE, were grown on coverslips, fixed with 3% paraformaldehyde, and ACE protein probed with rabbit anti-ACE antibodies, followed by a FITC-conjugated secondary antibody. The extracellular FITC label was detected using confocal microscopy, the digital pictures of which are shown. The same intensity setting was used for all pictures, allowing semi-quantitative comparison. These pictures are representative of the slide. Note the strong surface expression of ACEΔ61E, indicating good processing of this mutant to the surface and lack of shedding, leading to an accumulation on the plasma membrane. Both the ACE-Ndom and ACE-NBcl mutants are also processed to the cell surface.

Confocal microscopy was performed on fixed, un-permeabilised, CHO cells expressing ACE-Ndom. Good FITC labelling was achieved on the cell-surface (Fig. 6.3.5), indicating that the chimera is stable, is processed to the cell-surface and the abolition of shedding into the medium is not due to a failure of the secretory machinery in these cells.

In conclusion, the ACE-Ndom mutant is not shed. Although it is processed to the cell surface, as a mature, fully glycosylated enzyme, it does not release any protein into the medium after 4 hours of phorbol ester stimulation. This was corroborated using both the substrates HHL and Abz-SDK(Dnp)P-OH, which indicated that the enzyme was showing substrate preferences characteristic of the ACE N-domain, but was not released into the culture medium.

Thus, the ACE_S N-domain is unable to support ectodomain shedding when swapped into the exact position of the ACE_T 'C-domain'. If one assumes that the 54% identity (over 616 amino acids) between the N- and C-domains of ACE_S implies that they have the same structure, then one can conclude that the sheddase recognition motif is not structural *per se*, and that the 325 identical residues in this region do not play a direct role in shedding. In addition, a disorganised ectodomain is not essential for shedding, as both testis ACE (wtACE) and ACE-Ndom have cell-surface localised, functional ectodomains, but only wtACE is shed.

This is a very useful result, as a motif that was entirely structural and conserved between both domains would imply that the ACE sheddase is unique to ACE, and that there is a unique sheddase for each shed ectoprotein. Apart from being highly unlikely, given the precedent set by the promiscuous TACE sheddase that is responsible for the shedding of numerous ectodomains, it would also mean that a 'universal' shedding motif (whether sequence based or a localised 3D structure) would be impossible to find.

This leads one to examine the 262 non-identical amino acids more closely. Although spread out over the 584-residue ectodomain, there must be a region (or regions) that forms a specific structure that is recognised by the secretase, and has been inactivated by replacement with the residue found in the N-domain at that position. As numerous

sheddases position themselves for cleavage at a defined distance from the ectodomain [Ehlers *et al.*, 1996; Chapter 1], it seemed logical to start looking for this motif in the proximal ectodomain. Thus, the G_{583}-P_{623} region of human ACE_T was swapped for the homologous region in the ACE_S N-domain, to create the ACE-NBcl chimeric mutant (Fig. 6.3.1).

6.4) ACE-NBcl

The ACE-NBcl chimera is almost entirely the same as testis ACE, except for the 41-amino acid proximal ectodomain region (G_{583}-P_{623}) that has been replaced by the equivalent region of the ACE_S N-domain (G_{561}-P_{601}). The vector pLEN-ACE-NBcl was co-transfected with pSV2NEO into CHO-K1 cells using the calcium phosphate method. Pooled neomycin resistant cells were grown to confluence in 6-well dishes, and the cell-extracts assayed for ACE activity using the HHL hydrolysis protocol. The cell-associated activity was found to be 46.4 ±5.8 mU ACE per well (n = 6), 15-fold more than that of ACE-Ndom.

The cells were then subjected to the same 4-hour shedding study described above, and the cell-extract and medium samples assayed using HHL (Fig. 6.3.1a). Surprisingly, 20% of the ACE activity was shed into the medium without stimulation, and this increased to 64% with phorbol ester stimulation (Fig. 6.4.1b). This shedding activity was significantly inhibited by TAPI ($p<0.0005$, n = 6), indicating that a TAPI-inhibitable, phorbol ester-inducible sheddase is able to cleave the ACE-NBcl chimera, with much the same kinetics as wtACE.

Western blot analysis was performed on the cell-extract and medium samples collected in the 4-hour shedding kinetics study. The ACE-specific antibody clearly identifies both the precursor and mature forms of ACE-NBcl and that these have the same molecular weight as wtACE (Fig. 6.4.2). Furthermore, the mature form is reduced in the phorbol-stimulated sample lanes, and appears strongly in the medium after 4 hours, confirming the phorbol-induced activation of shedding. Similarly, the TAPI-inhibition of shedding can be seen with an increase in intensity in the mature band in the cell extract sample (lane 3) and the weak band in the medium sample

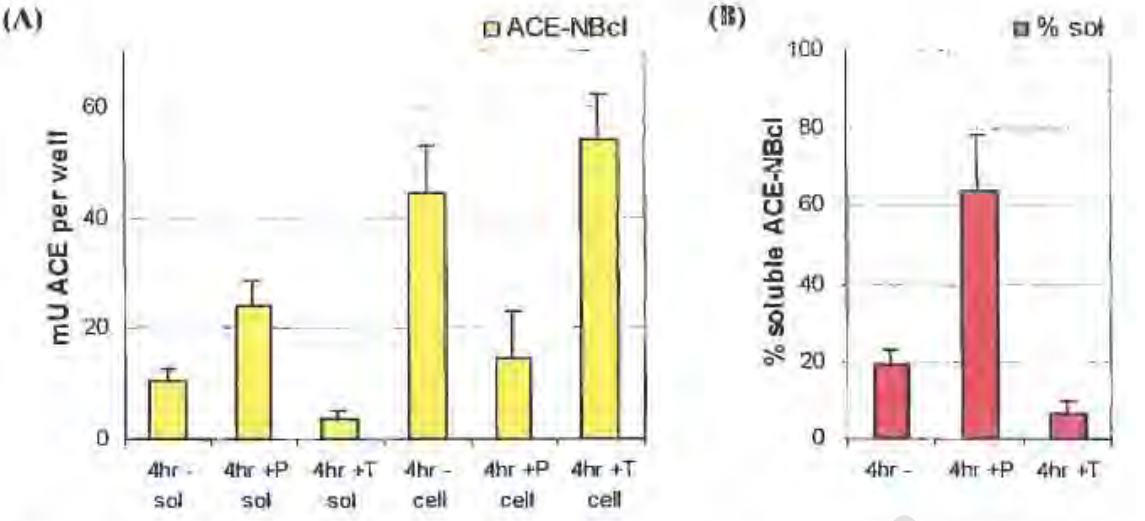

Figure 6.4.1) The shedding of ACE-NBcl – effect of PDBu and TAPI over 4 hours

Confluent CHO-K1 cells stably transfected with the pLEN-ACE-NBcl vector were incubated for 4 hours with fresh induction medium supplemented with nothing (-), 1 μM PDBu (+P) or 10 μM TAPI (+T). The medium (sol) and cell-extract (cell) samples were then assayed for ACE activity using HHL as substrate (A) [n=6]. The percentage soluble ACE activity after 4 hours is shown in (B).

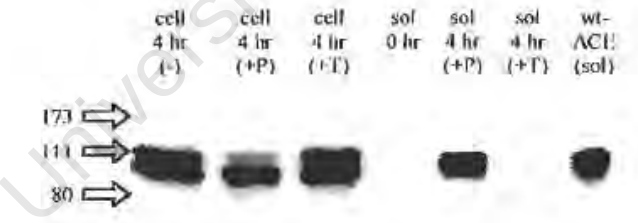

Figure 6.4.2) ACE-NBcl Western blot

Western blot analysis was performed on cell extract (cell) and medium (sol) samples of ACE-NBcl expressing CHO cells. Confluent 6-well dishes were incubated for 4 hours with either no supplements (-), or 1 μM PDBu (+P), or 10μM TAPI (+T). The medium was included as a negative control. The BenchMark prestained marker (GibcoBRL) positions and sizes (in kDa) are shown on the left. The soluble wtACE marker (50ng) is in the last lane (wtACE sol). Note the clear separation of the precursor (90 kDa) and mature (105 kDa) forms of ACE-NBcl in the cell-extract lanes. Note also the reduction in intensity of the mature band when cells are stimulated with phorbol ester, and the concomitant accumulation of the cleavage-secreted form in the medium. The inhibition of shedding by TAPI is seen with the weak band in lane 6. The minor contaminant seen at ~170 kDa also appears in the zero hour medium control lane.

(lane 6) after 4 hours of incubation with 10 μM TAPI. The Western-blot analysis also suggests that the mature, glycosylated form is shed, as the soluble form migrated with a similar R_f to the mature cellular form.

Confocal microscopy of paraformaldehyde-fixed, un-permeabilised, CHO cells expressing ACE-NBcl, which were probed with an anti-ACE antibody and a FITC-conjugated secondary antibody showed a strong signal on the cell-surface (Fig. 6.3.5, above). This confirmed the cell-surface localisation of ACE-NBcl, indicating that this mutant is processed adequately to the plasma membrane, where it is likely cleaved by the sheddase.

ACE-NBcl was affinity-purified from the culture medium, denatured, reduced, the cysteines protected with vinylpyridine, and then digested with endoproteinase Lys-C. MALDI-TOF analysis of the mixed peptide sample gave numerous *m/z* peaks, many of which could be assigned to known peptide sequences in the ACE_T ectodomain. One of the large peaks, at *m/z* 4062.7, related to the calculated mass of a putative C-terminal fragment Y_{573}-R_{605} (4060.4), placing the cleavage site at the R_{605}/S_{606} bond, which corresponds to R_{627}/S_{628} in ACE_T. Hence cleavage was predominantly occurring at the same bond used by the sheddase to cleave wtACE. Interestingly, two minor peaks of *m/z* 5058.9 and *m/z* 5391.3 relate well to the calculated masses of C-terminal peptides that end in R_{637} (5056.4) and F_{640} (5389.8) respectively. This suggests that the R_{637}/V_{638} and F_{640}/L_{641} bonds may act as secondary sites for sheddase cleavage, especially when considering their use for the shedding of ACE-Δ6JM, ACE-ΔR_{627} and ACE-ΔCYT, mentioned above.

In summary, the ACE-NBcl mutant is expressed in CHO cells and is processed to the cell-surface, presumably as the fully-glycosylated, mature protein seen on Western blotting analysis. It is shed from the cell by a sheddase that not only shows a characteristic 3-fold induction on phorbol stimulation, and inhibition with TAPI, but also hydrolyses the same R_{627}/S_{628} bond as in wtACE. Thus it is likely that the same sheddase cleaves both wtACE and the ACE-NBcl chimera.

Although specific activities were not calculated for the ACE-Ndom and ACE-NBcl mutants, the 15-fold increase in ACE activity of ACE-NBcl over that of ACE-Ndom, without the related increase in Western blot signal, suggests that the ACE-NBcl mutant has a C-domain-like catalytic activity, as opposed to the poor HHL hydrolysis of the N-domain. This would, at first, seem to be a trivial finding, as the ACE-NBcl chimera consists predominantly of wild-type ACE_T, with only 41 residues of the ectodomain replaced by the equivalent region of the N-domain. However, Williams *et al.* constructed N- and C-domain ACE chimeras that had the 60 residues spanning the active site swapped for the equivalent region of the other domain [Williams *et al.*, 1996]. Surprisingly, they found that the domain-specific characteristics did not transfer along with the catalytic site sequence, indicating that the substrate specificities must reside outside the immediate active site region. In an attempt to establish the importance of the first 141 amino acids of the N-domain, in terms of substrate specificity and structural stability, Marcic *et al.* made use of the two 'homologous' *Bgl*II sites in ACE_S. By deleting the *Bgl*II/*Bgl*II fragment, they created a chimera that contained the 5′-region of the N-domain and the 3′-end of the C-domain containing the catalytic site [Marcic *et al.*, 2000a]. Contrary to their expectations, this chimera did not act as either an N-domain or a C-domain (nor for that matter as an ACE_T or ACE_S enzyme), but instead has its own unique set of substrate specificities, inhibitor profile, ion dependence and thermostability. With this in mind, it is tempting to speculate that the ACE-NBcl mutant shows wtACE-like catalytic activity with the HHL substrate, and shedding characteristics, although this conjecture clearly needs to be proven with enzyme kinetics studies using purified wtACE, ACE-NBcl and ACE-Ndom.

Thus, the human somatic ACE N-domain, which is highly conserved across numerous species and both domains of ACE, does not support ectodomain shedding when placed in the exactly equivalent position as the ACE_T 'C'-domain. As the N-terminal highly O-glycosylated region of testis ACE does not play a role in shedding, one can conclude that the region defined by evolutionary conservation, namely D_{40}-P_{623} contains the relevant signals for the shedding of human testis ACE. Furthermore, 41 amino acids of the proximal ectodomain did not contain a shedding motif, as shedding was not abolished when the region G_{583}-P_{623} of ACE_T was swapped for the equivalent

region of the N-domain. Thus the sheddase recognition motif must reside in the distal ectodomain region of testis ACE (D_{40}-T_{582}), likely in a region that is not conserved between the two domains of somatic ACE.

The task of finding which of these 239 non-identical amino acids, spread out over this 544-residue region of the ectodomain is a daunting one. However, by systematically swapping different regions of testis ACE for equivalent regions of the somatic N-domain, one will be able to narrow down the exact motif used by the ACE sheddase to recognise its substrate. This motif is likely to be highly dependent on its structural context, as the inactive (and thus likely disorganised) ectodomain of the ACEΔ61E mutant is not shed and instead accumulates on the cell surface. Although it is tempting to speculate that the N-terminal 22 amino acids of ACE_T may contain a sheddase recognition motif, it is only through a swap-over approach that preserves enzymatic activity of the ectodomain, and thus likely the structural integrity, that one can meaningfully define the exact sheddase recognition domain. In fact, preliminary data from our laboratory, involving swap-over mutagenesis, suggests that this N-terminal region is not involved in shedding (in progress).

Similarly, the ACE-JMΔ47 mutant, in which the stalk region and 11 amino acids of the proximal ectodomain have been deleted, was found to be inactive and not shed [Ehlers *et al.*, 1996]. While the authors did not show that this mutant was processed to the surface, it is instead likely degraded intracellularly, like the ACE-Δ16JM mutant. Also, the findings from the ACE-NBcl swap-over chimera show conclusively that the sheddase recognition motif is not in this region. The sensitivity of the ACE ectodomain to deletions or mutations is clearly illustrated by both the work of Sadhukhan *et al.* in which they list ACE/CD4 chimeric mutants that failed to reach the cells surface [Sadhukhan *et al.*, 1998], and my own unpublished observation that a spurious $P_{576}L$ mutation in the ACE_S N-domain, 18 residues upstream of domain boundary, abolished enzymatic activity and that this activity could be restored with correction of the mutation.

This proves the point that the recognition motif is likely to be specific to a particular sequence in the ACE C-domain, which is absent in the N-domain, and that needs to be

in a particular 3D conformation. Attempts to delete or mutate residues within the region D_{40}-G_{615} of ACE_T are likely to result in an inactive protein that does not process to the cell surface and/or may have non-specifically disrupted a structurally sensitive sheddase recognition domain. This domain may, like the hypervariable regions of IgG, be composed of numerous folds from entirely different regions of the protein, any or all of which may be disrupted by deletions or mutations in the ACE ectodomain. Thus a swap-over mutagenesis approach, that preserves enzymatic activity, is the most feasible method for elucidating the exact sheddase recognition domain.

Chapter 7: Conclusions

The major goal of this thesis has been to attain a more complete understanding of the shedding apparatus responsible for releasing the ectodomain of ACE in transfected cells. At the start of the work leading to this thesis, many questions regarding the ACE sheddase, and shedding proteases in general, were unanswered, including the identities of the proteases, the factors involved in regulating the shedding machinery, and the determinants of substrate protein recognition by sheddases. Although the field is still in its infancy (the existence of sheddases as a distinct class of cellular proteases was first proposed in 1991 [Ehlers & Riordan, 1991b]), great strides have been made in the last five years, while this work was in progress.

Important discoveries in the sheddase field include:

- The discovery and cloning of TACE, the first sheddase to be identified, and the realization that it is a member of the recently discovered ADAM family of membrane-bound metalloproteases (ADAM-17). This family of proteases contains two additional sheddases, ADAM-10 and ADAM-9, and possibly others.

- The finding that each sheddase can cleave a broad range of substrate ectoproteins. Furthermore, a 'basal' sheddase exists that, unlike the ADAM proteases, is not induced with phorbol ester and is dependant on stalk structure.

- The discovery that the mechanistic basis for phorbol-ester-induced shedding of ectoproteins resides in interactions between PKC isoforms, calmodulin, and actin-binding proteins with substrate proteins and, likely, the sheddase.

- The realization that substrate protein recognition by sheddases is not dependent on precise sequence motifs or lengths of the juxtamembrane stalk. Instead, stalks must be accessible, preferably unfolded and/or disordered, of minimum length and sterically unhindered by the proximal TM and EC domains.

- Increasing evidence for the existence of one or more recognition motifs in the ectodomains of some substrate proteins that significantly enhance shedding rates. Such motifs are likely substrate- and sheddase-specific.

The work described in this thesis has addressed most of the above points. In particular, my work has shown that:

- The elusive sheddase recognition motif resides in the ectodomain of human testis ACE, in a region that is not conserved between the N- and C-domains of somatic ACE. More specifically, this recognition domain is in the distal ectodomain (D_{40}-T_{582}) and not in the proximal ectodomain (G_{583}-P_{623}), juxtamembrane stalk or cytoplasmic regions of human testis ACE.

- Deletions in the ectodomain of ACE abolish catalytic activity and/or protein stability and result in either rapidly degraded protein or potentially false-positive results. This sheddase recognition domain is likely to be structurally sensitive, akin to the hypervariable regions of IgG whose binding surface consists of numerous folds.

- In this regard the minimal catalytic unit of human testis ACE has been defined as the region D_{40}–G_{615}, with truncation mutations at either end inactivating the enzyme. A domain swap-over method for characterising the sheddase recognition domain has been developed, and the advantages of this approach over deletion mutagenesis or chimeric mutants involving CD4, expounded.

- The cytoplasmic tail of ACE plays a key role in the regulation of its cleavage-secretion, as removal results in deregulated shedding which is no longer responsive to phorbol ester activation and only partially inhibitable by TAPI. This indicates that the cytoplasmic tail may interact with an inhibitory factor in the cytoplasm of the cell, which is released on activation of shedding, possibly through PKC phosphorylation of either the ACE cytoplasmic domain or the inhibitory factor.

- This ACE cytoplasmic-tail-binding sheddase-inhibitory protein is likely to be either actin or an actin-binding protein, as the actin-depolymerising agent cytochalasin D significantly induces the shedding of wtACE. Thus, ACE may be localised to a particular microdomain of the plasma membrane that is inaccessible to the sheddase, and the increased lateral fluidity induced by PKC activation or the removal of the cytoplasmic tail results in greater accessibility for substrate/sheddase interactions. This may also explain the increased 'basal' shedding seen in the cytoplasmic-truncation mutant.

- The ACE sheddase does not position itself at a defined distance from the proximal ectodomain, but instead shows a particular preference for the native cleavage site (R_{627}/S_{628}). This site is not, however, essential for cleavage as shedding was not abolished when the preferred bond was occluded by a large N-linked oligosaccharide or the R_{627} residue removed. The sheddase instead uses alternate sites at the R_{637}/V_{638} and F_{640}/L_{641} bonds, which were used for shedding of three of the mutants presented here, but not for wtACE. This, and the finding that the regions of the ACE stalk can be deleted or replaced with entirely unrelated peptides without abolishing shedding, shows that the sheddase is not sequence-specific at the cleavage site.

- The region just downstream of the wtACE cleavage site may, however, contain a motif involved in recognition by a phorbol-ester induced sheddase, or confer a more favourable cleavage site conformation on the stalk region. This region, which shows some similarity to the cleavage site recognition domain of CSF-1[256], is deleted in the ACE-Δ5JM mutant. This mutant also explains the discrepancy seen in the shedding rates of the ACE-JMΔ17 and ACE-JMΔ24 mutants.

Thus, my work conclusively shows that the ACE sheddase recognition domain is in the distal ectodomain, and not the juxtamembrane stalk, cytoplasmic or proximal ectodomain regions of ACE. I have also developed a domain swap-over method for the further elucidation of the exact motif as deletion mutants have not and probably will not succeed, as this putative sequence-specific motif is likely to be structurally sensitive. Furthermore, I have discovered that the cytoplasmic domain of ACE is involved in shedding regulation, likely through binding to an inhibitory actin-binding factor. I have also shown that the 'headroom' region of the stalk is not necessary for sheddase recognition of ACE, and that the sheddase can use alternative cleavage sites when its preferred R_{627}/S_{628} bond is deleted or occluded by an N-linked oligosaccharide.

References:

Alele, J., Jiang, J., Goldsmith, J. F., Yang, X., Maheshwari, H. G., Black, R. A., Baumann, G., and Frank, S. J. (1998). Blockade of growth hormone receptor shedding by a metalloprotease inhibitor. *Endocrinology* **139**:1927-1935.

Alpaugh, M. L., Lee, M. C., Nguyen, M., Deato, M., Dishakjian, L., and Barsky, S. H. (2000). Myoepithelial-specific CD44 shedding contributes to the anti-invasive and antiangiogenic phenotype of myoepithelial cells. *Exp Cell Res* **261**:150-158.

Althoff, K., Reddy, P., Voltz, N., Rose-John, S., and Mullberg, J. (2000). Shedding of interleukin-6 receptor and tumor necrosis factor alpha. Contribution of the stalk sequence to the cleavage pattern of transmembrane proteins. *Eur J Biochem* **267**:2624-2631.

Althoff, K., Mullberg, J., Aasland, D., Voltz, N., Kallen, K., Grotzinger, J., and Rose-John, S. (2001). Recognition sequences and structural elements contribute to shedding susceptibility of membrane proteins. *Biochem J* **353**:663-672.

Amit, T., Amit, T., Hochberg, Z., Yogev-Falach, M., Youdim, M. B., Youdim, M. B., and Barkey, R. J. (2001). Shedding of growth hormone-binding protein is inhibited by hydroxamic acid-based protease inhibitors: proposed mechanism of activation of growth hormone-binding protein secretase. *J Endocrinol* **169**:397-407.

Araujo, M. C., Melo, R. l., Del Nery, E., Alves, M. F., Juliano, M. A., Casarini, D. E., Juliano, L., and Carmona, A. K. (1999). Internally quenched fluorogenic substrates for angiotensin I-converting enzyme. *J Hypertens* **17**:665-672.

Araujo, M. C., Melo, R. L., Cesari, M. H., Juliano, M. A., Juliano, L., and Carmona, A. K. (2000). Peptidase specificity characterization of C- and N-terminal catalytic sites of angiotensin I-converting enzyme. *Biochemistry* **39**:8519-8525.

Ariel Gomez, R. and Norwood, V. F. (1995). Developmental consequences of the Renin-Angiotensin System. *Am J Kidney Dis* **26**:409-431.

Arribas, J. and Massague, J. (1995). Transforming growth factor-alpha and beta-amyloid precursor protein share a secretory mechanism. *J Cell Biol* **128**:433-441.

Arribas, J., Coodly, L., Vollmer, P., Kishimoto, T. K., Rose-John, S., and Massague, J. (1996). Diverse cell surface protein ectodomains are shed by a system sensitive to metalloprotease inhibitors. *J Biol Chem* **271**:11376-11382.

Arribas, J., Lopez-Casillas, F., and Massague, J. (1997). Role of the juxtamembrane domains of the transforming growth factor- alpha precursor and the beta-amyloid precursor protein in regulated ectodomain shedding. *J Biol Chem* **272**:17160-17165.

Ashwell, G. and Morell, A. G. (1974). The role of surface carbohydrates in the hepatic recognition and transport of circulating glycoproteins. *Adv Enzymol Relat Areas Mol Biol* **41** :99-128.

Atochina, E. N., Muzykantov, V. R., Al Mehdi, A. B., Danilov, S. M., and Fisher, A. B. (1997). Normoxic lung ischemia/reperfusion accelerates shedding of angiotensin converting enzyme from the pulmonary endothelium. *Am J Respir Crit Care Med* **156**:1114-1119.

Azizi, M., Rousseau, A., Ezan, E., Guyene, T. T., Michelet, S., Grognet, J. M., Lenfant, M., Corvol, P., and Menard, J. (1996). Acute angiotensin-converting enzyme inhibition increases the plasma level of the natural stem cell regulator N-acetyl-seryl-aspartyl-lysyl- proline [see comments]. *J Clin Invest* **97**:839-844.

Bakhle, Y. S. (1968). Conversion of angiotensin I to angiotensin II by cell-free extracts of dog lung. *Nature* **220**:919-921.

Bayer-Garner, I. B., Sanderson, R. D., Dhodapkar, M. V., Owens, R. B., and Wilson, C. S. (2001). Syndecan-1 (cd138) immunoreactivity in bone marrow biopsies of multiple myeloma: shed syndecan-1 accumulates in fibrotic regions. *Mod Pathol* **14**:1052-1058.

Beer, S., Oleszewski, M., Gutwein, P., Geiger, C., and Altevogt, P. (1999). Metalloproteinase-mediated release of the ectodomain of L1 adhesion molecule. *J Cell Sci* **112 (Pt 16)**:2667-2675.

Beldent, V., Michaud, A., Bonnefoy, C., Chauvet, M. T., and Corvol, P. (1995). Cell surface localization of proteolysis of human endothelial angiotensin I-converting enzyme. Effect of the amino-terminal domain in the solubilization process. *J Biol Chem* **270**:28962-28969.

Bell, G. I., Fong, N. M., Stempien, M. M., Wormsted, M. A., Caput, D., Ku, L. L., Urdea, M. S., Rall, L. B., and Sanchez-Pescador, R. (1986). Human epidermal growth factor precursor: cDNA sequence, expression in vitro and gene organization. *Nucleic Acids Res* **14**:8427-8446.

Bernstein, K. E., Martin, B. M., Bernstein, E. A., Linton, J., Striker, L., and Striker, G. (1988). The isolation of angiotensin-converting enzyme cDNA. *J Biol Chem* **263**:11021-11024.

Black, R. A. and White, J. M. (1998). ADAMs: focus on the protease domain. *Curr Opin Cell Biol* **10**:654-659.

Black, R. A., Durie, F. H., Otten-Evans, C., Miller, R., Slack, J. L., Lynch, D. H., Castner, B., Mohler, K. M., Gerhart, M., Johnson, R. S., Itoh, Y., Okada, Y., and Nagase, H. (1996). Relaxed specificity of matrix metalloproteinases (MMPS) and TIMP insensitivity of tumor necrosis factor-alpha (TNF-alpha) production suggest the major TNF-alpha converting enzyme is not an MMP. *Biochem Biophys Res Commun* **225**:400-405.

Black, R. A., Rauch, C. T., Kozlosky, C. J., Peschon, J. J., Slack, J. L., Wolfson, M. F., Castner, B. J., Stocking, K. L., Reddy, P., Srinivasan, S., Nelson, N., Boiani, N., Schooley, K. A., Gerhart, M., Davis, R., Fitzner, J. N., Johnson, R. S., Paxton, R. J., March, C. J., and Cerretti, D. P. (1997). A metalloproteinase disintegrin that releases tumour-necrosis factor- alpha from cells. *Nature* **385**:729-733.

Blobel, C.P. (2000). Remarkable roles of proteolysis on and beyond the cell surface. *Curr Opin Cell Biol* **12**:606-12

Bodeau, A. L., Berrier, A. L., Mastrangelo, A. M., Martinez, R., and LaFlamme, S. E. (2001). A functional comparison of mutations in integrin beta cytoplasmic domains: effects on the regulation of tyrosine phosphorylation, cell spreading, cell attachment and beta1 integrin conformation. *J Cell Sci* **114**:2795-2807.

Bonnet, D., Lemoine, F. M., Pontvert-Delucq, S., Baillou, C., Najman, A., and Guigon, M. (1993). Direct and reversible inhibitory effect of the tetrapeptide acetyl-N- Ser-Asp-Lys-Pro (Seraspenide) on the growth of human CD34+ subpopulations in response to growth factors. *Blood* **82**:3307-3314.

Bordier, C. (1981). Phase separation of integral membrane proteins in Triton X-114 solution. *J Biol Chem* **256**:1604-1607.

Borland, G., Murphy, G., and Ager, A. (1999). Tissue inhibitor of metalloproteinases-3 inhibits shedding of L-selectin from leukocytes [In Process Citation]. *J Biol Chem* **274**:2810-2815.

Bosenberg, M. W., Pandiella, A., and Massague, J. (1993). Activated release of membrane-anchored TGF-alpha in the absence of cytosol. *J Cell Biol* **122**:95-101.

Bradford, M. M. (1976). A rapid and sensitive method for the quantitation of microgram quantities of protein utilizing the principle of protein-dye binding. *Anal Biochem* **72**:248-254.

Brakebusch, C., Nophar, Y., Kemper, O., Engelmann, H., and Wallach, D. (1992). Cytoplasmic truncation of the p55 tumour necrosis factor (TNF) receptor abolishes signalling, but not induced shedding of the receptor. *EMBO J* **11**:943-950.

Brakebusch, C., Varfolomeev, E. E., Batkin, M., and Wallach, D. (1994). Structural requirements for inducible shedding of the p55 tumor necrosis factor receptor. *J Biol Chem* **269**:32488-32496.

Brou, C., Logeat, F., Gupta, N., Bessia, C., LeBail, O., Doedens, J. R., Cumano, A., Roux, P., Black, R. A., and Israel, A. (2000). A novel proteolytic cleavage involved in Notch signaling: the role of the disintegrin-metalloprotease TACE. *Mol Cell* **5**:207-216.

Brown, C. L., Meise, K. S., Plowman, G. D., Coffey, R. J., and Dempsey, P. J. (1998). Cell surface ectodomain cleavage of human amphiregulin precursor is sensitive to a metalloprotease inhibitor. Release of a predominant N- glycosylated 43-kDa soluble form. *J Biol Chem* **273**:17258-17268.

Butler, G. S., Will, H., Atkinson, S. J., and Murphy, G. (1997). Membrane-type-2 matrix metalloproteinase can initiate the processing of progelatinase A and is regulated by the tissue inhibitors of metalloproteinases. *Eur J Biochem* **244**:653-657.

Buxbaum, J. D., Liu, K. N., Luo, Y., Slack, J. L., Stocking, K. L., Peschon, J. J., Johnson, R. S., Castner, B. J., Cerretti, D. P., and Black, R. A. (1998). Evidence that tumor necrosis factor alpha converting enzyme is

involved in regulated alpha-secretase cleavage of the alzheimer amyloid protein precursor. *J Biol Chem* **273**:27765-27767.

Cabrera, N., Diaz-Rodriguez, E., Becker, E., Martin-Zanca, D., and Pandiella, A. (1996). TrkA receptor ectodomain cleavage generates a tyrosine-phosphorylated cell-associated fragment. *J Cell Biol* **132**:427-436.

Caporaso, G. L., Gandy, S. E., Buxbaum, J. D., and Greengard, P. (1992). Chloroquine inhibits intracellular degradation but not secretion of Alzheimer beta/A4 amyloid precursor protein. *Proc Natl Acad Sci U S A* **89**:2252-2256.

Carman, C. V., Benovic, J. L. (1998). G-protein-coupled receptors: turn-ons and turn-offs. *Curr Opin Neurobiol* **8**(3):335-44

Caughey, G. H., Raymond, W. W., and Wolters, P. J. (2000). Angiotensin II generation by mast cell alpha- and beta-chymases. *Biochim Biophys Acta* **1480**:245-257.

Chai, S. Y., McKenzie, J. S., McKinley, M. J., and Mendelsohn, F. A. (1990). Angiotensin converting enzyme in the human basal forebrain and midbrain visualized by in vitro autoradiography. *J Comp Neurol* **291**:179-194.

Chandrasekharan, U. M., Sanker, S., Glynias, M. J., Karnik, S. S., and Husain, A. (1996). Angiotensin II-forming activity in a reconstructed ancestral chymase. *Science* **271**:502-505.

Cheng, H. J. and Flanagan, J. G. (1994). Transmembrane kit ligand cleavage does not require a signal in the cytoplasmic domain and occurs at a site dependent on spacing from the membrane. *Mol Biol Cell* **5**:943-953.

Citron, M., Teplow, D. B., and Selkoe, D. J. (1995). Generation of amyloid beta protein from its precursor is sequence specific. *Neuron* **14**:661-670.

Colman, A. (1991). An overview of conventional and novel routes of protein secretion. *Biochem Soc Trans* **19**:249-252.

Condon, T. P., Flournoy, S., Sawyer, G. J., Baker, B. F., Kishimoto, T. K., and Bennett, C. F. (2001). ADAM17 but not ADAM10 mediates tumor necrosis factor-alpha and L- selectin shedding from leukocyte membranes. *Antisense Nucleic Acid Drug Dev* **11**:107-116.

Cornell, M. J., Williams, T. A., Lamango, N. S., Coates, D., Corvol, P., Soubrier, F., Hoheisel, J., Lehrach, H., and Isaac, R. E. (1995). Cloning and expression of an evolutionary conserved single-domain angiotensin converting enzyme from Drosophila melanogaster. *J Biol Chem* **270**:13613-13619.

Corvol, P., Williams, T. A., and Soubrier, F. (1995). Peptidyl dipeptidase A: angiotensin I-converting enzyme. *Methods Enzymol* **248:283-305**:283-305.

Couet, J., Sar, S., Jolivet, A., Hai, M. T., Milgrom, E., and Misrahi, M. (1996). Shedding of human thyrotropin receptor ectodomain. Involvement of a matrix metalloprotease. *J Biol Chem* **271**:4545-4552.

Cuatrecasas, P. and Parikh, I. (1972). Adsorbents for affinity chromatography. Use of N-hydroxysuccinimide esters of agarose. *Biochemistry* **11**:2291-2299.

Cushman, D. W. and Cheung, H. S. (1971). Concentrations of angiotensin-converting enzyme in tissues of the rat. *Biochim Biophys Acta* **250**:261-265.

Dalbey, R. E., Von Heijne G. (1992). Signal peptidases in prokaryotes and eukaryotes--a new protease family. *Trends Biochem Sci* **17**(11):474-478.

Darnell, J. Lodish H. and Baltimore D. (1995). Cell-to-cell Signalling: Hormones and Receptors. *In* "Molecular Cell Biology" pp. 853-921, W.H. Freeman & Co., New York.

De Bernard, S., Misrahi, M., Huet, J. C., Beau, I., Desroches, A., Loosfelt, H., Pichon, C., Pernollet, J. C., and Milgrom, E. (1999). Sequential cleavage and excision of a segment of the thyrotropin receptor ectodomain. *J Biol Chem* **274**:101-107.

De Strooper, B., Craessaerts, K., Van Leuven, F., and Van Den Berghe, H. (1995). Exchanging the extracellular domain of amyloid precursor protein for horseradish peroxidase does not interfere with alpha-secretase cleavage of the beta-amyloid region, but randomizes secretion in Madin-Darby canine kidney cells. *J Biol Chem* **270**:30310-30314.

De Strooper, B., Saftig P., Craessaerts K., Vanderstichele H., Guhde G., Annaert W., Von Figura K., Van Leuven F. (1998). Deficiency of presenilin-1 inhibits the normal cleavage of amyloid precursor protein. *Nature* **391**:387-390.

De Strooper, B., Annaert W., Cupers P., Saftig P., Craessaerts K., Mumm J. S., Schroeter E. H., Schrijvers V., Wolfe M. S., Ray W. J., Goate A., Kopan R. (1999). A presenilin-1-dependent gamma-secretase-like protease mediates release of Notch intracellular domain. *Nature* **398**:518-522.

De Strooper, B. and Konig, G. (1999). Alzheimer's disease. A firm base for drug development. *Nature* **402**:471-472.

De Strooper, B. (2000). Alzheimer's disease. Closing in on gamma-secretase. *Nature* **405**:627-629.

Deddish, P. A., Wang, J., Michel, B., Morris, P. W., Davidson, N. O., Skidgel, R. A., and Erdos, E. G. (1994). Naturally occurring active N-domain of human angiotensin I-converting enzyme. *Proc Natl Acad Sci U S A* **91**:7807-7811.

Deddish, P. A., Jackman, H. L., Skidgel, R. A., and Erdos, E. G. (1997). Differences in the hydrolysis of enkephalin congeners by the two domains of angiotensin converting enzyme. *Biochem Pharmacol* **53**:1459-1463.

Deddish, P. A., Marcic, B., Jackman, H. L., Wang, H. Z., Skidgel, R. A., and Erdos, E. G. (1998). N-domain-specific substrate and C-domain inhibitors of angiotensin- converting enzyme: angiotensin-(1-7) and keto-ACE. *Hypertension* **31**:912-917.

Dempsey, P. J., Meise, K. S., Yoshitake, Y., Nishikawa, K., and Coffey, R. J. (1997). Apical enrichment of human EGF precursor in Madin-Darby canine kidney cells involves preferential basolateral ectodomain cleavage sensitive to a metalloprotease inhibitor. *J Cell Biol* **138**:747-758.

Deng, P., Rettenmier, C. W., and Pattengale, P. K. (1996). Structural requirements for the ectodomain cleavage of human cell surface macrophage colony-stimulating factor. *J Biol Chem* **271**:16338-16343.

Deng, P., Wang, Y. L., Haga, Y., and Pattengale, P. K. (1998). Multiple factors determine the selection of the ectodomain cleavage site of human cell surface macrophage colony-stimulating factor. *Biochemistry* **37**:17898-17904.

Denhardt, D. T. (1996). Signal-transducing protein phosphorylation cascades mediated by Ras/Rho proteins in the mammalian cell: the potential for multiplex signalling. *Biochem J* **318**:729-747.

Depierre, D., Bargetzi, J. P., and Roth, M. (1978). Dipeptidyl carboxypeptidase from human seminal plasma. *Biochim Biophys Acta* **523**:469-476.

Derynck, R., Roberts, A. B., Winkler, M. E., Chen, E. Y., and Goeddel, D. V. (1984). Human transforming growth factor-alpha: precursor structure and expression in E. coli. *Cell* **38**:287-297.

Diaz-Rodriguez, E., Esparis-Ogando, A., Montero, J. C., Yuste, L., and Pandiella, A. (2000). Stimulation of cleavage of membrane proteins by calmodulin inhibitors. *Biochem J* **346 Pt 2**:359-367.

Dickinson, E. S., Dennis, P. A., and Slakey, L. L. (1986). Time course of release into the medium of newly synthesized proteins by cultured aortic endothelial cells. Role of serum in preventing proteolytic degradation. *Arteriosclerosis* **6**:627-637.

Dive, V., Cotton, J., Yiotakis, A., Michaud, A., Vassiliou, S., Jiracek, J., Vazeux, G., Chauvet, M. T., Cuniasse, P., and Corvol, P. (1999). RXP 407, a phosphinic peptide, is a potent inhibitor of angiotensin I converting enzyme able to differentiate between its two active sites. *Proc Natl Acad Sci U S A* **96**:4330-4335.

Dobrinski, I., Ignotz, G. G., Fagnan, M. S., Yudin, S. I., and Ball, B. A. (1997). Isolation and characterization of a protein with homology to angiotensin converting enzyme from the periacrosomal plasma membrane of equine spermatozoa. *Mol Reprod Dev* **48**:251-260.

Dong J, Opresko LK, Dempsey PJ, Lauffenburger DA, Coffey RJ, Wiley HS. (1999). Metalloprotease-mediated ligand release regulates autocrine signaling through the epidermal growth factor receptor. *Proc Natl Acad Sci USA* **96**:6235-6240.

Donoghue, M., Hsieh, F., Baronas, E., Godbout, K., Gosselin, M., Stagliano, N., Donovan, M., Woolf, B., Robison, K., Jeyaseelan, R., Breitbart, R. E., and Acton, S. (2000). A novel angiotensin-converting enzyme-related carboxypeptidase (ACE2) converts angiotensin I to angiotensin 1-9. *Circ Res* **87**:E1-E9.

Dorer, F. E., Kahn, J. R., Lentz, K. E., Levine, M., and Skeggs, L. T. (1974). Hydrolysis of bradykinin by angiotensin-converting enzyme. *Circ Res* **34**:824-827.

Eguchi, S., Dempsey, P. J., Frank, G. D., Motley, E. D., and Inagami, T. (2001). Activation of MAPKs by angiotensin II in vascular smooth muscle cells. Metalloprotease-dependent EGF receptor activation is required for activation of ERK and p38 MAPK but not for JNK. *J Biol Chem* **276**:7957-7962.

Ehlers, M. R. and Riordan, J. F. (1989). Angiotensin-converting enzyme: new concepts concerning its biological role. *Biochemistry* **28**:5311-5318.

Ehlers, M. R. and Riordan, J. F. (1990). Angiotensin-Converting Enzyme, Biochemistry and Molecular Biology. *In* "Hypertension: Pathophysiology, Diagnosis, and Management" (J. H. Laragh and B. M. Brenner, Eds.), pp. 1217-1231, Raven Press, Ltd., NY.

Ehlers, M. R. and Riordan, J. F. (1991). Membrane proteins with soluble counterparts: role of proteolysis in the release of transmembrane proteins. *Biochemistry* **30**:10065-10074.

Ehlers, M. R. and Riordan, J. F. (1991a). Angiotensin-converting enzyme: zinc- and inhibitor-binding stoichiometries of the somatic and testis isozymes. *Biochemistry* **30**:7118-7126.

Ehlers, M. R. and Riordan, J. F. (1991b). Membrane proteins with soluble counterparts: role of proteolysis in the release of transmembrane proteins. *Biochemistry* **30**:10065-10074.

Ehlers, M. R., Maeder, D. L., and Kirsch, R. E. (1986). Rapid affinity chromatographic purification of human lung and kidney angiotensin-converting enzyme with the novel N-carboxyalkyl dipeptide inhibitor N-[1(S)-carboxy-5-aminopentyl]glycylglycine. *Biochim Biophys Acta* **883**:361-372.

Ehlers, M. R., Fox, E. A., Strydom, D. J., and Riordan, J. F. (1989a). Molecular cloning of human testicular angiotensin-converting enzyme: the testis isozyme is identical to the C-terminal half of endothelial angiotensin-converting enzyme. *Proc Natl Acad Sci U S A* **86**:7741-7745.

Ehlers, M. R., Chen, Y. N., and Riordan, J. F. (1991a). Purification and characterization of recombinant human testis angiotensin-converting enzyme expressed in Chinese hamster ovary cells. *Protein Expr Purif* **2**:1-9.

Ehlers, M. R., Chen, Y. N., and Riordan, J. F. (1991b). Spontaneous solubilization of membrane-bound human testis angiotensin- converting enzyme expressed in Chinese hamster ovary cells. *Proc Natl Acad Sci U S A* **88**:1009-1013.

Ehlers, M. R., Chen, Y. N., and Riordan, J. F. (1992). The unique N-terminal sequence of testis angiotensin-converting enzyme is heavily O-glycosylated and unessential for activity or stability. *Biochem Biophys Res Commun* **183**:199-205.

Ehlers, M. R., Scholle, R. R., and Riordan, J. F. (1995). Proteolytic release of human angiotensin-converting enzyme expressed in Chinese hamster ovary cells is enhanced by phorbol ester. *Biochem Biophys Res Commun* **206**:541-547.

Ehlers, M. R., Schwager, S. L., Scholle, R. R., Manji, G. A., Brandt, W. F., and Riordan, J. F. (1996). Proteolytic release of membrane-bound angiotensin-converting enzyme: role of the juxtamembrane stalk sequence. *Biochemistry* **35**:9549-9559.

Eisenberg, D., Marcotte, E. M., Xenarios, I., and Yeates, T. O. (2000). Protein function in the post-genomic era. *Nature* **405**:823-826.

El Dorry, H. A., Bull, H. G., Iwata, K., Thornberry, N. A., Cordes, E. H., and Soffer, R. L. (1982a). Molecular and catalytic properties of rabbit testicular dipeptidyl carboxypeptidase. *J Biol Chem* **257**:14128-14133.

El Dorry, H. A., Pickett, C. B., MacGregor, J. S., and Soffer, R. L. (1982b). Tissue-specific expression of mRNAs for dipeptidyl carboxypeptidase isoenzymes. *Proc Natl Acad Sci U S A* **79**:4295-4297.

El Dorry, H. A., MacGregor, J. S., and Soffer, R. L. (1983). Dipeptidyl carboxypeptidase from seminal fluid resembles the pulmonary rather than the testicular isoenzyme. *Biochem Biophys Res Commun* **115**:1096-1100.

Elenius K, Corfas G, Paul S, Choi CJ, Rio C, Plowman GD, Klagsbrun M. (1997). A novel juxtamembrane domain isoform of HER4/ErbB4. Isoform-specific tissue distribution and differential processing in response to phorbol ester. J Biol Chem. **272**(42):26761-8.

Ellis, S. and Mellor, H. (2000). The novel Rho-family GTPase rif regulates coordinated actin-based membrane rearrangements. *Curr Biol* **10**:1387-1390.

Elwood, P. C., Deutsch, J. C., and Kolhouse, J. F. (1991). The conversion of the human membrane-associated folate binding protein (folate receptor) to the soluble folate binding protein by a membrane- associated metalloprotease. *J Biol Chem* **266**:2346-2353.

Erdos, E. G. (1990). Angiotensin I converting enzyme and the changes in our concepts through the years. Lewis K. Dahl memorial lecture. *Hypertension* **16**:363-370.

Erdos, E. G. and Skidgel, R. A. (1987). The angiotensin I-converting enzyme. *Lab Invest* **56**:345-348.

Esch, F. S., Keim, P. S., Beattie, E. C., Blacher, R. W., Culwell, A. R., Oltersdorf, T., McClure, D., and Ward, P. J. (1990). Cleavage of amyloid beta peptide during constitutive processing of its precursor. *Science* **248**:1122-1124.

Esler, W. P., Kimberly, W. T., Ostaszewski, B. L., Diehl, T. S., Moore, C. L., Tsai, J. Y., Rahmati, T., Xia, W., Selkoe, D. J., and Wolfe, M. S. (2000). Transition-state analogue inhibitors of gamma-secretase bind directly to presenilin-1. *Nat Cell Biol* **2**:428-434.

Esther, C. R., Jr., Thomas, K. E., and Bernstein, K. E. (1994). Chicken lacks the testis specific isozyme of angiotensin converting enzyme found in mammals. *Biochem Biophys Res Commun* **205**:1916-1921.

Esther, C. R., Marino, E. M., Howard, T. E., Machaud, A., Corvol, P., Capecchi, M. R., and Bernstein, K. E. (1997). The critical role of tissue angiotensin-converting enzyme as revealed by gene targeting in mice. *J Clin Invest* **99**:2375-2385.

Eyries, M., Michaud, A., Deinum, J., Agrapart, M., Chomilier, J., Kramers, C., and Soubrier, F. (2001). Increased shedding of angiotensin-converting enzyme by a mutation identified in the stalk region. *J Biol Chem* **276**:5525-5532.

Fagerholm, S., Morrice, N., Gahmberg, C. G., and Cohen, P. (2001). Phosphorylation of the cytoplasmic domain of the integrin CD18 chain by protein kinase C isoforms in leukocytes. *J Biol Chem*.

Fan, H. and Derynck, R. (1999). Ectodomain shedding of TGF-alpha and other transmembrane proteins is induced by receptor tyrosine kinase activation and MAP kinase signaling cascades. *EMBO J* **18**:6962-6972.

Feehan, C., Darlak, K., Kahn, J., Walcheck, B., Spatola, A. F., and Kishimoto, T. K. (1996). Shedding of the lymphocyte L-selectin adhesion molecule is inhibited by a hydroxamic acid-based protease inhibitor. Identification with an L- selectin-alkaline phosphatase reporter. *J Biol Chem* **271**:7019-7024.

Ferreira, S. H. and Rocha e Silva (1965). Potentiation of bradykinin and eledoisin by BPF (bradykinin potentiating factor) from Bothrops jararaca venom. *Experientia* **21**:347-349.

Ferreira, S. H., Bartelt, D. C., and Greene, L. J. (1970a). Isolation of bradykinin-potentiating peptides from Bothrops jararaca venom. *Biochemistry* **9**:2583-2593.

Ferreira, S. H., Greene, L. H., Alabaster, V. A., Bakhle, Y. S., and Vane, J. R. (1970b). Activity of various fractions of bradykinin potentiating factor against angiotensin I converting enzyme. *Nature* **225**:379-380.

Fischer, M., Goldschmitt, J., Peschel, C., Brakenhoff, J. P., Kallen, K. J., Wollmer, A., Grotzinger, J., and Rose-John, S. (1997). I. A bioactive designer cytokine for human hematopoietic progenitor cell expansion. *Nat Biotechnol* **15**:142-145.

Fitzgerald, M. L., Wang, Z., Park, P. W., Murphy, G., and Bernfield, M. (2000). Shedding of syndecan-1 and -4 ectodomains is regulated by multiple signaling pathways and mediated by a TIMP-3-sensitive metalloproteinase. *J Cell Biol* **148**:811-824.

Foresta, C., Mioni, R., Rossato, M., Varotto, A., and Zorzi, M. (1991). Evidence for the involvement of sperm angiotensin converting enzyme in fertilization. *Int J Androl* **14**:333-339.

Garton, K. J., Gough, P. J., Blobel, C. P., Murphy, G., Greaves, D. R., Dempsey, P. J., and Raines, E. W. (2001). Tumor necrosis factor-alpha-converting enzyme (ADAM17) mediates the cleavage and shedding of fractalkine (CX3CL1). *J Biol Chem* **276**:37993-38001.

Gearing, A. J., Beckett, P., Christodoulou, M., Churchill, M., Clements, J., Davidson, A. H., Drummond, A. H., Galloway, W. A., Gilbert, R., and Gordon, J. L. (1994). Processing of tumour necrosis factor-alpha precursor by metalloproteinases. *Nature* **370**:555-557.

Gebbink M. F., Zondag G. C., Koningstein G. M., Feiken E., Wubbolts R. W., Moolenaar W. H. (1995). Cell surface expression of receptor protein tyrosine phosphatase RPTP mu is regulated by cell-cell contact. *J Cell Biol* **131**(1):251-260.

Gechtman, Z., Alonso, J. L., Raab, G., Ingber, D. E., and Klagsbrun, M. (1999). The shedding of membrane-anchored heparin-binding epidermal-like growth factor is regulated by the Raf/mitogen-activated protein kinase cascade and by cell adhesion and spreading. *J Biol Chem* **274**:28828-28835.

Glenner, G. G. and Wong, C. W. (1984). Alzheimer's disease: initial report of the purification and characterization of a novel cerebrovascular amyloid protein. *Biochem Biophys Res Commun* **120**:885-890.

Goishi, K., Higashiyama, S., Klagsbrun, M., Nakano, N., Umata, T., Ishikawa, M., Mekada, E., and Taniguchi, N. (1995). Phorbol ester induces the rapid processing of cell surface heparin- binding EGF-like growth factor: conversion from juxtacrine to paracrine growth factor activity. *Mol Biol Cell* **6**:967-980.

Gomez, D. E., Alonso, D. F., Yoshiji, H., and Thorgeirsson, U. P. (1997). Tissue inhibitors of metalloproteinases: structure, regulation and biological functions. *Eur J Cell Biol* **74**:111-122.

Gronhagen-Riska, C. and Fyhrquist, F. (1980). Purification of human lung angiotensin-converting enzyme. *Scand J Clin Lab Invest* **40**:711-719.

Gronhagen-Riska, C., Fyhrquist, F., Valimaki, M., and Lamberg, B. A. (1985). Thyroid hormones affect serum angiotensin I converting enzyme levels. *Acta Med Scand* **217**:259-264.

Gross E. Methods Enzymol. 11, 238-255. 1967.

Guan, R., Zhang, Y., Jiang, J., Baumann, C. A., Black, R. A., Baumann, G., and Frank, S. J. (2001). Phorbol ester- and growth factor-induced growth hormone (GH) receptor proteolysis and GH-binding protein shedding: relationship to GH receptor down-regulation. *Endocrinology* **142**:1137-1147.

Gutwein, P., Oleszewski, M., Mechtersheimer, S., Agmon-Levin, N., Krauss, K., and Altevogt, P. (2000). Role of Src kinases in the ADAM-mediated release of L1 adhesion molecule from human tumor cells. *J Biol Chem* **275**:15490-15497.

Haass, C. and Selkoe, D. J. (1993). Cellular processing of beta-amyloid precursor protein and the genesis of amyloid beta-peptide. *Cell* **75**:1039-1042.

Haass, C. and Selkoe, D. J. (1998). Alzheimer's disease. A technical KO of amyloid-beta peptide [news; comment]. *Nature* **391**:339-340.

Haass, C., Koo, E. H., Mellon, A., Hung, A. Y., and Selkoe, D. J. (1992). Targeting of cell-surface beta-amyloid precursor protein to lysosomes: alternative processing into amyloid-bearing fragments. *Nature* **357**:500-503.

Haass, C., Koo, E. H., Teplow, D. B., and Selkoe, D. J. (1994). Polarized secretion of beta-amyloid precursor protein and amyloid beta- peptide in MDCK cells. *Proc Natl Acad Sci U S A* **91**:1564-1568.

Hagaman, J. R., Moyer, J. S., Bachman, E. S., Sibony, M., Magyar, P. L., Welch, J. E., Smithies, O., Krege, J. H., and O'Brien, D. A. (1998). Angiotensin-converting enzyme and male fertility. *Proc Natl Acad Sci U S A* **95**:2552-2557.

Hamm, H. E. (2001). How activated receptors couple to G proteins. *Proc Natl Acad Sci U S A* **98**: 4819-4821.

Hampe, W., Riedel, I. B., Lintzel, J., Bader, C. O., Franke, I., and Schaller, H. C. (2000). Ectodomain shedding, translocation and synthesis of SorLA are stimulated by its ligand head activator. *J Cell Sci* **113 Pt 24**:4475-4485.

Hansen, H. P., Dietrich, S., Kisseleva, T., Mokros, T., Mentlein, R., Lange, H. H., Murphy, G., and Lemke, H. (2000). CD30 shedding from Karpas 299 lymphoma cells is mediated by TNF-alpha- converting enzyme. *J Immunol* **165**:6703-6709.

Hardy, J. (1997). The Alzheimer family of diseases: many etiologies, one pathogenesis? [comment]. *Proc Natl Acad Sci U S A* **94**:2095-2097.

Hattori, M., Osterfield, M., and Flanagan, J. G. (2000). Regulated cleavage of a contact-mediated axon repellent. *Science* **289**:1360-1365.

Helmer, O. M. (1957). Differentiation between different forms of angiotonin by means of spirally cut strips of of rabbit aorta. *Am J Physiol* **188**:571-577.

Hempstead, B. L., Patil, N., Thiel, B., and Chao, M. V. (1990). Deletion of cytoplasmic sequences of the nerve growth factor receptor leads to loss of high affinity ligand binding. *J Biol Chem* **265**:9595-9598.

Henkel, T., Machleidt, T., Alkalay, I., Kronke, M., Ben-Neriah, Y., and Baeuerle, P. A. (1993). Rapid proteolysis of I kappa B-alpha is necessary for activation of transcription factor NF-kappa B. *Nature* **365**:182-185.

Himmler A, Maurer-Fogy I, Kronke M, Scheurich P, Pfizenmaier K, Lantz M, Olsson I, Hauptmann R, Stratowa C, Adolf GR. (1990).Molecular cloning and expression of human and rat tumor necrosis factor receptor chain (p60) and its soluble derivative, tumor necrosis factor-binding protein. *DNA Cell Biol.* **9**(10):705-15.

Hino, T., Nakamura, H., Abe, S., Saito, H., Inage, M., Terashita, K., Kato, S., and Tomoike, H. (1999). Hydrogen peroxide enhances shedding of type I soluble tumor necrosis factor receptor from pulmonary epithelial cells. *Am J Respir Cell Mol Biol* **20**:122-128.

Holmes, W. E., Sliwkowski, M. X., Akita, R. W., Henzel, W. J., Lee, J., Park, J. W., Yansura, D., Abadi, N., Raab, H., and Lewis, G. D. (1992). Identification of heregulin, a specific activator of p185erbB2. *Science* **256**:1205-1210.

Holmquist, B., Bunning, P., and Riordan, J. F. (1979). A continuous spectrophotometric assay for angiotensin converting enzyme. *Anal Biochem* **95**:540-548.

Holsinger, L. J., Graef, I. A., Swat, W., Chi, T., Bautista, D. M., Davidson, L., Lewis, R. S., Alt, F. W., and Crabtree, G. R. (1998). Defects in actin-cap formation in Vav-deficient mice implicate an actin requirement for lymphocyte signal transduction. *Curr Biol* **8**:563-572.

Hooper, N. M. (1991a). Angiotensin converting enzyme: implications from molecular biology for its physiological functions. *Int J Biochem* **23**:641-647.

Hooper, N. M. (1994). Families of zinc metalloproteases. *FEBS Lett* **354**:1-6.

Hooper, N. M. and Turner, A. J. (1987). Isolation of two differentially glycosylated forms of peptidyl- dipeptidase A (angiotensin converting enzyme) from pig brain: a re- evaluation of their role in neuropeptide metabolism. *Biochem J* **241**:625-633.

Hooper, N. M. and Turner, A. J. (1989). Ectoenzymes of the kidney microvillar membrane. Isolation and characterization of the amphipathic form of renal dipeptidase and hydrolysis of its glycosyl-phosphatidylinositol anchor by an activity in plasma. *Biochem J* **261**:811-818.

Hooper, N. M., Keen, J., Pappin, D. J., and Turner, A. J. (1987). Pig kidney angiotensin converting enzyme. Purification and characterization of amphipathic and hydrophilic forms of the enzyme establishes C-terminal anchorage to the plasma membrane. *Biochem J* **247**:85-93.

Hooper, N. M., Karran, E. H., and Turner, A. J. (1997a). Membrane protein secretases. *Biochem J* **321 (Pt 2)**:265-279.

Howard, L., Nelson, K. K., Maciewicz, R. A., and Blobel, C. P. (1999). Interaction of the metalloprotease disintegrins MDC9 and MDC15 with two SH3 domain-containing proteins, endophilin I and SH3PX1. *J Biol Chem* **274**:31693-31699.

Hsiao, K. K., Borchelt, D. R., Olson, K., Johannsdottir, R., Kitt, C., Yunis, W., Xu, S., Eckman, C., Younkin, S., Price, D., and . (1995). Age-related CNS disorder and early death in transgenic FVB/N mice overexpressing Alzheimer amyloid precursor proteins. *Neuron* **15**:1203-1218.

Hu, J., Miyatake, F., Aizu, Y., Nakagawa, H., Nakamura, S., Tamaoka, A., Takahash, R., Urakami, K., and Shoji, M. (1999). Angiotensin-converting enzyme genotype is associated with Alzheimer disease in the Japanese population. *Neurosci Lett* **277**:65-67.

Hu, J., Igarashi, A., Kamata, M., and Nakagawa, H. (2001). Angiotensin-converting enzyme degrades Alzheimer amyloid {beta}-peptide (A{beta}), retards A{beta} aggregation, deposition, fibril formation and inhibits cytotoxicity. *J Biol Chem*.

Huang, E., Nocka, K., Beier, D. R., Chu, T. Y., Buck, J., Lahm, H. W., Wellner, D., Leder, P., and Besmer, P. (1990). The hematopoietic growth factor KL is encoded by the Sl locus and is the ligand of the c-kit receptor, the gene product of the W locus. *Cell* **63**:225-233.

Hubert, C., Houot A. M., Corvol P., Soubrier F. (1991). Structure of the angiotensin I-converting enzyme gene. Two alternate promoters correspond to evolutionary steps of a duplicated gene. *J Biol Chem* **266**(23):15377-15383

Hunter, A. J., Shimizu, Y.. (1997). Alpha 4 beta 1 integrin-mediated tyrosine phosphorylation in human T cells: characterization of Crk- and Fyn-associated substrates (pp105, pp115, and human enhancer of filamentation-1) and integrin-dependent activation of p59fyn1. *J Immunol* **159**(10):4806-4814.

Hussain, I., Powell, D., Howlett, D. R., Tew, D. G., Meek, T. D., Chapman, C., Gloger, I. S., Murphy, K. E., Southan, C. D., Ryan, D. M., Smith, T. S., Simmons, D. L., Walsh, F. S., Dingwall, C., and Christie, G. (1999). Identification of a novel aspartic protease (Asp 2) as beta-secretase. *Mol Cell Neurosci* **14**:419-427.

IHGSC (International Human Genome Sequencing Consortium). (2001). Initial sequencing and analysis of the human genome. *Nature* **409**, 860-921.

Inagami, T. (1994). The renin-angiotensin system. *Essays Biochem* **28**:147-164.

Ivetic, A., Deka, J., Ridley, A., and Ager, A. (2001). The cytoplasmic tail of L-selectin interacts with members of the ezrin- radixin-moesin (ERM) family of proteins: Activation dependent binding of moesin but not ezrin. *J Biol Chem.*

Iwata, K., Lai, C. Y., El Dorry, H. A., and Soffer, R. L. (1982). The NH2- and COOH-terminal sequences of the angiotensin-converting enzyme isozymes from rabbit lung and testis. *Biochem Biophys Res Commun* **107**:1097-1103.

Izumi, Y., Hirata, M., Hasuwa, H., Iwamoto, R., Umata, T., Miyado, K., Tamai, Y., Kurisaki, T., Sehara-Fujisawa, A., Ohno, S., and Mekada, E. (1998). A metalloprotease-disintegrin, MDC9/meltrin-gamma/ADAM9 and PKCdelta are involved in TPA-induced ectodomain shedding of membrane-anchored heparin-binding EGF-like growth factor. *EMBO J* **17**:7260-7272.

Jaspard, E., Wei, L., and Alhenc-Gelas, F. (1993). Differences in the properties and enzymatic specificities of the two active sites of angiotensin I-converting enzyme (kininase II). Studies with bradykinin and other natural peptides. *J Biol Chem* **268**:9496-9503.

Jiao, H., Cui, X. L., Torti, M., Chang, C. H., Alexander, L. D., Lapetina, E. G., Douglas, J. G. (1998). Arachidonic acid mediates angiotensin II effects on p21ras in renal proximal tubular cells via the tyrosine kinase-Shc-Grb2-Sos pathway. *Proc Natl Acad Sci USA* **95**(13):7417-7421.

Johnston, C. I. (2000). Angiotensin II type 1 receptor blockade: a novel therapeutic concept. *Blood Press Suppl* **1**:9-13.

Jones, S. A., Novick, D., Horiuchi, S., Yamamoto, N., Szalai, A. J., and Fuller, G. M. (1999). C-reactive protein: a physiological activator of interleukin 6 receptor shedding. *J Exp Med* **189**:599-604.

Junot, C., Gonzales, M. F., Ezan, E., Cotton, J., Vazeux, G., Michaud, A., Azizi, M., Vassiliou, S., Yiotakis, A., Corvol, P., and Dive, V. (2001). RXP 407, a selective inhibitor of the N-domain of angiotensin I- converting enzyme, blocks in vivo the degradation of hemoregulatory peptide acetyl-Ser-Asp-Lys-Pro with no effect on angiotensin I hydrolysis. *J Pharmacol Exp Ther* **297**:606-611.

Kahn, J., Ingraham, R. H., Shirley, F., Migaki, G. I., and Kishimoto, T. K. (1994). Membrane proximal cleavage of L-selectin: identification of the cleavage site and a 6-kD transmembrane peptide fragment of L-selectin. *J Cell Biol* **125**:461-470.

Kahn, J., Walcheck, B., Migaki, G. I., Jutila, M. A., and Kishimoto, T. K. (1998). Calmodulin regulates L-selectin adhesion molecule expression and function through a protease-dependent mechanism. *Cell* **92**:809-818.

Kajita, M., Itoh, Y., Chiba, T., Mori, H., Okada, A., Kinoh, H., and Seiki, M. (2001). Membrane-type 1 matrix metalloproteinase cleaves CD44 and promotes cell migration. *J Cell Biol* **153**:893-904.

Kamata, M., Hu, J., Shibahara, H., and Nakagawa, H. (2001). Assay of testicular angiotensin-converting enzyme activity in human spermatozoa. *Int J Androl* **24**:225-231.

Kang, J., Lemaire, H. G., Unterbeck, A., Salbaum, J. M., Masters, C. L., Grzeschik, K. H., Multhaup, G., Beyreuther, K., and Muller-Hill, B. (1987). The precursor of Alzheimer's disease amyloid A4 protein resembles a cell-surface receptor. *Nature* **325**:733-736.

Kansas, G. S., Ley, K., Munro, J. M., and Tedder, T. F. (1993). Regulation of leukocyte rolling and adhesion to high endothelial venules through the cytoplasmic domain of L-selectin. *J Exp Med* **177**:833-838.

Katayama, T., Imaizumi, K., Sato, N., Miyoshi, K., Kudo, T., Hitomi, J., Morihara, T., Yoneda, T., Gomi, F., Mori, Y., Nakano, Y., Takeda, J., Tsuda, T., Itoyama, Y., Murayama, O., Takashima, A., George-Hyslop, P., Takeda, M., and Tohyama, M. (1999). Presenilin-1 mutations downregulate the signalling pathway of the unfolded-protein response. *Nat Cell Biol* **1**:479-485.

Kawano, Y., Okamoto, I., Murakami, D., Itoh, H., Yoshida, M., Ueda, S., and Saya, H. (2000). Ras oncoprotein induces CD44 cleavage through phosphoinositide 3-OH kinase and the rho family of small G proteins. *J Biol Chem* **275**:29628-29635.

Kawaoka, Y. and Webster, R. G. (1989). Interplay between carbohydrate in the stalk and the length of the connecting peptide determines the cleavability of influenza virus hemagglutinin. *J Virol* **63**:3296-3300.

Keenan, R. J., Freymann D. M., Stroud R. M., Walter P. (2001). The signal recognition particle. *Annu Rev Biochem* **70**:755-75

Kendrew, J. and others (1995). "Encyclopedia of Molecular Biology," Blackwell Science Ltd, UK.

Kessler, S. P., Rowe, T. M., Blendy, J. A., Erickson, R. P., and Sen, G. C. (1998). A cyclic AMP response element in the angiotensin-converting enzyme gene and the transcription factor CREM are required for transcription of the mRNA for the testicular isozyme. *J Biol Chem* **273**:9971-9975.

Kessler, S. P., Rowe, T. M., Gomos, J. B., Kessler, P. M., and Sen, G. C. (2000). Physiological non-equivalence of the two isoforms of angiotensin- converting enzyme. *J Biol Chem* **275**:26259-26264.

Kim, H. S., Krege, J. H., Kluckman, K. D., Hagaman, J. R., Hodgin, J. B., Best, C. F., Jennette, J. C., Coffman, T. M., Maeda, N., and Smithies, O. (1995). Genetic control of blood pressure and the angiotensinogen locus. *Proc Natl Acad Sci U S A* **92**:2735-2739.

Kimberly, W. T., Zheng, J. B., Guenette, S. Y., and Selkoe, D. J. (2001). The Intracellular Domain of the beta - Amyloid Precursor Protein Is Stabilized by Fe65 and Translocates to the Nucleus in a Notch-like Manner. *J Biol Chem* **276**:40288-40292.

Kitazume, S., Tachida, Y., Oka, R., Shirotani, K., Saido, T. C., and Hashimoto, Y. (2001). Alzheimer's beta - secretase, beta -site amyloid precursor protein- cleaving enzyme, is responsible for cleavage secretion of a Golgi- resident sialyltransferase. *Proc Natl Acad Sci U S A*.

Kochanek, K. D., Smith, B. L., and Anderson, R. N. Deaths: Preliminary Data for 1999. National Vital Statistics Reports 49[3], 1-6. 2001. CDC.

Kohn, F. M., Dammshauser, I., Neukamm, C., Renneberg, H., Siems, W. E., Schill, W. B., and Aumuller, G. (1998). Ultrastructural localization of angiotensin-converting enzyme in ejaculated human spermatozoa. *Hum Reprod* **13**:604-610.

Kokubu, T. (1978). [Purification and properties of angiotensin I-converting enzyme (ACE) in human lung and its role on the metabolic regulation of vasoactive peptides in pulmonary circulation (author's transl)]. *Nihon Kyobu Shikkan Gakkai Zasshi* **16**:390-396.

Kozarsky, K., Kingsley, D., and Krieger, M. (1988). Use of a mutant cell line to study the kinetics and function of O-linked glycosylation of low density lipoprotein receptors. *Proc Natl Acad Sci U S A* **85**:4335-4339.

Kratzschmar, J., Lum, L., and Blobel, C. P. (1996). Metargidin, a membrane-anchored metalloprotease-disintegrin protein with an RGD integrin binding sequence. *J Biol Chem* **271**:4593-4596.

Krege, J. H., John, S. W., Langenbach, L. L., Hodgin, J. B., Hagaman, J. R., Bachman, E. S., Jennette, J. C., O'Brien, D. A., and Smithies, O. (1995). Male-female differences in fertility and blood pressure in ACE-deficient mice. *Nature* **375**:146-148.

Kriegler, M., Perez, C., DeFay, K., Albert, I., and Lu, S. D. (1988). A novel form of TNF/cachectin is a cell surface cytotoxic transmembrane protein: ramifications for the complex physiology of TNF. *Cell* **53**:45-53.

Kuster, B., Wheeler S. F., Hunter A. P., Dwek R. A., Harvey D. J. (1997) Sequencing of N-linked oligosaccharides directly from protein gels: in-gel deglycosylation followed by matrix-assisted laser desorption/ionization mass spectrometry and normal-phase high-performance liquid chromatography. *Anal Biochem* **250**(1):82-101.

Lamango, N. and Isaac, R. E. (1993). Identification of an ACE-like peptidyl dipeptidase activity in the housefly, Musca domestica. *Biochem Soc Trans* **21 (Pt 3)**:245S.

Lammich, S., Kojro, E., Postina, R., Gilbert, S., Pfeiffer, R., Jasionowski, M., Haass, C., and Fahrenholz, F. (1999). Constitutive and regulated alpha-secretase cleavage of Alzheimer's amyloid precursor protein by a disintegrin metalloprotease. *Proc Natl Acad Sci U S A* **96**:3922-3927.

Lander, E. S., *et al.*, (2001). Initial sequencing and analysis of the human genome. *Nature* **409**:860-921.

Langford, K. G., Shai, S. Y., Howard, T. E., Kovac, M. J., Overbeek, P. A., and Bernstein, K. E. (1991). Transgenic mice demonstrate a testis-specific promoter for angiotensin- converting enzyme. *J Biol Chem* **266**:15559-15562.

Langford, K. G., Zhou, Y., Russell, L. D., Wilcox, J. N., and Bernstein, K. E. (1993). Regulated expression of testis angiotensin-converting enzyme during spermatogenesis in mice. *Biol Reprod* **48**:1210-1218.

Lanzillo, J. J. and Fanburg, B. L. (1977). Angiotensin I converting enzyme from human plasma. *Biochemistry* **16**:5491-5495.

Lanzillo, J. J., Stevens, J., Dasarathy, Y., Yotsumoto, H., and Fanburg, B. L. (1985). Angiotensin-converting enzyme from human tissues. Physicochemical, catalytic, and immunological properties. *J Biol Chem* **260**:14938-14944.

Lattion, A. L., Soubrier, F., Allegrini, J., Hubert, C., Corvol, P., and Alhenc-Gelas, F. (1989). The testicular transcript of the angiotensin I-converting enzyme encodes for the ancestral, non-duplicated form of the enzyme. *FEBS Lett* **252**:99-104.

LeBel, D., Grondin G., Cook S., Hooper N. M. (1998). Membrane dipeptidase in the pig exocrine pancreas. Ultrastructural localization and secretion. *J Histochem Cytochem* **46**(7):841-6

Le Bivic, A., Sambuy, Y., Patzak, A., Patil, N., Chao, M., and Rodriguez-Boulan, E. (1991). An internal deletion in the cytoplasmic tail reverses the apical localization of human NGF receptor in transfected MDCK cells. *J Cell Biol* **115**:607-618.

Lenfant, M., Wdzieczak-Bakala, J., Guittet, E., Prome, J. C., Sotty, D., and Frindel, E. (1989). Inhibitor of hematopoietic pluripotent stem cell proliferation: purification and determination of its structure. *Proc Natl Acad Sci U S A* **86**:779-782.

Levitan, D., Lee, J., Song, L., Manning, R., Wong, G., Parker, E., and Zhang, L. (2001). PS1 N- and C-terminal fragments form a complex that functions in APP processing and Notch signaling. *Proc Natl Acad Sci U S A* **98**:12186-12190.

Li, Y. M., Xu, M., Lai, M. T., Huang, Q., Castro, J. L., DiMuzio-Mower, J., Harrison, T., Lellis, C., Nadin, A., Neduvelil, J. G., Register, R. B., Sardana, M. K., Shearman, M. S., Smith, A. L., Shi, X. P., Yin, K. C., Shafer, J. A., and Gardell, S. J. (2000). Photoactivated gamma-secretase inhibitors directed to the active site covalently label presenilin 1. *Nature* **405**:689-694.

Lightman, A., Tarlatzis, B. C., Rzasa, P. J., Culler, M. D., Caride, V. J., Negro-Vilar, A. F., Lennard, D., DeCherney, A. H., and Naftolin, F. (1987). The ovarian renin-angiotensin system: renin-like activity and angiotensin II/III immunoreactivity in gonadotropin-stimulated and unstimulated human follicular fluid. *Am J Obstet Gynecol* **156**:808-816.

Liu, X., Fernandez, M., Wouters, M. A., Heyberger, S., and Husain, A. (2001). Arg(1098) is critical for the chloride dependence of human angiotensin I-converting enzyme C-domain catalytic activity. *J Biol Chem* **276**:33518-33525.

Livneh, E., Benveniste, M., Prywes, R., Felder, S., Kam, Z., and Schlessinger, J. (1986a). Large deletions in the cytoplasmic kinase domain of the epidermal growth factor receptor do not affect its laternal mobility. *J Cell Biol* **103**:327-331.

Livneh, E., Prywes, R., Kashles, O., Reiss, N., Sasson, I., Mory, Y., Ullrich, A., and Schlessinger, J. (1986b). Reconstitution of human epidermal growth factor receptors and its deletion mutants in cultured hamster cells. *J Biol Chem* **261**:12490-12497.

Lum, L., Wong, B. R., Josien, R., Becherer, J. D., Erdjument-Bromage, H., Schlondorff, J., Tempst, P., Choi, Y., and Blobel, C. P. (1999). Evidence for a role of a tumor necrosis factor-alpha (TNF-alpha)- converting enzyme-like protease in shedding of TRANCE, a TNF family member involved in osteoclastogenesis and dendritic cell survival. *J Biol Chem* **274**:13613-13618.

Madge, L. A., Sierra-Honigmann, M. R., and Pober, J. S. (1999). Apoptosis-inducing agents cause rapid shedding of tumor necrosis factor receptor 1 (TNFR1). A nonpharmacological explanation for inhibition of TNF-mediated activation. *J Biol Chem* **274**:13643-13649.

Marcic, B., Deddish, P. A., Jackman, H. L., Erdos, E. G., and Tan, F. (2000a). Effects of the N-terminal sequence of ACE on the properties of its C- domain. *Hypertension* **36**:116-121.

Marcic, B., Deddish, P. A., Skidgel, R. A., Erdos, E. G., Minshall, R. D., and Tan, F. (2000b). Replacement of the transmembrane anchor in angiotensin I-converting enzyme (ACE) with a glycosylphosphatidylinositol tail affects activation of the B2 bradykinin receptor by ACE inhibitors. *J Biol Chem* **275**:16110-16118.

Marieb, E. N. (1995). "Human Anatomy and Physiology," The Benjamin/Cummings Publishing Company, Inc., NY.

Marron M. B., Hughes D. P., McCarthy M. J., Beaumont E. R., Brindle N. P. (2000). Tie-1 receptor tyrosine kinase endodomain interaction with SHP2: potential signalling mechanisms and roles in angiogenesis. *Adv Exp Med Biol* **476**:35-46.

Maruyama K, Terakado K, Usami M, Yoshikawa K. (1990). Formation of amyloid-like fibrils in COS cells overexpressing part of the Alzheimer amyloid protein precursor. Nature **347**(6293):566-9.

Maruyama, K., Kametani, F., Usami, M., Yamao-Harigaya, W., and Tanaka, K. (1991). "Secretase," Alzheimer amyloid protein precursor secreting enzyme is not sequence-specific. *Biochem Biophys Res Commun* **179**:1670-1676.

Maskos, K., Fernandez-Catalan, C., Huber, R., Bourenkov, G. P., Bartunik, H., Ellestad, G. A., Reddy, P., Wolfson, M. F., Rauch, C. T., Castner, B. J., Davis, R., Clarke, H. R., Petersen, M., Fitzner, J. N., Cerretti, D. P., March, C. J., Paxton, R. J., Black, R. A., and Bode, W. (1998). Crystal structure of the catalytic domain of human tumor necrosis factor-alpha-converting enzyme. *Proc Natl Acad Sci U S A* **95**:3408-3412.

Massague, J. and Pandiella, A. (1993). Membrane-anchored growth factors. *Annu Rev Biochem* **62**:515-541.

Masters, C. L., Simms, G., Weinman, N. A., Multhaup, G., McDonald, B. L., and Beyreuther, K. (1985). Amyloid plaque core protein in Alzheimer disease and Down syndrome. *Proc Natl Acad Sci U S A* **82**:4245-4249.

Matala, E., Alexander, S. R., Kishimoto, T. K., and Walcheck, B. (2001). The cytoplasmic domain of L-selectin participates in regulating L- selectin endoproteolysis. *J Immunol* **167**:1617-1623.

Matsuo, S., Caldwell, P. R., Brentjens, J. R., and Andres, G. (1985). In vivo interaction of antibodies with cell surface antigens. A mechanism responsible for in situ formation of immune deposits in the zona pellucida of rabbit oocytes. *J Clin Invest* **75**:1369-1380.

Mattei, M. G., Roeckel, N., Olsen, B. R., and Apte, S. S. (1997). Genes of the membrane-type matrix metalloproteinase (MT-MMP) gene family, MMP14, MMP15, and MMP16, localize to human chromosomes 14, 16, and 8, respectively. *Genomics* **40**:168-169.

McDermott, M. F., Aksentijevich, I., Galon, J., McDermott, E. M., Ogunkolade, B. W., Centola, M., Mansfield, E., Gadina, M., Karenko, L., Pettersson, T., McCarthy, J., Frucht, D. M., Aringer, M., Torosyan, Y., Teppo, A. M., Wilson, M., Karaarslan, H. M., Wan, Y., Todd, I., Wood, G., Schlimgen, R., Kumarajeewa, T. R., Cooper, S. M., Vella, J. P., Kastner, D. L., and . (1999). Germline mutations in the extracellular domains of the 55 kDa TNF receptor, TNFR1, define a family of dominantly inherited autoinflammatory syndromes. *Cell* **97**:133-144.

McDonald, M. P., Dahl, E. E., Overmier, J. B., Mantyh, P., and Cleary, J. (1994). Effects of an exogenous beta-amyloid peptide on retention for spatial learning. *Behav Neural Biol* **62**:60-67.

McGeehan, G. M., Becherer, J. D., Bast, R. C., Jr., Boyer, C. M., Champion, B., Connolly, K. M., Conway, J. G., Furdon, P., Karp, S., Kidao, S., and . (1994). Regulation of tumour necrosis factor-alpha processing by a metalloproteinase inhibitor. *Nature* **370**:558-561.

Mechtersheimer S, Gutwein P, Agmon-Levin N, Stoeck A, Oleszewski M, Riedle S, Fogel M, Lemmon V, Altevogt P. (2001). Ectodomain shedding of L1 adhesion molecule promotes cell migration by autocrine binding to integrins. J Cell Biol. **155**(4):661-74.

Mendelsohn, F. A., Lloyd, C. J., Kachel, C., and Funder, J. W. (1982). Induction by glucocorticoids of angiotensin converting enzyme production from bovine endothelial cells in culture and rat lung in vivo. *J Clin Invest* **70**:684-692.

Merlos-Suarez, A., Fernandez-Larrea, J., Reddy, P., Baselga, J., and Arribas, J. (1998). Pro-tumor necrosis factor-alpha processing activity is tightly controlled by a component that does not affect notch processing. *J Biol Chem* **273**:24955-24962.

Merlos-Suarez, A., Ruiz-Paz, S., Baselga, J., and Arribas, J. (2001). Metalloprotease-dependent proTGF-{alpha} ectodomain shedding in the absence of TACE. *J Biol Chem* **epub ahead of print**.

Meziane, H., Dodart, J. C., Mathis, C., Little, S., Clemens, J., Paul, S. M., and Ungerer, A. (1998). Memory-enhancing effects of secreted forms of the beta-amyloid precursor protein in normal and amnestic mice. *Proc Natl Acad Sci U S A* **95**:12683-12688.

Middelhoven, P. J., Ager A., Roos D., Verhoeven A. J. (1997). Involvement of a metalloprotease in the shedding of human neutrophil Fc gammaRIIIB. *FEBS Lett* **414**(1):14-18

Michalski, J. C., Wieruszeski J. M., Alonso C., Cache P., Montreuil J., Strecker G. (1991). Characterization and 400-MHz 1H-NMR analysis of urinary fucosyl glycoasparagines in fucosidosis. *Eur J Biochem* **201**(2):439-458.

Migaki GI, Kahn J, Kishimoto TK. (1995). Mutational analysis of the membrane-proximal cleavage site of L-selectin: relaxed sequence specificity surrounding the cleavage site. J Exp Med. **182**(2):549-57.

Mohler, K. M., Sleath, P. R., Fitzner, J. N., Cerretti, D. P., Alderson, M., Kerwar, S. S., Torrance, D. S., Otten-Evans, C., Greenstreet, T., Weerawarna, K., and . (1994). Protection against a lethal dose of endotoxin by an inhibitor of tumour necrosis factor processing. *Nature* **370**:218-220.

Montero, J. C., Yuste, L., Diaz-Rodriguez, E., Esparis-Ogando, A., and Pandiella, A. (2000). Differential shedding of transmembrane neuregulin isoforms by the tumor necrosis factor-alpha-converting enzyme. *Mol Cell Neurosci* **16**:631-648.

Moore, P. A., Belvedere, O., Orr, A., Pieri, K., LaFleur, D. W., Feng, P., Soppet, D., Charters, M., Gentz, R., Parmelee, D., Li, Y., Galperina, O., Giri, J., Roschke, V., Nardelli, B., Carrell, J., Sosnovtseva, S., Greenfield, W., Ruben, S. M., Olsen, H. S., Fikes, J., and Hilbert, D. M. (1999). BLyS: member of the tumor necrosis factor family and B lymphocyte stimulator. *Science* **285**:260-263.

Moss, M. L., Jin, S. L., Milla, M. E., Bickett, D. M., Burkhart, W., Carter, H. L., Chen, W. J., Clay, W. C., Didsbury, J. R., Hassler, D., Hoffman, C. R., Kost, T. A., Lambert, M. H., Leesnitzer, M. A., McCauley, P., McGeehan, G., Mitchell, J., Moyer, M., Pahel, G., Rocque, W., Overton, L. K., Schoenen, F., Seaton, T., Su, J. L., Becherer, J. D., and . (1997). Cloning of a disintegrin metalloproteinase that processes precursor tumour-necrosis factor-alpha. *Nature* **385**:733-736.

Mudher, A., Chapman, S., Richardson, J., Asuni, A., Gibb, G., Pollard, C., Killick, R., Iqbal, T., Raymond, L., Varndell, I., Sheppard, P., Makoff, A., Gower, E., Soden, P. E., Lewis, P., Murphy, M., Golde, T. E., Rupniak, H. T., Anderton, B. H., and Lovestone, S. (2001). Dishevelled regulates the metabolism of amyloid precursor protein via protein kinase C/mitogen-activated protein kinase and c-Jun terminal kinase. *J Neurosci* **21**:4987-4995.

Mullberg, J., Schooltink, H., Stoyan, T., Heinrich, P. C., and Rose-John, S. (1992). Protein kinase C activity is rate limiting for shedding of the interleukin-6 receptor. *Biochem Biophys Res Commun* **189**:794-800.

Mullberg, J., Oberthur, W., Lottspeich, F., Mehl, E., Dittrich, E., Graeve, L., Heinrich, P. C., and Rose-John, S. (1994). The soluble human IL-6 receptor. Mutational characterization of the proteolytic cleavage site. *J Immunol* **152**:4958-4968.

Muller, U., Cristina, N., Li, Z. W., Wolfer, D. P., Lipp, H. P., Rulicke, T., Brandner, S., Aguzzi, A., and Weissmann, C. (1994). Behavioral and anatomical deficits in mice homozygous for a modified beta-amyloid precursor protein gene. *Cell* **79**:755-765.

Murga, C., Fukuhara, S., Gutkind, J. S. (1999). Novel Molecular Mediators in the Pathway Connecting G-protein-coupled Receptors to MAP Kinase Cascades. *Trends Endocrinol Metab* **10**(4):122-127.

Naor, Z., Benard, O., Seger, R. (2000). Activation of MAPK cascades by G-protein-coupled receptors: the case of gonadotropin-releasing hormone receptor. *Trends Endocrinol Metab* **11**(3):91-99.

Nath, D., Williamson, N. J., Jarvis, R., and Murphy, G. (2001). Shedding of c-Met is regulated by crosstalk between a G-protein coupled receptor and the EGF receptor and is mediated by a TIMP-3 sensitive metalloproteinase. *J Cell Sci* **114**:1213-1220.

Nelson, K. K., Schlondorff, J., and Blobel, C. P. (1999). Evidence for an interaction of the metalloprotease-disintegrin tumour necrosis factor alpha convertase (TACE) with mitotic arrest deficient 2 (MAD2), and of the metalloprotease-disintegrin MDC9 with a novel MAD2- related protein, MAD2beta. *Biochem J* **343 Pt 3**:673-680.

Ng, K. K. and Vane, J. R. (1967). Conversion of angiotensin I to angiotensin II. *Nature* **216**:762-766.

Ng, K. K. and Vane, J. R. (1968). Fate of angiotensin I in the circulation. *Nature* **218**:144-150.

Nielsen, O. H., Langholz, E., Hendel, J., and Brynskov, J. (1994). Circulating soluble intercellular adhesion molecule-1 (sICAM-1) in active inflammatory bowel disease. *Dig Dis Sci* **39**:1918-1923.

Nophar, Y., Kemper, O., Brakebusch, C., Englemann, H., Zwang, R., Aderka, D., Holtmann, H., and Wallach, D. (1990). Soluble forms of tumor necrosis factor receptors (TNF-Rs). The cDNA for the type I TNF-R, cloned

using amino acid sequence data of its soluble form, encodes both the cell surface and a soluble form of the receptor. *EMBO J* **9**:3269-3278.

Nye, J. S. (1997). Developmental signaling: notch signals Kuz it's cleaved. *Curr Biol* **7**:R716-R720.

Oliverio, M. I., Kim, H. S., Ito, M., Le, T., Audoly, L., Best, C. F., Hiller, S., Kluckman, K., Maeda, N., Smithies, O., and Coffman, T. M. (1998). Reduced growth, abnormal kidney structure, and type 2 (AT2) angiotensin receptor-mediated blood pressure regulation in mice lacking both AT1A and AT1B receptors for angiotensin II. *Proc Natl Acad Sci U S A* **95**:15496-15501.

Ondetti, M. A., Williams, N. J., Sabo, E. F., Pluscec, J., Weaver, E. R., and Kocy, O. (1971). Angiotensin-converting enzyme inhibitors from the venom of Bothrops jararaca. Isolation, elucidation of structure, and synthesis. *Biochemistry* **10**:4033-4039.

Ondetti, M. A., Rubin, B., and Cushman, D. W. (1977). Design of specific inhibitors of angiotensin-converting enzyme: new class of orally active antihypertensive agents. *Science* **196**:441-444.

Oppong, S. Y. and Hooper, N. M. (1993). Characterization of a secretase activity which releases angiotensin-converting enzyme from the membrane. *Biochem J* **292 (Pt 2)**:597-603.

Pandiella, A., Bosenberg, M. W., Huang, E. J., Besmer, P., and Massague, J. (1992). Cleavage of membrane-anchored growth factors involves distinct protease activities regulated through common mechanisms. *J Biol Chem* **267**:24028-24033.

Pan, D. and Rubin, G. M. (1997). Kuzbanian controls proteolytic processing of Notch and mediates lateral inhibition during Drosophila and vertebrate neurogenesis. *Cell* **90**:271-280.

Pang, S., Chubb, A. J., Schwager, S. L., Ehlers, M. R., Sturrock, E. D., and Hooper, N. M. (2001). Roles of the juxtamembrane and extracellular domains of angiotensin- converting enzyme in ectodomain shedding. *Biochem J* **358**:185-192.

Pantoliano, M. W., Holmquist, B., and Riordan, J. F. (1984). Affinity chromatographic purification of angiotensin converting enzyme. *Biochemistry* **23**:1037-1042.

Park, P. W., Pier, G. B., Preston, M. J., Goldberger, O., Fitzgerald, M. L., and Bernfield, M. (2000). Syndecan-1 shedding is enhanced by LasA, a secreted virulence factor of Pseudomonas aeruginosa. *J Biol Chem* **275**:3057-3064.

Parvathy, S., Oppong, S. Y., Karran, E. H., Buckle, D. R., Turner, A. J., and Hooper, N. M. (1997). Angiotensin-converting enzyme secretase is inhibited by zinc metalloprotease inhibitors and requires its substrate to be inserted in a lipid bilayer. *Biochem J* **327 (Pt 1)**:37-43.

Parvathy, S., Karran, E. H., Turner, A. J., and Hooper, N. M. (1998). The secretases that cleave angiotensin converting enzyme and the amyloid precursor protein are distinct from tumour necrosis factor- alpha convertase. *FEBS Lett* **431**:63-65.

Parvathy, S., Hussain, I., Karran, E. H., Turner, A. J., and Hooper, N. M. (1999). Cleavage of Alzheimer's amyloid precursor protein by alpha-secretase occurs at the surface of neuronal cells. *Biochemistry* **38**:9728-9734.

Patwardhan, S. A., Pandey, R. C., and Dev, S. (1974). Toxic cytochalasins of Phomopsis paspalli a pathogen of Kodo millet. *Phytochemistry* **13**:1985-1988.

Pavalko, F. M., Walker, D. M., Graham, L., Goheen, M., Doerschuk, C. M., and Kansas, G. S. (1995). The cytoplasmic domain of L-selectin interacts with cytoskeletal proteins via alpha-actinin: receptor positioning in microvilli does not require interaction with alpha-actinin. *J Cell Biol* **129**:1155-1164.

Pearse, B. M. (1988). Receptors compete for adaptors found in plasma membrane coated pits. *EMBO J* **7**:3331-3336.

Pepperell, J. R., Nemeth, G., Roa, L., Yamada, Y., Palumbo, A., and Naftolin, F. (1994). Intraovarian regulation by the ovarian renin-angiotensin system. *Aust N Z J Obstet Gynaecol* **34**:288-292.

Peschon, J. J., Slack, J. L., Reddy, P., Stocking, K. L., Sunnarborg, S. W., Lee, D. C., Russell, W. E., Castner, B. J., Johnson, R. S., Fitzner, J. N., Boyce, R. W., Nelson, N., Kozlosky, C. J., Wolfson, M. F., Rauch, C. T., Cerretti, D. P., Paxton, R. J., March, C. J., and Black, R. A. (1998). An essential role for ectodomain shedding in mammalian development. *Science* **282**:1281-1284.

Piquilloud, Y., Reinharz, A., and Roth, M. (1970). Studies on the angiotensin converting enzyme with different substrates. *Biochim Biophys Acta* **206**:136-142.

Pischitzis, A., Hahn, D., Leuenberger, B., and Sterchi, E. E. (1999). N-Benzoyl-L-tyrosyl-p-aminobenzoic acid hydrolase beta (human meprinbeta). A 13-amino-acid sequence is required for proteolyticprocessing and subsequent secretion. *Eur J Biochem* **261**:421-429.

Plowman, G. D., Green, J. M., Neubauer, M. G., Buckley, S. D., McDonald, V. L., Todaro, G. J., and Shoyab, M. (1992). The epithelin precursor encodes two proteins with opposing activities on epithelial cell growth. *J Biol Chem* **267**:13073-13078.

Poloso, N. J., Nagarajan S., Mejia-Oneta J. M., Selvaraj P. (2002) GPI-anchoring of GM-CSF results in active membrane-bound and partially shed cytokine. *Mol Immunol* **38**(11):803-816

Polsky-Cynkin, R. and Fanburg, B. L. (1979). Immunochemical comparison of angiotensin 1 converting enzymes from different rat organs. *Int J Biochem* **10**:669-674.

Porteu, F. and Hieblot, C. (1994). Tumor necrosis factor induces a selective shedding of its p75 receptor from human neutrophils. *J Biol Chem* **269**:2834-2840.

Porteu, F. and Nathan, C. (1990). Shedding of tumor necrosis factor receptors by activated human neutrophils. *J Exp Med* **172**:599-607.

Prenzel, N., Zwick, E., Daub, H., Leserer, M., Abraham, R., Wallasch, C., and Ullrich, A. (1999). EGF receptor transactivation by G-protein-coupled receptors requires metalloproteinase cleavage of proHB-EGF. *Nature* **402**:884-888.

Primakoff, P. and Myles, D. G. (2000). The ADAM gene family: surface proteins with adhesion and protease activity. *Trends Genet* **16**:83-87.

Puck TT. Genetics of somatic mammalian cells III. Long-term cultivation of euploid cells from human and animal subjects. J.Exp.Med. 108, 945-956. 1958.

Pugsley, AP. (1993). The complete general secretory pathway in gram-negative bacteria. *Microbiol Rev* **57**:50-108.

Qi, H., Rand, M. D., Wu, X., Sestan, N., Wang, W., Rakic, P., Xu, T., and Artavanis-Tsakonas, S. (1999). Processing of the notch ligand delta by the metalloprotease Kuzbanian. *Science* **283**:91-94.

Quinn KA, Pye VJ, Dai YP, Chesterman CN, Owensby DA. Characterization of the soluble form of the low density lipoprotein receptor-related protein (LRP). (1999). *Exp Cell Res.* **251**(2):433-41.

Raizada, M. K., Francis, S. C., Wang, H., Gelband, C. H., Reaves, P. Y., and Katovich, M. J. (2000). Targeting of the renin-angiotensin system by antisense gene therapy: a possible strategy for the long-term control of hypertension. *J Hypertens* **18**:353-362.

Ramaraj, P., Kessler, S. P., Colmenares, C., and Sen, G. C. (1998). Selective restoration of male fertility in mice lacking angiotensin- converting enzymes by sperm-specific expression of the testicular isozyme. *J Clin Invest* **102**:371-378.

Ramchandran, R. and Sen, I. (1995). Cleavage processing of angiotensin-converting enzyme by a membrane-associated metalloprotease. *Biochemistry* **34**:12645-12652.

Ramchandran, R., Sen, G. C., Misono, K., and Sen, I. (1994). Regulated cleavage-secretion of the membrane-bound angiotensin- converting enzyme. *J Biol Chem* **269**:2125-2130.

Rawlings, N. D. and Barrett, A. J. (1995). Evolutionary families of metallopeptidases. *Methods Enzymol* **248**:183-228.

Ray, W. J., Ashall, F., and Goate, A. M. (1998). Molecular pathogenesis of sporadic and familial forms of Alzheimer's disease. *Mol Med Today* **4**:151-157.

Ray, W. J., Yao, M., Mumm, J., Schroeter, E. H., Saftig, P., Wolfe, M., Selkoe, D. J., Kopan, R., and Goate, A. M. (1999). Cell surface presenilin-1 participates in the gamma-secretase-like proteolysis of Notch. *J Biol Chem* **274**:36801-36807.

Reddy, P., Caras, I., and Krieger, M. (1989). Effects of O-linked glycosylation on the cell surface expression and stability of decay-accelerating factor, a glycophospholipid-anchored membrane protein. *J Biol Chem* **264**:17329-17336.

Reddy, P., Slack, J. L., Davis, R., Cerretti, D. P., Kozlosky, C. J., Blanton, R. A., Shows, D., Peschon, J. J., and Black, R. A. (2000). Functional analysis of the domain structure of tumor necrosis factor- alpha converting enzyme. *J Biol Chem* **275**:14608-14614.

Rieger, K. J., Saez-Servent, N., Papet, M. P., Wdzieczak-Bakala, J., Morgat, J. L., Thierry, J., Voelter, W., and Lenfant, M. (1993). Involvement of human plasma angiotensin I-converting enzyme in the degradation of the haemoregulatory peptide N-acetyl-seryl-aspartyl- lysyl-proline. *Biochem J* **296 (Pt 2)**:373-378.

Rigat, B., Hubert, C., Alhenc-Gelas, F., Cambien, F., Corvol, P., and Soubrier, F. (1990). An insertion/deletion polymorphism in the angiotensin I-converting enzyme gene accounting for half the variance of serum enzyme levels. *J Clin Invest* **86**:1343-1346.

Rio, C., Buxbaum, J. D., Peschon, J. J., and Corfas, G. (2000). Tumor necrosis factor-alpha-converting enzyme is required for cleavage of erbB4/HER4. *J Biol Chem* **275**:10379-10387.

Roberts, S. B., Ripellino, J. A., Ingalls, K. M., Robakis, N. K., and Felsenstein, K. M. (1994). Non-amyloidogenic cleavage of the beta-amyloid precursor protein by an integral membrane metalloendopeptidase. *J Biol Chem* **269**:3111-3116.

Roghani, M., Becherer, J. D., Moss, M. L., Atherton, R. E., Erdjument-Bromage, H., Arribas, J., Blackburn, R. K., Weskamp, G., Tempst, P., and Blobel, C. P. (1999). Metalloprotease-disintegrin MDC9: intracellular maturation and catalytic activity. *J Biol Chem* **274**:3531-3540.

Roher, A. E., Lowenson, J. D., Clarke, S., Woods, A. S., Cotter, R. J., Gowing, E., and Ball, M. J. (1993). beta-Amyloid-(1-42) is a major component of cerebrovascular amyloid deposits: implications for the pathology of Alzheimer disease. *Proc Natl Acad Sci U S A* **90**:10836-10840.

Ronin, C., Granier, C., Caseti, C., Bouchilloux, S., and Van Rietschoten, J. (1981). Synthetic substrates for thyroid oligosaccharide transferase. Effects of peptide chain length and modifications in the Asn-Xaa-Thr-region. *Eur J Biochem* **118**:159-164.

Rooke, J., Pan, D., Xu, T., and Rubin, G. M. (1996). KUZ, a conserved metalloprotease-disintegrin protein with two roles in Drosophila neurogenesis. *Science* **273**:1227-1231.

Rose-John, S. and Heinrich, P. C. (1994). Soluble receptors for cytokines and growth factors: generation and biological function. *Biochem J* **300 (Pt 2)**:281-290.

Rosendahl, M. S., Ko, S. C., Long, D. L., Brewer, M. T., Rosenzweig, B., Hedl, E., Anderson, L., Pyle, S. M., Moreland, J., Meyers, M. A., Kohno, T., Lyons, D., and Lichenstein, H. S. (1997). Identification and characterization of a pro-tumor necrosis factor- alpha-processing enzyme from the ADAM family of zinc metalloproteases. *J Biol Chem* **272**:24588-24593.

Rossner, S., Beck, M., Stahl, T., Mendla, K., Schliebs, R., and Bigl, V. (2000). Constitutive overactivation of protein kinase C in guinea pig brain increases alpha-secretory APP processing without decreasing beta-amyloid generation. *Eur J Neurosci* **12**:3191-3200.

Rossner, S., Mendla, K., Schliebs, R., and Bigl, V. (2001). Protein kinase Calpha and beta1 isoforms are regulators of alpha- secretory proteolytic processing of amyloid precursor protein in vivo. *Eur J Neurosci* **13**:1644-1648.

Rousseau, A., Michaud, A., Chauvet, M. T., Lenfant, M., and Corvol, P. (1995). The hemoregulatory peptide N-acetyl-Ser-Asp-Lys-Pro is a natural and specific substrate of the N-terminal active site of human angiotensin- converting enzyme. *J Biol Chem* **270**:3656-3661.

Rutledge, E. A., Root, B. J., Lucas, J. J., and Enns, C. A. (1994). Elimination of the O-linked glycosylation site at Thr 104 results in the generation of a soluble human-transferrin receptor. *Blood* **83**:580-586.

Ryan, J. W. (1988). Angiotensin-converting enzyme, dipeptidyl carboxypeptidase I, and its inhibitors. *Methods Enzymol* **163**:194-210.

Sadhukhan, R. and Sen, I. (1996). Different glycosylation requirements for the synthesis of enzymatically active angiotensin-converting enzyme in mammalian cells and yeast. *J Biol Chem* **271**:6429-6434.

Sadhukhan, R., Sen, G. C., and Sen, I. (1996). Synthesis and cleavage- secretion of enzymatically active rabbit angiotensin-converting enzyme in Pichia pastoris. *J Biol Chem* **271**:18310-18313.

Sadhukhan, R., Sen, G. C., Ramchandran, R., and Sen, I. (1998). The distal ectodomain of angiotensin-converting enzyme regulates its cleavage-secretion from the cell surface. *Proc Natl Acad Sci U S A* **95**:138-143.

Sadhukhan, R., Santhamma, K. R., Reddy, P., Peschon, J. J., Black, R. A., and Sen, I. (1999). Unaltered cleavage and secretion of angiotensin-converting enzyme in tumor necrosis factor-alpha-converting enzyme-deficient mice. *J Biol Chem* **274**:10511-10516.

Sanger, F., Niklen, S., and Coulson, A.R. (1977). *Proc. Nat. Acad. Sci. USA* **74**:5463-546.

Sahasrabudhe, S. R., Spruyt, M. A., Muenkel, H. A., Blume, A. J., Vitek, M. P., and Jacobsen, J. S. (1992). Release of amino-terminal fragments from amyloid precursor protein reporter and mutated derivatives in cultured cells. *J Biol Chem* **267**:25602-25608.

Santhamma, K. R. and Sen, I. (2000). Specific cellular proteins associate with angiotensin-converting enzyme and regulate its intracellular transport and cleavage-secretion. *J Biol Chem* **275**:23253-23258.

Schechter I., Berger A. (1967). On the size of the active site in proteases. I. Papain. *Biochem Biophys Res Commun* **27**:157-162

Scheele, G. A. (1988). Molecular sorting of proteins into the cisternal secretory pathway. *Biochimie* **70**(9):1269-1276.

Schekman, R. (1994). Translocation gets a push. *Cell* **78**:911-913.

Schenk, D., Barbour, R., Dunn, W., Gordon, G., Grajeda, H., Guido, T., Hu, K., Huang, J., Johnson-Wood, K., Khan, K., Kholodenko, D., Lee, M., Liao, Z., Lieberburg, I., Motter, R., Mutter, L., Soriano, F., Shopp, G., Vasquez, N., Vandevert, C., Walker, S., Wogulis, M., Yednock, T., Games, D., and Seubert, P. (1999). Immunization with amyloid-beta attenuates Alzheimer-disease-like pathology in the PDAPP mouse. *Nature* **400**:173-177.

Schlondorff, J. and Blobel, C. P. (1999). Metalloprotease-disintegrins: modular proteins capable of promoting cell-cell interactions and triggering signals by protein-ectodomain shedding. *J Cell Sci* **112 (Pt 21)**:3603-3617.

Schwager, S. L., Chubb, A. J., Scholle, R. R., Brandt, W. F., Eckerskorn, C., Sturrock, E. D., and Ehlers, M. R. (1998). Phorbol ester-induced juxtamembrane cleavage of angiotensin-converting enzyme is not inhibited by a stalk containing intrachain disulfides. *Biochemistry* **37**:15449-15456.

Schwager, S. L., Chubb, A. J., Scholle, R. R., Brandt, W. F., Mentele, R., Riordan, J. F., Sturrock, E. D., and Ehlers, M. R. (1999). Modulation of juxtamembrane cleavage ("shedding") of angiotensin- converting enzyme by stalk glycosylation: evidence for an alternative shedding protease. *Biochemistry* **38**:10388-10397.

Schwager, S. L., Chubb, A. J., Woodman ,Z. L., Yan, L. , Mentele, R., Ehlers, M. R. and Sturrock, E. D., (2001). Cleavage of Disulfide-Bridged Stalk Domains during Shedding of Angiotensin-Converting Enzyme Occurs at Multiplying Juxtamembrane Sites. *Biochemistry* **40**:15624-15630.

Selkoe, D. J. (1991). Amyloid protein and Alzheimer's disease. *Sci Am* **265**:68-6, 78.

Selkoe, D. J. (1998). The cell biology of beta-amyloid precursor protein and presenilin in Alzheimer's disease. *Trends Cell Biol* **8**:447-453.

Sen, I., Samanta, H., Livingston, W., III, and Sen, G. C. (1991). Establishment of transfected cell lines producing testicular angiotensin-converting enzyme. Structural relationship between its secreted and cellular forms. *J Biol Chem* **266**:21985-21990.

Seubert, P., Vigo-Pelfrey, C., Esch, F., Lee, M., Dovey, H., Davis, D., Sinha, S., Schlossmacher, M., Whaley, J., Swindlehurst, C., and . (1992). Isolation and quantification of soluble Alzheimer's beta-peptide from biological fluids. *Nature* **359**:325-327.

Shakin-Eshleman, S. H., Spitalnik, S. L., and Kasturi, L. (1996). The amino acid at the X position of an Asn-X-Ser sequon is an important determinant of N-linked core-glycosylation efficiency. *J Biol Chem* **271**:6363-6366.

Shapiro, R. and Riordan, J. F. (1983). Critical lysine residue at the chloride binding site of angiotensin converting enzyme. *Biochemistry* **22**:5315-5321.

Shapiro, R., Holmquist, B., and Riordan, J. F. (1983). Anion activation of angiotensin converting enzyme: dependence on nature of substrate. *Biochemistry* **22**:3850-3857.

Sherrington, R., Rogaev, E. I., Liang, Y., Rogaeva, E. A., Levesque, G., Ikeda, M., Chi, H., Lin, C., Li, G., Holman, K., and . (1995). Cloning of a gene bearing missense mutations in early-onset familial Alzheimer's disease. *Nature* **375**:754-760.

Shi, M., Dennis, K., Peschon, J. J., Chandrasekaran, R., and Mikecz, K. (2001). Antibody-induced shedding of CD44 from adherent cells is linked to the assembly of the cytoskeleton. *J Immunol* **167**:123-131.

Sinha, S., Anderson, J. P., Barbour, R., Basi, G. S., Caccavello, R., Davis, D., Doan, M., Dovey, H. F., Frigon, N., Hong, J., Jacobson-Croak, K., Jewett, N., Keim, P., Knops, J., Lieberburg, I., Power, M., Tan, H., Tatsuno,

G., Tung, J., Schenk, D., Seubert, P., Suomensaari, S. M., Wang, S., Walker, D., John, V., and . (1999). Purification and cloning of amyloid precursor protein beta-secretase from human brain. *Nature* **402**:537-540.

Sisodia, S. S. (1992). Beta-amyloid precursor protein cleavage by a membrane-bound protease. *Proc Natl Acad Sci U S A* **89**:6075-6079.

Sisodia, S. S. and Gallagher, M. (1998). A role for the beta-amyloid precursor protein in memory? [In Process Citation]. *Proc Natl Acad Sci U S A* **95**:12074-12076.

Sisodia, S. S., Koo, E. H., Beyreuther, K., Unterbeck, A., and Price, D. L. (1990). Evidence that beta-amyloid protein in Alzheimer's disease is not derived by normal processing. *Science* **248**:492-495.

Skeggs, L. T., Jr., Marsh, W. H., Kahn, J. R., and Shumway, N. P. (1954). The existance of two forms of hypertensin. *J Exp Med* **99**:275-282.

Skeggs, L. T., Jr., Kahn, J. R., and Shumway, N. P. (1956). The preparation and function of the hypertensin-converting enzyme. *J Exp Med* **103**:295.

Skidgel, R. A. and Erdos, E. G. (1985). Novel activity of human angiotensin I converting enzyme: release of the NH2- and COOH-terminal tripeptides from the luteinizing hormone- releasing hormone. *Proc Natl Acad Sci U S A* **82**:1025-1029.

Soubrier, F., Alhenc-Gelas, F., Hubert, C., Allegrini, J., John, M., Tregear, G., and Corvol, P. (1988). Two putative active centers in human angiotensin I-converting enzyme revealed by molecular cloning. *Proc Natl Acad Sci U S A* **85**:9386-9390.

Southern, P. J. and Berg, P. (1982). Transformation of mammalian cells to antibiotic resistance with a bacterial gene under control of the SV40 early region promoter. *J Mol Appl Genet* **1**:327-341.

Steinhusen, U., Weiske, J., Badock, V., Tauber, R., Bommert, K., and Huber, O. (2001). Cleavage and shedding of E-cadherin after induction of apoptosis. *J Biol Chem* **276**:4972-4980.

Strittmatter, S. M. and Snyder, S. H. (1984). Angiotensin-converting enzyme in the male rat reproductive system: autoradiographic visualization with [3H]captopril. *Endocrinology* **115**:2332-2341.

Struhl, G. and Greenwald, I. (1999). Presenilin is required for activity and nuclear access of Notch in Drosophila [see comments]. *Nature* **398**:522-525.

Sturrock, E. D., Yu, X. C., Wu, Z., Biemann, K., and Riordan, J. F. (1996). Assignment of free and disulfide-bonded cysteine residues in testis angiotensin-converting enzyme: functional implications. *Biochemistry* **35**:9560-9566.

Sturrock, E. D., Danilov, S. M., and Riordan, J. F. (1997). Limited proteolysis of human kidney angiotensin-converting enzyme and generation of catalytically active N- and C-terminal domains. *Biochem Biophys Res Commun* **236**:16-19.

Subramanian, S. V., Fitzgerald, M. L., and Bernfield, M. (1997). Regulated shedding of syndecan-1 and -4 ectodomains by thrombin and growth factor receptor activation. *J Biol Chem* **272**:14713-14720.

Sugimura, K., Tian, X. L., Hoffmann, S., Ganten, D., and Bader, M. (1998). Alternative splicing of the mRNA coding for the human endothelial angiotensin-converting enzyme: a new mechanism for solubilization. *Biochem Biophys Res Commun* **247**:466-472.

Swales, J. D. (1995). "Manual of Hypertension," Blackwell Science, Oxford.

Swedberg, K. (2000). Exploring new treatment strategies in heart failure. *Blood Press Suppl* **1**:44-48.

Tang, P., Hung, M.-C., and Klostergaard, J. (1996a). Human pro-tumor necrosis factor is a homotrimer. *Biochemistry* **35**:8216-8225.

Tang, P., Hung, M.-C., and Klostergaard, J. (1996b). Length of the linking domain of human pro-tumor necrosis factor determines the cleavage processing. *Biochemistry* **35**:8226-8233.

Tanimoto, K., Sugiyama, F., Goto, Y., Ishida, J., Takimoto, E., Yagami, K., Fukamizu, A., and Murakami, K. (1994). Angiotensinogen-deficient mice with hypotension. *J Biol Chem* **269**:31334-31337.

Tatei, K., Cai, H., Ip, Y. T., and Levine, M. (1995). Race: a Drosophila homologue of the angiotensin converting enzyme. *Mech Dev* **51**:157-168.

The *C.elegans* Sequencing Consortium (1998). Genome sequence of the nematode *C. elegans*: a platform for investigating biology. *Science* **282**:2012-2018.

Tipnis, S. R., Hooper, N. M., Hyde, R., Karran, E., Christie, G., and Turner, A. J. (2000). A human homolog of angiotensin-converting enzyme. Cloning and functional expression as a captopril-insensitive carboxypeptidase. *J Biol Chem* **275**:33238-33243.

Tomita, S., Kirino, Y., and Suzuki, T. (1998). A basic amino acid in the cytoplasmic domain of Alzheimer's beta-amyloid precursor protein (APP) is essential for cleavage of APP at the alpha-site. *J Biol Chem* **273**:19304-19310.

Toyama, S. and Toyama, S. (1988). Functional alterations in beta'-actin from a KB cell mutant resistant to cytochalasin B. *J Cell Biol* **107**:1499-1504.

Tsukita, S. and Yonemura, S. (1999). Cortical actin organization: lessons from ERM (ezrin/radixin/moesin) proteins. *J Biol Chem* **274**:34507-34510.

Turner, A. J., Hryszko, J., Hooper, N. M., and Dowdall, M. J. (1987). Purification and characterization of a peptidyl dipeptidase resembling angiotensin converting enzyme from the electric organ of Torpedo marmorata. *J Neurochem* **48**:910-916.

Tyndall, J. D. and Fairlie, D. P. (1999). Conformational homogeneity in molecular recognition by proteolytic enzymes. *J Mol Recognit* **12**:363-370.

Unger, T., Azizi, M., and Belz, G. G. (2000). Blocking the tissue renin-angiotensin system: the future cornerstone of therapy. *J Hum Hypertens* **14 Suppl 2**:S23-S31.

Urena, J. M., Merlos-Suarez, A., Baselga, J., and Arribas, J. (1999). The cytoplasmic carboxy-terminal amino acid determines the subcellular localization of proTGF-(alpha) and membrane type matrix metalloprotease (MT1-MMP). *J Cell Sci* **112 (Pt 6)**:773-784.

Vassalli, P. (1992). The pathophysiology of tumor necrosis factors. *Annu Rev Immunol* **10**:411-452.

Vassar, R., Bennett, B. D., Babu-Khan, S., Kahn, S., Mendiaz, E. A., Denis, P., Teplow, D. B., Ross, S., Amarante, P., Loeloff, R., Luo, Y., Fisher, S., Fuller, J., Edenson, S., Lile, J., Jarosinski, M. A., Biere, A. L., Curran, E., Burgess, T., Louis, J. C., Collins, F., Treanor, J., Rogers, G., and Citron, M. (1999). Beta-secretase cleavage of Alzheimer's amyloid precursor protein by the transmembrane aspartic protease BACE. *Science* **286**:735-741.

Vecchi M, Baulida J, Carpenter G. (1996). Selective cleavage of the heregulin receptor ErbB-4 by protein kinase C activation. J Biol Chem. **271**(31):18989-95.

Vecchi, M., Rudolph-Owen, L. A., Brown, C. L., Dempsey, P. J., and Carpenter, G. (1998). Tyrosine phosphorylation and proteolysis. Pervanadate-induced, metalloprotease-dependent cleavage of the ErbB-4 receptor and amphiregulin. *J Biol Chem* **273**:20589-20595.

Venter, J. C. *et al.*, (2001). The sequence of the human genome. *Science* **291**:1304-1351.

Walcheck, B., Kahn, J., Fisher, J. M., Wang, B. B., Fisk, R. S., Payan, D. G., Feehan, C., Betageri, R., Darlak, K., Spatola, A. F., and Kishimoto, T. K. (1996). Neutrophil rolling altered by inhibition of L-selectin shedding in vitro. *Nature* **380**:720-723.

Walter, J., Fluhrer, R., Hartung, B., Willem, M., Kaether, C., Capell, A., Lammich, S., Multhaup, G., and Haass, C. (2001). Phosphorylation regulates intracellular trafficking of beta-secretase. *J Biol Chem* **276**:14634-14641.

Wear, M. A., Schafer, D. A., and Cooper, J. A. (2000). Actin dynamics: assembly and disassembly of actin networks. *Curr Biol* **10**:R891-R895.

Wei, L., Alhenc-Gelas, F., Corvol, P., and Clauser, E. (1991a). The two homologous domains of human angiotensin I-converting enzyme are both catalytically active. *J Biol Chem* **266** :9002-9008.

Wei, L., Alhenc-Gelas, F., Soubrier, F., Michaud, A., Corvol, P., and Clauser, E. (1991b). Expression and characterization of recombinant human angiotensin I- converting enzyme. Evidence for a C-terminal transmembrane anchor and for a proteolytic processing of the secreted recombinant and plasma enzymes. *J Biol Chem* **266**:5540-5546.

Wendorf, P., Linder D., Sziegoleit A., Geyer R. (1991). Carbohydrate structure of human pancreatic elastase 1. *Biochem J* **278**:505-514

Weskamp, G., Kratzschmar, J., Reid, M. S., and Blobel, C. P. (1996). MDC9, a widely expressed cellular disintegrin containing cytoplasmic SH3 ligand domains. *J Cell Biol* **132**:717-726.

WHO. World Health Report 2000 - Statistical Annex. 143-206. 2001. World Health Organisation. Ref Type: Report

Wilkinson, B. M., Regnacq M., Stirling C. J. (1997). Protein translocation across the membrane of the endoplasmic reticulum. *J Membr Biol* **155**(3):189-197.

Williams, T. A., Corvol, P., and Soubrier, F. (1994). Identification of two active site residues in human angiotensin I- converting enzyme. *J Biol Chem* **269**:29430-29434.

Williams, T. A., Danilov, S., Alhenc-Gelas, F., and Soubrier, F. (1996). A study of chimeras constructed with the two domains of angiotensin I- converting enzyme. *Biochem Pharmacol* **51**:11-14.

Williams, T. A., Gouttaya, M., Tougard, C., Michaud, A., Chauvet, M. T., and Corvol, P. (1997). Cleavage-secretion of angiotensin I-converting enzyme in yeast. *Mol Cell Endocrinol* **128**:39-45.

Williams, T. A., Hooper, N. M., Kenny, A. J., and Turner, A. J. (1990). Molecular forms of angiotensin-converting enzyme in brain microvessels. *Biochem Soc Trans* **18**:887.

Williams, T. A., Michaud, A., Houard, X., Chauvet, M. T., Soubrier, F., and Corvol, P. (1996). Drosophila melanogaster angiotensin I-converting enzyme expressed in Pichia pastoris resembles the C domain of the mammalian homologue and does not require glycosylation for secretion and enzymic activity. *Biochem J* **318**:125-131.

Williamson, R. A., Hutton, M., Vogt, G., Rapti, M., Knauper, V., Carr, M. D., and Murphy, G. (2001). Tyrosine 36 Plays a Critical Role in the Interaction of the AB Loop of Tissue Inhibitor of Metalloproteinases-2 with Matrix Metalloproteinase-14. *J Biol Chem* **276**:32966-32970.

Winckler, B., Forscher, P., and Mellman, I. (1999). A diffusion barrier maintains distribution of membrane proteins in polarized neurons. *Nature* **397**:698-701.

Wolfe, M. S. and Haass, C. (2001). The Role of presenilins in gamma-secretase activity. *J Biol Chem* **276**:5413-5416.

Wolfe, M. S., Xia, W., Ostaszewski, B. L., Diehl, T. S., Kimberly, W. T., and Selkoe, D. J. (1999). Two transmembrane aspartates in presenilin-1 required for presenilin endoproteolysis and gamma-secretase activity [see comments]. *Nature* **398**:513-517.

Wong, P. Y. and Uchendu, C. N. (1990). The role of angiotensin-converting enzyme in the rat epididymis. *J Endocrinol* **125**:457-465.

Woodman, Z. L., Oppong, S. Y., Cook, S., Hooper, N. M., Schwager, S. L., Brandt, W. F., Ehlers, M. R., and Sturrock, E. D. (2000). Shedding of somatic angiotensin-converting enzyme (ACE) is inefficient compared with testis ACE despite cleavage at identical stalk sites. *Biochem J* **347 Pt 3**:711-718.

Yan, R., Bienkowski, M. J., Shuck, M. E., Miao, H., Tory, M. C., Pauley, A. M., Brashier, J. R., Stratman, N. C., Mathews, W. R., Buhl, A. E., Carter, D. B., Tomasselli, A. G., Parodi, L. A., Heinrikson, R. L., and Gurney, M. E. (1999). Membrane-anchored aspartyl protease with Alzheimer's disease beta- secretase activity. *Nature* **402**:533-537.

Yang, H. Y. and Erdos, E. G. (1967). Second kininase in human blood plasma. *Nature* **215**:1402-1403.

Yang, H. Y., Erdos, E. G., and Levin, Y. (1970). A dipeptidyl carboxypeptidase that converts angiotensin I and inhibits bradykinin. *Biochem Biophys Acta* **214**:374-376.

Yaron, A., Carmel, A., and Katchalski-Katzir, E. (1979). Intramolecularly quenched fluorogenic substrates for hydrolytic enzymes. *Anal Biochem* **95**:228-235.

Ye, Y., Lukinova, N., and Fortini, M. E. (1999). Neurogenic phenotypes and altered Notch processing in Drosophila Presenilin mutants [see comments]. *Nature* **398**:525-529.

Yotsumoto, H., Lanzillo, J. J., and Fanburg, B. L. (1983). Generation of a 90 000 molecular weight fragment from human plasma angiotensin-I-converting enzyme by enzymatic or alkaline hydrolysis. *Biochim Biophys Acta* **749**:180-184.

Yotsumoto, H., Sato, S., and Shibuya, M. (1984). Localization of angiotensin converting enzyme (dipeptidyl carboxypeptidase) in swine sperm by immunofluorescence. *Life Sci* **35**:1257-1261.

Yu, X. C., Sturrock, E. D., Wu, Z., Biemann, K., Ehlers, M. R., and Riordan, J. F. (1997). Identification of N-linked glycosylation sites in human testis angiotensin-converting enzyme and expression of an active deglycosylated form. *J Biol Chem* **272**:3511-3519.

Zamze, S., Harvey D. J., Pesheva P., Mattu T. S., Schachner M., Dwek R. A., Wing D. R. (1999). Glycosylation of a CNS-specific extracellular matrix glycoprotein, tenascin-R, is dominated by O-linked sialylated glycans and "brain-type" neutral N-glycans. *Glycobiology* **9**(8):823-831.

Zee, R. Y., Lou, Y. K., Griffiths, L. R., and Morris, B. J. (1992). Association of a polymorphism of the angiotensin I-converting enzyme gene with essential hypertension. *Biochem Biophys Res Commun* **184**:9-15.

Zhang, H., Wada, J., Hida, K., Tsuchiyama, Y., Hiragushi, K., Shikata, K., Wang, H., Lin, S., Kanwar, Y. S., and Makino, H. (2001). Collectrin, a collecting duct-specific transmembrane glycoprotein, is a novel homolog of ACE2 and is developmentally regulated in embryonic kidneys. *J Biol Chem* **276**:17132-17139.

Zhang, Y., Jiang, J., Black, R. A., Baumann, G., and Frank, S. J. (2000a). Tumor necrosis factor-alpha converting enzyme (TACE) is a growth hormone binding protein (GHBP) sheddase: the metalloprotease TACE/ADAM- 17 is critical for (PMA-induced) GH receptor proteolysis and GHBP generation. *Endocrinology* **141**:4342-4348.

Zhang, Z., Cork, J., Ye, P., Lei, D., Schwarzenberger, P. O., Summer, W. R., Shellito, J. E., Nelson, S., and Kolls, J. K. (2000b). Inhibition of TNF-alpha processing and TACE-mediated ectodomain shedding by ethanol. *J Leukoc Biol* **67**:856-862.

Zhang, Z., Kolls, J. K., Oliver, P., Good, D., Schwarzenberger, P. O., Joshi, M. S., Ponthier, J. L., and Lancaster, J. R., Jr. (2000c). Activation of tumor necrosis factor-alpha-converting enzyme-mediated ectodomain shedding by nitric oxide. *J Biol Chem* **275** :15839-15844.

Zhao, L., Shey, M., Farnsworth, M., and Dailey, M. O. (2001). Regulation of membrane metalloproteolytic cleavage of L-selectin (CD62l) by the epidermal growth factor domain. *J Biol Chem* **276**:30631-30640.

Zhong, Z., Higaki, J., Murakami, K., Wang, Y., Catalano, R., Quon, D., and Cordell, B. (1994). Secretion of beta-amyloid precursor protein involves multiple cleavage sites. *J Biol Chem* **269**:627-632.

Appendix I: Supplementary Tables and Figures

Table AI.1) Abbreviations

A	Ala, alanine
Abz	*ortho*-aminobenzoic acid
Ao	Angiotensinogen
Beta-A4	β-amyloid protein (40-42 aa, of β-APP, causes AD)
β-APP	β-Amyloid precursor protein
ACE	Angiotensin Converting Enzyme (ACE1, DCP1)
ACE_E	Endothelial ACE
ACE_I	Ilial ACE
ACE_P	Pulmonary ACE
ACE_S	Somatic ACE
ACE_T	Testicular ACE
AD	Alzheimer's disease
ADH	Anti-diuretic hormone
AngI	Angiotensin I (10 aa) [DRVYIHPFHL]
AngII	Angiotensin II (8 aa) [DRVYIHPF]
AR	Breast tumor cell line
AT_1	Angiotensin II type-1 receptor
ATCC	American Type Culture Collection
bp	Base pairs (nt)
pBS	pBlueScript SK (Stratagene)
BIM	bisindolylmaleimide
C	Cys, cysteine
C-terminal	COOH-terminal
CaM	Calmodulin
cAMP	Cyclic adenosine monophosphate
CD	Clusters of Differentiation
CHCA	α-cyano-4-hydroxycinnamic acid
CHO	Chinese Hamster Ovary
CNBr	Cyanogen bromide
COS1	African green monkey cell line
CRP	C-reactive protein
CRE	cAMP response element
CREM	cAMP response element modulator
cytoD	Cytochalasin D
D	Asp, aspartic acid
DAG	Diacylglycerol, activates PKC
DABCO	1,4-diazobicyclo-[2,2,2]-octane
DCP1	dipeptidyl carboxypeptidase 1 (ACE)
DEPC	Diethyl Pyrocarbonate
DHB	2,5-dihydroxybenzoic acid
DNA	Deoxyribonucleic acid
Dnp	2,4-dinitrophenyl
E	Glu, glutamic acid
EC	Extracellular
EDTA	Ethylenediaminetetraacetic acid
EGF	Epidermal growth factor
EGFR	Epidermal growth factor receptor
EPA	Erythroid-potentiating activity
ER	Endoplasmic reticulum

ERK	Extracellular signal-regulated protein kinase
F	Phe, phenylalanine
Fa-FGG	2-furanacryloyl-L-phenylalanylglycylglycine
FasL	Fas ligand
FCS	Foetal Calf Serum
FGF	Fibroblast growth factor
FMet-Leu-Phe	N-formylmethionyl-leucyl-phenylalanine
FU	Fluorescence units (arbitrary)
G	Gly, glycine
GDP	Guanosine diphosphate
GTP	Guanosine triphosphate
GH	Growth hormone
GHBP	GH binding protein
GHR	GH receptor
GPI	glycosylphosphatidylinositol
GRB2	Growth factor receptor-bound protein 2
H	His, histidine
H_2O_2	Hydrogen peroxide
HA	Hemagglutinin
HB-EGF	Heparin-binding epidermal growth factor
HEPES	4-(2-Hydroxyethyl)-1-piperazineethanesulfonic acid
HHL	Hippuryl-His-Leu
HMEC-1	An endothelial dermal microvessel cell line
HRP	Horseradish peroxidase
HUVEC	human umbilical vein endothelial cell
I	Ile, isoleucine
IC3	Immunex compound 3
IL-6	Interleukine-6
IL-6R	IL-6 receptor
IP_3	Ins(1,4,5)P_3, inositol 1,4,5-tiphosphate
JNK	Janus kinase
K	Lys, lysine
Kb	Kilo bases (nucleotides)
KO	Knockout
L	Leu, leucine
LDL	Low density lipoprotein
LDLR	LDL receptor
Lisinopril	N alpha-[(S)-1-carboxy-3-phenylpropyl]L-lysyl-L-proline
LPA	Lysophosphatidic acid
M	Met, methionine
mAb	Monoclonal antibody
MALDI-TOF	Matrix-assisted laser-desorption-ionisation time-of-flight
MAP	Mitogen activated protein kinase
MAPK	MAP kinase
MAPKK	MAP kinase kinase, (alias MEK)
MAPKKK	MAP kinase kinase kinase, (alias Raf)
MEK	MAP and ERK kinase
Met	Hepatocyte growth factor receptor
MHC	Major Histocompatibility Complex
MS	Mass spectroscopy
MWCO	molecular weight cutoff
N	Asn, asparagine
N-terminal	NH_2-terminal
NEM	N-ethylmaleimide
NEP	neutral endopeptidase-24.11

neu-α2c	pro-neuregulin-α2c
NGF	Nerve growth factor
NMuMG	Normal murine mammary gland cells
nt	nucleotide
O/N	overnight
OVCAR-3	Ovarian tumour cell line
OVRAS	Ovarian RAS
ORF	Open reading frame
P	Pro, proline
pAb	Polyclonal antibody
PAO	phenylarsine oxide, an inhibitor of PTP
PBS	Phosphate buffered saline
PCR	Polymerase chain reaction
PDBu	Phorbol 12,13-dibutyrate
PDGF	Platelet-derived growth factor
PDTC	pyrrolidine dithiocarbomate (PV inhibitor)
PI	Phosphatidylinositol
PI3K	phosphoinositide 3-kinase
PIP_2	Phosphatidylinositol 4,5-bisphosphate
PKC	Protein kinase C
PLC-β	phospholipase C-β (activated by G-proteins)
PLC-γ	phospholipase C-γ (activated by RTKs)
PM	Plasma membrane
PMA	phorbol 12-myristate 13-acetate
PP2	Src kinase inhibitor [4-Amino-5-(4-chlorophenyl)-7-(*t*-butyl)pyrazolo[3,4-d]pyrimidine]
PP3	Negative control for PP2 [4-Amino-7-phenylpyrazol[3,4-d]pyrimidine]
PPHβ	*N*-Benzoyl-L-tyrosyl-*p*-aminobenzoic acid hydrolase
PTH	Phenylthiohydantoin (Edman deg.)
PTK	Protein tryrosine kinase
PTPase	protein-tyrosine phosphatase
R	Arg, arginine
Ras	Small GTP-binding protein, activated by GDP-releasing factors
Raf	MEK kinase, MAPKK kinase, activated by Ras
RNA	ribonucleicacid
mRNA	Messenger RNA
RP-HPLC	Reverse phase high performance liquid chromatography
RTK	Receptor tyrosine kinase
RT	Room temperature (~25°C)
S	Ser, serine
$sACE_S$	Soluble somatic ACE
$sACE_T$	Soluble testicular ACE
SDS-PAGE	Sodium dodecyl sulphate-polyacrylamide gel electrophoresis
SH2	Src homology 2 (domain)
SorLA	Sorting protein-related receptor containing LDLR class A repeats
SOS	Son of Sevenless
T	Thr, threonine
T47D	Mammary tumour cell line
TACE	TNFα converting enzyme
TAPI	TNFα protease inhibitor, Immunex compound 2, [Mohler *et al.*, 1994] N-(D,L-[2-(hydroxyaminocarbonyl)methyl]-4-methylpentanoyl)L-3-(2'naphthyl)-alanyl-L-alanine, 2-aminoethyl amide
TBE	Tris buffered EDTA
TFP	trifluoroperazine
TIGR	The Institute of Genomic Research
TLN	thermolysin

TPA	12-O-tetradecanoylphorbol 13-acetate (PMA)
TNFα	Tumor necrosis factor α
TNFRI	p55 TNFα receptor I
TNFRII	p75 TNFα receptor II
TRAP	Thrombin receptor agonist peptide
TRANCE	TNF-related activation-induced cytokine
TrkA	receptor tyrosine kinase
TSHR	thyrotropin receptor
U	units
V	Val, valine
W	Trp, tryptophan
W7	N-(6-Aminohexyl)-5-chloro-1-naphthalenesulfonamide
Wt	Wild type
Y	Tyr, tyrosine

Table AI.2) Stalk region of numerous ectoproteins

Name:	Stalk sequence:	Cut?
wtACE	SYFKPLLDWLRTENELHGEKLGWPQYNWTPNSARSEGPLPDSGRVSFLGLDLDAQQARVGQWLL	Y
ACE-Ndom	KYFQPVTQWLQEQNQQNGEVLGWPEYQWHPNSARSEGPLPDSGRVSFLGLDLDAQQARVGQWLL	N
ACE-Δ17	SYFKPLLDWLRTENELHGEKLGWPQYNWTPNSARSEGPLPDSGR.....WLL	Y
ACE-Δ24	SYFKPLLDWLRTENELHGEKLGWPQYNWTPNSAR.....VGQWLL	Y
ACE-Δ47	SYFKPLLDWLR.....VGQWLL	N
ACE-Δ6	SYFKPLLDWLRTENELHGEKLGWPQYN.....RSEGPLPDSGRVSFLGLDLDAQQARVGQWLL	Y
ACE-Δ11	SYFKPLLDWLRTENELHGEKLG.....RSEGPLPDSGRVSFLGLDLDAQQARVGQWLL	Y
ACE-Δ16	SYFKPLLDWLR.....WTPNSARSEGPLPDSGRVSFLGLDLDAQQARVGQWLL	N?
ACE-Δ5	SYFKPLLDWLRTENELHGEKLGWPQYNWTPNSARSE.....SGRVSFLGLDLDAQQARVGQWLL	Y?
ACE-ΔR627	SYFKPLLDWLRTENELHGEKLGWPQYNWTPNSA.SEGPLPDSGRVSFLGLDLDAQQARVGQWLL	Y
ACE-JGL	SYFKPLLDWLRTENELHGEKLGWPQYNWTPNS.VTVTHGTSSQATTSSQTTTHQATARVGQWLL	Y
ACE-LDL	SYFKPLLDWLRTENELHGEKLGWPQYNWTPNSHQALGDVAGRGNEKKPSSV.....RVGQWLL	Y
ACE-EGF	ELHGEKLGWPQYNWTPNSECLDNNGGCSH..VCNDLKIGYECLCPDGFQLVAQRRCERVGQWLL	Y
ACE-FIXEGF	GEKLGWPQYNWTPNSDGDQCE..SNPCLNGGSCKDDINSYECWCPFGFE...GKNCERVGQWLL	Y
ACE-MINI23	GEKLGWPQYNWTPNS.LMRCKQDS.DCLAGSVCGPNGF...CG.....VGQWLL	Y
PPHα	PLEDHNWPQYFRDPCDPNPCQNDGICVNVKGMASCRCISGHAFFYTGERCQSAEVHGSVLGMVI	Y
Meprin A α (mouse)	PMEDHNWPQYFRDPCDPNPCQNEGTCVNVKGMASCRCVSGHAFFYAGERCQAMHVHGSLLGLLI	Y
PPHβ	QIQLTPAPSVQDLCSKTTCKNDGVCTVRDGKAECRCQSGEDWWYMGERCEKRGSTRDTIVIAVS	Y
Meprin A β (mouse)	VPDPVPTLAVHNACSEVVCQNGGICVVQDGRAECKCPAGEDWWYMGKRCEKRGSTRDTVIIAVS	N
L-Selectin	PLASFSFTSACTFICSEGTELIGKKKTICESSGIWSNPSPICQKLDKSFSMIKEGDYNPLFIPV	Y
E-selectin	VPGKINMSCSGEPVFGTVCKFACPEGWTLNGSAARTCGATGHWSGLLPTCEAPTESNIPLVAGL	N
P-selectin	AMNCSNLWGNFSYGSICSFHCLEGQLLNGSAQTACQENGHWSTTVPTCQAGPLTIQEALTYFGG	N
L-CDX (E-sel stalk)	LGIMNCSHPLASFSFTSACTFICSEGTELIGKKKTICESSGIWSNPSPICEAPTESNIPLFIPV	N
TGFα	VSHFNDCPDSHTQFCFHGTCRFLVQEDKPACVCHSGYVGARCEHADLLAVVAASQKKQAITALV	Y
EGFR	GPHCVKTCPAGVMGENNTLVWKYADAGHVCHLCHPNCTYGCTGPGLEGCPTNGPKIPSIATGMV	N
EGFR/TNFRI	VKTCPAGVMGENNTLVWKYADAGHVCHLCHPNCTYGCTGPGLEGIENVKGTEDSGTTSIATGMV	Y
hu-p55-TNF-RI	VHLSCQEKQNTVCTCHAGFFLRENECVSCSNCKKSLECTKLCLPQIENVKGTEDSGTTVLLPLV	Y
TNFRI-NV172/3AA	VHLSCQEKQNTVCTCHAGFFLRENECVSCSNCKKSLECTKLCLPQIEAAKGTEDSGTTVLLPLV	Y
TNFRI-Δ172/3	VHLSCQEKQNTVCTCHAGFFLRENECVSCSNCKKSLECTKLCLPQIE--KGTEDSGTTVLLPLV	N
TNFRI-Δ174/5	VHLSCQEKQNTVCTCHAGFFLRENECVSCSNCKKSLECTKLCLPQIENV--TEDSGTTVLLPLV	Y
TNFRI-Δ177/8/9	VHLSCQEKQNTVCTCHAGFFLRENECVSCSNCKKSLECTKLCLPQIENVKGT---GTTVLLPLV	N
P75 TNFRII	CTSTSPTRSMAPGAVHLPQPVSTRSQHTQPTPEPSTAPSTSFLLPMGPSPPAEGSTGDEALPVG	Y
HER2	CVARCPSGVKPDLSYMPIWKFPDEEGACQPCPINCTHSCVDLDDKGCPAEQRASPLTSIVSAVV	N
HER4 JM-a	PDGLQGANSFIFKYADPDRECHPCHPNCTQGC***NGPTSHDCIYYPWTGHSTLPQHA***RTPLIAAGV	Y
HER4 JM-b	KDGPNCVEKCPDGLQGANSFIFKYADPDRECHPCHPNCTQGC***IGSSIEDCIGLM***DRTPLIAAGV	N
CD4	MLSLKLENKEAKVSKREKAVWVLNPEAGMWQCLLSDSGQVLLESNIKVLPTWSTPVQPMALIVL	N
ACE/CD4-5	MLSLKLENKEAKVSKREKAVWVLNPEAGMWQCLLSDSGQVLLESNIKVLPTWSTPVQPMALIVL	Y
MDP (pig)	ELLRRQWTEAEVRGALADNLLRVFEAVEQASNHAQVPGEEPIPLGQLEASCRTNYGYS---GPI	N
MDP-STM	SNHAQVPGEEPIPLGQLEASCRTNYGYWTPNSARSEGPLPDSGRVSFLGLDLDAQQARVGQWLL	Y
MDP-TM	AELLRRQWTEAEVRGALADNLLRVFEAVEQASNHAQVPGEEPIPLGQLEASCRTNYGYWLLLFL	N
β-glycan (rat)	DACTSLDATMIWTMMQNKKTFTKPLAVVLQVDYKENVPSTKDSSPIPPPPPQIFHGLDTLTVMG	N
β-G-TGFα	DACTSLDATMIWTMMQNKKTFTKPLAVVLQVDYKENVPSTKDSSDLLAVVAASQKKQATLTVMG	Y
β-G-APP	DACTSLDATMIWTMMQNKKTFTKPLAVVLQVDYKENVPSTKDSSHQKLVFFAEDVGSNTLTVMG	Y
IL6R	PEAMGTPWTESRSPPAENEVSTPMQALTTNKDDDNILFRDSANATSLPVQDSSSVPLPTFLVAG	Y
gp130	AVNVDSSHTEYTLSSLTSDTLYMVRMAAYTDEGGKDGPEFTFTTPKF.....AQGEIEAIVVPV	N
gp130Q615S	AVNVDSSHTEYTLSSLTSDTLYMVRMAAYTDEGGKDGPEFTFTTPKF.....ASGEIEAIVVPV	N
gpIL130 (IL6R)	AVNVDSSHTEYTLSSLTSDTLYMVRMAAYTDEGGKDGPEFTSLPVQDSSSVPASGEIEAIVVPV	Y
gp8IL130	AVNVDSSHTEYTLSSLTSDTLYMVRMAAYTDEGGKDGPEF..LPVQDSSS..ASGEIEAIVVPV	Y
gp4IL130	AVNVDSSHTEYTLSSLTSDTLYMVRMAAYTDEGGKDGPEF....VQDS....ASGEIEAIVVPV	Y

gpΔ41L130	AVNVDSSHTEYTLSSLTSDTLYMVRMAAYTDEGGKDGPEFTSLP....SSVPASGEIEAIVVPV	Y
gpΔ81L130	AVNVDSSHTEYTLSSLTSDTLYMVRMAAYTDEGGKDGPEFTS.....VPASGEIEAIVVPV	Y
gpTN130 (TNFα)	AVNVDSSHTEYTLSSLTSDTLYMVRMAAYTDEGGKDGPEFSPLAQAVRSSSRASGEIEAIVVPV	Y
gpRT130 (rev.TNFα)	AVNVDSSHTEYTLSSLTSDTLYMVRMAAYTDEGGKDGPEFRSSSRVAQALPSASGEIEAIVVPV	Y
gpTG130 (TGFα)	AVNVDSSHTEYTLSSLTSDTLYMVRMAAYTDEGGKDGPEFHADLLAVVAASQASGEIEAIVVPV	Y
LIFR	SDIKVKNITDISQKTLRIADLQGKTSYHLVLRAYTDGGVGPEKSMYVVTKEN.....SVGLIIA	N
gpSLIFR130	AVNVDSSHTEYTLSSLTSDTLYMVRMAAYTDEGGKDGPEF...SMYVVTK..ASGEIEAIVVPV	Y
gpLLIFR130	AVNVDSSHTEYTLSSLTSDTLYMVRMAAYTDEGGKDGPEF...SMYVVTKENASGEIEAIVVPV	Y
APP	ARPAADRGLTTRPGSGLTNIKTEEISEVKMDAEFRHDSGYEVHHQKLVFFAEDVGSNKGAIIGL	Y
APPQ611A/K612A	ARPAADRGLTTRPGSGLTNIKTEEISEVKMDAEFRHDSGYEVHHAALVFFAEDVGSNKGAIIGL	Y
APPQ611A/K612T	ARPAADRGLTTRPGSGLTNIKTEEISEVKMDAEFRHDSGYEVHHATLVFFAEDVGSNKGAIIGL	Y
APPΔL601-D619	ARPAADRGLTTRPGSGLTNIKTEEISEVKMDAEF.....VGSNKGAIIGL	Y
APPΔL613-F616	ARPAADRGLTTRPGSGLTNIKTEEISEVKMDAEFRHDSGYEVHHQK....AEDVGSNKGAIIGL	Y
APPΔL613-E618	ARPAADRGLTTRPGSGLTNIKTEEISEVKMDAEFRHDSGYEVHHQK.....DVGSNKGAIIGL	Y
Ephrin $A2^{wt}$	KFQLFTPFEFRPGHEYYYISATPPNAVDRPCLRLKVYVRPTNETLYEAPEPIFTSNNS===GPI	Y
Ephrin $A2^{ΔS1}$	FRPGHEYYYISATPPNAVDRPCLRLKVYVRPTNETLVDYKDDDKYYEAPEPIFTSNNS===GPI	Y
Ephrin $A2^{ΔS2}$	FTPFEFRPGHEYYYISATPPNAVDRPCLRLKVYVRPTNETLYELDYKDDDKQFTSNNS===GPI	N
Ephrin $A2^{ΔS3}$	RPGHEYYYISATPPNAVDRPCLRLKVYVRPTNETLYEAPEPSVDYKDDDKPIFTSNNS===GPI	N
N-CAM L1	LSPQYVSYNQSSYTQWDLQPDTDYEIHLFKERMFRHQMAVKTNGTGRVRLPPAGFATEGWFIGF	Y
N-CAM L1 [conf.]	SPQYVSYNQSSYTQWDLQPDTDYEIHLFKERMFRHQMAVKTNGTGRVRLPPAWLCATEGWFIGF	Y
CSF1	ETPLQLLEKVKNVFNETKNLLDKDWNIFSKNCNNSFAECSSQGHERQSEGSSSPQLQESVFHLL	Y
HB-EGF	KKRDPCLRKYKDFCIHGECKYVKELRAPSCICHPGYHGERCHGLSLPVENRLYTYDHTTILAVV	Y
CD44	GDSNSNVNRSLSGDQDTFHPSGGSHTTHGSESDGHSHGSQEGGANTTSGPIRTPQIPEWLIILA	Y
LDL-R	VSSTAVRTQHTTTRPVPDTSRLPGATPGLTTVEIVTMSHQALGDVAGRGNEKKPSSVRALSIVL	Y?
SorLA (~LDL-R)	TDNFFKISNLKMGHNYTFTVQARCLFGNQICGEPAILLYDELGSGADASATQAARSTDVAAVVV	Y
LRP1	CNCTDGRVAPSCLTCVGHCSNGGSCTMNSKMMPECQCPPHMTGPRCEEHVFSQQQPGHIASILI	Y
TNF-α	LHFGVIGPQREEFPRDLSLISPLAQAVRSSSRTPSDKPVAHVVANPQAEGQLQWLNRRANALLA	Y
BLyS	QVAALQGDLASLRAELQGHHAEKLPAGAGAPKAGLEEAPAVTAGLKIFEPPAPGEGNSSQNSRN KRAVQGPEETVTQDCLQLI	Y

All sequences are of human origin, unless otherwise stated. The TM domain is highlighted in blue, and the proximal ectodomain (where annotated in GenBank) in yellow. Known cleavage sites are shown with a black arrow. GPI-linked anchors are indicated with "===GPI". Interesting features such as chimeric sequences, putative N-linked sites, alternative splicing sequences and cysteines are shown in bold. The sequence of testis ACE is in blue type while the N-domain sequence and insertion mutants are in red type. The region thought to be responsible for the shedding of PPHβ is highlighted in green. Part of the βA4 peptide is highlighted in grey.

References for Table AI.2:

wtACE	Ehlers *et al.*, 1996
ACE-Ndom	Pang *et al.*, 2001
ACE-Δ17	Ehlers *et al.*, 1996
ACE-Δ24	
ACE-Δ47	
ACE-Δ6	Schwager *et al.*, 1999
ACE-Δ11	This thesis
ACE-Δ16	
ACE-Δ5	
ACE-ΔR627	
ACE-JGL	Schwager *et al.*, 1999
ACE-LDL	Ehlers *et al.*, 1996
ACE-EGF	Schwager *et al.*, 1998
ACE-FIXEGF	Schwager *et al.*, in press
ACE-MINI23	
Meprin A α human	Pischitzis *et al.*, 1999
Meprin A α mouse	
Meprin A β human	
Meprin A β mouse	
L-Selectin	Kahn *et al.*, 1994
E-selectin	
P-selectin	
L-CDX (E-sel stalk)	Migaki *et al.*, 1995
TGFα	Derynck *et al.*, 1984
EGFR	Brakebusch *et al.*, 1994; Himmler *et al.*, 1990
EGFR/TNFRI	
hu-p55-TNF-RI	
TNFRI-NV172/3AA	
TNFRI-Δ172/3	
TNFRI-Δ174/5	
TNFRI-Δ177/8/9	
P75 TNFRII	Nophar *et al.*, 1990
HER2	Vecchi *et al.*, 1996
HER4 JM-a	Elenius *et al.*, 1997
HER4 JM-b	
CD4	Sadhukhan *et al.*, 1998
ACE/CD4-5	
MDP (pig)	Pang *et al.*, 2001
MDP-STM	
MDP-TM	

β-glycan (rat)	Arribas *et al.* 1997
β-G-TGFα	
β-G-APP	
IL6R	Mullberg *et al.*, 1994
gp130	Althoff *et al.*, 2001
gp130Q615S	
gpIL130 (IL6R)	
gp8IL130	
gp4IL130	
gpΔ4IL130	
gpΔ8IL130	
gpTN130 (TNFα)	
gpRT130 (rev.TNFα)	
gpTG130 (TGFα)	
LIFR	
gpSLIFR130	
gpLLIFR130	
βAPP	Esch *et al.*, 1990; Maruyama *et al.*, 1990; Masters *et al.*, 1985
APPQ611A/K612A	Zhong *et al.*, 1994; Maruyama *et al.*, 1990
APPQ611A/K612T	
APPΔL601-D619	
APPΔL613-F616	
APPΔL613-E618	
Ephrin $A2^{wt}$	Hattori *et al.*, 2000
Ephrin $A2^{IS1}$	
Ephrin $A2^{IS2}$	
Ephrin $A2^{IS3}$	
N-CAM L1	Beer *et al.*, 1999; Mechtersheimer *et al.*, 2001
N-CAM L1 [conf.]	
CSF1	Deng *et al.*, 1996; Halenbeck *et al.*, 1988
HB-EGF	Goishi *et al.*, 1995; Izumi *et al.*, 1998
CD44	Kajita *et al.*, 2001
LDL-R human	M. Begg, unpublished data
SorLA human	Hampe *et al.*, 2000
LRP1	Quinne *et al.*, 1999

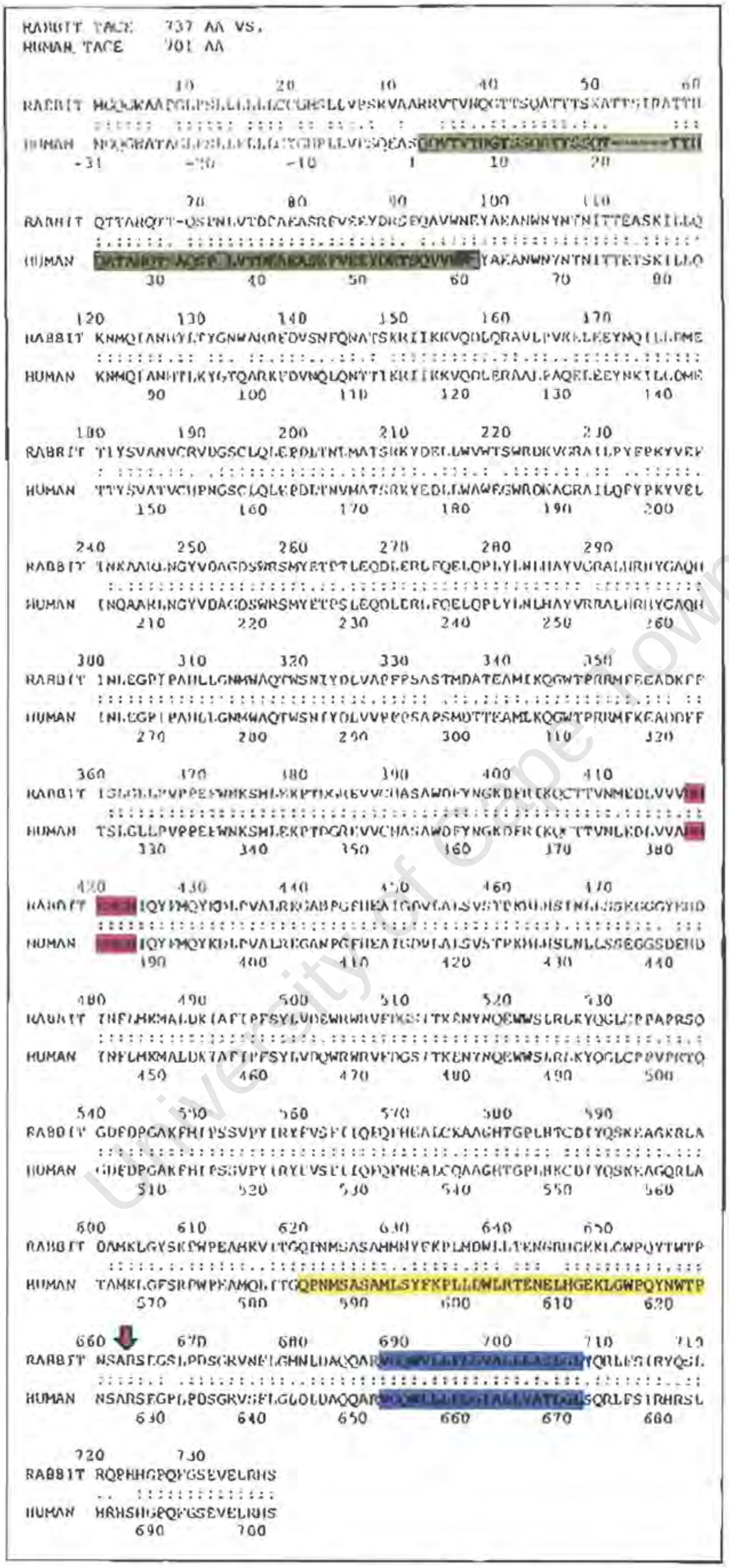

Figure AI.1) Comparison of rabbit and human ACE_T sequences

The peptide sequences of rabbit and human testis ACE are aligned here to aid comprehension of the paper by Sadhukhan *et al*, which is particularly relevant to this thesis [Sadhukhan, 1998]. The TM is highlighted in blue, the proximal ectodomain mutant in yellow, and the region deleted in ACEΔ36N-wt, ACEΔ61E in green and the catalytic site in mauve. The cleavage site is indicated with an arrow.

Table AI.3) Taxonomic lineage of species whose ACE cDNA is cloned		
Name:		**Lineage:**
Common	**Species**	
Humans	*Homo sapiens*	Eukaryota; Metazoa; Chordata; Craniata; Vertebrata; Euteleostomi; **Mammalia**; Eutheria; **Primates**; Catarrhini; **Hominidae**; Homo
Chimpanzee	*Pan troglodytes*	Eukaryota; Metazoa; Chordata; Craniata; Vertebrata; Euteleostomi; **Mammalia**; Eutheria; **Primates**; Catarrhini; **Hominidae**; Pan
Rabbit	*Oryctolagus cuniculus*	Eukaryota; Metazoa; Chordata; Craniata; Vertebrata; Euteleostomi; **Mammalia**; Eutheria; **Lagomorpha**; Leporidae; Oryctolagus
Cow	*Bos taurus*	Eukaryota; Metazoa; Chordata; Craniata; Vertebrata; Euteleostomi; **Mammalia**; Eutheria; Cetartiodactyla; **Ruminantia**; Pecora; Bovoidea; Bovidae; **Bovinae**; Bos
Dog	*Canis familiaris*	Eukaryota; Metazoa; Chordata; Craniata; Vertebrata; Euteleostomi; **Mammalia**; Eutheria; **Carnivora**; Fissipedia; **Canidae**; Canis
Rat	*Rattus norvegicus*	Eukaryota; Metazoa; Chordata; Craniata; Vertebrata; Euteleostomi; **Mammalia**; Eutheria; **Rodentia**; Sciurognathi; Muridae; **Murinae**; Rattus
Mouse	*Mus musculus*	**Eukaryota**; **Metazoa**; Chordata; Craniata; **Vertebrata**; Euteleostomi; **Mammalia**; **Eutheria**; **Rodentia**; Sciurognathi; Muridae; **Murinae**; Mus
Chicken	*Gallus gallus*	**Eukaryota**; **Metazoa**; **Chordata**; Craniata; **Vertebrata**; Euteleostomi; Archosauria; **Aves**; Neognathae; Galliformes; Phasianidae; Phasianinae; Gallus
Worm	*Caenorhabditis elegans*	**Eukaryota**; **Metazoa**; **Nematoda**; Chromadorea; Rhabditida; Rhabditoidea; Rhabditidae; Peloderinae; Caenorhabditis
Fruit fly	*Drosophila melanogaster*	**Eukaryota**; **Metazoa**; **Arthropoda**; Tracheata; Hexapoda; **Insecta**; Pterygota; Neoptera; Endopterygota; **Diptera**; Brachycera; Muscomorpha; **Ephydroidea**; Drosophilidae; Drosophila
Buffalo fly	*Haematobia irritans exigua*	**Eukaryota**; **Metazoa**; **Arthropoda**; Tracheata; Hexapoda; **Insecta**; Pterygota; Neoptera; Endopterygota; **Diptera**; Brachycera; Muscomorpha; **Muscoidea**; Muscidae; Haematobia; Haematobia irritans
Silkworm	*Bombyx mori*	Eukaryota; Metazoa; **Arthropoda**; Tracheata; Hexapoda; **Insecta**; Pterygota; Neoptera; Endopterygota; **Lepidoptera**; Glossata; Ditrysia; Bombycoidea; Bombycidae; Bombyx
Tick	*Boophilus microplus*	Eukaryota; Metazoa; **Arthropoda**; Chelicerata; **Arachnida**; **Acari**; **Parasitiformes**; Ixodida; Ixodidae; Boophilus
Zebrafish EST db[Ψ]	*Danio rerio*	Eukaryota; **Metazoa**; Chordata; Craniata; **Vertebrata**; **Euteleostomi**; **Actinopterygii**; Neopterygii; Teleostei; Euteleostei; **Ostariophysi**; Cypriniformes; **Cyprinidae**; Rasborinae; Danio

Lineages obtained from the NCBI Taxonomy database.
[Ψ]The full cDNA for Zebrafish ACE has not, as yet, been cloned.

The Taxonomic 'history' of ACE Evolution

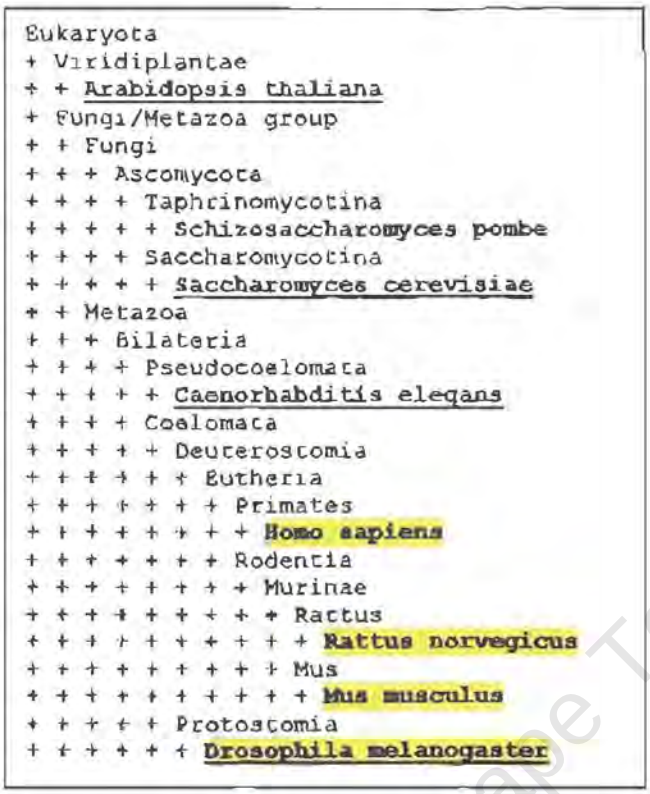

Figure A1.2) Fully sequenced genomes that do/do not contain an ACE gene

The taxonomic, and thus likely evolutionary, relationship between species (bold) that have an ACE gene (highlighted in yellow) and those that do not. Note that of the four eukaryotic species whose genomes have been completely sequenced (underlined), three do not contain ACE related sequences, namely *Caenorhabditis elegans* (nematode worm), *Saccharomyces cerevisiae* (yeast) and *Arabidopsis thaliana* (mouse-ear cress) [NCBI, Entrez BLASTp, November 2001]. Output generated from the NCBI Entrez Taxonomy homepage: [http://www.ncbi.nlm.nih.gov/entrez/query.fcgi?db=Taxonomy].

Table AI.4) ACE homologues								
Name		Type	Length (p#)	% ID (ACE_T)$^{\psi}$		% ID (N-dom)$^{\xi}$		Seq. #$^{\tau}$
Common	Species			%	aa	%	aa	
Humans	*Homo sapiens*	ACE_T	732	100%	732			sp|P22966|
Humans	*Homo sapiens*	ACE_S	1306	100%	665	54%	616	sp|P12821|
Human ACEH	*Homo sapiens*	?	805	41%				gi|8650466|
Chimpanzee	*Pan troglodytes*	ACE_S	1304	99%	666	54%	616	gi|11138413|
		ACE_T	732	99%	732			gi|11138414|
Rabbit	*Oryctolagus cuniculus*	ACE_S	1310	87%	666	53%	605	sp|P12822|
		ACE_T	737	84%	737			sp|P22968|
Cow	*Bos taurus*	ACE_S	1306	81%	666	53%	608	gi|449408|
Rat	*Rattus norvegicus*	ACE_S	1313	80%	667	53%	639	sp|P47820|
Mouse	*Mus musculus*	ACE_S	1312	79%	667	52%	637	sp|P09470|
		ACE_T	732	78%	733			sp|P22967|
Chicken	*Gallus gallus*	ACE_S	1193	63%	650	59%	510	sp|Q10751|
Worm	*Caenorhabditis elegans*	ACE_S?	907					
Fruit fly	*Drosophila melanogaster*	AnCE	615?	44%	600			gi|1373008|
	D. melanogaster	ACEr	?					gi|1405881|
Buffalo fly	*Haematobia irritans exigua*	ACE_T	611	43%	573			sp|Q10715|
Silkworm	*Bombyx mori*	ACE_S?	648	45%	595			gi|8918492|
Tick	*Boophilus microplus*	ACE_S?	660	42%	588			gi|1468981|
Zebrafish EST db	*Danio rerio*	ACE2	59?					
Worm	*Caenorhabditis elegans*	No HExxH	907	28%	616			AAA98719.1

All data obtained using NCBI's BLASTp search. Sequences shown with an identity to ACE_T >40% have an 'expect' value of <e-136 and are thus significantly homologous to human testis ACE. (ψ), percentage identity to human testis ACE. (ξ), percentage identity of N-domain to human ACE_T. (ψ,ξ), aa refers here to range of amino acid showing identity. (τ), sequence ID number (SwissProt or GenBank). References: Human ACES [Soubrier *et al.*, 1988]; Human ACET [Ehlers *et al.*, 1989; Lattion *et al.*, 1989]; Human ACEH/ACE2 [Tipnis *et al.*, 2000; Donoghue *et al.*, 2000; Suzuki Y, unpublished;]; Chimpanzee [Dufour *et al.*, 2000]; Cow [Shai *et al.*, 1992]; Rat [Tatei *et al.*, 1995]; Mouse [Bernstein *et al.*, 1988]; Rabbit ACE [Kumar *et al.*, 1991]; Chicken [Esther, Jr. *et al.*, 1994b]; Fruit fly [Cornell *et al.*, 1995; Tatei *et al.*, 1995]; Buffalo Fly ACET [Wijffels *et al.*, 1996]; Silkworm [Quan *et al.*, 2001].

Appendix II: Methods

The methods used in this thesis were predominantly derived from Short Protocols in Molecular Biology, 2nd edition, John Wiley & sons, N.Y., 1992. Reagents or short protocols that appear in Appendix III are highlighted in bold.

AII.1) Recombinant DNA methods:

AII.1.1) Polymerase chain reaction (PCR)

PCR DNA amplifications were performed in a final volume of 50 µl, using a Hybaid DNASprint PCR apparatus. The heated lid function of these machines allows one to leave out the mineral oil drop layering that is usually needed to prevent evaporation. The final reaction is: 1 ng to 1 µg DNA template, each primer at a final concetration of 800 nM, 200 µM dNTP (dATP, dGTP, dCTP and dTTP), 1x *pfu* buffer, 5 U *pfu* DNA polymerase (Promega) in a final volume of 50 µl. A stock solution was prepared containing 1 µl of a 10 µM dNTP stock, 5 µl of the 10x buffer, and 39 µl H_2O for each 45 µl, which was then placed into 200 µl tubes on ice. The DNA template (1µl) and 2 µl of each primer stock (20 µM) was then added, and finally 1-2 µl *pfu* DNA polymerase was added immediately prior to the PCR. The lid of the PCR machine was pre-heated to ensure an immediate start of the reaction which is a 3 minute denaturation step at 94°C. This is followed by 30 cycles of denaturation at 94°C for 30 seconds, annealing at between 50°C and 70°C for 60 seconds, and elongation at 70°C for 90 seconds. A final elongation step at 70°C for 5 min was performed to ensure that all DNA was double stranded, before holding at 4°C O/N. **DNA loading buffer** was added (6 µl), and the full 56 µl mixture was analysed on **1.5% agarose** gels in an electric field of 70V for 1 hr, and photographed or printed using a video camera. The gels were then scanned.

The thermostable *pfu* DNA polymerase supplied by Promega, isolated from *Pyrococcus furiosis*, is ideal for high fidelity amplification of DNA.

AII.I.2) Restriction enzyme digestion of DNA and electrophoresis

All restriction enzyme digests of mini-preparation or Qiagen isolated DNA were prepared in a total reaction volume of 20 µl. This contained the appropriate enzyme buffer(A, B, L, M or H) at 1x concentration, between 5 and 10 units of each enzyme, and approximately 1 µg DNA. The digestion cocktails were incubated at 37°C for at least 1 hour (except for digestions involving *BclI*), after which the reaction was terminated with the addition of 0.1 volumes of 10x sucrose loading dye. When digesting with *BclI*, the reaction was incubated at 37°C for 1 hour, and then at 55°C for a further hour, before being terminated. The digested DNA was separated using electrophoresis through 6x10 cm agarose gels (TBE[EtBr]). The percentage agarose used depended on the size of the fragments being analysed; **0.8%** and **1.5% agarose** gels were used to separate large (>1000 bp) and small (<1000 bp) DNA molecules respectively. The gel was immersed in **TBE[EtBr] buffer** and a constant voltage of

70 V was applied until the dark blue Bromophenol Blue band had run 2/3 of the length of the gel. The DNA was then visualised using an ultraviolet light box a Polaroid picture was taken using a 1 second exposure at F_o = 5.6 or 8. The relevant bands were then excised using sterile scalpel blades.

AII.1.3) DNA extraction from *Escherichia coli*

Plasmid-containing *E. coli* were grown O/N in either 5 ml or 50 ml LB supplemented with 100 µg/ml ampicillin and plasmids extracted using the mini- and midi-kit (Qiagen) respectively, according to the manufacturers instructions. DNA was quantitated by making a 1:100 dilution and recording the A_{260} and A_{280} in a Anthelite Advanced spectrophotometer (Secoman), and the equation: 1 A_{260} Unit of dsDNA = 50 µg/ml H_2O. All sequencing was done on DNA prepared using the Midi-kit with a A_{260}/A_{280} ratio of greater than 1.8.

AII.1.4) Cloning a DNA fragment into a plasmid vector

The relevant restriction digested bands were excised out of agarose gels, after electrophoresis, and placed together in a GenElute agarose spin column (Sigma) which had previously been equilibrated with 100 µl 1x TE. The slices were spun to near desiccation (10 min) in a Sorvall MC 12C desktop microcentrifuge, and the fluid phase collected in a 1.5 ml tube. The DNA was then co-precipitated by adding $1/10^{th}$ volume 3M sodium acetate (pH 5.2) and 2.5 volumes ice-cold ethanol, mixing and incubating at -20°C for 60 min. The DNA was pelleted for 10 minutes in a microcentrifuge, washed with 500 µl 70 % ethanol, and dried using a Speedyvac centrifuge. The pellet was resuspended in 8 µl H_2O, to which 1 µl 10x ligase buffer was added, and 1 µl T4 DNA ligase (Roche). Ligation was allowed to proceed for 60 min at 37°C, after which the 10 µl mixture was transformed directly into competent *E. coli* cells.

AII.1.5) Transforming *Escherichia coli*

The RbCl method for competent *E. coli* was preferred, as cells can be frozen at -70°C for long periods without losing their transfection efficiency. A single colony of XL1 blue *E. coli* (Stratagene) was inoculated in 5 ml **Ψ-broth** and the cells grown O/N at 37°C. The following day the broth was added to 100 ml of pre-warmed Ψ-broth, and the cell growth measured every 30 min by reading the OD_{550}. When the OD_{550} was greater than 0.35 the cells were chilled rapidly on ice and centrifuged in 2x 35 ml SS34 tubes in a pre-chilled Beckman J2-21 centrifuge at 2500 rpm for 5 min at 4°C. Cells were resuspended gently in 2x 10.5 ml ice-cold **TFB1**, pooled and incubated on ice for 90 min. Cells were again centrifuged at 2500 rpm for 5 min at 4°C, and resuspended in 3.5 ml ice-cold **TBF2**. 100 µl aliquots were placed in individual 1.5 ml Eppendorf microfuge tubes, and flash-frozen in liquid nitrogen, and stored at -70°C.

To transform these cells with Plasmid, the cells were first thawed to just molten at RT, and then incubated on ice for 10 min. The ligation mixture, or up to 10 ng of plasmid DNA, was then added and the cells further incubated on ice for 20 min. Heat shock was performed by placing the tubes in a 42°C water bath for exactly 60 sec, followed by a 2 min incubation on ice. 900 µl Ψ-broth was then added, and the cells

allowed to recover at 37°C, shaking, for 50 min, after which they were plated onto LA plates containing 100 μg/ml ampicillin.

AII.1.6) DNA sequencing

All PCR products used for mutant construction were sequenced in both directions, twice, using both the SequiTherm Excel II DNA Sequencing Kit (Epicentre Technologies) and an ALFexpress DNA Automated Sequencer (APBiotech).

SequiTherm Excel II Cycle sequencing:
PCR products were cloned into pBS SK (Stratagene) and sequenced using either the T3 or T4 primers. The PCR-based cycle-sequencing was done using the SequiTherm Excel II DNA Sequencing Kit (Epicentre Technologies) exactly as per manufacturers instructions, using [α-^{35}S]-dATP (Amersham) and a PCRSprint PCR machine (Hybaid). The radioactive products were then electrophoresed through a 0.5 mm thick 6% acrylamide/bisacrylamide DNA sequencing gel containing 7M urea, at 96 W, 2000V, 55°C for about 1.5 hours each run. The gels were dried onto blotting paper and autoradiographed. The sequences were read manually and processed using the GCG[Seqed] function.

ALF sequencing:
Sequencing was done by the Specialist Sequencing Service, Department of Microbiology, University of Cape Town, using Thermo Sequenase fluorescent labelled primer cycle sequencing kit with 7-deaza-dGTP (Amersham Pharmacia Biotech AB) according to the manufacturer's instructions and cycle sequenced. The chain termination technique of Sanger *et al.*, 1977 was employed. Electrophoresis was done using 5% Long Ranger gel solution (FMC BioProducts), 5% gel run according to the manufacturer's operating procedure for 13 hrs at 55 deg C, using standard gel cassette, 0.5mm spacers and controlled by ALFwin 2.1 software. Data was processed by ALFwin version 2.1 software (APBiotech).

AII.2) Tissue culture:

AII.2.1) CaPO4 Transfection

The mammalian expression vector pLEN-ACE, and mutants thereof, were co-transfected with pSV2-NEO into CHO-K1 cells using the ProFection Calcium Phosphate Mammalian Transfection System kit, according to the manufacturer's instructions (Promega). pSV2-NEO containing cells were selected using 0.8 mg/ml G418 (GibcoBRL) or Genetesin (Sigma). Resistant cells were cloned using either the cloning ring method or limiting dilution.

AII.2.2) Cloning CHO cells

Cloning rings:
Cloning rings were prepared by cutting the top 1cm off blue 1000 μl pipette tips with a hot scalpel blade, and inverting onto a glass Petri dish smeared with vacuum grease. This was then wrapped in foil and autoclaved. The 100 mm dish containing neomycin resistant colonies was washed with PBS, and the cloning rings carefully placed on

each colony. Cells were lifted by adding 100 µl 5 mM EDTA in PBS, incubating for 5 min at 37°C, and transferring to 12-well (4.0 cm^2) dishes.

Limiting dilution:
Neomycin resistant CHO cells were lifted from 100 mm dishes using 5 mM EDTA in PBS and resuspended in 10 ml medium. 100 µl was added to 9.9 ml isoton solution, and cell number counted in a coulter counter. 8x 10 ml tubes were prepared, the first containing 2 ml of medium each. The volume containing 3600 cells was added to the first tube, and this was made up to 4 ml. A sterile 5 ml pipette was then used to mix the contents of each tube and transfer 2 ml to the next tube. This results in 1600, 800, 400, 200, 100, 50, 25, and 12.5 cells per tube respectively. Two drops of each dilution were added to each well of a 96-well plate, using a 5 ml pipette and starting at the lowest dilution. This results in each row of the 96 well containing an average of 64, 32, 16, 8, 4, 2, 1 or 0.5 cells per well. A further 2 drops of fresh medium was added to each well, and the plate incubated at 37°C, 5% CO_2, humidified. Each well is monitored for colony formation, and any which have more than one were discarded.

AII.3) Protein analysis:

AII.3.1) Western Blot analysis

SDS-PAGE: Proteins were electrophoresed through a 10% acrylamide, Sodium dodecyl sulphate gel, with a 3% stacking gel, using the Bio-Rad Gel electrophoresis apparatus and according to the manufacturers instructions [Bio-Rad]. 6 µl **5x SDS loading buffer** was added to 24 µl of each sample and boiled for 5 minutes prior to loading. Samples were run at 50 mA for 1 hour.
Blotting: Gels were soaked in blotting buffer for 15 min prior to assembly in the blotting apparatus (Bio-Rad). Proteins were electophoresed onto nitrocellulose in **blotting buffer** at 100 V for 1 hours, with cooling.
Immunodetection: Any non-specific sites on the nitrocellulose blots were blocked using 5% skim milk **blocking buffer** for 1 hour. A 1:1000 dilution of the rabbit anti-ace serum was then used to probe ACE, for 1.5 hours while shaking, followed by washing with copious quantities of blocking buffer. The rabbit antibody was then probed using 1:2000 dilution of goat anti-rabbit/HRP conjugated antibody, for 1 hour. After extensive washing with blocking buffer, the HRP was detected using the ECL chemiluminescence kit (Amersham).

AII.3.2) Protein concentration determination

The Bradford method was used to determine protein concentration [Bradford, 1976]. 800 µl of sample was added to 200 µl Bio-Rad protein assay solution (Bio-Rad), incubated at RT for 5 min, and the A_{595} determined in a spectrophotometer. A standard curve using 0, 1, 2, 4, 8, 12, 16, 20 and 24 µg/ml BSA was used to convert the A_{595} to µg protein/ml.

AII.3.3) Triton X114 separation of ACE

Medium and cell extract samples were centrifuged in 1.5 ml Eppendorf tubes for 3 min to remove any cells or debris. 50 µl of each sample was mixed with 50 µl Triton extraction buffer [10mM Tris, pH 7.5, 150 mM NaCl]. An equal volume (100µl) of

2% Triton X114 (in Triton extraction buffer) was added and mixed thoroughly. After allowing the cloudy solution to clear on ice (5 min), the samples were placed at 30°C for 3 minutes. The samples were immediately centrifuged at RT for 3 minutes. The aqueous phase (~180 µl) was carefully removed, and placed in a new Eppendorf. To equalise the volumes, the detergent droplet was resuspended in ~146 µl Triton extraction buffer, and placed on ice to allow the micelles to dissolve. HHL assays were performed on 20 µl of both the detergent and aqueous phase samples, and the percentage activity in the aqueous phase determined.

AII.3.4) Affinity purification of ACE:

A 10 ml column was with packed with Sepharose-[28Å]-Lisinopril. The column was pre-equilibrated with **wash buffer** [20 mM HEPES, pH 7.5; 0.5 M NaCl], and the medium sample (~400 ml cell-free medium) loaded over 12 hours using a Minipuls3 peristaltic pump (Gilson). The protein was washed extensively O/N using copious quantities of wash buffer, and the protein eluted off using 50 mM borate, pH 9.5. Fractions were collected and analysed for ACE activity using HHL as substrate, and the ACE-containing fractions pooled, dialysed against H_2O and freeze-dried.

Appendix III: Reagents and Miscellaneous data

Reagents:

Abz/Dnp substrate solution
[0.1 M Tris/HCl, pH 7.0, 50 mM NaCl and 10 μM $ZnCl_2$].

40% Acrylamide stock (100 ml)
[40% acylamide (w/v), 2% bis-acrylamide (w/v)]. Add 38.0 g Acrylamide and 2.0 g Bis-acrylamide to 100 ml sdH_2O. Store in a foil-wrapped blue-topped bottle at 4°C.

Agarose gels (50 ml)
Agarose gels were made by adding either 0.4 g or 0.75 g Agarose to 50 ml TBE[EtBr], boiling for 2.5 minutes, and then allowing to set at room temperature (RT) in a 5 cm × 8 cm casting well.

Ampicillin stock (100 mg/ml, 1 ml)
100 mg Ampicillin was dissolved in 1000 μl H_2O and stored at 4°C. 1μl of this stock was added to 1 ml of LB for a final antibiotic concentration of 100 μg/ml.

10% Amps (1 ml)
[10% Ammonium persulphate (w/v)]
Dissolve 0.1 g Ammonium persulphate $[(NH_4)_2S_2O_8]$ in 1ml sdH_2O.

Blocking buffer (1L)
Mix 25 g skim milk powder, 500 μl Tween-20, 50 ml 2 M NaCl and 25 ml 1 M Tris pH 7.4.

Blotting buffer (1L)
Mix 3.025 g Tris, 14.4 g glycine in 800 ml H_2O. Add 200 ml methanol.

10× Boric Acid (500 ml, pH 9.5)
15.46 g Boric acid was added to 400ml H_2O. This was adjusted to a pH of 9.5 using 10M NaOH. The final volume was corrected to 500ml with H_2O.

Boric Acid (50 mM, pH 9.5)
A 1:10 dilution of the 500 mM Borate (pH 9.5) was made in H_2O and used to elute the purified ACE off a lisinopril-sepharose column.

1% Bromophenol Blue (1 ml)
Dissolve 10 mg Bromophenol Blue in 1000 μl H_2O.

3% BSA in PBS^{++} (20 ml)
Dissolve 600 mg BSA fraction V in 20 ml PBS^{++}.

10 mM chloroquine stock
5.15 mg chloroquine dissolved in 1ml water, filter sterilised.

CHO-K1 cells
[*Cricetulus griseus* (Chinese hamster) ovary cell line; ATCC: CCL-61]
ATCC have this to say about the CHO-K1 cell line: The CHO-K1 cell line was derived as a subclone from the parental CHO Chinese Hamster (*Cricetulus griseus*) cell line initiated from a biopsy of an ovary of an adult Chinese hamster by T. T. Puck in 1957 [Puck, 1958]. The cells require proline in the medium for growth. The cells should be propagated using Ham's F12K medium with 2 mM L-glutamine (achieved with 50% Hams F-12/50% DMEM mixture) adjusted to contain 1.5 g/L sodium bicarbonate, 90%; fetal bovine serum, 10%. The ATCC website is: http://www.atcc.org.

Column Wash Buffer
[0.5 M NaCl, 20 mM HEPES, pH 7,5]
29.22 g NaCl was dissolved in 980 ml H_2O, to which 20 ml 1 M HEPES (pH 7.5) was added, and then sterilised by autoclaving.

COS-1 cells
[*Cercopithecus aethiops* [African green monkey] cell line; ATCC, CRL-1650]

Complete medium
[50% Ham's F-12/50% DMEM supplemented with 20 mM HEPES, pH 7.5, 20 mM L-glutamine and 10 % heat-inactivated foetal calf serum (FCS)]
22 ml Ham's F-12, 22 ml DMEM, 5 ml heat inactivated FCS (56°C for 30 minutes) and 1 ml 1 M HEPES, pH 7.5, was mixed in a 50 ml tube and filter sterilised.

1× DEAE-Dextran/DMEM/PS
Dilute 10× HBS/DEAE-Dextran stock 1:10 in DMEM/PS

DEPC water (1 L)
[0.02% DEPC in H_2O (0.1% recommended by Sigma)]
Add 200 µl diethyl pyrocarbonate [Sigma, D5758] to 1 l H_2O.

DMEM Tissue Culture Medium
Laboratory stocks were used for growing CHO cells. DMEM was bought from Highveld Biological [P.O. Box 488, Kelvin, 2054, South Africa] in a powder form which was hydrated and filter sterilised
References: Dulbecco R., G. Freeman, Virology 8, 395, (1959); Smith, J. D., et al., Virology 12, 185 (1960). Composition (amounts in mg/l): NaCl (6400), KCl (400), $CaCl_2$ (200), $MgSO_4.7H_2O$ (200), NaH_2PO_4 (124), D-glucose (1000), $Fe(NO_3)_3.9H_2O$ (0.1), Na-Pyruvate (110), Phenol Red (15), NaHCO3 (3700), L-Arginine.HCl (84), L-Cysteine (48), L-Glutamine (580), L-Histidine.HCl.H_2O (42), L-Isoleucine (105), L-Leucine (105), L-Lysine.HCl (146), L-Methionine (30), L-Phenylalanine (66), L-Threonine (95), L-Tryptophan (16), L-Tyrosine (72), L-Valine (94), Glycine (30), L-Serine (42), Choline Chloride (4), Folic Acid (4), I-Inositol (7.2), Nicotinamide (4), D-Ca-Pantothenate (4), Pyridoxal.HCl (4), Riboflavin (0.4), Thiamine.HCl (4).

DMEM/PS
[DMEM supplemented with 100 U/ml penicillin and 100 µg/ml streptomycin]
Dilute 500 µl PenStrep stock (100x) in 50 ml DMEM. Filter sterilise and store at 4°C.

DMEM/PSH
[DMEM supplemented with 100 U/ml penicillin, 100 µg/ml streptomycin and 20 mM HEPES, pH7.5]
Add 1 ml 1 M HEPES (pH 7.5) and 500 µl PenStrep stock (100x) to 50 ml DMEM. Filter sterilise and store at 4°C.

DNA Loading Buffer (20 ml)
[0.25% Bromophenol Blue, 0.25% Xylene Cyanol FF, 30% Glycerol]
Dissolve 50 mg Bromophenol Blue, 50 mg Xylene Cyanol FF, and 6.0g Glycerol in sdH_2O. Adjust to 20ml. Filter sterilise and store at 4°C.

0.5 M EDTA (200 ml, pH 8.0)
Dissolve 37.2 g EDTA in 150 ml H_2O. Adjust pH to 8.0 with 10 M NaOH, then the volume to 200ml with H_2O. Autoclave and store at RT.

5 mM EDTA/PBS (50 ml, pH 8.0)
Add 500 µl of 0.5 M EDTA to 50 ml PBS. Filter sterilise and store at 4°C.

Ethidium Bromide Stock [EtBr] (10 ml)
Warning: Ethidium Bromide is highly mutagenic.
[1000× stock solution, 0.5 mg/ml]
Dissolve 5 mg of ethidium bromide [Sigma, E8751] in 10 ml H_2O. Cover with foil and store at RT.

FCS
Foetal calf serum (Amersham) was heat inactivated at 56°C for 30 min. prior to use in complete medium. For use in induction medium, the FCS was further heat inactivated to 70 °C for 15 min.

10% FCS/DMEM/PSH
Mix 5 ml FCS, 44 ml DMEM, 50 µl PenStrep and 1 ml 1 M HEPES pH 7.5 in a 50 ml tube. Filter sterilise.

Formaldehyde agarose gels (40 ml)
Boil 0.4 g agarose in 27.3 ml H_2O with 4 ml 10× RNA Running Buffer for 2.5 minutes. Immediately add 8.53 ml formaldehyde, in a fume hood and pour into a gel chamber as soon as possible. Allow to set in a fume hood.

Formaldehyde loading mix
For each 5 µg RNA sample (made up to 10 µl with H_2O), add 15µl of the formaldehyde loading mix: 3.3 µl H_2O, 1,5 µl 10× RNA running buffer, 7,5 µl deionised formamide, 2,7 µl formaldehyde and 1,5 µl RNA loading buffer.

6 M GnCl buffer
[6 M GnCl, 0.1 M Tris, pH 8.5]

200 mM L-glutamine
Dissolve 292 mg L-glutamine [GibcoBRL; 146 g/mol] in 10 ml H_2O, filter sterilise.

Hams F-12 Tissue Culture Medium
Laboratory stocks were used for growing CHO cells. Hams F-12 was bought from Highveld Biological [P.O. Box 488, Kelvin, 2054, South Africa] in a powder form which was hydrated and filter sterilised.
References: Ham, R. G., PNAS, 53, 288 (1965). Composition (amounts in mg/l): NaCl (7599), KCl (223.6), Na_2HPO_4 (142), $CaCl_2.2H_2O$ (44), $MgCl_2.6H_2O$ (122), $FeSO_4.7H_2O$ (0.834), $CuSO_4.5H_2O$ (0.00249), $ZnSO_4.7H_2O$ (0.863), D-Glucose (1802), Na-Pyruvate (110), Phenol Red (1.2) [10 mg/l final], $NaHCO_3$ (1176), L-Alanine (9), L-Arginine.HCl (211), L-Asparagine (13.2), L-Aspartic Acid (13.3), L-Cysteine.HCl (31.5), L-Glutamine (146), L-Glutamic acid (14.7), Glycine (7.5), L-Histidine.HCl.H_2O (21), L-Isoleucine (4), L-Leucine (13), L-Lysine.HCl (36.5), L-Methionine (4.47), L-Phenylalanine (5), L-Proline (34.5), L-Serine (10.5), L-Threonine (12), L-Tryptophan (2), L-Tyrosine (5.4), L-Valine (11.7), Biotin (0.0073), D-Ca-Pantothenate (0.48), Folic acid (1.3), I-Inositol (18), Nicotinic acid amide (0.037), Pyridoxine.HCl (0.062), Riboflavin (0.038), Thiamine.HCl (0.34), Vitamin B12 (1.36), Hypoxanthine (4.1), Thymidine (0.73), Lipoic acid (0.21), Linoleic acid (0.084), Putrescine.$2H_2O$ (0.161).

10× HBS/DEAE-Dextran stock
30mg/ml DEAE-Dextran (white powder, RT, brown bottle) in HBS (in frozen 1,5ml aliquots)

1M HEPES (500 ml, pH 7.5)
Dissolve 119.15g N-[2-Hydroxyethyl]piperazine-N'-[2-ethanesulfonic acid] (HEPES) [Sigma: H3375] in 400ml H_2O, adjust to pH 7.5 with 10M NaOH and 500ml with H_2O.

HHL assay solution (24 ml)
58.2 mg Hippuryl-His-Leu [Sigma: H1635] was dissolved in 5 ml 0.025 M NaOH, with heating. Once all white powder was dissolved, 1250 µl 1 M HEPES, pH 7.5, 3750 µl 2 M NaCl and 14 ml H_2O were added. Stored at 4 °C.

Induction medium
[Ham's F-12/DMEM supplemented with 20 mM HEPES, pH 7.5, 2 % FCS (70°C, 15 min heat-inactivated) and 40µM $ZnCl_2$]
24 ml Ham's F-12, 24 ml DMEM, 1 ml heat inactivated FCS (70°C for 15 minutes), 1 ml 1 M HEPES, pH 7.5, and 20 µl 0.1 M $ZnCl_2$ was mixed in a 50 ml tube and filter sterilised. Ham's F-12 and DMEM were obtained from laboratory stocks, while FCS from Amersham Pharmacia Biotech.

Sepharose-[28Å]-lisinopril column wash buffer (1 L)
[0.5 M NaCl, 20 mM HEPES, pH 7,5]
29.22 g NaCl was dissolved in 980 ml H_2O, to which 20 ml 1 M HEPES (pH 7.5) was added, and then sterilised by autoclaving. When equilibrating the Lisinopril-sepharose column for cell extract samples, the wash buffer was further supplemented with 10 ml Triton X-100 (1% final) and 10 ml 100 mM PMSF (1 mM final). The columns are stored in wash buffer with the addition of 0.02% Sodium azide. [Warning: Sodium azide causes explosions in lead pipes - check the drains!]

Luria Agar Plates (400 ml, 20 plates)
[10 g/l Tryptone, 5 g/l Yeast Extract Powder, 10 g/l NaCl, 15 g/l Bacteriological Agar, 100 μg/ml Ampicillin]
Luria agar plates were made by adding Tryptone (4 g), Yeast Extract (2 g), NaCl (4 g) and Bacteriological Agar (6g) to 400 ml H_2O in a 500 ml blue-capped bottle. This was autoclaved at 121°C for 30 min, and allowed to cool to 50°C in a water bath. Ampicillin (40 mg) was added and the solution was mixed thoroughly, but gently. The liquid agar was poured into 20 sterile Petri dishes. After the agar had set, the plates were dried in a tissue culture hood, wrapped in cling-wrap and stored at 4°C.

Luria Broth (500 ml)
[10 g/l Tryptone, 5 g/l Yeast extract powder, 10 g/l NaCl, 100 μg/ml Ampicillin]
Tryptone (5 g), Yeast Extract (2.5 g) and NaCl (5 g) was dissolved in 500 ml H_2O. This was allocated into 20 ml Universals (5 ml), or foil wrapped 500 ml flasks (50 ml), and autoclaved at 121°C for 30 minutes. 1.0 μl/ml of the Ampicillin stock (100 mg/ml) was added when inoculating the broth. Bacteria were grown in inoculated LB at 37°C overnight.

β-mercaptoethanol
[100%, 78.43 g/mol]

MOWIOL mounting solution
Add 2 ml glycerol to 2 g MOWIOL (CalBiochem), and mix. Add 4 ml H_2O, mix, and leave for 4 hours at RT. Add 8ml 0.2 M Tris-HCl, pH 8.5, and incubate at 50°C with intermittent shaking until MOWIOL is completely dissolved (~1,5 hrs). Centrifuge for 15 minutes at 5000 × g, collect supernatant, and add 1,4-diazobicyclo-[2,2,2]-octane (DABCO) to a final concentration of 2.5% (0.25 g in 10 ml). Store 2 ml aliquots at -20°C (storage), else 4°C (working).

1 M Na_2HPO_4 (10 ml, pH ~8.0)
(Disodium phosphate)
Dissolve 1.42 g of Na_2HPO_4 [Sigma, S7907] in 10 ml H_2O.

1 mM Na_2HPO_4 (10 ml, pH >7.5)
Add 10 μl of 1 M Na_2HPO_4 to 10 ml H_2O. Use for RNA absorption reading.

***o*-phthaldiadehyde (20 mg/ml in methanol)**
Dissolve 100 mg o-phthaldiadehyde in 5 ml methanol.

10× PBS (1 L)
(Phosphate buffered saline)
[1,37 M NaCl, 27 mM KCl, 43 mM $Na_2HPO_4.2H_2O$, 14 mM KH_2PO_4]
Dissolve 80 g NaCl, 2 g KCl, 7.7 g $Na_2HPO_4.2H_2O$ and 2 g KH_2PO_4 in ~800 ml H_2O. Adjust the pH to 7.4, and make up to 1 L. Autoclave.

PBS^{++} (1 L)
[PBS + 1 mM $CaCl_2$ + 1mM $MgCl_2$]
Dilute 100 ml 10× PBS in 800 ml of H_2O and add 147 mg $CaCl_2.2H_2O$ and 200 mg $MgCl_2.6H_2O$. Make up to 1 L with H_2O.

PenStrep stock (100x)
[10000 U/ml penicillin, 10000 μg/ml streptomycin]

Mix 1 ml NovoPen with 3 ml NovoStrep and 96 ml PBS. Filter-sterilize, freeze in 5 ml aliquots.

8% PFA (100ml)
(paraformaldehyde – TOXIC!!!! Use in fume hood only.)
Add 8 g paraformaldehyde to 90 ml H_2O while stirring. Warm to 60°C, then check pH – should be acidic. Neutralise with 1 M NaOH, stir until dissolved (some always remains insoluble). Cool to RT, adjust volume to 100 ml, filter through 0.22 µm filter. Store in 5 ml aliquots at -20°C.

3% PFA in PBS (10ml)
Thaw one 5 ml aliquot of 8% PFA to 60°C. Mix 3.75 ml 8% PFA, 1 ml 10× PBS and 5.25 ml H_2O in fume hood.

PMSF (100 mM)
HIGHLY TOXIC! 348 mg phenylmethylsulfonyl flouride (PMSF) [Sigma: P-7626] was dissolved in to 20 ml methanol.

2 µM Propidium Iodide
A 1:2500 dilution of a 5 mM stock of propidium iodide was made. Invert coverslip on 50 µl drop. in the dark.

5 mM Propidium Iodide stock
HIGHLY TOXIC/CARCINOGENIC!!!! 5 mg of propidium iodide (668.4 g/mol) was dissolved in 1.5 ml isopropanol. Store at -20°C in foil.

10× RNA Loading buffer (2 ml)
[1mM EDTA, pH 8.0, 0.25% Bromophenol Blue. 0.25% Xylene Cyanol, 50% Glycerol]
Mix 4 µl 0.5 M EDTA (pH 8.0), 500 µl 1% Bromophenol Blue, 500 µl 1% Xylene Cyanol and 1000µl 100% glycerol.

10× RNA Running Buffer (500 ml)
Add 20.9 g MOPS [Sigma, M5162] to 400 ml DEPC treated H_2O. Adjust to pH 7.0 with NaOH or acetic acid, then add 8.3 ml of 3M NaAc (pH 5.5) and 20 ml of 0.5 M EDTA (pH 8). Adjust volume to 500 ml with DEPC treated H_2O, autoclave and store wrapped in foil at RT.

10% Sarkosyl (100ml)
[10% (w/v) *N*-Lauroylsarcosine (Sarkosyl)]
Dissolve 10 mg *N*-Lauroylsarcosine (Sarkosyl) [Sigma, L5777] in 100 ml of DEPC H_2O.

Sephadex G-50 column
A small amount of Sephadex G-50 powder was re-hydrated in 8 volumes of H_2O, and autoclaved in a blue-topped bottle. Similarly glass wool was autoclaved in H_2O in a small bottle. The column was prepared on the day that the probe was made, using a sterile Pasteur pipette. Sterilised tweezers were used to stopper the tube with a small ball of glass wool. Sephadex beads were then added up to 1 cm from the top of the tube. The column was transferred to the first of 15 1,5 ml Eppendorf, and the 150 µl of nick-translated probe added. When no more fluid runs out, the column was transferred to the next tube, and 150 µl sterile water added. After all 15 150 µl eluent samples were obtained, the most radioactive samples (usually numbers 7 and 8) were pooled, and 10 µl counted using a scintillation counter (3 ml scintillation fluid used).

2× SDS Loading buffer (20 ml)
[0.0625M Tris, pH 6.8, 2% SDS, 10% Glycerol, 0.001% Bromophenol Blue]
Mix 625 µl of 2 M Tris (pH 6.8), 400 mg of SDS, 2 ml of Glycerol, 0.2 µg of Bromophenol Blue and 14 ml of H_2O. Adjust to 20ml with H_2O.

2× SDS Reducing buffer (2.5 ml)
[0.0625 M Tris (pH 6.8), 2% SDS, 10% Glycerol, 0.001% Bromophenol Blue, 5% β-mercaptoethanol]
Add 125µl of β-mercaptoethanol to 2.375 ml of 2× SDS loading buffer. Mix and use immediately.

5× SDS Loading Buffer (20 ml)
[0.1563M Tris (pH 6.8), 5% SDS, 25% Glycerol, 0.0025% Bromophenol Blue]
Mix 1.563 ml of 2 M Tris (pH 6.8), 1 g of SDS, 5 ml of Glycerol, 0.5 µg of Bromophenol Blue and 10 ml of H_2O. Adjust to 20 ml with H_2O.

5× SDS Reducing Buffer (4 ml)
[0.1563 M Tris (pH 6.8), 5% SDS, 25% Glycerol, 0.0025% Bromophenol Blue, 12.5% β-mercaptoethanol]
Add 500 µl β-mercaptoethanol to 3.5 ml 5× SDS loading buffer. Mix and use immediately.

SDS Running Gel Buffer (250 ml)
[1.125 M Tris (pH 8.8), 0.3% SDS]
Dissolve 34.07 g of Trisma Base and 0.75 g of SDS in 200 ml H_2O. Adjust the pH to 8.8 with HCl and the volume to 250 ml with H_2O.

SDS Stacking Gel Buffer (250 ml)
[0.375 M Tris (pH 6.8), 0.3% SDS]
Dissolve 11.36 g of Trisma Base and 0.75 g of SDS in 200 ml H_2O. Adjust the pH to 6.8 with HCl and the volume to 250 ml with H_2O.

10× SDS Tank Buffer (500 ml)
[1% SDS, 0.25 M Tris (pH 8.3), 1.92 M Glycine]
Dissolve 15.14 g of Trisma Base, 72.06 g of Glycine and 5 g of SDS in 400 ml of H_2O. Adjust the pH to 8.3 using 10 M NaOH and adjust the volume to 500 ml with H_2O.

[^{35}S] labelling medium
(2% dialysed FCS in minimal Eagles medium (MEM) supplemented with 4 mM L-glutamine and 100 µCi [^{35}S]-methionine/[^{35}S]-cysteine per ml)
5× aliquots of 200 µCi [^{35}S]-methionine/[^{35}S]-cysteine were added to 10 ml starvation medium. 500 µl of this was added to confluent cells in 6-well dishes for metabolic labelling (i.e. 50 µCi per well).

2M Sodium Acetate (20 ml, pH 4.0)
Dissolve 3.28 g anhydrous Sodium Acetate (NaAc) [ ] in 10 ml sdH_2O. Adjust to pH 4.0 with pure Glacial Acetic acid, then 20 ml with H_2O. Autoclave. Store at RT.

3M Sodium Acetate (20 ml, pH 5.2)
Dissolve 4.92 g anhydrous Sodium Acetate (NaAc) in about 10 ml sdH_2O. Adjust the pH to 5.2 using Pure Glacial Acetic acid (~ 7 ml). Make up to 20 ml with sdH_2O. Autoclave. Store at RT.

0.75 M Sodium Citrate (100 ml, pH 7.0)
Dissolve 22.05 g sodium citrate [Sigma, S4641] in 80 ml DEPC H_2O. Adjust to pH 7.0 with 10 M NaOH, and 100 ml with DEPC treated H_2O.

Solution D, stock (100 ml)
[4M guanidine thiocyanate, 25 mM sodium citrate (pH 7.0), 0.5% (w/v) Sarkosyl]
For 100 ml of Solution D; mix 58.6 ml H_2O, 3.52 ml of 0.75 M sodium citrate (pH 7.0), and 5.28 ml of 10% (w/v) *N*-Lauroylsarcosine (Sarkosyl) [Sigma, L5777]. Add 50g guanine thiocyanate [Sigma, G9277] and stir at 65°C to dissolve. Autoclave and store at RT for up to 3 months.

Solution D, working (25 ml)
[4M guanidine thiocyanate, 25 mM sodium citrate (pH 7.0), 0.5% (w/v) Sarkosyl, 100 mM β-mercaptoethanol]
Add 175 µl β-mercaptoethanol to 25 ml of Solution D stock. Store at RT for up to 1 month.

Solvent A (HPLC)
[0.1% trifluoroacetic acid (TFA) in H_2O; pH ~1.0]

Solvent B (HPLC)
[0.1% TFA in acetonitrile]

20× SSC (1 L)
[3 M NaCl, 0.3 M sodium citrate, pH 7.0]
Dissolve 175 g of NaCl and 88 g of sodium citrate (Na_3citrate.$2H_2O$) [Sigma, S4641] in 800 ml H_2O. Adjust the pH to 7.0 with HCl, then the volume to 1000 ml with H_2O. Autoclave and store at RT.

Starvation medium
(2% dialysed FCS in minimal Eagles medium (MEM) supplemented with 4 mM L-glutamine)
400 µl dialysed FCS [GibcoBRL, 10110-153], 400 µl 200 mM L-glutamine [GibcoBRL, 21051-024] and 19.2 ml minimal Eagles medium [ICN, 1641447]. 10 ml is used for staving 3× 6-well dishes for 30 min (500 µl per well), while the remainder is used for metabolic labelling (5× [^{35}S] methionine/cysteine aliquots [200 µCi each] are added) – 500 µl of mixture per well.

TBE (1 L)
[89 mM Tris.Base (pH 8.0), 89 mM boric acid, 2.5 mM EDTA]
Add 100 ml 10× TBE to 900 ml H_2O.

TBE [EtBr]
[89 mM Tris.Base (pH 8.0), 89 mM boric acid, 2 mM EDTA and 0.5 µg/l EtBr]
Add 1 ml 0.5 mg/l Ethidium Bromide Stock to 1 L of TBE.

10× TBE (1 L)
[890 mM Tris.Base (pH 8.0), 890 mM boric acid, 25 mM EDTA]
Dissolve 108 g Trisma Base, 55g boric acid and 9.3g EDTA in 800 ml H_2O. Adjust the pH to 8.0 with concentrated HCl. Adjust the volume to 1000 ml with H_2O and autoclave.

Terrific Broth (Ψ-broth)
[2% (w/v) Difco Bacto Tryptone, 0.5% (w/v) Difco Bacto Yeast Extract, 0.4% (w/v) $MgSO_4$, 10 mM KCl]

TFB1
[100 mM RbCl, 50 mM $MnCl_2$, 30 mM KOAc, 10 mM $CaCl_2$, 15% glycerol]

TFB2
[10 mM MOPS pH 7.0, 10 mM RbCl, 75 mM $CaCl_2$, 15% glycerol]

Tris, Tris.Base, Trisma Base
Sigma [T1503]. Mw = 121.1g/mol.

0. 2M Tris (100 ml, pH8.5)
Dissolve 2.42 g Trisma Base in ~70 ml H_2O. Adjust to pH 8.5 with concentrated HCl, and 100ml with H_2O. Autoclave.

2M Tris (100 ml, pH 6.8)
Dissolve 24.2 g Trisma Base in ~70 ml H_2O. Adjust to pH 6.8 with concentrated HCl, and 100ml with H_2O. Autoclave.

Triton-lysis buffer
[1% Triton X-100, 50 mM HEPES, pH 7.5, 0.5 M NaCl, 1 mM PMSF].
Mix 29.5 ml H_2O, 2.5 ml 1 M HEPES, pH 7.5, 12.5 ml 2 M NaCl, 5.0 ml 10 % Triton X-100, 500 µl 100 mM PMSF. Store at RT.

0.1% Triton X-100 (100 ml)
Dilute 100 µl Triton X-100 in 100 ml PBS^{++}.

Triton X-114 (pre-condensed, 1 L)

[11% final in 10mM Tris, pH 7.5, 150 mM NaCl]

Dissolve 20g Triton X114 in 980ml on ice. Place the clear solution at RT (to allow micelle formation) and allow it to stand until the phases have separated. Remove the aqueous phase and replace with fresh Triton extraction buffer and allow it to stand overnight. Repeat this 3 times, and remove the aqueous phase thereafter. This results in an 11% solution of Triton X114 which can then be diluted to 2 % for phase separations.

Triton X-114 extraction buffer (200ml, pH 7.5)

[10mM Tris, pH 7.5, 150 mM NaCl]

Dissolve 242mg Trisma base (121.1 g/mol) and 1,75 g NaCl (58.4 g/mol) in 160ml H_2O. Adjust the pH to 7.5 using HCl, and make up to 200ml.

2% Triton X-114 (100 ml, pH 7.5)

[2% Triton X-114, 10mM Tris, pH 7.5, 150 mM NaCl]

Dilute 18.2 ml pre-condensed Triton X-114 (11%) in 100 ml Triton X-114 extraction buffer [10 mM Tris, pH 7.5, 150 mM NaCl].

Trypsin/EDTA

[0.5 mg/ml Trypsin in 5 mM EDTA/PBS]

Wash buffer

[20 mM HEPES, pH 7.5; 0.5 M NaCl]

29.22 g NaCl was dissolved in 980 ml H_2O, to which 20 ml 1 M HEPES (pH 7.5) was added, and then sterilised by autoclaving.

Western Blocking Buffer (500 ml)

[5% Skim milk, 0.1% Tween-20, 0.2 M NaCl, 0.05 M Tris (pH 7.4)]

Mix 25 g of Skim Milk powder, 500 µl of Tween-20, 50 ml of 2 M NaCl, 25 ml of 1 M Tris (pH 7.4) and 400ml H_2O. Adjust to 500ml with H_2O.

Western Blotting Buffer (1 L)

Dissolve 3.025 g Trisma Base and 14.4 g of Glycine in 800 ml H_2O, then add 200 ml methanol. This should have a pH of 8.3.

1% Xylene Cyanol (1 ml)

Dissolve 10 mg Xylene Cyanol in 1000µl H_2O.

0.1 M $ZnCl_2$

Dissolve 682 mg $ZnCl_2$ (Sigma, Z0152; 136.3 g/mol) in 50 ml H_2O. Add a 10 µl drop of conc. HCl to aid dissolution. Filter sterilise.

Primers:

Table AIII.1) List of Primers			
Testis ACE Mutant:	**Primer Name:**	**DNA sequence (5' to 3')**	**Silent restriction sites / notes:**
WtACE	ACE-MP2	GTCGACGGTATCGATTCAGGAGTGTCTCAGCTC	*Sal*I, *Cla*I
	ACE-MP3	ACTAGT*GGATCCT*GATCACGGGCCAGCCCA	*Spe*I, *Bam*HI, *Bcl*I
ACE-Δ6JM	ANT-d6B	GGGCCCTTCTGAGCGGTTGTACTGCGGCCA	
	ANT-d6C	TGGCCGCAGTACAACCGCTCAGAAGGGCCC	Ant-d6B^{-1}
ACE-Δ11JM	ANT-d11B	GGGCCCTTCTGAGCGGCC**AAGCTT**CTCCCC	*Hind*III
	ANT-d11C	GGGGAG**AAGCTT**GGCCGCTCAGAAGGGCCC	*Hind*III, Ant-d11B^{-1}
ACE-Δ16JM	ANT-d16B	G**GAATTC**GGCGTCCAGCGGAGCCAGTCCAG	*Eco*RI
	ANT-d16C	CTGGACTGGCTCCGCTGGACGCC**GAATTC**C	*Eco*RI, Ant-d16B^{-1}
ACE-Δ5JM	ANT-d5B	G**AAGCTT**ACGCGGCCCCCTTCTGAGCGAGC	*Hind*III
	ANT-d5C	GCTCGCTCAGAAGGGGGCCGCGT**AAGCTT**C	*Hind*III, Ant-d5B^{-1}
ACE-ΔR_{627}	ACE-R627-1	GGACGCC**GAATTC**CGCTTCAGAAGGGCCCCTC	*Eco*RI
	ACE-R627-2	GAGGGGCCCTTCTGAAGCG**GAATTC**GGCGTCC	*Eco*RI, ACE-R627-1^{-1}
ACE-ΔRS	ACE-RS628-1	GGACGCC**GAATTC**CGCTGAAGGGCCCCTCCCA	*Eco*RI
	ACE-RS628-2	TGGGAGGGGCCCTTCAGCG**GAATTC**GGCGTCC	*Eco*RI, ACE-RS628-1^{-1}
ACE-R627P	ACE-P627-1	GGACGCC**GAATTC**CGCTCCCTCAGAAGGGCCCCTC	*Eco*RI
	ACE-P627-2	GAGGGGCCCTTCTGAGGGAGCG**GAATTC**GGCGTCC	*Eco*RI, ACE-P627-1^{-1}
ACE-ΔCYT	ANT-dCYT	**GTCGAC***ATCGAT*TCACCGCTGGCTGACGCC	*Sal*I, *Cla*I
ACE-Ndom	SomN1	TACCAGTGGCACCCGAACTCCGCTCGC	
	SomN2	GCGAGCGGAGTTCGGGTGCCACTGGTAC	SomN1^{-1}
	Pcr2f	*CCCGGG***GAATTC**ATCT**ACCGGT**CCACC	*Sma*I, *Eco*RI, *Pin*AI
	Pcr3r	GAGCGGAGTTCGGCGTCCACTGGTACTCGGGC	
	Pcr4f	GGCCCGAGTACCAGTGGACGCCGAACTCCGCTC	Pcr3r^{-1}
	SomNDra	CC**ATCGAT**C**AC**TGG***GTG***ACTGGCTGGAAG	*Dra*III, *Cla*I
ACE-NBcl	SomNBcl	**GGAATTCC***TGATCA*CGGGCTTAGATGCCCTG	*Eco*RI, *Bcl*I
	SomN3	GAGGAATATGACCGGCCGAACTCCGCTGCG	Ndom Bridge primers
	SomN4	GCGAGCGGAGTTCGGCCGGTCATATTCCTC	SomN3^{-1}
ACE-JMflX	Antfix1	CCG**GAATTC**CGATGGAGATCAGTGT	*Eco*RI
	Antfix2	CCACTGGCCCACGCGTTCACAGTTCTTTCC	
	Antfix3	GGAAAGAACTGTGAACGCGTGGGCCAGTGG	Antfix2^{-1}
ACEΔ61E	PCR1	*ACTAGT***GGATCC***GTCGAC***AAGCTT**CTAGACTCTGCTCT CCTGCGGCC	*Spe*I, *Bam*HI, *Sal*I *Hind*III
	Zen3r	TCCAGTTGGCCTCGGCATATTGGGATGCCTCCTGGCTG	
	Zen3f	GCCAGGAGGCATCCCAATATGCCGAGGCCAACTGGAAC	
	ACERT	ATTTCCGGGATGTGGCCATCACATT	

Relevant restriction sites, either engineered or naturally occurring, are indicated in bold, italics or both.

Protein Sequences used in alignments:

All sequences obtained from the NCBI Entrez database:
http://www.ncbi.nlm.nih.gov:80/entrez/query.fcgi?db=Protein.

Signal Peptides found using the SignalP server:
http://www.cbs.dtu.dk/services/SignalP/

Transmembrane regions found using the TMPred server:
http://www.ch.embnet.org/software/TMPRED_form.html

Human ACE_S (Human {*Homo sapiens*} somatic ACE derived from P12821 (J04144); mature protein)

```
-29     MGAASGRRGP GLLLPLPLLL LLPPQPALA    (-1)
1       LDPGLQPGNF SADEAGAQLF AQSYNSSAEQ VLFQSVAASW AHDTNITAEN ARRQEEAALL
61      SQEFAEAWGQ KAKELYEPIW QNFTDPQLRR IIGAVRTLGS ANLPLAKRQQ YNALLSNMSR
121     IYSTAKVCLP NKTATCWSLD PDLTNILASS RSYAMLLFAW EGWHNAAGIP LKPLYEDFTA
181     LSNEAYKQDG FTDTGAYWRS WYNSPTFEDD LEHLYQQLEP LYLNLHAFVR RALHRRYGDR
241     YINLRGPIPA HLLGDMWAQS WENIYDMVVP FPDKPNLDVT STMLQQGWNA THMFRVAEEF
301     FTSLELSPMP PEFWEGSMLE KPADGREVVC HASAWDFYNR KDFRIKQCTR VTMDQLSTVH
361     HEMGHIQYYL QYKDLPVSLR RGANPGFHEA IGDVLALSVS TPEHLHKIGL LDRVTNDTES
421     DINYLLKMAL EKIAFLPFGY LVDQWRWGVF SGRTPPSRYN FDWWYLRTKY QGICPPVTRN
481     ETHFDAGAKF HVPNVTPYIR YFVSFVLQFQ FHEALCKEAG YEGPLHQCDI YRSTKAGAKL
541     RKVLQAGSSR PWQEVLKDMV GLDALDAQPL LKYFQPVTQW LQEQNQQNGE VLGWPEYQWH
601     PPLPDNYPEG IDLVTDEAEA SKFVEEYDRT SQVVWNEYAE ANWNYNTNIT TETSKILLQK
661     NMQIANHTLK YGTQARKFDV NQLQNTTIKR IIKKVQDLER AALPAQELEE YNKILLDMET
721     TYSVATVCHP NGSCLQLEPD LTNVMATSRK YEDLLWAWEG WRDKAGRAIL QFYPKYVELI
781     NQAARLNGYV DAGDSWRSMY ETPSLEQDLE RLFQELQPLY LNLHAYVRRA LHRHYGAQHI
841     NLEGPIPAHL LGNMWAQTWS NIYDLVVPFP SAPSMDTTEA MLKQGWTPRR MFKEADDFFT
901     SLGLLPVPPE FWNKSMLEKP TDGREVVCHA SAWDFYNGKD FRIKQCTTVN LEDLVVAHHE
961     MGHIQYFMQY KDLPVALREG ANPGFHEAIG DVLALSVSTP KHLHSLNLLS SEGGSDEHDI
1021    NFLMKMALDK IAFIPFSYLV DQWRWRVFDG SITKENYNQE WWSLRLKYQG LCPPVPRTQG
1081    DFDPGAKFHI PSSVPYIRYF VSFIIQFQFH EALCQAAGHT GPLHKCDIYQ SKEAGQRLAT
1141    AMKLGFSRPW PEAMQLITGQ PNMSASAMLS YFKPLLDWLR TENELHGEKL GWPQYNWTPN
1201    SARSEGPLPD SGRVSFLGLD LDAQQARVGQ WLLLFLGIAL LVATLGLSQR LFSIRHRSLH
1261    RHSHGPQFGS EVELRHS
```

Human ACE_T (Human {*Homo sapiens*} testis ACE derived from P22966 (M26657); mature protein)

```
(-31)   MGQGWATAGL PSLLFLLLCY GHPLLVPSQE A  (-1)
1       SQQVTVTHGT SSQATTSSQT TTHQATAHQT SAQSPNLVTD EAEASKFVEE YDRTSQVVWN
61      EYAEANWNYN TNITTETSKI LLQKNMQIAN HTLKYGTQAR KFDVNQLQNT TIKRIIKKVQ
121     DLERAALPAQ ELEEYNKILL DMETTYSVAT VCHPNGSCLQ LEPDLTNVMA TSRKYEDLLW
181     AWEGWRDKAG RAILQFYPKY VELINQAARL NGYVDAGDSW RSMYETPSLE QDLERLFQEL
241     QPLYLNLHAY VRRALHRHYG AQHINLEGPI PAHLLGNMWA QTWSNIYDLV VPFPSAPSMD
301     TTEAMLKQGW TPRRMFKEAD DFFTSLGLLP VPPEFWNKSM LEKPTDGREV VCHASAWDFY
361     NGKDFRIKQC TTVNLEDLVV AHHEMGHIQY FMQYKDLPVA LREGANPGFH EAIGDVLALS
421     VSTPKHLHSL NLLSSEGGSD EHDINFLMKM ALDKIAFIPF SYLVDQWRWR VFDGSITKEN
481     YNQEWWSLRL KYQGLCPPVP RTQGDFDPGA KFHIPSSVPY IRYFVSFIIQ FQFHEALCQA
541     AGHTGPLHKC DIYQSKEAGQ RLATAMKLGF SRPWPEAMQL ITGQPNMSAS AMLSYFKPLL
601     DWLRTENELH GEKLGWPQYN WTPNSARSEG PLPDSGRVSF LGLDLDAQQA RVGQWLLLFL
661     GIALLVATLG LSQRLFSIRH RSLHRHSHGP QFGSEVELRH S
```

Human ACEH/ACE2 (Human {*Homo sapiens*} ACE homologue (AAF78220/ BAB40370/ AAF99721; mature protein)

```
(-17)   MSSSSWLLLS LVAVTAA   (-1)
1       QSTIEEQAKT FLDKFNHEAE DLFYQSSLAS WNYNTNITEE NVQNMNNAGD KWSAFLKEQS
61      TLAQMYPLQE IQNLTVKLQL QALQQNGSSV LSEDKSKRLN TILNTMSTIY STGKVCNPDN
121     PQECLLLEPG LNEIMANSLD YNERLWAWES WRSEVGKQLR PLYEEYVVLK NEMARANHYE
181     DYGDYWRGDY EVNGVDGYDY SRGQLIEDVE HTFEEIKPLY EHLHAYVRAK LMNAYPSYIS
241     PIGCLPAHLL GDMWGRFWTN LYSLTVPFGQ KPNIDVTDAM VDQAWDAQRI FKEAEKFFVS
301     VGLPNMTQGF WENSMLTDPG NVQKAVCHPT AWDLGKGDFR ILMCTKVTMD DFLTAHHEMG
```

```
361     HIQYDMAYAA QPFLLRNGAN EGFHEAVGEI MSLSAATPKH LKSIGLLSPD FQEDNETEIN
421     FLLKQALTIV GTLPFTYMLE KWRWMVFKGE IPKDQWMKKW WEMKREIVGV VEPVPHDETY
481     CDPASLFHVS NDYSFIRYYT RTLYQFQFQE ALCQAAKHEG PLHKCDISNS TEAGQKLFNM
541     LRLGKSEPWT LALENVVGAK NMNVRPLLNY FEPLFTWLKD QNKNSFVGWS TDWSPYADQS
601     IKVRISLKSA LGDKAYEWND NEMYLFRSSV AYAMRQYFLK VKNQMILFGE EDVRVANLKP
661     RISFNFFVTA PKNVSDIIPR TEVEKAIRMS RSRINDAFRL NDNSLEFLGI QPTLGPPNQP
721     PVSIWLIVFG VVMGVIVVGI VILIFTGIRD RKKKNKARSG ENPYASIDIS KGENNPGFQN
781     TDDVQTSF
```

Chimp ACE_T (Chimpanzee {*Pan troglodytes*} testis ACE derived from AF193487_2; mature protein)

```
(-30)   MGQGWATAGL PSLLFLLLCY GHPLLVPSQE    (-1)
1       APRQVTVTHG TSSQATTSGQ TTTHQATAHQ TSAQSPNLVT DEAEASKFVE EYDRTSQVVW
61      NEYAEANWNY NTNITTETSK ILLQKNMQIA NHTLKYGTQA RRFDVNQLQN TTIKRIIKKV
121     QDLERAALPA QELEEYNKIL LDMETTYSVA TVCHTNGSCL QLEPDLTNVM ATSRKYEDLL
181     WAWEGWRDKA GRAILQFYPK YVELINQAAR LNGYVDAGDS WRSMYETPSL EQDLERLFQE
241     LQPLYLNLHA YVRRALHRHY GAQHINLEGP IPAHLLGNMW AQTWSNIYDL VVPFPSAPSM
301     DTTEAMLKQG WTPRRMFKEA DDFFTSLGLL PVPPEFWNKS MLEKPTDGRE VVCHASAWDF
361     YNGKDFRIKQ CTTVNLEDLV VAHHEMGHIQ YFMQYKDLPV ALREGANPGF HEAIGDVLAL
421     SVSTPKHLHS LNLLSSEGGS DEHDINFLMK MALDKIAFIP FSYLVDQWRW RVFDGSITKE
481     NYNQEWWSLR LKYQGLCPPV PRTQGDFDPG AKFHIPSSVP YIRYFVSFII QFQFHEALCQ
541     AAGHTGPLHK CDIYQSKEAG QRLATAMKLG FSRPWPEAMQ LITGQPNMSA SAMLSYFKPL
601     LDWLRTENEL HGEKLGWPQY NWTPNSARSE GPLPDSGRVS FLGLDLDAQQ ARVGQWLLLF
661     LGIALLVATL GLSQRLFSIR HRSLHRHSHG PQFDSEVELR HS
```

Rabbit ACE_T (Rabbit {*Oryctolagus cuniculus*} testis ACE derived from P22968; mature protein)

```
(-32)   MGQGWAAPGL PSLLLLLLCC GHSLLVPSRV AA    (-1)
1       RRVTVNQGTT SQATTTSKAT TSIRATTHQT TAHQTTQSPN LVTDEAEASR FVEEYDRSFQ
61      AVWNEYAEAN WNYNTNITTE ASKILLQKNM QIANHTLTYG NWARRFDVSN FQNATSKRII
121     KKVQDLQRAV LPVKELEEYN QILLDMETIY SVANVCRVDG SCLQLEPDLT NLMATSRKYD
181     ELLWVWTSWR DKVGRAILPY FPKYVEFTNK AARLNGYVDA GDSWRSMYET PTLEQDLERL
241     FQELQPLYLN LHAYVGRALH RHYGAQHINL EGPIPAHLLG NMWAQTWSNI YDLVAPFPSA
301     STMDATEAMI KQGWTPRRMF EEADKFFISL GLLPVPPEFW NKSMLEKPTD GREVVCHASA
361     WDFYNGKDFR IKQCTTVNME DLVVVHHEMG HIQYFMQYKD LPVALREGAN PGFHEAIGDV
421     LALSVSTPKH LHSINLLSSE GGGYEHDINF LMKMALDKIA FIPFSYLVDE WRWRVFDGSI
481     TKENYNQEWW SLRLKYQGLC PPAPRSQGDF DPGAKFHIPS SVPYIRYFVS FIIQFQFHEA
541     LCKAAGHTGP LHTCDIYQSK EAGKRLADAM KLGYSKPWPE AMKVITGQPN MSASAMMNYF
601     KPLMDWLLTE NGRHGEKLGW PQYTWTPNSA RSEGSLPDSG RVNFLGMNLD AQQARVGQWV
661     LLFLGVALLL ASLGLTQRLF SIRYQSLRQP HHGPQFGSEV ELRHS
```

Rabbit ACE_T (Rabbit {*Oryctolagus cuniculus*} ACE_T derived from P22968; full pre-protein)

```
1       MGQGWAAPGL PSLLLLLLCC GHSLLVPSRV AARRVTVNQG TTSQATTTSK ATTSIRATTH
61      QTTAHQTTQS PNLVTDEAEA SRFVEEYDRS FQAVWNEYAE ANWNYNTNIT TEASKILLQK
121     NMQIANHTLT YGNWARRFDV SNFQNATSKR IIKKVQDLQR AVLPVKELEE YNQILLDMET
181     IYSVANVCRV DGSCLQLEPD LTNLMATSRK YDELLWVWTS WRDKVGRAIL PYFPKYVEFT
241     NKAARLNGYV DAGDSWRSMY ETPTLEQDLE RLFQELQPLY LNLHAYVGRA LHRHYGAQHI
301     NLEGPIPAHL LGNMWAQTWS NIYDLVAPFP SASTMDATEA MIKQGWTPRR MFEEADKFFI
361     SLGLLPVPPE FWNKSMLEKP TDGREVVCHA SAWDFYNGKD FRIKQCTTVN MEDLVVVHHE
421     MGHIQYFMQY KDLPVALREG ANPGFHEAIG DVLALSVSTP KHLHSINLLS SEGGGYEHDI
481     NFLMKMALDK IAFIPFSYLV DEWRWRVFDG SITKENYNQE WWSLRLKYQG LCPPAPRSQG
541     DFDPGAKFHI PSSVPYIRYF VSFIIQFQFH EALCKAAGHT GPLHTCDIYQ SKEAGKRLAD
601     AMKLGYSKPW PEAMKVITGQ PNMSASAMMN YFKPLMDWLL TENGRHGEKL GWPQYTWTPN
661     SARSEGSLPD SGRVNFLGMN LDAQQARVGQ WVLLFLGVAL LLASLGLTQR LFSIRYQSLR
721     QPHHGPQFGS EVELRHS
```

Mouse ACE_T (Mouse {*Mus musculus*} testis ACE derived from P22967; mature protein)

```
(-31)   MGQGWATPGL PSFLFLLLCC GHHLLVLSQV A    (-1)
1       TDHVTANQGI TNQATTRSQT TTHQATIDQT TQIPNLETDE AKADRFVEEY DRTAQVLLNE
61      YAEANWQYNT NITIEGSKIL LEKSTEVSNH TLKYGTRAKT FDVSNFQNSS IKRIIKKLQN
121     LDRAVLPPKE LEEYNQILLD METTYSLSNI CYTNGTCMPL EPDLTNMMAT SRKYEELLWA
181     WKSWRDKVGR AILPFFPKYV EFSNKIAKLN GYTDAGDSWR SLYESDNLEQ DLEKLYQELQ
241     PLYLNLHAYV RRSLHRHYGS EYINLDGPIP AHLLGNMWAQ TWSNIYDLVA PFPSAPNIDA
301     TEAMIKQGWT PRRIFKEADN FFTSLGLLPV PPEFWNKSML EKPTDGREVV CHPSAWDFYN
361     GKDFRIKQCT SVNMEDLVIA HHEMGHIQYF MQYKDLPVTF REGANPGFHE AIGDIMALSV
```

```
421    STPKHLYSLN LLSTEGSGYE YDINFLMKMA LDKIAFIPFS YLIDQWRWRV FDGSITKENY
481    NQEWWSLRLK YQGLCPPVPR SQGDFDPGSK FHVPANVPYV RYFVSFIIQF QFHEALCRAA
541    GHTGPLHKCD IYQSKEAGKL LADAMKLGYS KPWPEAMKLI TGQPNMSASA MMNYFKPLTE
601    WLVTENRRHG ETLGWPEYNW APNTARAEGS TAESNRVNFL GLYLEPQQAR VGQWVLLFLG
661    VALLVATVGL AHRLYNIRNH HSLRRPHRGP QFGSEVELRH S
```

Bovine Cdom (Bovine {*Bos taurus*} ACE_S C-domain derived from g449408; starting D616)

```
616                   DEDEA RKFVEEYDRR SQVVWNEYAE ANWNYSTDIS TDNSKLLMEK
661    NLQMANHTVK YGTWASKFDV TNFQNATMKR MIKKIQDLER AALPTKELEE YNQILLDMET
721    VYSVASVCHE NGTCLRLEPD LTNLMATSRN YQDLAWAWKS WRDKVGRSIL PYFPKYVELT
781    NKAARLNGYQ DGGDSWRSMY EMPFLEEELE QLFQELQPLY LNLHAYVRRA LHRHYGPDVI
841    NLEGPIPAHL LGNMWAQSWS NIYDLVAPFP SAPKMDATEA MIKQGWTPLR MFKEADNFFT
901    SLGLLPMPPE FWNKSMLEKP TDGREVVCHA SAWDFFNGKD FRIKQCTSVN MEDLVVAHHE
961    MGHIQYFMQY KDLPVTFREG ANPGFHEAIG DVLALSVSTP THLHKINLLS SGDGGYEEDI
1021   NFLMKMALEK IAFIPFSFLV DQWRWRVFDG SVTRENYNQE WWSLRLKYQG VCPPLARSQD
1081   DFDPGAKFHI PASVPYVRYF VSFVIQFQFH QALCQAAGHQ GPLHKCDIYQ SKEAGKLLAD
1141   AMKLGFSQPW PEAMRLITGQ SNMSASAMMT YPKPLVDWLV TENGRHGEKL GWPQYNWTPN
1201   SARPGGPFVG SGRVNFLGLN LEEQQARVGQ WVLLFLGVAL LVATLGLTQR LFSIRHHSLR
1261   GPHRGPQFGS EVELRHS
```

Rat Cdom (Rat {*Rattus norvegicus*} ACE_S C-domain derived from P47820; starting D616)

```
616                   DEAKA NRFVEEYDRT AKVLWNEYAE ANWHYNTNIT IEGSKILLQK
661    NKEVSNHTLK YGTWAKTFDV SNFQNSTIKR IIKKVQNVDR AVLPPNELEE YNQILLDMET
721    TYSVANVCYT NGTCLSLEPD LTNIMATSRK YEELLWVWKS WRDKVGRAIL PFFPKYVDFS
781    NKIAKLNGYS DAGDSWRSSY ESDDLEQDLE KLYQELQPLY LNLHAYVRRS LHRHYGSEYI
841    NLDGPIPAHL LGNMWAQTWS NIYDLVAPFP SAPSIDATEA MIKQGWTPRR IFKEADNFFT
901    SLGLLPVPPE FWNKSMLEKP TDGREVVCHA SAWDFYNGKD FRIKQCTSVN MEELVIAHHE
961    MGHIQYFMQY KDLPVTFREG ANPGFHEAIG DVLALSVSTP KHLHSLNLLS SEGSGYEHDI
1021   NFLMKMALDK IAFIPFSYLI DQWRWRVFDG SITKENYNQE WWSLRLKYQG LCPPVPRSQG
1081   DFDPGSKFHV PANVPYIRYF ISFIIQFQFH EALCRAAGHT GPLYKCDIYQ SKEAGKLLAD
1141   AMKLGYSKQW PEAMKIITGQ PNMSASAIMN YFKPLTEWLV TENRRHGETL GWPEYTWTPN
1201   TARAEGSLPE SSRVNFLGMY LEPQQARVGQ WVLLFLGVAL LVATVGLAHR LYNIHNHHSL
1261   RRPHRGPQFG SEVELRHS
```

Human Ndom (Human {*Homo sapiens*} ACE_S N-domain derived from P12821 (J04144); mature)

```
(-29)  MGAASGRRGP GLLLPLPLLL LLPPQPALA   (-1)
1      LDPGLQPGNF SADEAGAQLF AQSYNSSAEQ VLFQSVAASW AHDTNITAEN ARRQEEAALL
61     SQEFAEAWGQ KAKELYEPIW QNFTDPQLRR IIGAVRTLGS ANLPLAKRQQ YNALLSNMSR
121    IYSTAKVCLP NKTATCWSLD PDLTNILASS RSYAMLLFAW EGWHNAAGIP LKPLYEDFTA
181    LSNEAYKQDG FTHTGAYWRS WYNSPTFEDD LEHLYQQLEP LYLNLHAFVR RALHRRYGDR
241    YINLRGPIPA HLLGDMWAQS WENIYDMVVP FPDKPNLDVT STMLQQGWNA THMFRVAEEF
301    FTSLELSPMP PEFWEGSMLE KPADGREVVC HASAWDFYNR KDFRIKQCTR VTMDQLSTVH
361    HEMGHIQYYL QYKDLPVSLR RGANPGFHEA IGDVLALSVS TPEHLHKIGL LDRVTNDTES
421    DINYLLKMAL EKIAFLPFGY LVDQWRWGVF SGRTPPSRYN FDWWYLRTKY QGICPPVTRN
481    ETHFDAGAKF HVPNVTPYIR YFVSFVLQFQ FHEALCKEAG YEGPLHQCDI YRSTKAGAKL
541    RKVLQAGSSR PWQEVLKDMV GLDALDAQPL LKYFQPVTQW LQEQNQQNGE VLGWPEYQWH
601    PPLPDNYPEG IDLVTDEA    (A618)
```

Chimp Ndom (Chimpanzee {*Pan troglodytes*} ACE_S N-domain derived from AF193487_1; mature)

```
(-27)  MGAASGRRGP GLLLPLLLLL PPQPALA    (-1)
1      LDPGLQPGNF SADEAGAQLF AQSYNSSAEQ VLFQSVAASW AHDTNITAEN ARRQEEAALL
61     SQEFAEAWGQ KAKELYEPVW QNFTDPQLRR IIGAVRTLGS ANLPLAKRQQ YNALLSNMSR
121    IYSTAKVCLP NKTATCWSLD PDLTNILASS RSYAMLLFAW EGWHNAAGIP LKPLYEDFTA
181    LSNEAYKQDG FTDTGAYWRS WYNSPTFEDD LEHLYQQLEP LYLNLHAFVR RALHRRYGDR
241    YINLRGPIPA HLLGDMWAQS WENIYDMVVP FPDKPNLDVT STMLQQGWNA THMFRVAEEF
301    FTSLELSPMP PEFWEGSMLE KPADGREVVC HASAWDFYNR KDFRIKQCTR VTMDQLSTVH
361    HEMGHIQYYL QYKDLPVSLR GGANPGFHEA IGDVLALSVS TPAHLHKIGL LDNVTNDTES
421    DINYLLKMAL EKIAFLPFGY LVDQWRWGVF SGRTPNSRYN FDWWYLRTKY QGICPPVTRN
481    ETHFDAGAKF HVPNVTPYIR YFVSFVLQFQ FHEALCKEAG YEGPLHQCDI YQSTKAGAKL
541    RKVLQAGSSR PWQEVLKDMV GLDALDAQPL LKYFQPVTQW LQEQNQQNGE VLGWPEYQWH
601    PPLPDNYPEG IDLVTDEA    (A618)
```

Rabbit Ndom (Rabbit {*Oryctolagus cuniculus*} ACE_S N-domain derived from P12822; mature protein)

```
(-33)   MGAAPGRRGP RLLRPPPPLL LLLLLLRPPP AAL    (-1)
1       TLDPGLLPGD FAADEAGARL FASSYNSSAE QVLFRSTAAS WAHDTNITAE NARRQEEEAL
61      LSQEFAEAWG KKAKELYDPV WQNFTDPELR RIIGAVRTLG PANLPLAKRQ QYNSLLSNMS
121     QIYSTGKVCF PNKTASCWSL DPDLNNILAS SRSYAMLLFA WEGWHNAVGI PLKPLYQEFT
181     ALSNEAYRQD GFSDTGAYWR SWYDSPTFEE DLERIYHQLE PLYLNLHAYV RRVLHRRYGD
241     RYINLRGPIP AHLLGNMWAQ SWESIYDMVV PFPDKPNLDV TSTMVQKGWN ATHMFRVAEE
301     FFTSLGLLPM PPEFWAESML EKPEDGREVV CHASAWDFYN RKDFRIKQCT QVTMDQLSTV
361     HHEMGHVQYY LQYKDQPVSL RRANPGFHEA IGDVLALSVS TPAHLHKIGL LDHVTNDTES
421     DINYLLKMAL EKIAFLPFGY LVDQWRWGVF SGRTPSSRYN FDWWYLRTKY QGICPPVVRN
481     ETHFDAGAKF HIPSVTPYIR YFVSFVLQFQ FHQALCMEAG HQGPLHQCDI YQSTRAGAKL
541     RAVLQAGCSR PWQEVLKDMV ASDALDAQPL LDYFQPVTQW LQEQNERNGE VLGWPEYQWR
601     PPLPNNYPEG IDLVTDEA    (A618)
```

Bovine Ndom (Bovine {*Bos taurus*} ACE_S N-domain derived from g449408, mature protein)

```
(-29)   MGAASGRRSP PLLLPLLLLL LPPPPVILE    (-1)
1       LDPALQPGNF PADEAGAQIF AASFNSSAEQ VLFQSTAASW AHDTNITEEN ARLQEEAALL
61      SQEFSEAWGQ KAKDLFDFVW QNFTDPTLLR IIGAVRTLGP ANLDLEKRQK YNSLLSNMSR
121     IYSTAKVCFP NKTAPCWSLD PELTNILASS RSYTLLLYAW EGWHNAAGIP LKPLYQDFTA
181     LSNEAYKQDG FSDTGAYWRS WYDSPTFTED LERLYQQLEP LYLNLHAYVR RALHRRYGDR
241     YINLRGPIPA HLLGNMWAQS WENIYDTVVP FPDKPNLDVT DVMVQKGWNA THMFRVAEEF
301     FTSLGLLPMP PEFWAESMLE KPSDGREVVC HASAWDFYNR KDFRIKQCTR VTMDQLSTVH
361     HEMGHVQYYL QYKGQHVSLR RGANPGFHEA IGDVLALSVS TPAHLHKIGL LDQVTNDTES
421     DINYLLKMAL EKIAFLPFGY LVDQWRWGVF SGRTRPCRYN YDWWYLRTKY QGICPPVVRN
481     ETHFDAGAKF HVPNVTPYIR YFVSFVLQFQ FHEALCKEAG HQGPLHQCDI YQSTQAGAKL
541     RALLQAGSSR PWQEVLKDMV GSDNLDARPL LSYFQPVTQW LEEQNQQNGE VLGWPEYQWR
601     PPMPDNYPEG IDLVSDED    (D618)
```

Mouse Ndom (Mouse {*Mus musculus*} ACE_S N-domain derived from P09470, mature protein)

```
(-34)   MGAASGQRGR WPLSPPLLML SLLVLLLQPS PAPA    (-1)
1       LDPGLQPGNF SPDEAGAQLF AESYNSSAEV VMFQSTVASW AHDTNITEEN ARRQEEAALV
61      SQEFAEVWGK KAKELYESIW QNFTDSKLRR IIGSIRTLGP ANLPLAQRQQ YNSLLSNMSR
121     IYSTGKVCFP NKTATCWSLD PELTNILASS RSYAKLLFAW EGWHDAVGIP LKPLYQDFTA
181     ISNEAYRQDD FSDTGAFWRS WYESPSFEES LEHIYHQLEP LYLNLHAYVR RALHRRYGDK
241     YVNLRGPIPA HLLGDMWAQS WENIYDMVVP FPDKPNLDVT STMVQKGWNA THMFRVSEEF
301     FTSLGLSPMP PEFWAESMLE KPTDGREVVC HASAWDFYNR KDFRIKQCTR VTMEQLATVH
361     HEMGHVQYYL QYKDLHVSLR RGANPGFHEA IGDVLALSVS TPAHLHKIGL LDHVTNDIES
421     DINYLLKMAL EKIAFLPFGY LVDQWRWGVF SGRTPPSRYN FDWWYLRTKY QGICPPVARN
481     ETHFDAGAKF HIPNVTPYIR YFVSFVLQFQ FHQALCKEAG HQGPLHQCDI YQSTQAGAKL
541     KQVLQAGCSR PWQEVLKDLV GSDALDAKAL LEYFQPVSQW LEEQNQRNGE VLGWPENQWR
601     PPLPDNYPEG IDLETDEA    (A618)
```

Rat Ndom (Rat {*Rattus norvegicus*} ACE_S N-domain derived from P47820, mature protein)

```
(-35)   MGAASGQRGR WPLSPPLLML SLLLLLLLPP SPAPA    (-1)
1       LDPGLQPGNF SADEAGAQLF ADSYNSSAEV VMFQSTAASW AHDTNITEEN ARLQEEAALI
61      NQEFAEVWGK KAKELYESIW QNFTDQKLRR IIGSVQTLGP ANLPLTQRLQ YNSLLSNMSR
121     IYSTGKVCFP NKTATCWSLD PELTNILASS RNYAKVLFAW EGWHDAVGIP LRPLYQDFTA
181     LSNEAYRQDG FSDTGAYWRS WYESPSFEES LEHLYHQVEP LYLNLHAFVR RALHRRYGDK
241     YINLRGPIPA HLLGDMWAQS WENIYDMVVP FPDKPNLDVT STMVQKGWNA THMFRVAEEF
301     FTSLGLSPMP PEFWAESMLE KPADGREVVC HASAWDFYNR KDFRIKQCTR VTMDQLSTVH
361     HEMGHVQYYL QYKDLHVSLR RGANPGFHEA IGDVLALSVS TPAHLHKIGL LDRVANDIES
421     DINYLLKMAL EKIAFLPFGY LVDQWRWGVF SGRTPPSRYN YDWWYLRTKY QGICPPVARN
481     ETHFDAGAKF HIPSVTPYIR YFVSFVLQFQ FHQALCKEAG HQGPLHQCDI YQSTKAGAKL
541     QQVLQAGCSR PWQEVLKDLV GSDALDASAL MEYFQPVSQW LQEQNQRNGE VLGWPEYQWR
601     PPLPDNYPEG IDLETDEA    (A618)
```

Chick ACE (Chicken {*Gallus gallus*} partial ACE, Q10751)

```
1       AKELYGNIWS NFSDPQLKKI IGSIQTLGPS NLPLDKRQQY NTILSDMDKI YSTAKVCLDN
61      GTCWDLEPDI SDIMATSRSY KKLLYAWEGW HNAAGNPLRA KYQEFVTLSN EAYQMDGFED
121     TGSYWRSWYD STTFEDDLEH LYNQLEPLYL NLHAFVRRKL YDRYGPKYIN LKGPIPAHLL
181     GNMWAQQWNN IYDLMVPYPD KPNLDVTNTM VNQGWNATHM FRVSEEFFTS LGLLEMPPEF
241     WEKSMLEKPA DGREVVCHAS AWDFYNRKDF RIKQCTTVTM EQLFTVHHEM GHVQYYLQYK
301     DQPVSFRGGA NPGFHEAIGD VLSLSVSTPS HLQKIGLLSS AVEDEESNIN YLLKMALEKI
361     AFLPFGYLID QWRWNVFSGR TPPSRYNYDW WYLRTKYQGI CAPVSRNESN FDPGAKYHIP
421     GNTPYIRYFV SFILQFQFHK ALCQAANHTG PLHTCDIYMS KEAGAKLREV LKAGSSKSWQ
481     EILFNLTGTD KMDAGALLEY FSPVTTWLQE QNNKTNEVLG WPEFDWRSPI PEGYPEGIDK
541     IVDEAQAKEF LSEYNSTAEV VWNAYTEASW EYNTNITDHN KEVMLEKNLA MSKHTIEYGM
601     RARQFDPSDF QDETVTRILN KLSVLERAAL PEDELKEYNT LLSDMETTYS VAKVCRENNT
661     FHPLDPDLTD ILATSRDYNE LLFAWKGWWD ASGAKIKDKY KRYVELSNKA AVLNGYTDNG
721     AYWRSLYETP TFEEDLERLY LQLQPLYLNL HAYVRRALYN KYGAEHISLK GPIPAHLLGN
781     MWAQSWSNIF DLVMPFPDAT KVDATPAMKQ QGWTPKMMFE ESDRFFTSLG LIPMPQEFWD
841     KSMIEKPADG REVVCHASAW DFYNRKDFRI KQCTVVNMDD LITVHHEMGH VQYFLQYMDQ
901     PISFRDGANP GFHEAIGDVM ALSVSTPKHL HSINLLDQVT ENEESDINYL MSIALDKIAF
961     LPFGYLMDQW RWKVFDGRIK EDEYNQQWWN LRLKYQGLCP PVPRSEDDFD PGAKFHIPAN
1021    VPYIRYFVSF VIQFQFHQAL CKAAGHTGPL HTCDIYQSKE AGKLLGDAMK LGFSKPWPEA
1081    MQLITGQPNM SAEALMSYFE PLMTWLVKKN TENGEVLGWP EYSWTPYAVT EFHAATDTAD
1141    FLGMSVGTKQ ATAGAWVLLA LALVFLITSI FLGVKLFSSR RKAFKSSSEM ELK
```

Dros AnCE (Fruit fly {*Drosophila melanogaster*} ACE, derived from (Q10714); mature)

```
(-17)   MRLFLLALLA TLAVTQA   (-1)
1       LVKEEIQAKE YLENLNKELA KRTNVETEAA WAYGSNITDE NEKKKNEISA ELAKFMKEVA
61      SDTTKFQWRS YQSEDLKRQF KALTKLGYAA LPEDDYAELL DTLSAMESNF AKVKVCDYKD
121     STKCDLALDP EIEEVISKSR DHEELAYYWR EFYDKAGTAV RSQFERYVEL NTKAAKLNNF
181     TSGAEAWLDE YEDDTFEQQL EDIFADIRPL YQQIHGYVRF RLRKHYGDAV VSETGPIPMH
241     LLGNMWAQQW SEIADIVSPF PEKPLVDVSA EMEKQAYTPL KMFQMGDDFF TSMNLTKLPQ
301     DFWDKSIIEK PTDGRDLVCH ASAWDFYLID DVRIKQCTRV TQDQLFTVHH ELGHIQYFLQ
361     YQHQPFVYRT GANPGFHEAV GDVLSLSVST PKHLEKIGLL KDYVRDDEAR INQLFLTALD
421     KIVFLPFAFT MDKYRWSLFR GEVDKANWNC AFWKLRDEYS GIEPPVVRSE KDFDAPAKYH
481     ISADVEYLRY LVSFIIQFQF YKSACIKAGQ YDPDNVELPL DNCDIYGSAR AGAAFHNMLS
541     MGASKPWPDA LEAFNGERIM SGKAIAEYFE PLRVWLEAEN IKNNVHIGWT TSNKCVSS
```

Dros ACEr (Fruit fly {*Drosophila melanogaster*} ACE, derived from (X96913); mature)

```
(-22)   MGACNITVLL LVIMLWLPHG LS    (-1)
1       MGNSCSASVL EARRFFELEN EQLRRRFHEE FLSGYNYNTN VTEANRQAMI EVYARNAELN
61      KRLAQQIKSS DYVQSEDADI RRQAEHLSKL GASALNADDY LALQNAISSM QTNYATATVC
121     SYTNRSDCSL TLEPHIQERL SHSRDPAELA WYWREWHDKS GTPMRQNFAE YVRLTRKASQ
181     LNGHRSYADY WVQFYEDPDF ERQLDATFKQ LLPLYRQLHG YVRFRLRQHY GPDVMPAEGN
241     IPISLLGNMW GQSWNELLDL FTPYPEKPFV DVKAEMEKQG YTVQKLFELG DQFFQSLGMR
301     ALPPSFWNLS VLTRPDDRQV VCHASAWDFY QDSDVRIKMC TEVDSHYFYV VHHELGHIQY
361     YLQYEQQPAV YRGAPNPGFH EAVGDVIALS VMSAKHLKAI GLIENGRLDE KSRINQLFKQ
421     ALSKIVFLPF GYAVDKYRYA VFRNELDESQ WNCGFWQMRS EFGGVEPPVF RTEKDFDPPA
481     KYHIDADVEY LRYFAAHIFQ FQFHKVLCRK AGQYAPNNSR LTLDNCDIFG SKAAGRSLSQ
541     FLSKGNSRHW KEVLEEFTGE TEMDPAALLE YFEPLYQWLK QENSRLGVPL GWGPTDKIPS
601     DCCGTFST
```

Buffalo fly ACE (Buffalo fly {*Haematobia irritans exigua*} ACE derived from (Q10715); mature)

```
(-18)   MKLLVVTILA GLAVCHG    (-1)
1       ATKEEIVATE YLQNINKELA KHTNVETEVS WAYASNITDE NERLRNEISA ENAKFLKEVA
61      KDIQKFNWRT YGSADVRRQF KSLSKTGYSA LPAEDYAELL EVLSAMESNF AKVRVCDYKN
121     SAKCDLSLDP EIEEIITKSR DPEELKYYWT QFYDKAGTPT RSNFEKYVEL NTKSAKLNNF
181     TDGAEVWLDE YEDATFEDQL EAIFEDIKPL YDQVHGYVRY RLNKFYGDEV VSKTGPLPMH
241     LLGNMWAQQW SSIADIVSPF PEKPLVDVSD EMVAQGYTPL KMFQMGDDFF QSMGLKKLPQ
301     EFWDKSILEK PDDGRDLVCH ASAWDFYLTD DVRIKQCTRV TQDQFFTVHH EMGHIQYFLQ
361     YQHQPFVYRT GANPGFHEAV GDVLSLSVST PKHLERVGLL KNYVSDNEAR INQLFLTALD
421     KIVFLPFAFT MDKYRWALFR GQADKSEWNC AFWKLREEYS GIEPPVVRTE KDFDAPAKYH
481     VSADVEYLRY LVSFIIQFQF YKSACITAGE YVPNQTEYPL DNCDIYGSKE AGKLFENMLS
541     LGASKPWPDA LEAFNGERTM TGKAIAEYFE PLRVWLEAVA VESLCHQRYK NVDL
```

Silkworm ACE (Silkworm {*Bombyx mori*} ACE derived from (BAA97657); mature)

```
(-24)  MLKVGGGAVL IAAIVAVFIV ATQG   (-1)
1      RDPDLEAREH EAREYMLHLD KATGLRKNRA SLAEWEYTSN ITKENEEKSI QTHLELSRQE
61     KAAWEETKMY GWQDFQDFTL RRMFKKYSQL GVAALPDDKF QALMRTVSGM ESNYATAKIC
121    SYKNESKCDL SLEPEITEIF STSQDPEELK HAWVEWHNAA GATAKKNFTD YVNLYNEAAK
181    LNGFDNVAEW WQSEYEVPDF EEQLAKLWED VKPLYQQLHA YVRKRLRDKY GDKVVSARGP
241    IPAHLLGNMW AQTWNNIESF TRPYPDKKEI DVTQAMRDQN YTPMKMFQMS DEFFRSLNLT
301    AMPEKFWKNS IIEKPTDREI VCHASAWDFF DGEDFRIKQC TTVDYEYFQT THHEMGHIQY
361    YLQYRDQPVV FRDGANQGFH EAVGDTIALS VSSPKHLRRV GLATGDAEDE QTEINQLYKM
421    GIDKIAFLPF AYTLDLFRYG VFRRKTLPED YNCHYWKLRE QLQGVEPPVN RTEDDFDAAA
481    KYHVSSNVEY ARYYVSFIIQ FQFHRGVCQL AGEHAAGDPN KKLVDCDIYQ SVAAGNALAN
541    MLKMGSSKPW PDAMEALTGQ REMKADGLLE YFRPLHDWLR AENQRTGEHI GWEPTNMEYC
601    TPSQLSELNV KEPSSSPATQ QSDS
```

Tick ACE (Tick {*Boophilus microplus*} ACE derived from (U62809); mature)

```
(-29)  MAARSGSSAA DRFVAVALLA TALYATAAA   (-1)
1      DNFDTYLATL SNVSALIKDE AMGVAFIEGL NDPYTTINNV DSSSSWDYAS NITDYNQNMS
61     NKVSTEVSKM ERQFGITAKR FDWHNFKNDS LKRLFRHVAT IGLAALPDDK LENATSLSSK
121    MAAIYGSTKV TVGKDKDLPL EPDLTRNMKE VGNYDKLLQT WLAWHNAVGP AIKQYYIPYI
181    KLSNEAASLD GYDNIKSAWL SDYETENMTE IVDKLWEDLS PLYKKLHAYV RMKLREIYPG
241    RLPEDGTIPA HLLGNMWAQE WGTLYPHLTM EDKPLDISKT MVEQKWDAQK MFHAAEDFFT
301    SLGLDNMTSE FWSKSILTKP EDREIQCHAS AWNMYNGDDF RIKMCTDPSV EELRTVHHEM
361    GHIEYYMQYK HLHVLLQEGA NEGFHEAVGD LIALSVATKT HYGKLSLLKP TDKYNAVDLL
421    LMSALDKIAF LPFGYLLDKW RWTIFTGETP FDKMNEKFWE YRIKYQGVSP PVKRNESFFD
481    GGAKYHVALH VPYLRYFVAF ILQFQFHEHL CTVAKKVDEH HPFHECDIYG EKNAGDVLKK
541    GLSLGRSKPW PDVLEIMAGT RQMSASSLKK YYEPLEKWLD ERIKNEVVGW DKANVQDYMG
601    VPSFANKVDF SAAAVLASIG VILFCWKNIS L
```

SomNdom (mature protein; PLP)

```
1      LDPGLQPGNF SADEAGAQLF AQSYNSSAEQ VLFQSVAASW AHDTNITAEN ARRQEEAALL
61     SQEFAEAWGQ KAKELYEPIW QNFTDPQLRR IIGAVRTLGS ANLPLAKRQQ YNALLSNMSR
121    IYSTAKVCLP NKTATCWSLD PDLTNILASS RSYAMLLFAW EGWHNAAGIP LKPLYEDFTA
181    LSNEAYKQDG FTDTGAYWRS WYNSPTFEDD LEHLYQQLEP LYLNLHAFVR RALHRRYGDR
241    YINLRGPIPA HLLGDMWAQS WENIYDMVVP FPDKPNLDVT STMLQQGWNA THMFRVAEEF
301    FTSLELSPMP PEFWEGSMLE KPADGREVVC HASAWDFYNR KDFRIKQCTR VTMDQLSTVH
361    HEMGHIQYYL QYKDLPVSLR RGANPGFHEA IGDVLALSVS TPEHLHKIGL LDRVTNDTES
421    DINYLLKMAL EKIAFLPFGY LVDQWRWGVF SGRTPPSRYN FDWWYLRTKY QGICPPVTRN
481    ETHFDAGAKF HVPNVTPYIR YFVSFVLQFQ FHEALCKEAG YEGPLHQCDI YRSTKAGAKL
541    RKVLQAGSSR PWQEVLKDMV GLDALDAQPL LKYFQPVTQW LQEQNQQNGE VLGWPEYQWH
601    PNSARSEGPL PDSGRVSFLG LDLDAQQARV GQWLLLFLGI ALLVATLGLS QRLFSIRHRS
661    LHRHSHGPQF GSEVELRHS
```

SomNBcl (mature protein; ACE_S N-domain in bold; PLP)

```
1      SQQVTVTHGT SSQATTSSQT TTHQATAHQT SAQSPNLVTD EAEASKFVEE YDRTSQVVWN
61     EYAEANWNYN TNITTETSKI LLQKNMQIAN HTLKYGTQAR KFDVNQLQNT TIKRIIKKVQ
121    DLERAALPAQ ELEEYNKILL DMETTYSVAT VCHPNGSCLQ LEPDLTNVMA TSRKYEDLLW
181    AWEGWRDKAG RAILQFYPKY VELINQAARL NGYVDAGDSW RSMYETPSLE QDLERLFQEL
241    QPLYLNLHAY VRRALHRHYG AQHINLEGPI PAHLLGNMWA QTWSNIYDLV VPFPSAPSMD
301    TTEAMLKQGW TPRRMFKEAD DFFTSLGLLP VPPEFWNKSM LEKPTDGREV VCHASAWDFY
361    NGKDFRIKQC TTVNLEDLVV AHHEMGHIQY FMQYKDLPVA LREGANPGFH EAIGDVLALS
421    VSTPKHLHSL NLLSSEGGSD EHDINFLMKM ALDKIAFIPF SYLVDQWRWR VFDGSITKEN
481    YNQEWWSLRL KYQGLCPPVP RTQGDFDPGA KFHIPSSVPY IRYFVSFIIQ FQFHEALCQA
541    AGHTGPLHKC DIYQSKEAGQ RLATAMKLGF SRPWPEAMQL ITGLDALDAQ PLLKYFQPVT
601    QWLQEQNQQN GEVLGWPEYQ WHPNSARSEG PLPDSGRVSF LGLDLDAQQA RVGQWLLLFL
661    GIALLVATLG LSQRLFSIRH RSLHRHSHGP QFGSEVELRH S
```

Useful websites:

Table AIII.2) Useful websites		
Name	**Use**	**URL**
NCBI Entrez	PubMed & protein databases	http://www.ncbi.nlm.nih.gov/Entrez/
	Entrez Genome	http://www.ncbi.nlm.nih.gov:80/entrez/query.fcgi?db=Genome
	Taxonomy	http://www.ncbi.nlm.nih.gov/htbin-post/Taxonomy/wgetorg
	Taxonomy searches	http://www.ncbi.nlm.nih.gov/entrez/query.fcgi?db=Taxonomy
Chemfinder	Chemical structures	http://www.chemfinder.com
PubMed	Literature searches	http://www.ncbi.nlm.nih.gov/entrez/query.fcgi?db=PubMed
ExPASy tools	Protein analysis	http://www.expasy.ch/tools/
TMPred	Transmembrane prediction	http://www.ch.embnet.org/software/TMPRED_form.html
SignalP	Signal sequence prediction	http://www.cbs.dtu.dk/services/SignalP/
BLAST	Protein homology searches	http://www.ncbi.nlm.nih.gov:80/BLAST/
ATCC	Cell line data	http://www.atcc.org/
NEB	Restriction enzymes	http://www.neb.com/neb/products/res_enzymes/re_frame.html
PDB lite	Find 3D structures	http://pdb.weizmann.ac.il/pdb-bin/pdblite
Amos' links	Everything	http://www.expasy.ch/alinks.html
JBC	J. Biological Chemistry	http://www.jbc.org/search.dtl
PNAS	Proc. Nat. Acad. Sci.	http://www.pnas.org/all.shtml
PredictProtein	Predicts secondary structure	http://cubic.bioc.columbia.edu/predictprotein/
Google	Awesome search engine	http://www.google.com/
Framingham	Largest hypertension study	http://rover.nhlbi.nih.gov/about/framingham/index.html

As the WWW is constantly updated, these sites may not be functional after 2001.